

Final Report HRC 51

Prepared By
Arkansas State Highway and Transportation Department
Materials and Research Division
In Cooperation With
U.S. Department of Transportation
Federal Highway Administration

Stresses and Strains in ACHM Overlays on PCC Pavements



Arkansas



1. Report No. FHWA/AR-84/005	2. Government Accession No.	3. Recipient's Catalog No.	
4. Title and Subtitle Stresses and Strains in ACHM Overlays on PCC Pavements		5. Report Date February, 1983	
		6. Performing Organization Code	
7. Author(s) Robert C. Welch, Terry J. Dantin, & Charles W. Caldwell		8. Performing Organization Report No. 1	
9. Performing Organization Name and Address Department of Civil Engineering University of Arkansas Fayetteville, Arkansas 72701		10. Work Unit No.	
		11. Contract or Grant No. HRC-51	
		13. Type of Report and Period Covered Final Report	
12. Sponsoring Agency Name and Address* Arkansas State Highway & Transportation Department P.O. Box 2261 Little Rock, Arkansas 72203		14. Sponsoring Agency Code	
15. Supplementary Notes This study was conducted in cooperation with the Arkansas State Highway and Transportation Department and the U.S. Department of Transportation, Federal Highway Administration.			
16. Abstract An instrumentation system which is capable of measuring both static and dynamic performance of pavement systems has been designed and implemented. Pavement deformations are measured by using induction coil pairs. Stresses are measured by strain gage pressure cells and temperatures are measured by thermistors. The behavior of several different overlay sections was measured under various axle loadings and speeds and at different times of the year. The results are to be used in the development of a design procedure to minimize reflection cracking in overlays.			
17. Key Words Pavement Behavior, Instrumentation, Dynamic Loading, Reflection, Cracking		18. Distribution Statement	
19. Security Classif. (of this report)	20. Security Classif. (of this page)	21. No. of Pages	22. Price

Arkansas Highway and Transportation Department's

ADDENDUM

The following comment by Dr. Welch describing the temperatures recorded during the field study phase of this research project is considered noteworthy and is therefore quoted below:

"... only two of the temperature sensors were operable during the summer of 1980 and they operated only intermittently. These sensors were in the three layer overlay at the interface between the surface course and binder course and at the interface between the open-graded course and the concrete pavement. In January, 1981 only one temperature sensor was operable. The temperatures recorded were:

Date	<u>Time</u>	<u>Top of Binder</u>	<u>Top of Concrete</u>
7/9/80	14:43	141°F	104°F
7/9/80	16:35	142°F	104°F
1/27/81	10:51	50	
1/27/81	12:24	50	
1/27/81	13:16	50	"

STRESSES AND STRAINS
IN ACHM OVERLAYS
ON PCC PAVEMENTS

by

Robert C. Welch
Terry J. Dantin
Charles W. Caldwell

FINAL REPORT
HIGHWAY RESEARCH PROJECT NO. 51

conducted for

The Arkansas State Highway and Transportation Department

in cooperation with

The U. S. Department of Transportation

Federal Highway Administration

The opinions, findings, and conclusions are those of the author and not necessarily those of the Arkansas State Highway and Transportation Department or the Federal Highway Administration.

February 1983

FINDINGS AND CONCLUSIONS

The findings and conclusions resulting from this research are:

1. The behavior of pavement systems under static and dynamic loading can be measured using the instrumentation system developed in this project.
2. The data acquisition system developed in this project is capable of acquiring and recording the data in a convenient and accurate manner.

IMPLEMENTATION

The instrumentation and data acquisition systems developed in this project have been proven through field use. These systems can now be used to measure the performance of various types of pavement structures and to compare the performance of different designs. Much useful data, not previously available, can be gathered by using the systems developed in this project.

TABLE OF CONTENTS

Chapter	Page
I. INTRODUCTION	1
Background	1
Project Objective	3
II. LITERATURE REVIEW	6
Failure Mechanics	6
Methods of Prevention	23
Methods of Prediction	30
Summary	40
III. INSTRUMENTATION	42
General	42
Sensors	43
Sensor Calibrations	48
Static Displacement Data Acquisition	55
Dynamic Data Acquisition	55
Field Installation	75
IV. MATERIAL PROPERTIES	93
Properties of the Subgrade	93
Properties of the Asphaltic Concrete	95
V. DATA ACQUISITION AND RESULTS	112
Procedure - Static Data Acquisition	112
Vertical Movements - Top of PCC Pavement	114
Vertical Movements - Top of Open Grade	120
Vertical Movement - Top of Binder	124
Horizontal Strains - Top of PCC Pavement	129
Horizontal Strains - Top of Open-Grade	133
Horizontal Strains - Top of Binder	133
Procedure - Dynamic Data Acquisition	137

Chapter	Page
Data Reduction	139
Results of Dynamic Data Acquisition	140
VI. CONCLUSIONS AND RECOMMENDATIONS	176
BIBLIOGRAPHY	177
APPENDIX	180

LIST OF FIGURES

<u>No.</u>	<u>Title</u>	<u>Page</u>
2.1	Theoretical Stresses in ACHM Overlay at Joint . . .	9
2.2	Closing of a Crack Tip	12
2.3	Modes of Crack Tip Deformation	12
2.4	Local State in the Vicinity of a Crack Tip	12
2.5	Increase in Transverse Joint Reflection	24
2.6	Dependence of Square of Stress-Intensity Coefficient on Relative Crack Depth.	31
2.7	K/P versus c/d	33
2.8	K/P - c Relation for Beams on Elastic Foundation Tests	33
2.9	Two Dimensional Overlay Model	39
2.10	Crack Growth Rate versus S_{min}	39
3.1	Bison Strain Gage Console with a Pair of 2 in. and a Pair of 1 in. Diameter Induction Coil Sensors. . .	43
3.2	Basic Inductive Coil Displacement Transducer. . . .	44
3.3	Coil Configuration in Three Layered Overlay	45
3.4	Detail of Vertical Extensometer	46
3.5	Remote Temperature Indicator with System Expansion Box and Thermistor	47
3.6	Typical Calibration Curves for 2 in. Diameter Sensors	50
3.7	Calibration Mounts for a Pair of 2 in. Sensors in Coaxial Orientation	51
3.8	Calibration Mounts for a Pair of 2 in. Sensors in Coplanar Orientation	52
3.9	Extensometer Calibration Set-Up	54
3.10	Typical Calibration Curve for Pressure Cell	56
3.11	Typical Crack in CRC Pavement, I-40 near Forrest City, Arkansas	76
3.12	Typical Contraction Joint in PCC Pavement, I-30 at Benton, Arkansas	76

<u>No.</u>	<u>Title</u>	<u>Page</u>
3.13	Typical Sensor Embedment Plan	78
3.14	Typical Sensor Embedment Profiles for (a) One, (b) Two and (c) Three Layered Overlays.	79
3.15	Extensometer Locations Marked for Coring	80
3.16	Truck-Mounted Coring Rig	80
3.17	Extensometer Locations After Coring	81
3.18	Dismantled Parts of a Pair of Extensometer Ready for Assembly	81
3.19	One Inch Sensor and Aluminum Cap being secured to Top of One-Half Inch Steel Rod	82
3.20	Aluminum Pipe Sleeve inserted into Hole	82
3.21	Packing Pipe Sleeve tightly in Hole	82
3.22	Applying Epoxy to Bottom Face of Plexiglass Cap	83
3.23	Attaching Plexiglass Cap to Top of Pipe Sleeve	83
3.24	Contact Cement bonds Cap to Concrete Pavement	84
3.25	Applying Epoxy to Bottom Face of Two in. Diameter Sensor	84
3.26	Attaching Sensor to Top of Plexiglass Cap to complete Extensometer	84
3.27	Completed Pair of Extensometers across Contraction Joint in PCC Pavement.	84
3.28	Establishing reference line from marks on top of each curb on opposite sides of highway	85
3.29	Measuring distances from the top of the near curb to the sensors	85
3.30	A pair of 2 in. sensors set on top of Binder Course and across overlaid joint in PCC Pavement.	86
3.31	Checking sensors for continuity	86
3.32	Check sensor to assure that they are within range	86
3.33	Completed Installation of Sensors on top of PCC Pavement	87

<u>No.</u>	<u>Title</u>	<u>Page</u>
3.34	Instrumented Section after Lay-Down of Open-Grade Course	88
3.35	Completed Installation of Sensors on top of Open-Grade	88
3.36	First Lift of Binder being Laid-Down over Open-Grade	89
3.37	Rolling of Binder Course at Instrumented Section. .	89
3.38	Completed Installation of Sensors on Top of Binder.	90
3.39	Instrumented section complete with Surface Course .	90
3.40	Sensor wires extending beyond shoulder are buried in conduits and terminate in a fiberglass enclosure	91
3.41	Checking system after completion of installation. .	92
4.1	6" x 12" cylinder use to mold open-graded test samples	97
4.2	Molded and capped open-graded test sample	97
4.3	Volume Change Measuring Device	99
4.4	Open-Graded Sample being tested in compression. . .	9 {
4.5	Stress-Strain curves at various Temperatures Asphaltic Concrete Open-Graded Course	100
4.6	Change in Volume per Unit Volume vs. Strain at Various Temperatures	101
4.7	Binder sample being compacted in Hveem kneading compactor	103
4.8	Binder sample being capped prior to testing	103
4.9	Inserting binder sample into Texas triaxial cylinder prior to testing.	104
4.10	Binder sample in compression machine ready for testing	104
4.11	Stress-Strain Curves at Various Temperatures Asphaltic Concrete Binder Course	105
4.12	Change in Volume per Unit Volume vs. Strain at various Temperature	107
4.13	Stress-Strain Curves at various Temperatures . . .	108
4.14	Change in Volume per Unit Volume vs. Strain at Various Temperature	109

<u>No.</u>	<u>Title</u>	<u>Page</u>
4.15	Modulus of Elasticity vs. Temperature Curves Asphaltic Concrete Overlay Courses	110
5.1 through 5.35		141 - 175

LIST OF TABLES

<u>No.</u>	<u>Title</u>	<u>Page</u>
4.1	Subgrade Material Properties	94
4.2	Asphaltic Concrete Hot Mix Design Data	97
4.3	Asphaltic Concrete Properties	111

CHAPTER I

INTRODUCTION

A. BACKGROUND

Asphalt overlays are the most common remedy for the problem of distressed concrete pavements. An overlay will consist of one or more layers of asphaltic concrete placed on an existing pavement. Overlaying an existing Portland cement concrete pavement with an asphaltic concrete pavement structure is a highway rehabilitation technique which has been used by highway agencies since the mid-1940's. At that time, highway engineers were predicting increased traffic volumes and heavier wheel loads for the late 1940's and early 1950's on highway pavements originally constructed in the 1930's and minimally maintained throughout the early 1940's. Rehabilitation of these original pavements was given considerable attention, but during this period of highway rehabilitation, overlays were constructed with little or no corrective treatment to the existing pavement or sub-grade. Consequently, by the late 1940's and early 1950's the new overlay pavement structures had begun developing unexpected failure mechanisms in the form of cracks which penetrated through the full depth of the overlay. It was soon recognized that the developing crack patterns closely followed that of existing joints and cracks in the overlaid pavement and, thus, the highway engineer was confronted with a new problem that has become known as reflection cracking.

Reflection cracks are cracks in asphaltic concrete overlays that reflect the joint and/or crack pattern in the pavement structure underneath. Although asphaltic concrete overlays will strengthen the pavement structure and prevent large quantities of water from penetrating to the base,

if joints and cracks of the underlying pavement are reflected through the overlay and cracks are exposed at the surface, the overlay loses its waterproofing characteristic. Water can then seep into the base and create detrimental conditions which produce structural damage to the layered system, and thereby reduce the supporting power of the pavement. The edges of the cracks become vulnerable to dynamic impact forces due to traffic loads. These impact forces can cause pumping action, widening of the cracks and deterioration of the surface.

Although attention was being given to this new problem of reflection cracking in asphaltic concrete overlays, in 1956 the Interstate system was initiated and emphasis was shifted from rehabilitation of existing highways to construction of new ones. The new Interstate and other new primary and secondary highways were generally constructed with superior geometric designs which have resulted in pleasing horizontal and vertical alignments. This was done with the foresight that reconstruction or rehabilitation of the Interstate and other major elements of the national highway network could be accomplished on their existing alignment. However, pavement rehabilitation has been required on many miles of highway much sooner than had been originally anticipated because traffic volumes have far exceeded projections. Many more miles of Interstate and other Federal and state highways have prematurely reached or are approaching the end of their structural life and they currently require or in the near future will require pavement rehabilitation. Therefore, once again emphasis is shifting to reconstruction or rehabilitation of existing highways with an additional major problem of developing design and construction procedures to greatly reduce or completely eliminate reflection cracking in an asphaltic concrete overlay system.

Reflection cracks are believed to be caused primarily by horizontal movements of the pavement beneath the overlay, brought on by expansion and contraction with temperature change or change in moisture content. They may also be caused by vertical movements created by traffic loads, earth movements, or change of moisture in subgrades with high clay contents.

The development of reflection cracks in asphalt overlays usually results in high maintenance cost. One of the major factors limiting the engineer's ability to efficiently design for reduction or elimination of reflection cracks in asphalt overlays is the lack of knowledge of the actual causes of these cracks. Stress and strain are fundamental measures of asphalt overlay response and a knowledge of the stress-strain-time relationship should hold the key to understanding and solving reflection cracking problems. In situ measurements of stresses and strains are essential if knowledge about the true behavior of the overlay mass is to be obtained.

B. PROJECT OBJECTIVE

The overall objective of this project is to measure the actual behavior, in the field, of asphalt overlay structures in the vicinity of joints in the overlaid concrete pavement. The measurements will be used in a subsequent study to develop design procedures for asphalt overlays over concrete pavement.

The tasks involved in the measurement of overlay performance, along with a brief description of the methods used, are described below.

1. To develop and implement a system for measuring horizontal strains at each interface, and vertical movements in each layer, of a

multilayered asphaltic concrete hot mixed overlay structure in the vicinity of a joint in an overlaid Portland cement concrete pavement. Measurements were made using pairs of induction coils. These coils were embedded in the asphaltic concrete without any physical connection between the coils so that movements in the region of the discs are not constrained. Changes in the spacing of the coils are recorded as differential voltages which can be displayed and recorded.

2. To calibrate the sensors in coplanar and coaxial alignments. A calibration device was fabricated so that sensor pairs could be mounted in a coplanar or coaxial orientation, from which relationships between instrument readings and sensor spacings can be determined.

3. To determine the effects of misalignment of sensor pairs. Calibrations were performed with various lateral displacements and/or rotation of one sensor relative to another. The misaligned calibrations were compared with the aligned calibrations.

4. To determine the physical properties of the subgrade material and of each course of the asphaltic concrete overlay. Field samples were obtained from the site and laboratory tests were performed to evaluate the properties of each material.

5. To record cumulative seasonal and daily movements occurring in three different overlay structures. Sensors were installed in a one, two, and three layer overlay system, in the vicinity of joints in the overlaid PCC pavement.

6. To measure vertical stresses and vertical displacements under dynamic traffic loading. A dynamic data acquisition system capable of acquiring 40,000 data points per second was designed and constructed to record data from strain gage stress cells and induction coil sensors.

7. To measure the pavement temperature profile. Thermistors were installed to measure temperature at layer interfaces in the overlay systems.

CHAPTER II

LITERATURE REVIEW

A. FAILURE MECHANISM

Reflection cracking, in asphaltic concrete overlay construction, is a major problem which has confronted highway engineers for nearly thirty years. Although numerous trial and error methods and experimental methods have been used and studied in attempts to eliminate or reduce reflection cracking, it is perhaps remarkable that at the present time there is very little knowledge of the actual distress mechanism which creates reflection cracking. This is primarily due to the fact that until recent technological developments, sensors that could accurately measure both static and dynamic strains were not available. Therefore, the mechanism of reflection cracking is based totally on theoretical assumptions.

As first reported by Bone, et al. (1954), reflection cracks are believed to be caused primarily by horizontal movements in the pavement slabs beneath the overlay, brought on by expansion and contraction with temperature and/or moisture changes. Because the asphalt is bonded to the pavement, tensile stresses are induced in the asphaltic concrete overlaying the joint when contraction of the pavement causes the joint to open. If the joint opening induces a tensile stress greater than the tensile strength of the asphaltic concrete, then failure occurs and cracking is initiated. Reflection cracks may also be caused by vertical movements due to excessive deflections under traffic loads such as occur when there is pumping of slabs or due to differential settlement of adjacent slabs or due to earth movements or due to loss of moisture in

subgrades with high clay contents. Vertical movements induce shear stresses in the asphaltic concrete in the plane of the overlaid joint.

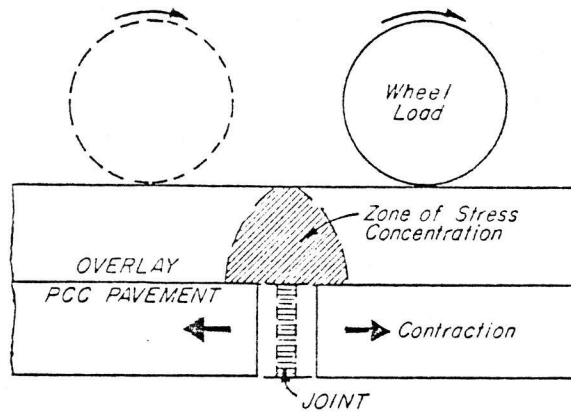
Bone supports this belief by comparing field measurements of the opening and closing of joints between pavement slabs with laboratory determinations of the strength and elongation characteristics of the asphaltic concrete. It was concluded that joints in concrete pavements are subjected to a maximum opening and closing of from 0.1 to 0.2 inch, depending on the location and severity of temperature changes. Laboratory tension tests showed that the most any of the asphaltic concrete mixes stretched at 30°F was 0.05 inch in a 4-inch gage length. It is further concluded that since the asphaltic concrete can only stretch about one fourth of the total seasonal movement of the joints in the underlying concrete pavement, then reflection cracking is inevitable in those types mixes tested.

Some shortcomings of the results reported by Bone follow. First, field measurements of the pavement joints opening and closing are compared with laboratory measurements of the asphaltic concrete elongation. Because the asphalt in the field is subjected to traffic loads, changing temperature cycles, and aging, its properties can be considerably different from laboratory samples molded with the same initial specifications. Second, the assumptions are based on a single asphaltic course overlay. Most overlays are presently two or three layered systems. Third, vertical movements are considered negligible under the assumption that they can usually be controlled by adequate subgrade support. No studies could be found where field measurements of vertical movement of an overlaid pavement were made.

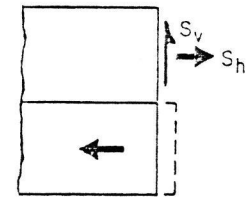
Hensley, 1975, presents theoretical stress diagrams in an attempt to

show the stresses that take place to produce reflection cracks. As the underlying pavement contracts the joint or crack opens and creates horizontal stress concentrations in the overlay above the joint (Fig. 2.1-a). If differential movements of the adjacent slabs occur as a wheel load crosses the joint, then vertical shear stresses are included in the overlay above the joint (Fig. 2.1-b). Hensley theorizes that the majority of the cracks are caused by the horizontal stress (Fig. 2.1-c) as a result of the existing pavement characteristics of expansion and contraction with changes in temperature and moisture, and that reflective cracking becomes a result of tensile failure in the overlay. As the overlay begins to fail small cracks develop at the bottom of the overlay and propagate toward the surface as the bottom cracks grow progressively larger (Fig. 2.1-d).

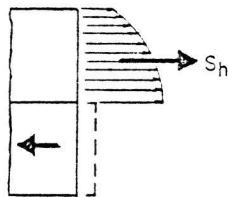
Recent studies have applied theories of fracture mechanics to develop design systems capable of solving various boundary value problems associated with overlay design, joint stress analysis and fatigue crack propagation (Ramsamooj, 1970 and 1973; Luther, 1973; Luther et al., 1976, Majidzadeh et al., 1971; Majidzadeh et al., 1977). Linear fracture mechanics is a structural study which considers crack extension behavior as a function of applied loads, in the absence of large plastically yielded regions surrounding existing cracks or flaws (Kobayashi, 1973). The application of linear fracture mechanics to asphaltic concrete overlay systems hypothesized that small flaws exist in the asphaltic concrete above a joint or crack, which develop zones of stress concentration. Overstresses in these zones, induced by wheel loads and/or thermal changes produce fatigue failures from which cracks are initiated with the growth of the flaw. Ramsamooj (1970) and Kauffman (1973) provide



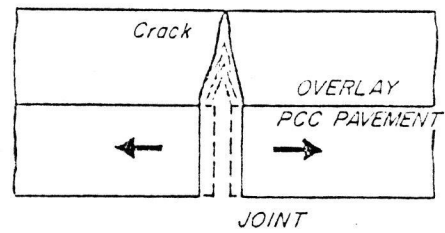
(a) OVERLAY OVER JOINT



(b) ACTIVE STRESSES



(c) HORIZONTAL STRESSES



(d) CRACK GROWTH

Figure 2.1 Theoretical Stresses in ACHM Overlay at Joint
(From Hensley, 1975)

evidence that small flaws do exist in asphaltic concrete and that the asphaltic concrete does crack from fatigue failure.

The process of crack initiation and growth is associated with the energy balance in the flaw regions. The work of external forces producing deformations at the tip of regions of discontinuities can be divided into elastic energy, the energy required for irreversible changes in the material body of a viscous or plastic flow, and the surface energy required to form a crack. The rate of crack growth then depends on the energy balance, and the path it follows is governed by the minimum energy requirement (Ramsamooj, 1970).

The original Griffith (1921) theory formulates the basis of linear fracture mechanics. Griffith proposed that the rupture of brittle material occurred when the surface area of a flaw of a body under load increased such that the rate of decrease in potential energy was greater than the rate of increase in surface energy due to the increased crack surface area. In order to apply the Griffith theory to metals, Irwin (1952) replaced the rate of increase in surface energy by the increased plastic-energy-dissipation rate. Irwin justified this by recognizing that the surface-energy-dissipation rate was negligible when compared to the magnitude of the plastic-energy-dissipation rate. Furthermore, Irwin postulated that the plastic-energy-dissipation rate is a material property which can be determined by standardized test at the onset of fracture or when it is equal to the rate of decrease in potential energy. The Griffith-Irwin theory of fracture then states that when the strain-energy-release rate is equal to or exceeds the plastic-energy-dissipation rate, instability occurs and the crack will run (Kobayashi, 1973). The strain-energy-release rate depends on the loading condition and crack geometry,

therefore, the problem of determining the strain-energy-release rate reduces to a boundary-value problem.

Kobayashi presents the relation between the strain-energy-release rate, δU_σ , and the local stress field by considering the reverse problem where a short segment, δx , of a two dimensional crack is closed by imposing a force of σ_{yy}^* $(-\delta x, 0)$ on the crack surface as shown in Figure 2.2. The total strain-energy absorption rate in this reverse loading problem is equal to the input-energy absorption rate, δU_σ , which in turn, is equal to the strain-energy-release rate, g , for a crack extension of δx or

$$\delta U_\sigma = g \cdot \delta x = \int_0^{\delta x} u_y(0,0) \cdot \sigma_{yy}^*(-\delta x, 0) dx \quad (2.1)$$

where, assuming that the plastically yielded region ahead of the crack tip does not change the state of stress significantly, then $u_y(0,0)$ is the crack-closing displacement with the crack tip located at the origin of the coordinates, $(0,0)$, and σ_{yy}^* is the associated closing stress which is equal to the normal stress ahead of the crack tip located at $(-\delta x, 0)$. Thus, all problems in linear fracture mechanics can be converted to problems in linear elasticity.

Irwin (1958) recognized the association of crack movements with stress fields in the immediate vicinity of the crack tip. Irwin developed the concepts of stress-intensity factors and proposed three modes of crack tip deformation to classify crack behavior. The three modes of relative displacement of the crack surfaces, as shown in Figure 2.3 are Mode I - the opening mode, Mode II - the inplane sliding mode, and Mode III - the tearing mode.

If analysis is confined to a small region in the vicinity of a crack

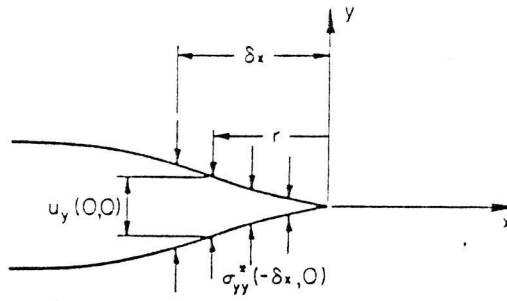


Figure 2.2 Closing of a Crack Tip.
(From Kobayashi, 1973)

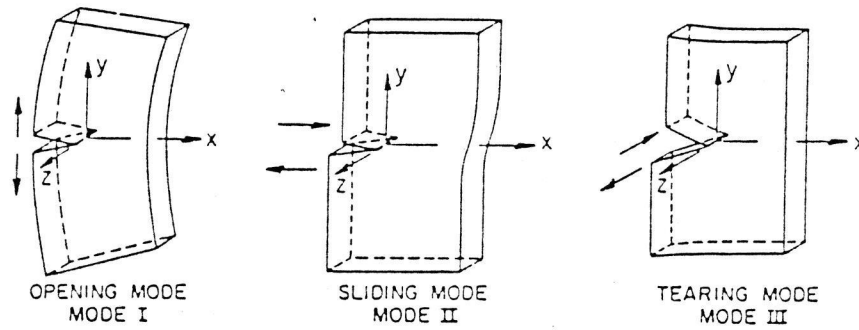


Figure 2.3 Modes of Crack Tip Deformation.
(From Kobayashi, 1973)

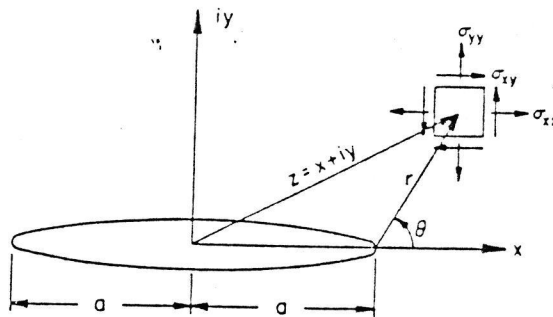


Figure 2.4 Local State in the Vicinity of a Crack Tip.
(From Kobayashi, 1973)

tip, as shown in Figure 2.4, and all stresses and stress functions are represented in terms of a local polar-coordinate system of r and θ , then Westergaard's stress function Z is applicable (Kobayashi, 1973).

$$Z = \frac{f(\rho)}{\sqrt{\rho}} \quad \text{where } \rho = re^{i\theta} \quad (2.2)$$

As $\rho \rightarrow 0$, the complex analytic function $f(\rho)$ approaches a real constant equal to $K/\sqrt{2\pi}$ for Mode I, $K_{II}/\sqrt{2\pi}$ for Mode II and $K_{III}/\sqrt{2\pi}$ for Mode III crack tip deformation. K , K_{II} , and K_{III} are stress-intensity factors for each respective mode of deformation.

1. MODE I - OPENING MODE - The stress-intensity factor, K , for the opening mode is defined as

$$K = \lim_{r \rightarrow 0} \sigma_{yy}(r, \theta = 0) \cdot \sqrt{2\pi r} \quad (2.3)$$

The local stresses in terms of local polar coordinates are:

$$\begin{aligned} \sigma_{xx} &= \frac{K}{\sqrt{2\pi r}} \cos \frac{\theta}{2} \left[1 - \sin \frac{\theta}{2} \cdot \sin \frac{3\theta}{2} \right] \\ \sigma_{yy} &= \frac{K}{\sqrt{2\pi r}} \cos \frac{\theta}{2} \left[1 + \sin \frac{\theta}{2} \cdot \sin \frac{3\theta}{2} \right] \\ \sigma_{xy} &= \frac{K}{\sqrt{2\pi r}} \sin \frac{\theta}{2} \cdot \cos \frac{\theta}{2} \cdot \cos \frac{3\theta}{2} \end{aligned} \quad (2.4)$$

The displacement components in the x and y directions become:

a. for the state of plane stress

$$\begin{aligned} u_x &= \frac{K}{G} \sqrt{\frac{r}{2\pi}} \cos \frac{\theta}{2} \left[\frac{1-\nu}{1+\nu} + \sin^2 \frac{\theta}{2} \right] \\ u_y &= \frac{K}{G} \sqrt{\frac{r}{2\pi}} \sin \frac{\theta}{2} \left[\frac{2}{1+\nu} - \cos^2 \frac{\theta}{2} \right] \end{aligned} \quad (2.5)$$

where G = the shear modulus

ν = the Poisson's ratio

b. for the state of plane strain

$$\begin{aligned} u_x &= \frac{K_I}{G} \sqrt{\frac{r}{2\pi}} \cos \frac{\theta}{2} \left[1 - 2\nu + \sin^2 \frac{\theta}{2} \right] \\ u_y &= \frac{K_I}{G} \sqrt{\frac{r}{2\pi}} \sin \frac{\theta}{2} \left[2 - 2\nu - \cos^2 \frac{\theta}{2} \right] \end{aligned} \quad (2.6)$$

K_I denotes that K for the state of plane strain is restricted to tensile fracture.

The strain-energy-release rate due to crack extension can now be determined by evaluating $u_y(0,0)$ and $\sigma_{yy}^*(-\delta x, 0)$ at a distance r from the crack tip, from equations (2.4) and (2.6)

$$\begin{aligned} \sigma_{yy}^*(-\delta x, 0) &= \frac{K_I}{\sqrt{2\pi(\delta x - r)}} \\ u_y(0, 0) &= \frac{2(1-\nu)}{G} \frac{K_I}{\sqrt{2\pi}} \sqrt{r} \quad (\text{Plane strain}) \end{aligned} \quad (2.7)$$

and then substituted into equation (2.1)

$$\begin{aligned} \delta U_\sigma &= g \cdot \delta x = \int_0^{\delta x} u_y(0, 0) \cdot \sigma_{yy}^*(-\delta x, 0) dx \\ \delta U_\sigma &= g_I \delta x = \frac{1-\nu}{G} K_I^2 \int_0^{\delta x} \sqrt{\frac{r}{\delta x - r}} dr = \frac{1-\nu}{2G} K_I^2 \delta x \end{aligned} \quad (2.8)$$

The characteristic quantity of strain-energy-release rate is also referred to as a crack-opening force and can be represented as

$$g_I = \frac{1-\nu}{2G} K_I^2 \quad (2.9)$$

or replacing ν with $\nu/(1+\nu)$ and obtaining

$$G = K^2/E \quad (2.10)$$

where E is the modulus of elasticity.

The plastic-energy-dissipation rate which is a material constant following the Griffith-Irwin theory can be replaced by an equivalent material constant G_{IC} which is the critical strain-energy-release rate at the onset of rapid fracture. Since K_I is directly related to G_I from equation (2.9), the Griffith-Irwin theory can be restated in terms of K_I which becomes a material constant, K_{IC} , at the onset of rapid fracture. K_{IC} , the critical stress-intensity factor, is referred to as the fracture toughness of the material and has the dimension of stress $\cdot \sqrt{\text{length}}$ (Kobayashi).

2. MODE II - INPLANE-SLIDING MODE - Similar expressions of stresses and displacements as for Mode I have been developed for Mode II. The stress-intensity factor for Mode II crack tip displacement is obtained by

$$K_{II} = \lim_{r \rightarrow 0} \sigma_{xy}(r, \theta = 0) \cdot \sqrt{2\pi r} \quad (2.11)$$

The local stresses in terms of local polar coordinates for the inplane-sliding mode are:

$$\begin{aligned} \sigma_{xx} &= \frac{-K_{II}}{\sqrt{2\pi r}} \sin \frac{\theta}{2} \left[2 + \cos \frac{\theta}{2} \cdot \cos \frac{3\theta}{2} \right] \\ \sigma_{yy} &= \frac{K_{II}}{\sqrt{2\pi r}} \cos \frac{\theta}{2} \cdot \sin \frac{\theta}{2} \cdot \cos \frac{3\theta}{2} \\ \sigma_{xy} &= \frac{K_{II}}{\sqrt{2\pi r}} \cos \frac{\theta}{2} \cdot \left[1 - \sin \frac{\theta}{2} \sin \frac{3\theta}{2} \right] \end{aligned} \quad (2.12)$$

The displacement components in the x and y directions become:

a. for the state of plane stress

$$\begin{aligned} u_x &= \frac{K_{II}}{G} \sqrt{\frac{r}{2\pi}} \sin \frac{\theta}{2} \left[\frac{2}{1+\nu} + \cos^2 \frac{\theta}{2} \right] \\ u_y &= \frac{K_{II}}{G} \sqrt{\frac{r}{2\pi}} \cos \frac{\theta}{2} \left[\frac{1-\nu}{1+\nu} + \sin^2 \frac{\theta}{2} \right] \end{aligned} \quad (2.13)$$

b. for the state of plane strain

$$\begin{aligned} u_x &= \frac{K_{II}}{G} \sqrt{\frac{r}{2\pi}} \sin \frac{\theta}{2} \left[2 - 2\nu + \cos^2 \frac{\theta}{2} \right] \\ u_y &= \frac{K_{II}}{G} \sqrt{\frac{r}{2\pi}} \cos \frac{\theta}{2} \left[1 - 2\nu + \sin^2 \frac{\theta}{2} \right] \end{aligned} \quad (2.14)$$

The strain-energy-release rate for the Mode II deformation takes on an identical form as equation (2.9)

$$\mathcal{G}_{II} = \frac{1-\nu}{2G} K_{II}^2 \quad (2.15)$$

3. MODE III - TEARING MODE - The Mode III deformation is due to an out-of-plane shear which can be produced locally in torsion loading. The stress-intensity factor, K_{III} , is determined by

$$K_{III} = \lim_{r \rightarrow 0} \sigma_{yz}(r, \theta = 0) \cdot \sqrt{2\pi r} \quad (2.16)$$

The local stresses in terms of local polar coordinates for the tearing mode are

$$\begin{aligned} \sigma_{xx} &= \sigma_{yy} = \sigma_{xy} = 0 \\ \sigma_{xz} &= \frac{K_{III}}{\sqrt{2\pi r}} \sin \frac{\theta}{2} \\ \sigma_{yz} &= \frac{K_{III}}{\sqrt{2\pi r}} \cos \frac{\theta}{2} \end{aligned} \quad (2.17)$$

and the displacements become

$$u_x = u_y = 0$$

$$u_z = w = \frac{K_{III}}{G} \sqrt{\frac{2r}{\pi}} \sin \frac{\theta}{2} \quad (2.18)$$

where w is the deformation due to out-of-plane warping.

The strain-energy-release rate for the Mode III deformation is represented by

$$\mathcal{G}_{III} = \frac{1}{2G} K_{III}^2 \quad (2.19)$$

4. SUPERPOSITION OF MODES - The theory of fracture mechanics described above is based on the linear theory of elasticity, therefore, stress functions for other boundary value problems with identical geometries and same opening modes can be superimposed. The corresponding stress-intensity factors for the same mode of crack deformation can be superimposed as

$$\begin{aligned} K_I &= K_{I1} + K_{I2} + \cdots + K_{Im} \\ K_{II} &= K_{II1} + K_{II2} + \cdots + K_{II_n} \\ K_{III} &= K_{III1} + K_{III2} + \cdots + K_{III_p} \end{aligned} \quad (2.20)$$

where m , n , and p are integers.

The crack-opening forces are scalar terms involving the strain-energy-release rates and, therefore, crack opening forces for different modes of crack deformation can be superimposed as

$$\mathcal{G} = \mathcal{G}_I + \mathcal{G}_{II} + \mathcal{G}_{III} = \frac{1-\nu}{2G} K_I^2 + \frac{1-\nu}{2G} K_{II}^2 + \frac{1}{2G} K_{III}^2 \quad (2.21)$$

The elastic plane state of stress in the vicinity of the crack tip in terms of local polar coordinates can be obtained by the linear superposition of equations (2.4) and 2.12) as

$$\begin{aligned}
\sigma_{xx} &= \frac{K}{\sqrt{2\pi r}} \cos \frac{\theta}{2} \left[1 - \sin \frac{\theta}{2} \sin \frac{3\theta}{2} \right] - \frac{K_{II}}{\sqrt{2\pi r}} \sin \frac{\theta}{2} \left[2 + \cos \frac{\theta}{2} \cdot \cos \frac{3\theta}{2} \right] \\
\sigma_{yy} &= \frac{K}{\sqrt{2\pi r}} \cos \frac{\theta}{2} \left[1 + \sin \frac{\theta}{2} \sin \frac{3\theta}{2} \right] + \frac{K_{II}}{\sqrt{2\pi r}} \cos \frac{\theta}{2} \sin \frac{\theta}{2} \cos \frac{3\theta}{2} \\
\sigma_{xy} &= \frac{K}{\sqrt{2\pi r}} \sin \frac{\theta}{2} \cos \frac{\theta}{2} \cos \frac{3\theta}{2} + \frac{K_{II}}{\sqrt{2\pi r}} \cos \frac{\theta}{2} \left[1 - \sin \frac{\theta}{2} \cdot \sin \frac{3\theta}{2} \right]
\end{aligned} \tag{2.22}$$

The elastic plane-stress state of displacement in the vicinity of the crack tip can be obtained by the linear superposition of equations (2.5) and 2.13) as

$$\begin{aligned}
u_x &= \frac{K}{G} \sqrt{\frac{r}{2\pi}} \cos \frac{\theta}{2} \left[\frac{1-\nu}{1+\nu} + \sin^2 \frac{\theta}{2} \right] + \frac{K_{II}}{G} \sqrt{\frac{r}{2\pi}} \sin \frac{\theta}{2} \cdot \left[\frac{2}{1+\nu} + \cos^2 \frac{\theta}{2} \right] \\
u_y &= \frac{K}{G} \sqrt{\frac{r}{2\pi}} \sin \frac{\theta}{2} \left[\frac{2}{1+\nu} - \cos^2 \frac{\theta}{2} \right] + \frac{K_{II}}{G} \sqrt{\frac{r}{2\pi}} \cos \frac{\theta}{2} \cdot \left[\frac{1-\nu}{1+\nu} + \sin^2 \frac{\theta}{2} \right]
\end{aligned} \tag{2.23}$$

The analytical solutions to the methods presented yield stress-intensity factors for only a limited number of simple problems, and lengthy exact solutions to idealized problems only approximate the actual conditions. Therefore, numerical methods, in particular the method of finite-element analysis, have been used to obtain numerical solutions to actual two dimensional crack problems. If the state of stress or displacement in the vicinity of the crack tip can be determined within a reasonable degree of accuracy, the stress intensity factors can be computed by the use of equations (2.22) or (2.23). The finite-element analysis must then produce sufficiently accurate states of stress or displacement within the local region where these equations are valid.

As a well known rule of thumb, this local region has been defined as $r < (a/20)$, where a is the half-crack length of a straight crack (Kobayashi).

The stress-intensity factor depends on the load, specimen geometry, and crack configuration and can be evaluated experimentally or by analytical techniques. The critical stress-intensity factors are material properties. K_{IC} has been determined by using beam specimens whose dimensions fulfill the established fracture mechanics criteria (Ramsamooj, 1970). However, standard criteria to perform K_{IIC} and K_{IIIC} tests or values for K_{IIC} and K_{IIIC} for asphalt or other materials have not been established (Luther et al., 1976).

The strain energy density criterion of fracture or S-criterion was introduced by Sih (1973). This new criterion assumes that failure starts by breaking material elements at finite distances away from the crack front. The locations of these elements are determined from the relative minimum of strain energy density. Sih established that for most loading conditions the energy of volume change is larger than the energy of shape change at these locations. As a result of the material elements breaking up, the crack grows in certain preferred directions which can be computed and the load required to produce a certain value of strain energy density, characteristic of the material at fracture, can also be obtained.

In two dimensions, fracture initiates from a point element ahead of the crack where the strain energy density factor, S , reaches a critical value, S_{cr} , and if the fracture is considered as three dimensional, then there is a whole line of critical elements parallel to the straight crack edge. When all three stress intensity factors, K , K_{II} and K_{III} , are present along the crack border, the fracture criterion should express

that fracture occurs when some combination of them reaches a critical value such that

$$f(K, K_{II}, K_{III}) = f_{cr}$$

Such a criterion is developed by referring to the strain energy stored in a volume element ahead of the crack. The strain energy stored in a volume element $dV = dx dy dz$ is a quadratic form of the stresses σ_{xx} , σ_{yy} , σ_{zz} , σ_{xy} , σ_{xz} and σ_{yz} such that

$$\begin{aligned} \frac{dW}{dV} = & \frac{1}{2E} (\sigma_{xx}^2 + \sigma_{yy}^2 + \sigma_{zz}^2) - \frac{\nu}{E} (\sigma_{xx}\sigma_{yy} + \sigma_{yy}\sigma_{zz} + \sigma_{zz}\sigma_{xx}) \\ & + \frac{1+\nu}{E} (\sigma_{xy}^2 + \sigma_{xz}^2 + \sigma_{yz}^2) \end{aligned} \quad (2.24)$$

where ν is Poisson's ratio, E is Young's modulus of the material, and σ_{xx} , σ_{yy} , and σ_{xy} are expressed by equations (2.22) and σ_{zz} , σ_{xz} , and σ_{yz} are given by

$$\begin{aligned} \sigma_{zz} &= 2\nu \frac{K}{\sqrt{2\pi r}} \cos \frac{\theta}{2} - 2\nu \frac{K_{II}}{\sqrt{2\pi r}} \sin \frac{\theta}{2} \\ \sigma_{xz} &= - \frac{K_{III}}{\sqrt{2\pi r}} \sin \frac{\theta}{2} \\ \sigma_{yz} &= \frac{K_{III}}{\sqrt{2\pi r}} \cos \frac{\theta}{2} \end{aligned} \quad (2.25)$$

Substituting the stresses from equations (2.22) and (2.25) into (2.24), the strain energy per unit volume may be written as

$$\frac{dW}{dV} = \frac{S}{r} + \text{non-singular terms} \quad (2.26)$$

which become singular in the limit as $r \rightarrow 0$. The strain energy density S is defined only if $r \neq 0$ and hence the volume element is always kept at a finite distance away from the crack border. S is expressed as a quadratic form in the stress intensity factors k_1 , k_2 and k_3 :

$$S = a_{11} k_1^2 + 2a_{12} k_1 k_2 + a_{22} k_2^2 + a_{33} k_3^2 \quad (2.27)$$

where $k = \frac{K}{\sqrt{\pi}}$. In two dimensional problems the factors k_1 , k_2 and k_3 are constant along the crack front and S is only dependent on the polar angle θ . The coefficients a_{11} , a_{12} , a_{22} and a_{33} are given by

$$\begin{aligned} a_{11} &= \frac{1}{16G} \{(3-4\nu-\cos\theta)(1+\cos\theta)\} \\ a_{12} &= \frac{1}{16G} \{(2\sin\theta)(\cos\theta) - (1-2\nu)\} \\ a_{22} &= \frac{1}{16G} \{4(1-\nu)(1-\cos\theta) + (1+\cos\theta)(3\cos\theta-1)\} \\ a_{33} &= \frac{1}{4G} \end{aligned} \quad (2.28)$$

Sih (1975) has proposed that crack propagation initiating from an inherent flaw in the material is determined by the energy density in the region of high stress elevation. The locations of maximum yielding and of brittle fracture can be found from the stationary values of the strain energy density factor, S . The basic hypotheses of the strain energy density factor theory as applied to two-dimensional crack problems are outlined as follows:

Hypothesis (1): The direction of crack propagation at any point along the crack border is toward the region with the minimum value of strain energy density factor, S , as compared with other regions on the same spherical surface surrounding the point.

Hypothesis (2): Crack extension occurs when the strain energy density factor in the region determined by hypotheses (1), $S = S_{\min}$, reaches a critical value, S_{cr} .

Hypotheses (1) and (2) are sufficient for determining where and when unstable crack propagation occurs in a two-dimensional problem in which all the elements at the same distance r_0 from the straight crack front are assumed to fail simultaneously. The relation $S_{cr} = r_0(dW/dV)_{cr}$ implies that if r_0 is constant along the crack front then the value S_{cr} is uniquely related to $(dW/dV)_{cr}$.

In order to apply the strain energy density theory, the minimum value of S along the crack border is required. It is seen from equation (2.27) that S is a function of θ through the coefficients A_{ij} . The range of θ is $(-\pi, \pi)$. The function $S(\theta)$ is said to have a local minimum at (θ_0) in the region $R(-\pi \leq \theta \leq \pi)$, if $S(\theta) \geq S(\theta_0)$ for all points (θ) in the neighborhood of the point (θ_0) in R .

If the function $S(\theta)$ is differentiable in the region R and a stationary value is attained at an interior point (θ_0) , then the first derivative of $S(\theta)$ with respect to (θ) vanishes at (θ_0) , i.e.,

$$\frac{\partial S}{\partial \theta} = 0 \text{ at } (\theta_0) \quad (2.29)$$

If S is a relative minimum at (θ_0) , then usually the second derivative of S satisfied the condition

$$\frac{\partial^2 S}{\partial \theta^2} > 0 \text{ at } (\theta_0) \quad (2.30)$$

Sih's strain energy density theory provides an analytical method for investigating mixed mode fracture and the propagation of cracks.

B. METHODS OF PREVENTION

Many highway agencies have experimented with numerous methods of asphaltic concrete overlay construction. The five methods generally used by most highway departments in attempting to prevent reflection cracking in an asphaltic concrete overlay, implemented either independently or in combinations, are: (1) increase the thickness of the asphaltic concrete overlay, (2) use an intermediate layer of granular base (cushion course), (3) reseal the slabs by rolling, (4) break the slabs into small segments, and (5) use a stress relief (open-grade asphalt) base course. Although not widely used, several other experimental methods have been extensively studied. These other methods fall into two general categories. One category gives three methods that may be considered in the design of the asphaltic concrete overlay. These three methods provide the use of: (1) reinforcement, (2) admixtures, or (3) asphalt stiffness. The second category gives three methods of treatment of the joints and cracks. The three joint treatment methods consist of: (1) filling existing joints with incompressibles, (2) breaking bond between asphalt and pavement, or (3) replicating the existing joints by sawing the overlay layer.

1. INCREASED THICKNESS OF ASPHALTIC CONCRETE OVERLAY - Several studies investigated the effects of overlay thicknesses in conjunction with other methods such as wire mesh reinforcement (Zube, 1956) and pavement breaker-rolling (Korfhage, 1970). Regardless of the overlay thickness

used, all studies show some degree of reflection cracking. Figure 2.5, from Korfhage's report, indicates that an increase in thickness tends to reduce the amount of reflected cracking. Note that for the 5, 6, and 9

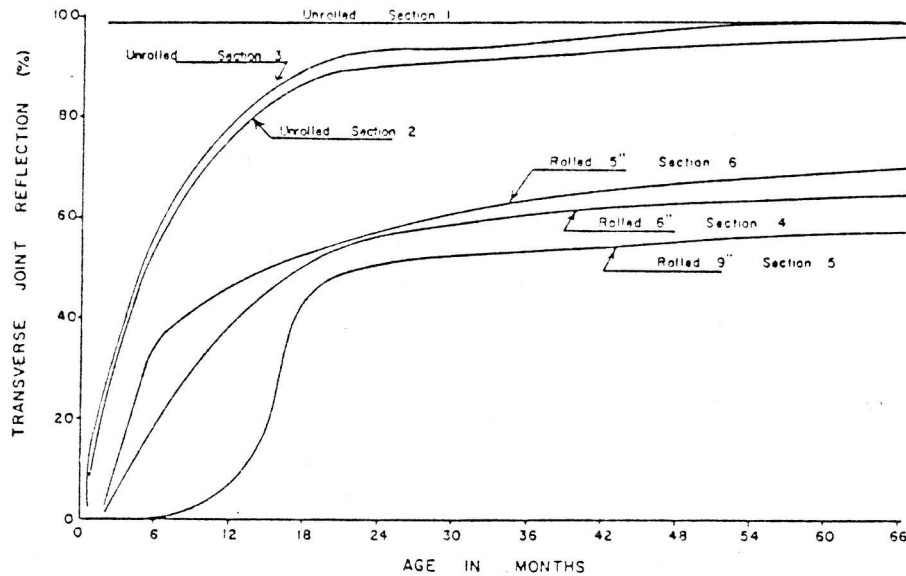


Figure 2.5 Increase in Transverse Joint Reflection.
(From Korfhage, 1970)

inch overlays a roller was used to break the existing pavement. A majority of the joint reflections occurred during the first year. After five years, all of the sections had developed sixty or more percent joint reflections with only about a ten percent reduction between the 5 inch and the 9 inch overlays.

2. INTERMEDIATE GRANULAR BASE - A base of crushed gravel overlaying a portland-cement concrete pavement has been effective in reducing reflective cracking. It is assumed that the cushion absorbs most of the slab movement without transmitting detrimental effects to the overlay. Erickson and Marsh, 1956, reported that after five years one pavement with a

layer of crushed gravel base three inches thick laid over the old pavement reflected joints but not serious enough to impair riding quality. A pavement with a six inches thick crushed gravel base was in excellent condition and did not reflect cracks.

Billingsley, 1966, experimented with a cushion course over regular jointed slabs that had been broken into approximately one foot segments. Comparison, over a seven year period, of the cushion course section to one where the asphaltic concrete pavement was placed directly on top of the pavement, indicated the cushion course section to be superior.

Copple and Ochler, 1968, reported varying results from their investigation. Although cushions did reduce reflection cracking, thicknesses of eight inches did not completely eliminate them. This method does not appear to be economically feasible because of the large quantity of aggregate required both in terms of cost and availability, because of the additional problems created during overlay operations, and because of the lack of structural stability of the aggregate layer.

3. RESEAT SLABS BY ROLLING - The purpose of seating the existing concrete pavement slabs is to eliminate excessive vertical movements or rocking of the slabs. This is accomplished by applying sufficient weight and roller applications to the pavement that will place the slab in contact with the base at all points. The continuity of the slab is thus maintained and the load carrying capacity is increased. Figure 2.5 shows that rolling of the pavement slabs prior to a 5 inch overlay reduced reflection cracks by over 30 percent when compared to the unrolled 4½ inch overlays. However, over 50 percent of the joints had reflected in the 5 inch overlay within two years. This method reduces reflection cracking caused by excessive vertical movement of the slab, but has little effect

on the magnitude of movement due to thermal changes (Highway Research Board, 1972).

4. BREAKING SLABS INTO SMALL SEGMENTS - Techniques which break up the existing cracked or jointed pavement slabs into small pieces or small blocks are used to minimize or delay the occurrence of reflection cracking. Smith and Bartner (1962) found that breaking of the existing rigid pavement into approximately 3-ft. pieces prevented the reflection of original cracks and joints. Only a few cracks were noted where the pavement was broken. In all cases these cracks were reported to be fine in magnitude and short in length. Lyon (1970) reports on a ten year study where significant reduction of reflection cracking was observed on one project where the original rigid pavement had been broken down by rolling. However, on subsequent projects, the use of heavy rollers failed to crush the base pavement. In other studies results were inconclusive because, although there were significant reductions of reflection cracks, other type cracks, such as longitudinal and alligator cracking had developed (Korfhage, 1970). The disadvantages of this technique are the large loss in load-carrying capacity caused by breaking up the slabs, and the added construction costs involved.

5. STRESS RELIEF BASE COURSE - An open-grade asphaltic concrete mix having interconnecting voids in the range of 25 to 35 percent, was proposed by Hensley (1975). The open-grade course is used in two and three layer systems. It is laid on top of the existing concrete pavement and then overlaid with a conventional binder course and/or a surface course. Hensley recommends the three layer system because the surface course of the two layer system infiltrates into the voids of the open-grade course and defeats the purpose of the mix. With the three layer system an

intermediate binder course overlays the open-grade course with aggregates sufficiently sized to prevent infiltration. The purpose of the open-grade course is to dissipate the crack action before it reaches the surface course.

Arkansas has experimented with both a two layer system and a three layer system. Approximately two years after the construction of a two layer system, using a 2-inch top-size aggregate open-grade course overlaid with a surface course, approximately 25 percent of the joints and cracks had reflected to the surface. To date, approximately seven years after construction with the three layer system using a 3-inch top-size aggregate open-grade course overlaid with a binder and a surface course, the system has been 100 percent effective in eliminating reflection cracking. However, rutting has occurred on some sections and it may be a major concern for this type of construction.

6. REINFORCEMENT - Bone et al. (1954), Zube (1956), Tons et al. (1961), Smith and Cartner (1962), Chastain and Mitchell (1964), and Bushing et al. (1970) have experimented with the use of welded wire mesh reinforcing in the asphaltic concrete overlay in attempts to distribute the stresses induced by opening of a joint or crack to values insufficient to cause the overlay to crack. Experiments, varying from short strips placed directly over the joints or cracks to continuous reinforcement, have had from good to poor degrees of success in the prevention of reflection cracking. Fabric reinforcement such as polyester fabric, non-woven polypropylene fabric, asbestos fabric, and other synthetic fiber materials are being studied for use in the prevention or retardation of reflection cracking. Because of the variability in results, wire mesh and fabric reinforcing is considered to be experimental construction.

7. ADMIXTURES - Additives have been introduced into asphaltic concrete mixes in attempts to increase the ductility or stretchability of the asphaltic concrete so that it can absorb the joint and crack movements of the concrete pavement slabs. Roggween and Tons (1956) experimented with emulsified rubber asphalt, synthetic rubber and natural rubber crumbs, but no difference in performance was observed between sections with or without additives. Bone and Crump (1956) reported that various types of rubber added to asphaltic concrete mixes can significantly increase the ductility of the mix, but there is no indication that the increase is sufficient to prevent reflection cracking. Gould (1961) and a study of the Road Research Laboratory in England indicated that rubber in the asphalt did not reduce cracking. Several agencies have experimented with the use of asbestos additives in asphaltic concrete overlays, but results have been inconclusive.

8. ASPHALT STIFFNESS - Roberts (1954) compared reflection cracking in two different penetration grades of asphalt. The softer asphalt (115-penetration) reduced reflection cracking to approximately one-half of that in the stiffer asphalt (80-penetration). This study indicated that the asphalt stiffness may play a significant role in the amount of reflection cracking. Although rubber additives and softer asphalts have been used in overlays, precautions should be taken in the mix design to develop mixes that are not as susceptible to temperature changes (Hass 1970 and Burgen et al. 1971).

9. FILLING EXISTING JOINTS WITH INCOMPRESSIBLES - One project attempted to reduce movement at the joints of an overlaid concrete pavement by filling the joints with incompressible material. This resulted in disastrous blowups occurring at every fifth joint (Synthesis of Highway

Practice 9, HRB, 1972). Because of the results of this study, no further investigation of this method has been done.

10. BREAKING BOND BETWEEN ASPHALT AND PAVEMENT - An experimental test section by the Road Research Laboratory implemented the use of smooth plates and expanded metal strip between the concrete pavement and the asphaltic concrete overlay, in an attempt to have a longer gage length for the asphalt to absorb joint movements. Reflection cracking was reduced slightly, but those sections that did crack had severe disintegration. Vicelja (1963) used aluminum foil, building paper, sheet metal, stone dust, and wax paper as bond breakers. The sheet metal and building paper were eliminated early because of construction problems. Vicelja reported approximately 50 percent reduction in reflection cracking in the test sections utilizing wax paper and aluminum foil. During the four years covered by the report, no cracks had occurred in the section where stone dust was used, whereas cracks developed throughout the entire untreated control section. Luther (1973) reports that in addition to construction problems in placing the bond breaking material, detrimental effects may result from their use by setting up an additional free surface into which air and water may more readily attack the resurfacing material.

11. REPLICATE JOINTS BY SAWING THE ASPHALTIC CONCRETE LAYER - Wilson (1962) experimented with controlling reflection cracking by sawing three-eighths inch wide, and from one-half to one and three-quarters inch deep joints in the asphaltic concrete overlay above the existing concrete pavement joints. This substantially extended the maintenance-free life of the overlay, but it did not reduce reflection cracking.

Practically all studies reviewed that attempted methods to control

reflection cracking, reported the occurrence of reflection cracking in varying degrees. The most promising method appears to be a three layer asphaltic concrete structure which uses a stress relief base course overlaid with a binder and surface course. The economic value of this method, in relation to anticipated maintenance cost savings compared to the system cost, are still to be determined.

C. METHODS OF PREDICTION

Predicting the rate at which joints or cracks in an underlying layer of a pavement will reflect through an asphaltic concrete overlay has been the objective of several research projects. The basic approach to the problem of predicting the initiation and growth of reflection cracks, under the combined influence of repeated vehicular loading and changes in temperature, has been an application of the principles of fracture mechanics.

Substantial work has been done on Mode I fracture in bituminous materials where damage growth is represented in accordance with Paris' law

$$\frac{dc}{dN} = AK^4 \quad (2.32)$$

where c is the crack length, N is the number of cycles, $\frac{dc}{dN}$ is the rate of crack propagation, A is a material property and K is the stress-intensity factor (Ramsamooj, 1970; Luther, 1973; Ramsamooj, 1975; Majidzadeh and Ramsamooj, 1973; Luther et al., 1976; Majidzadeh et al., 1977).

Analytical methods have been developed to determine the stress-intensity factor K for a given crack size and specimen geometry and for various boundary conditions. Figure 2.6 shows the results of Gross and Srawley's analysis of K values for a simply supported beam acted on by a load at the center. The K -value for a beam supported on an elastic foundation with a central load was determined by Ramsamooj (1970) by the

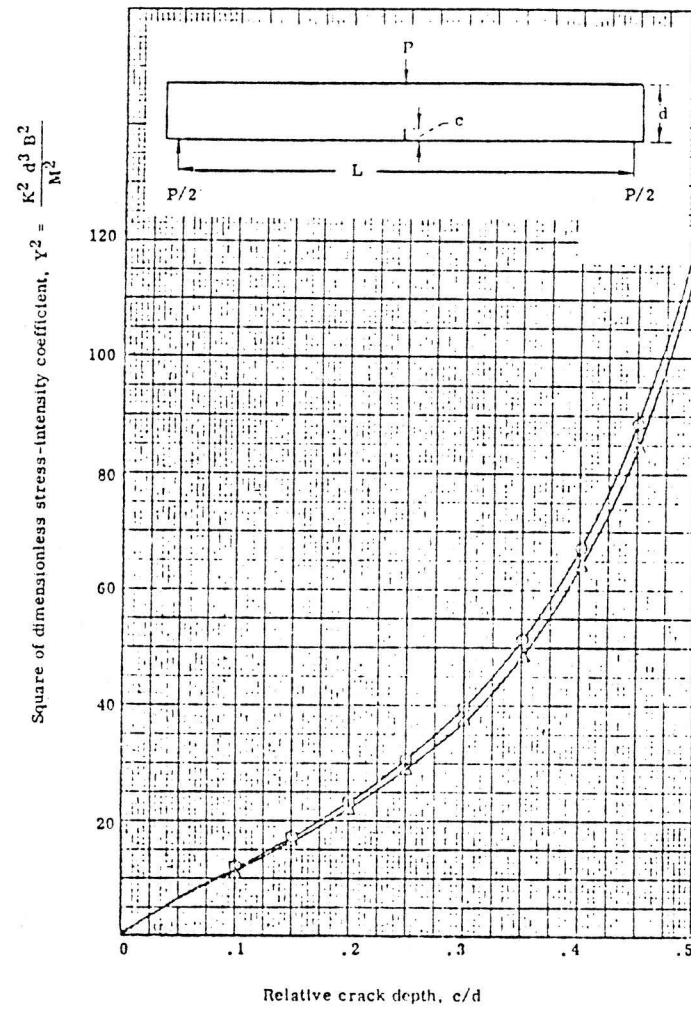


Figure 2.6 Dependence of Square of Stress-Intensity Coefficient on Relative Crack Depth. (From Majidzadeh and Ramsamoj, 1973)

boundary collocation method and by a finite element program. Ramsamooj's results for the stress-intensity factors versus crack lengths for two types of foundations are reproduced in Figure 2.7. For beams on elastic foundations, Majidzadeh and Ramsamooj (1973) report that K for any type loading, crack pattern, and geometry can be determined experimentally by measuring the change in deflection as the crack grows and by applying the formula

$$K^2 = \frac{P^2 E}{2(1-\nu^2)} \frac{\delta L}{\delta c} \quad (2.33)$$

where P is the load, E is Young's modulus, ν is Poisson's ratio, L is the compliance (the inverse slope of the load-deflection diagram), c is the crack length, and $\delta L/\delta c$ is the rate of change of the compliance of the system with crack depth. Figure 2.8, reproduced from Ramsamooj (1970), shows K versus c curves for the experimentally deduced K values compared with the boundary collocation and finite element solutions.

In the research work carried out at the Ohio State University, the applicability of the theory to asphaltic materials has been examined in the light of two important assumptions made in the theoretical concepts (Majidzadeh and Ramsamooj, 1973):

1. The material must be homogeneous, isotropic, and essentially elastic-plastic, and
2. The size of the plastic zone at the tip of the crack must be small in comparison to the crack and specimen dimension.

The first assumption is one that is generally accepted for asphaltic materials. With regard to the second assumption, the size of the plastic

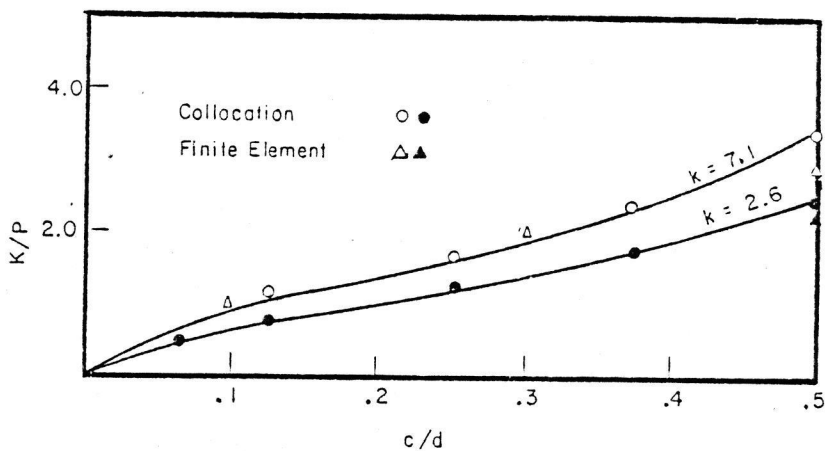


Figure 2.7 K/P versus c/d (Beam on Elastic Foundation)
 (From Ramsamooj, 1970)

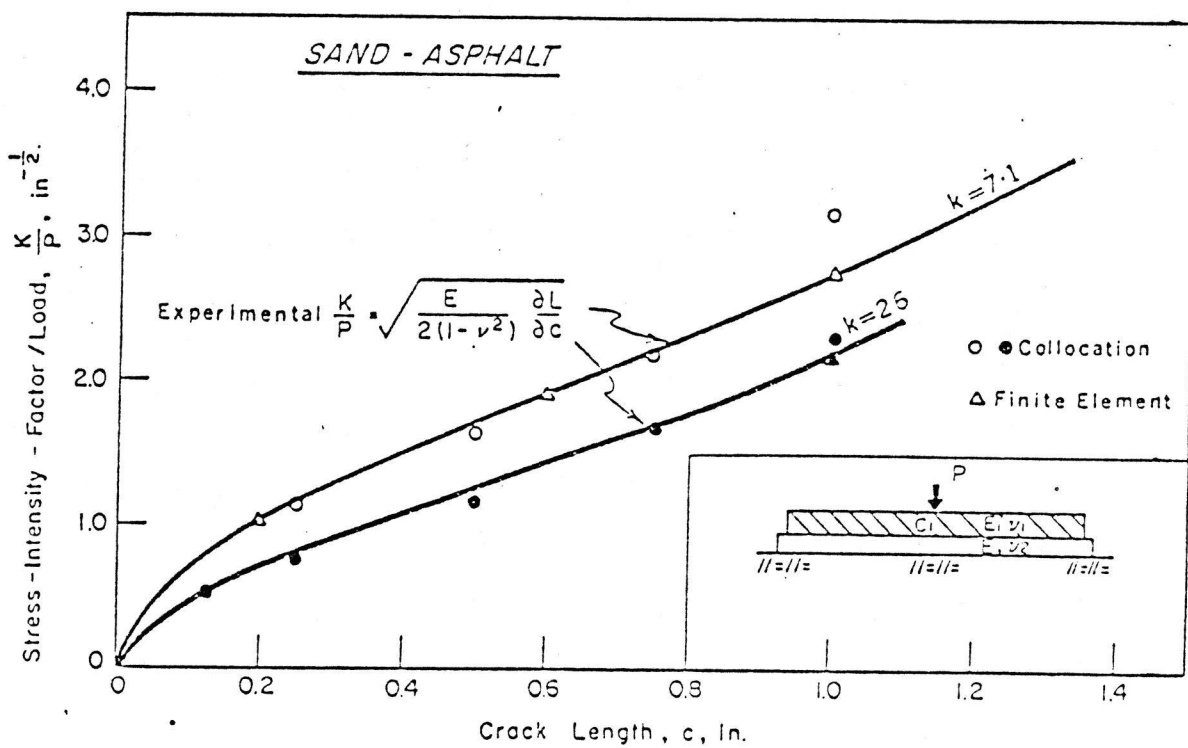


Figure 2.8 $K/P - c$ Relation for Beams on Elastic Foundation Tests.
 (From Ramsamooj, 1970)

zone r_y can be calculated from the formula

$$r_y = \frac{1}{2\pi} \left(\frac{K_I}{\sigma_y} \right)^2 \quad (2.34)$$

where σ_y is the yield stress in tension.

Using this estimate of the size of the plastic zone, Srawley and Roberts (1969) established criteria for the crack length, width, and depth of beam to ensure plane strain conditions and the applicability of linear elastic fracture mechanics. The criteria state that both the crack depth and width of the beam should exceed

$$2.5 \left(\frac{K_I}{\sigma_y} \right)^2 \quad (2.35)$$

For a pavement the theory is applicable if the thickness of the asphaltic layer is greater than $1.25 (K_I/\sigma_y)^2$.

Results of experiments conducted at Ohio State University from tests on simply supported beams of sand asphalt tested at 23⁰F showed that the rate of crack propagation correlated well with the stress-intensity factor in accordance with Paris' law, equation (2.32). The beams failed when the crack reached the critical crack length c_f corresponding to the critical stress-intensity factor K_{IC} . The fatigue life N_f of the beam was expressed as

$$N_f = \int_{c_0}^{c_f} \frac{1}{AK^m} dc \quad (2.36)$$

where c_0 is the starter flaw. The fatigue life may be considered as the

number of cycles of repeated loading to propagate a starter flaw, c_0 , into a crack of critical size, c_f . The starter flaw is a material constant, but is subjected to statistical variation and is believed to be principally responsible for the statistical variation of fatigue life.

The cracking of flexible pavements under moving load was investigated by Majidzadeh and Ramsamooj (1973). They presented a growth law in the form of

$$\frac{dc}{dN} = A_1 K_I^{n_1} \text{ and } A_2 K_{II}^{n_2} \quad (2.37)$$

where K_I and K_{II} are stress-intensity factors for Mode I and Mode II cracking. The obvious assumption here is that the damage resulting from the action of each fracture mode is additive and independent.

Ramsamooj (1973) formulated a method of solution to the problem of the initiation and growth of reflection cracks under the combined influence of repeated vehicular loading and changes in temperature. Both the theory of linear elastic fracture mechanics and that of delayed fracture in viscoelastic materials are used. Ramsamooj assumes that the crack will propagate in two modes: the opening mode and the in-plane sliding mode, with the opening mode being of greater importance. Once the range and distribution of starter flaws in the overlay along the potential line of cracking and the properties of the component layers of the pavement have been determined experimentally, Ramsamooj theorizes that the rate of crack propagation can be obtained from the crack growth law:

$$\frac{dc}{dN} = A_1 (\Delta K_I)^4 + A_2 (\Delta K_{II})^4 \quad (2.38)$$

where ΔK is the increment in K due to the passage of a wheel load, K_I and K_{II} are the stress-intensity factors for Modes I and II cracking under the stresses produced by traffic loading. Equation (2.38) is applicable when the mean load is constant. For a variable mean load the rate of crack propagation is given by

$$\frac{dc}{dN} = A' (1+\beta)^2 (\Delta K)^4 \quad (2.39)$$

where $K < K_{cr}$, $\beta = (K_{max} + K_{min})/2\Delta K$ and A' is the crack propagation constant. Equation (2.39) is applicable if the vehicle speed is greater than 15 mph so that the response of the pavement due to the passage of wheel loads may be considered elastic.

The response of the pavement due to stresses produced by slowly varying temperatures is essentially viscoelastic in nature. A crack in a viscoelastic material initiates after a time

$$t_i = \psi^{-1}(m) \quad (2.40)$$

where m is equal to $(K_{IC}/K_I)^2$, $J(t)$ is the the compliance at time t , ψ is the compliance function equal to $J(t)/J(0)$ and ψ^{-1} is the inverse compliance function. The crack then grows at a finite rate until eventually at time, t_{cr} , when the stress-intensity factor reaches its critical value, K_{IC} , catastrophic failure occurs. The rate at which the subcritical crack grows, for $t_i < t < t_{cr}$, is given by

$$\frac{dc}{dt} = \frac{\Delta}{\psi^{-1}(K_{IC}/K_I)^2} \quad (2.41)$$

$$\text{where } \Delta = \frac{\pi(K_I/\sigma_y)^2}{8(1-\nu^2)}$$

If the wheel loads pass over the crack at regular intervals at the rate of n per day, where $N = nt$, then the total rate of crack growth, $(dc/dt)_t$, due to both vehicular loading and temperature stresses will be given by (for $t_i < t < t_{cr}$)

$$\begin{aligned} \left(\frac{dc}{dt}\right)_t &= nA_1'(1+\beta)^2(\Delta K_I)^4 + nA_2'(1+\beta)^2(\Delta K_{II})^4 \\ &+ \frac{\Delta}{\psi^{-1} (K_{IC}/K_I)^2} \end{aligned} \quad (2.42)$$

and for $t < t_i$

$$\left(\frac{dc}{dt}\right)_t = nA_1'(1+\beta)^2(\Delta K_I)^4 + nA_2'(1+\beta)^2(\Delta K_{II})^4 \quad (2.43)$$

Ramsamooj states that equations (2.42) and (2.43) are sufficient to completely describe the rate of growth of reflection crack at any time during the loading history. However, in providing an example applying these principles, it was assumed that the resistance to cracking in the in-plane sliding mode was much greater than that in the opening mode and, therefore, the in-plane sliding mode was neglected. Ramsamooj recognized that this assumption may not be true and recommended that the method be completely verified experimentally.

Luther et al. (1976) conducted fatigue tests to verify the hypothesis that reflection cracking is of mixed-mode fracture (specifically not Mode I) and to observe the general propagation and mechanics of crack growth. The general concept of Sih's strain-energy-density factor is presented as a method of analysis for mixed-mode fracture experienced in asphalt overlays. The finite element method was used to evaluate the minimum strain-energy-density factor, S_{\min} , and θ_0 for various initial flaw crack lengths of a two dimensional overlay model shown in Figure 2.9. The θ_0 angles were all calculated to be about 12 degrees and agreed well with the observed fracture angle obtained during fatigue tests on the models. From the crack length versus cycle data obtained during these fatigue tests dc/dN was obtained, and its relation with S_{\min} is shown in Figure 2.10. The growth is described by

$$\frac{dc}{dN} = A' S_{\min}^n \quad (2.44)$$

where $A' = 6.8 \times 10^{-6}$ in./cycle and $n = 2.309$. Equation (2.44) was derived for the same sand-asphalt material as that used in modeling flexible pavements where crack growth was found to be proportional to K_I^4 . Since K is proportional to $S^{1/2}$, Luther, et al. conclude that any growth law involving S_{\min} for sand asphalt would expect to have an n power of about 2.0. They further conclude that, pending further investigation of the constants n and A' , the fatigue life of an asphalt overlay (for load-endured reflection cracking) may be expressed by

$$N = \int_{c_0}^{c_f} \frac{1}{A' S_{\min}^n} dc \quad (2.45)$$

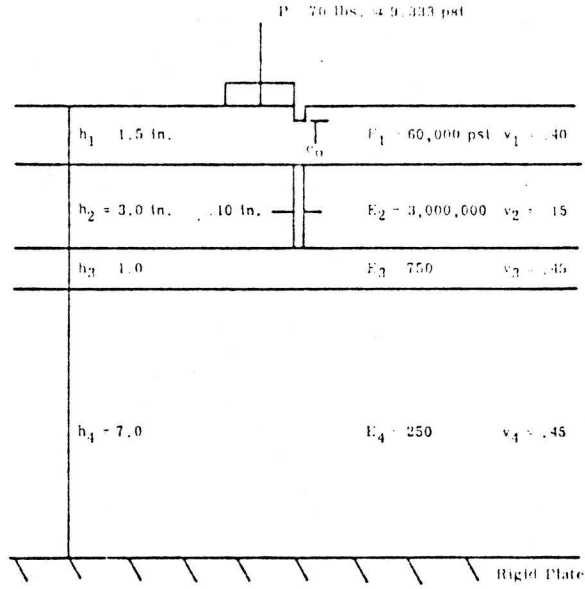


Figure 2.9 Two Dimensional Overlay Model
(From Luther, et al., 1976)

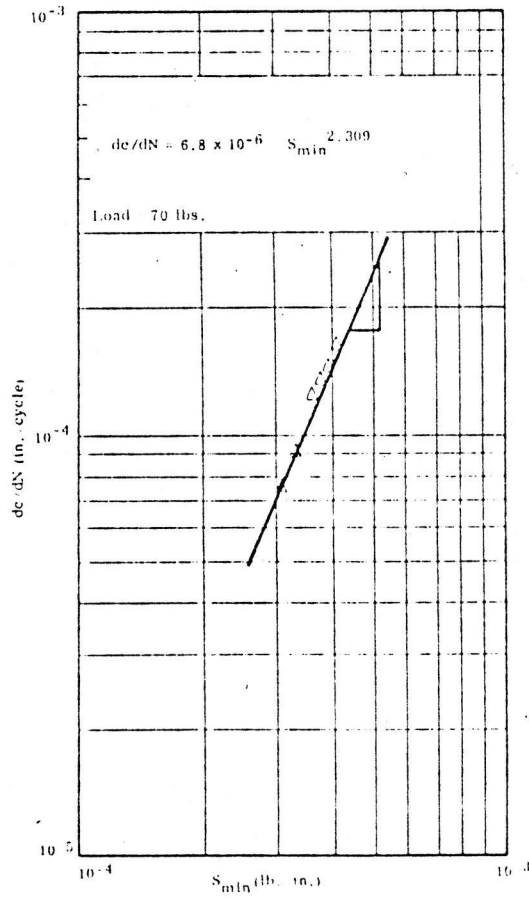


Figure 2.10 Crack Growth Rate versus S_{min} .
(From Luther, et al., 1976)

where c_0 = initial flaw and c_f is the crack length at which S_{cr} is reached or the overlay thickness, whichever is less.

D. SUMMARY

Attempts at reducing or eliminating reflection cracking by implementing trial and error methods have resulted in moderate to poor degrees of success. Trial and error design methods based on experience and empirical testing cannot incorporate the many variables involved in the design of pavements, nor can they incorporate new advances in technology and products. However, the modern day computers can be programmed for these variables and changes to aid in the solution of these problems. With the aid of the computer, several analytical methods have been developed which predict crack initiation and rate of crack growth to aid in the design of asphaltic concrete overlays that will eliminate or retard the development of reflection cracking and thereby increase the maintenance-free life of the overlay.

One computer model reviewed makes simplifying assumptions which have been neither experimentally nor field verified and which may or may not be applicable. They recommend the need for verification. Another model analyzed the effects of Modes I and II type failures and their findings reportedly verified by instrumentation of laboratory models. This, however, dealt with a single layer overlay system. Most computer models provide analysis of multilayered systems, but the asphaltic concrete overlay is generally treated as a single layer with the other layers being the subgrade and/or the concrete pavement. When a multilayered asphaltic concrete overlay is considered, especially when an open-graded base course is used, the properties of the open-graded course and that of the binder course are considerably different, and.

therefore, must be treated as a separate layer. There are also significantly different properties between the binder and surface courses. This literature review did not produce any studies on the determination of the physical properties of an open-graded asphaltic concrete mix. Although surface deflections have been commonly measured using the Benkelman beam or the method of dynaflect deflection, the literature reviewed did not produce any studies where actual movements were measured within a multilayered overlay structure in the vicinity of an overlaid joint to verify a computer analysis.

One of the objectives of this research project is to obtain field measurements of vertical and horizontal movements within a multilayered overlay structure in the vicinity of an overlaid joint. The instrumentation which will be used to monitor these movements is presented in the following chapter.

CHAPTER III

INSTRUMENTATION

A. GENERAL

The instrumentation system is designed to measure horizontal movements at each interface and vertical movements in each layer of a multi-layered asphaltic concrete hot mixed overlay structure in the vicinity of a joint in an overlaid Portland cement concrete pavement. It is also designed to measure the temperature at each interface of the overlay. This system will provide both static and dynamic measurements of vertical and horizontal movements in the vicinity of an overlaid joint. Static measurements will provide data to determine daily movements and cumulative long-term movements primarily associated with daily and seasonal temperature changes. The dynamic measurements will provide data to determine instantaneous movements in the vicinity of an overlaid joint as a wheel load travels across the joint.

Embedded induction coil sensors will provide the signals for both static and dynamic measurements of displacement. Thermistors will provide temperature measurements. Stresses at layer interfaces will be measured by strain gage diaphragm-type pressure cells.

Data acquisition or readout of static displacements will be accomplished using a single channel battery-operated meter. Dynamic displacements will be recorded using a 20-channel data acquisition system controlled by a microprocessor. Stress cell data will be taken with the dynamic data acquisition system. Temperature data from the thermistors will be taken with a battery-operated analog meter. Details of the sensors used and the data acquisition devices are given in this chapter.

B. SENSORS

1. INDUCTION COIL SENSORS - The two basic components used to make the static displacement measurements are a pair of wire wound induction coil discs and an external instrument package (Figure 3.1). Pairs of sensors are placed in coaxial and coplanar alignment. A pair of sensors does not require any physical connection between the two coils, except for the coaxial cables independently running back to the signal conditioner. When a pair of sensors is energized, one becomes the transmitting coil and the other the receiving coil. The separation of the pair is sensed by using the electromagnetic coupling between the two because they operate on the basic principle that two electrical coils in proximity will couple energy from one to the other (Figure 3.2). The electrical output of the

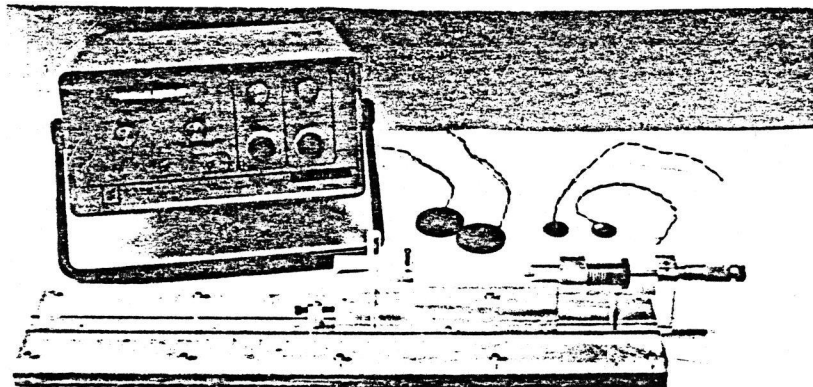
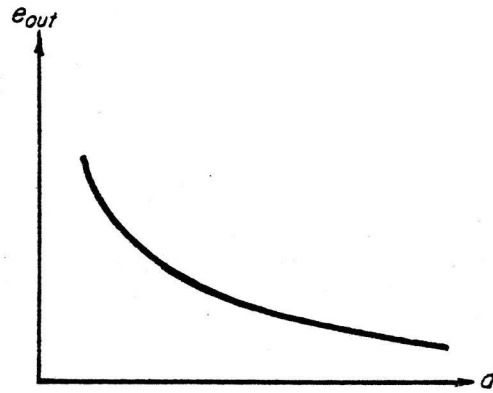
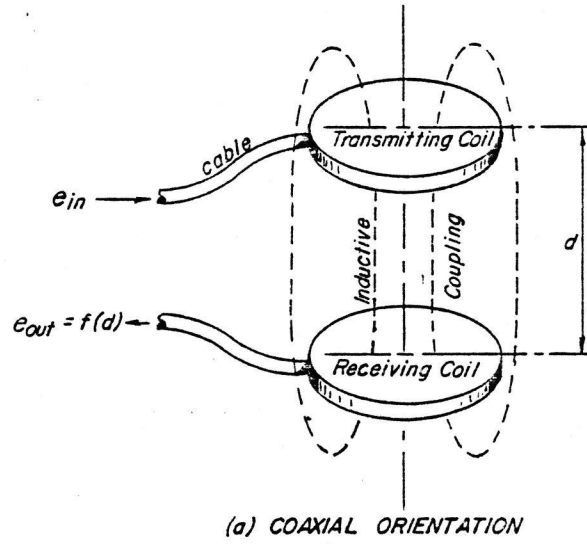


Figure 3.1 Bison Strain Gage Console with a Pair of 2 in. and a Pair of 1 in. Diameter Induction Coil Sensors. Calibration Apparatus is in the Foreground.

receiving coil will be an inverse and nonlinear function of the spacing between the coils (Figure 3.2b). An induction bridge allows the output



(b) RECEIVED SIGNAL VS SPACING

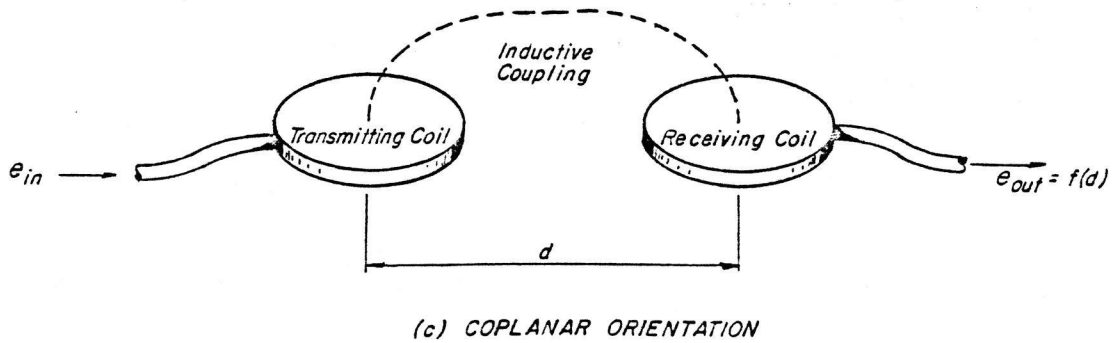


Figure 3.2 Basic Inductive Coil Displacement Transducer.

voltage to be measured as a function of strain, since a change in spacing from the initial spacing produces a bridge unbalance. The sensor pairs can generally operate at any spacing between one and four times the nominal coil diameter. They are capable of measuring dynamic strains of 0.005 percent and long term static strains of 0.05 percent with an accuracy of 1 percent.

The two axis, two-inch diameter coil configuration shown in Figure 3.3 was selected for six locations along the contraction joint in the outside lane of the overlaid concrete pavement, to measure vertical movements in each course of the overlay and horizontal movements across the joint at each interface of the overlay. The three axis configuration shown in Figure 3.3 was selected for the center line joint between the outside and inside lanes.

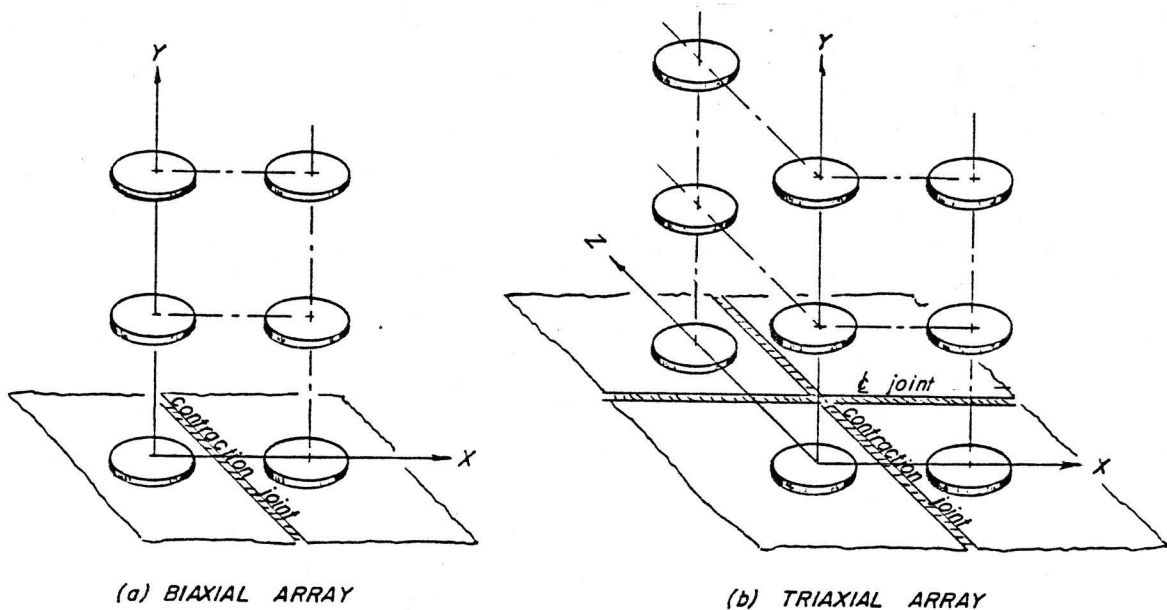


Figure 3.3 Coil Configuration in Three Layered Overlay.

The vertical extensometer (Figure 3.4) is designed to measure the vertical movement of the overlaid concrete slab at the joint. The

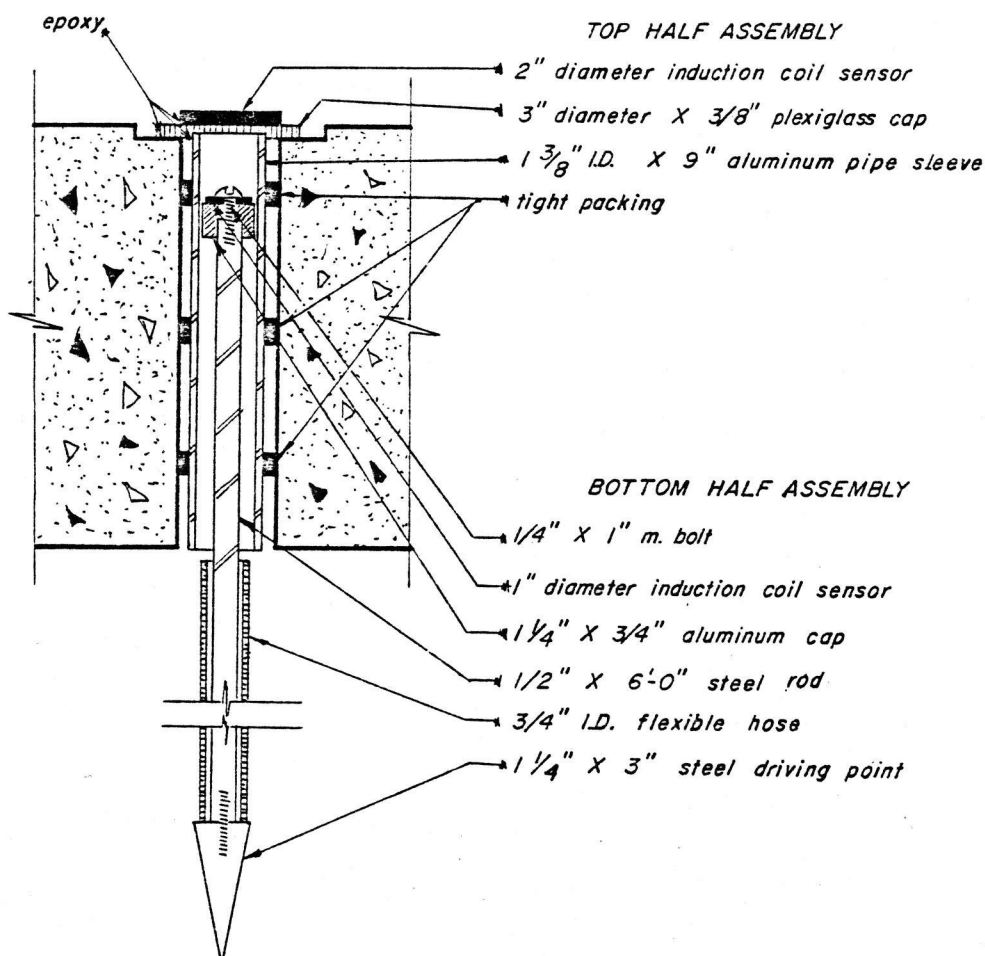


Figure 3.4 Detail of Vertical Extensometer.

sensor pair used with the extensometer consists of a one-inch and a two-inch diameter sensor.

The extensometer is assembled in the field. A two-inch diameter hole is cored through the existing concrete pavement. A one-half inch diameter steel rod six feet in length is driven through the center of the hole and into the undisturbed subgrade until the top of the rod is approximately two and one-half inches below the top of the concrete pavement. The rod is encased in a three-quarter-inch diameter flexible hose

to prevent the development of frictional stresses between the rod and the subgrade soil. A one-inch diameter sensor set on an aluminum cap is secured to the top of the rod. This completes the bottom half assembly of the extensometer. The top half assembly consists of a two-inch diameter sensor set on a plexiglass cap and secured to the top of an aluminum pipe sleeve. The pipe sleeve is placed in the cored hole and encases the one-inch diameter sensor. This maintains a coaxial alignment between the one-inch and two-inch sensors. Using epoxy and contact cement the top half assembly is secured to the concrete pavement. For further discussion and illustrations on the extensometer, refer to the section on Field Installation.

2. TEMPERATURE SENSORS - The temperature measuring system (Figure 3.5), consists of thermistors embedded at each interface of the overlay at the approximate center line of the outside traffic lane. The sensors, which have the capability of measuring temperature between -20°F and 212°F , are connected to a remote temperature indicator which has a resolution of 2°F accuracy of \pm one percent of full range.

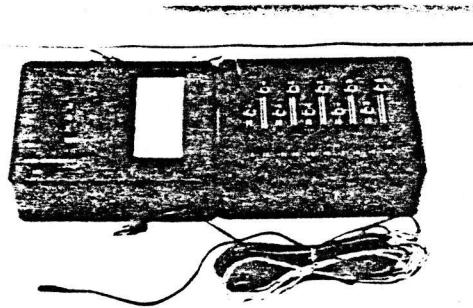


Figure 3.5 Remote Temperature Indicator with System Expansion Box and Thermistor.

3. STRESS CELLS - Stress cells designed as a flat circular diaphragm with fixed edges were constructed for installation at the layer interfaces within the overlays. Strains induced by externally applied stress were sensed by semiconductor strain gages bonded to the diaphragm. A full bridge circuit was used with connections made to give the maximum output. Two sizes were used, one for placement on top of the existing concrete pavement, and the other smaller size for embedment in the asphaltic concrete. The cell placed on top of the concrete pavement was 11 inches in diameter and 1 inch thick with one active diaphragm 7 inches in diameter and 0.250 inches thick. The free field cells embedded in the overlay material were 4.50 inches in diameter and 0.500 inches thick with two active diaphragms (opposing faces of the cell) 3 inches in diameter and 0.125 inches thick.

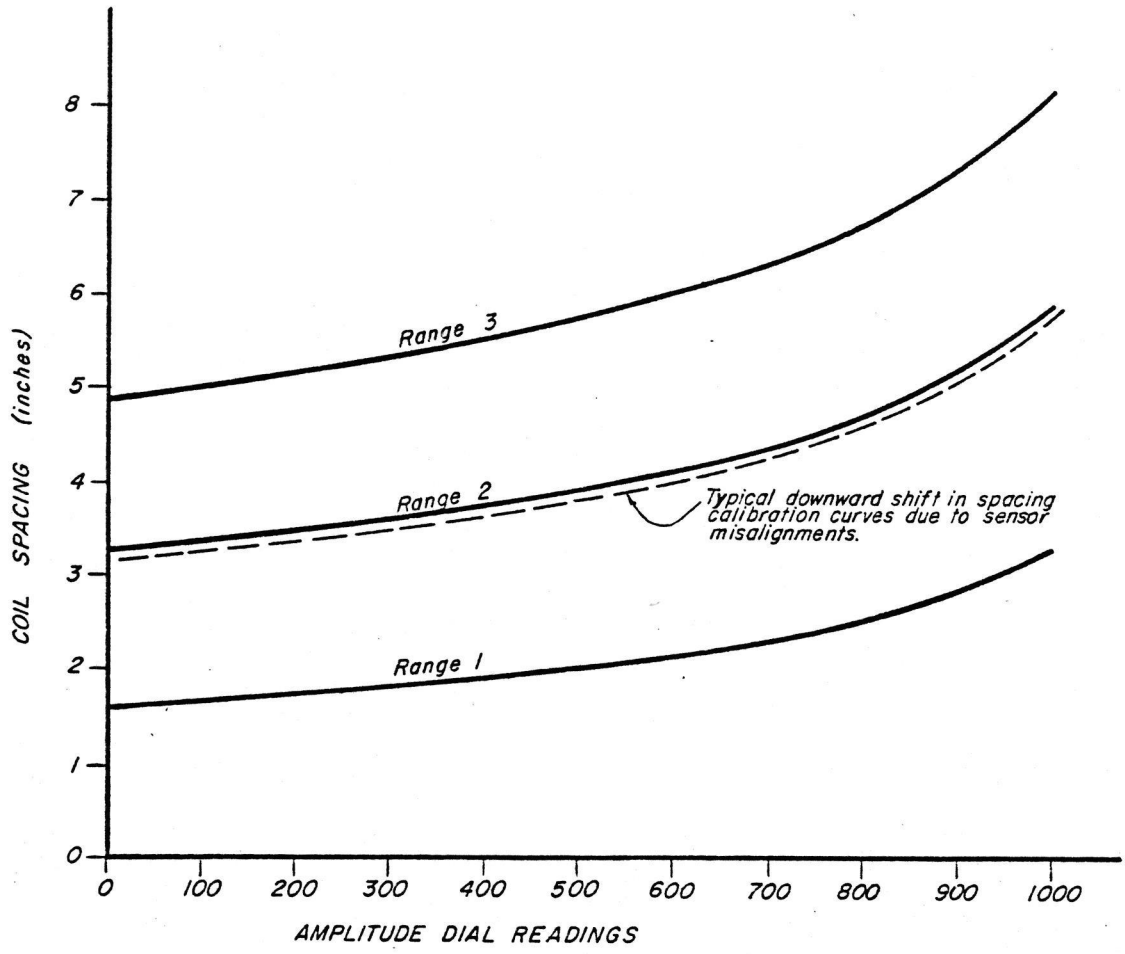
C. SENSOR CALIBRATIONS

1. INDUCTION COIL SENSORS - The calibration apparatus shown in Figure 3.1 is used to obtain spacing calibration curves for pairs of induction coil sensors. With the proper accessories, a pair of sensors is attached to the apparatus in either a coaxial or coplanar orientation. The extension and retraction of the micrometer, which is mounted on the apparatus, produces accurate changes in the spacing between the two sensors. The sensors are connected to the strain instrument which has three coarse balance settings to permit operation over the entire range from one to four nominal coil diameters. For each coarse setting the spacings of the sensors are correlated with the amplitude dial readings. This is accomplished by setting the amplitude dial reading and then adjusting the spacing and phase balance so that both are nulled. This is repeated for every fifty or one hundred unit increments over the full one thousand

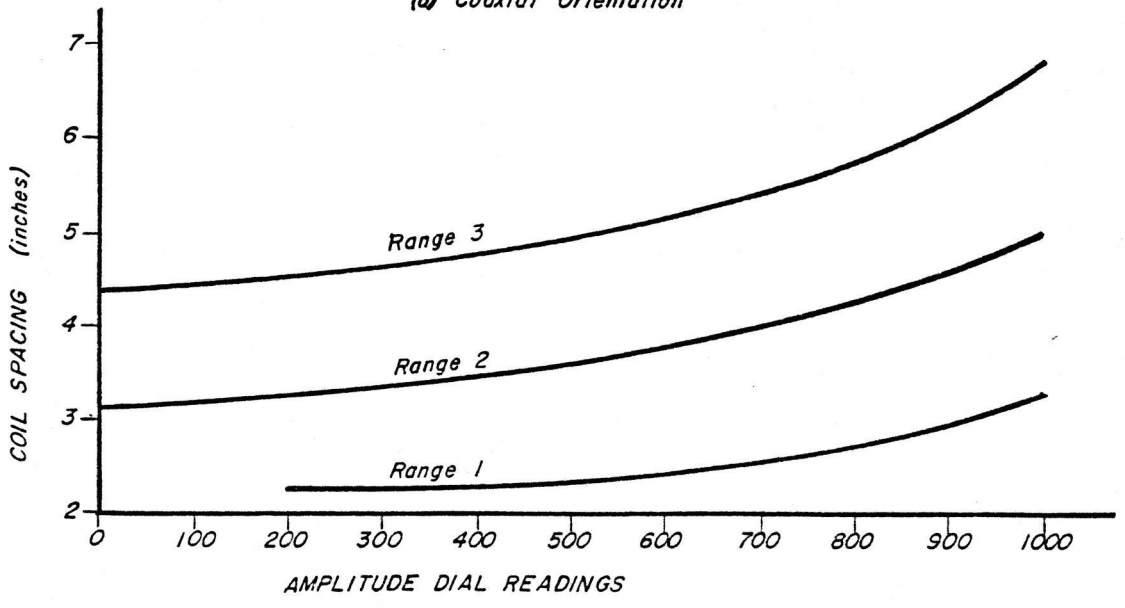
units range of the amplitude dial, and for each of the three coarse settings on the strain instrument. A typical set of spacing calibration curves for a pair of sensors, first in coaxial orientation and then in coplanar orientation, is shown in Figure 3.6

To investigate the effect of misalignment through lateral translation and rotation that may occur with the free floating sensors, numerous calibrations were conducted with various misalignments of the sensors, Figures 3.7 and 3.8. Essentially misalignment causes a downward shift in the spacing calibration curves as shown in Figure 3.6. Since the slopes of the curves remain about the same, the measured spacing change will still be correct. The sensors, however, will appear to be farther apart than they actually are. This will introduce a small error in strain because too large a gage length will be specified. Analysis of the calibration data for lateral displacements of up to 1/4 of an inch and for rotations of up to ten degrees about a longitudinal or a transverse axis, indicate an error of less than one percent of the computed strain when the sensors are in alignment. Misalignment, therefore, is not a critical factor, because a lateral shift or a small rotation produces a signal which is an order of magnitude smaller than an equal axial or an equal planar movement. The gage is practically insensitive to lateral movements or small rotations in the vicinity of a coaxial and coplanar alignment. A study by Selig and Grangaard (1970) presents similar conclusions, and adds that a rotation of ± 10 degrees is not significant and that a rotation of ± 20 degrees causes an error usually less than 10 percent.

Due to the method and precision with which the sensors were installed and the nature of the material into which they were embedded, it is

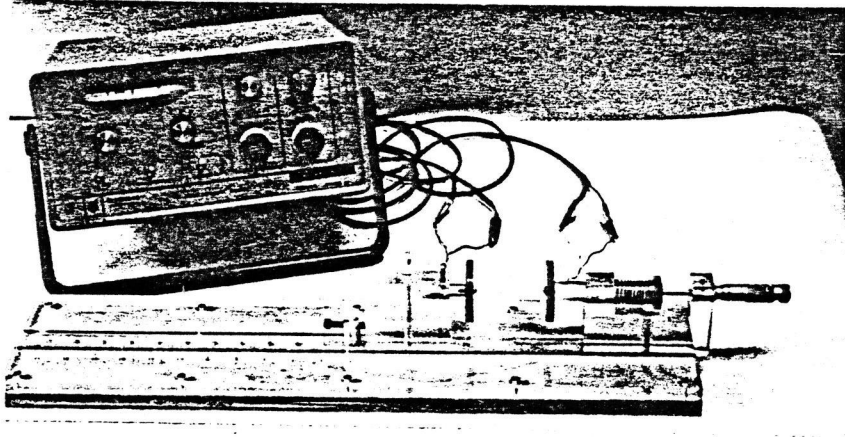


(a) Coaxial Orientation

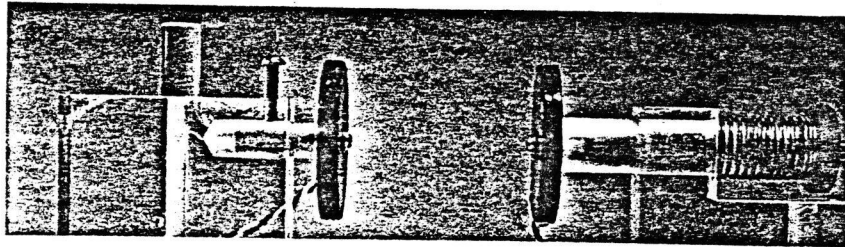


(b) Coplanar Orientation

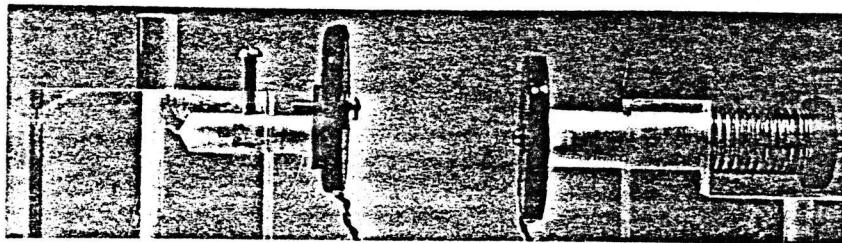
Figure 3.6 Typical Calibration Curves for 2 in. Diameter Sensors.



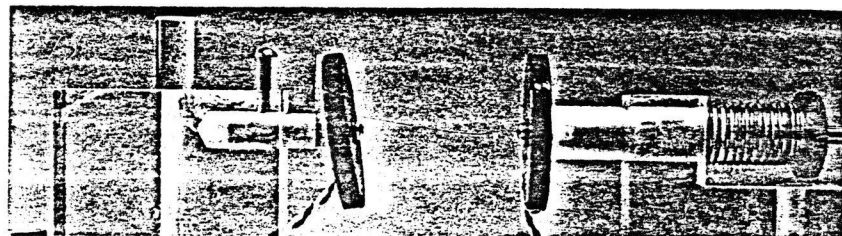
(a) *Set-up for Coaxial Calibration of Sensors.*



(b) *Coaxial Calibration Mount.*

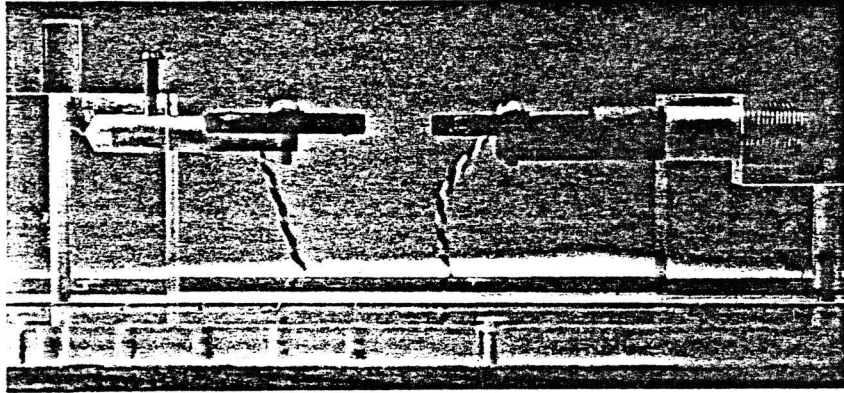


(c) *Calibration Mount for Coaxial Misalignment.*

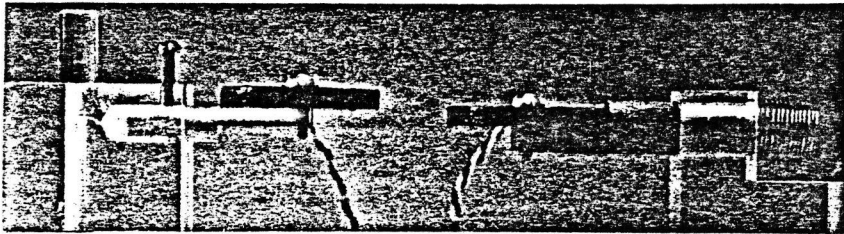


(d) *Calibration Mount for Coaxial Rotation.*

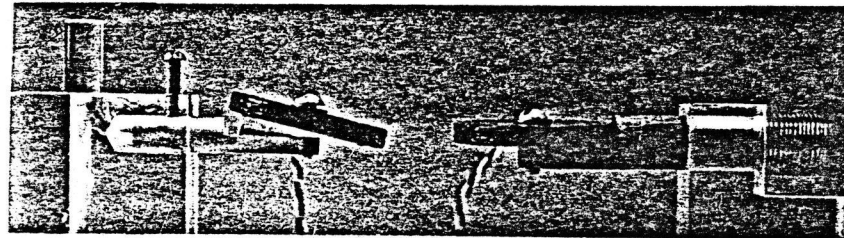
Figure 3.7 Calibration Mounts for a Pair of 2 in. Sensors in Coaxial Orientation.



(a) *Coplanar Calibration Mount.*



(b) *Calibration Mount for Coplanar Misalignment.*



(c) *Calibration Mount for Coplanar Single Axis Rotation.*



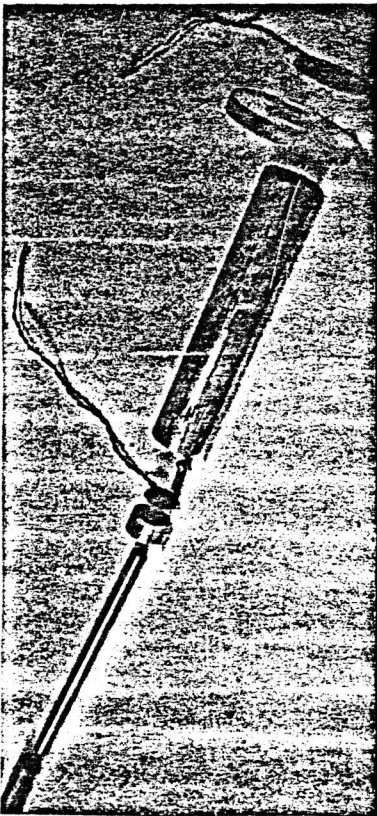
(d) *Calibration Mount for Coplanar Double Axis Rotation.*

Figure 3.8 Calibration Mounts for a Pair of 2 in. Sensors in Coplanar Orientation.

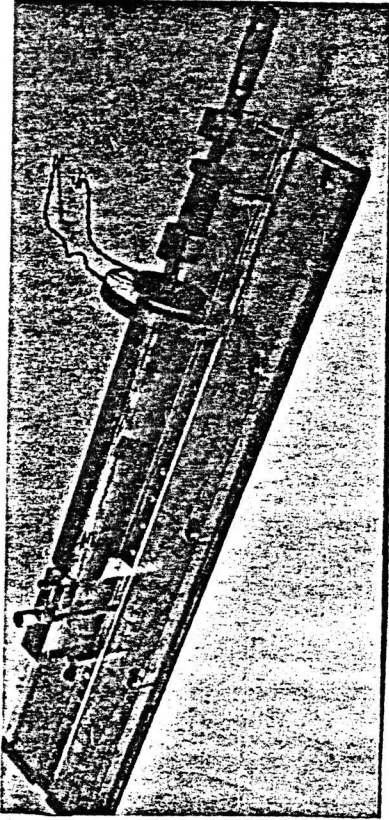
doubtful that misalignments having the magnitude of those calibrated will occur. Additional support for this belief was obtained by the examination of two cores taken from a three layered overlay site, with each containing a stack of three sensors. In both stacks, the three sensors were in very near coaxial alignment. The top and bottom sensors in each stack were very near parallel. The center sensors (on top of the open grade course) had rotated. One sensor rotated approximately 6 degrees and the other approximately 3 degrees from parallel with the others in their respective stack. It is concluded that the effects of sensor lateral movement and rotation are generally small and thus it is possible to accurately measure strain.

Calibration of the extensometer is performed by assembling the extensometer on the calibration device as shown in Figure 3.9. The same procedure as outlined above for coaxial orientation of sensors is followed and a similar set of spacing calibration curves as shown in Figure 3.6 is obtained.

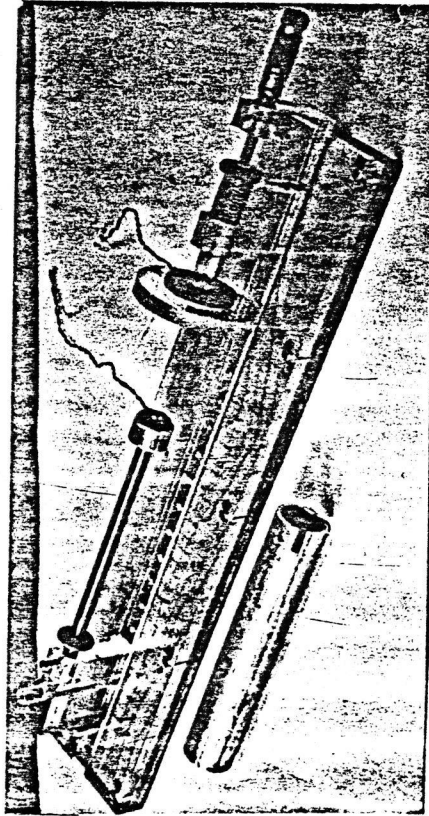
2. STRESS CELLS - The calibration of the stress cells was accomplished in the laboratory by constructing pressure chambers, filling them with sand, embedding the stress cells within the sand, and applying pressure to the sand using air pressure and a flexible membrane. Since the stress cell is very stiff compared to either sand or asphaltic overlay material, no significant error will be introduced by calibrating the cell in sand rather than in the overlay material. The gage factor of the semiconductor gages used changes with temperature, thus requiring calibration for the range of service temperatures expected. The pressure chambers containing the stress cells were placed in freezer units and allowed to cool to 10⁰F and then calibration data was obtained. Calibration data



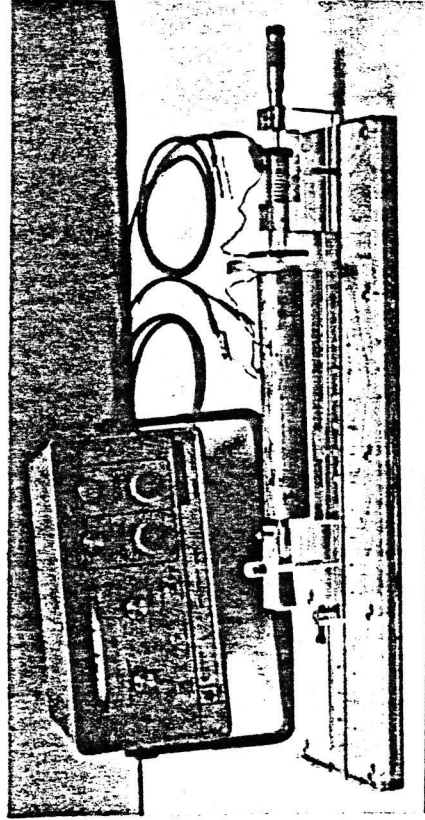
(a) Blow-out of Extensometer Parts.



(c) Complete Mounting of Extensometer.



(b) Extensometer Mounted on Calibration Apparatus with out Pipe Sleeve.



(d) Extensometer Ready for Calibration.

Figure 3.9 Extensometer Calibration Set-Up.

was also obtained at room temperature of 72⁰F and the final calibration was done after heating the chamber and stress cell in an oven to a temperature of 140⁰F. Typical calibration curves are shown in Figure 3.10.

3. THERMISTORS - The manufacturer's calibration of the thermistors used for temperature measurement was checked by immersing the sensors in ice water and hot water, checking the temperature with a mercury thermometer. The supplied calibration was sufficiently accurate and was used.

D. STATIC DISPLACEMENT DATA ACQUISITION

The external instrument package to be used for static measurements is a commercial soil strain instrument introduced in 1970 by Bison Instruments, Inc., Minneapolis, Minnesota. The Bison instrument to which the sensors are connected contains all necessary driving, amplification, balance, readout, and calibration controls along with a self-contained power supply. The bridge balance is accomplished by means of the phase and amplitude controls, using the meter to indicate null. The amplitude dial reading corresponds to the sensor spacing. Changes in spacing may be determined by renulling and noting the changes in the amplitude reading. They may also be determined by meter deflection from zero or by voltage output on a recorder connected to the rear panel.

E. DYNAMIC DATA ACQUISITION

The field instrumentation system developed specifically for this project was designed to meet the following goals:

- 1) Acquisition and conditioning of at least 20 signals from induction coil pairs;
- 2) Digitization of each channel at a maximum sampling rate of 2000 Hz/channel (40 KHz sampling rate total) with a resolution of at least 8 bits;

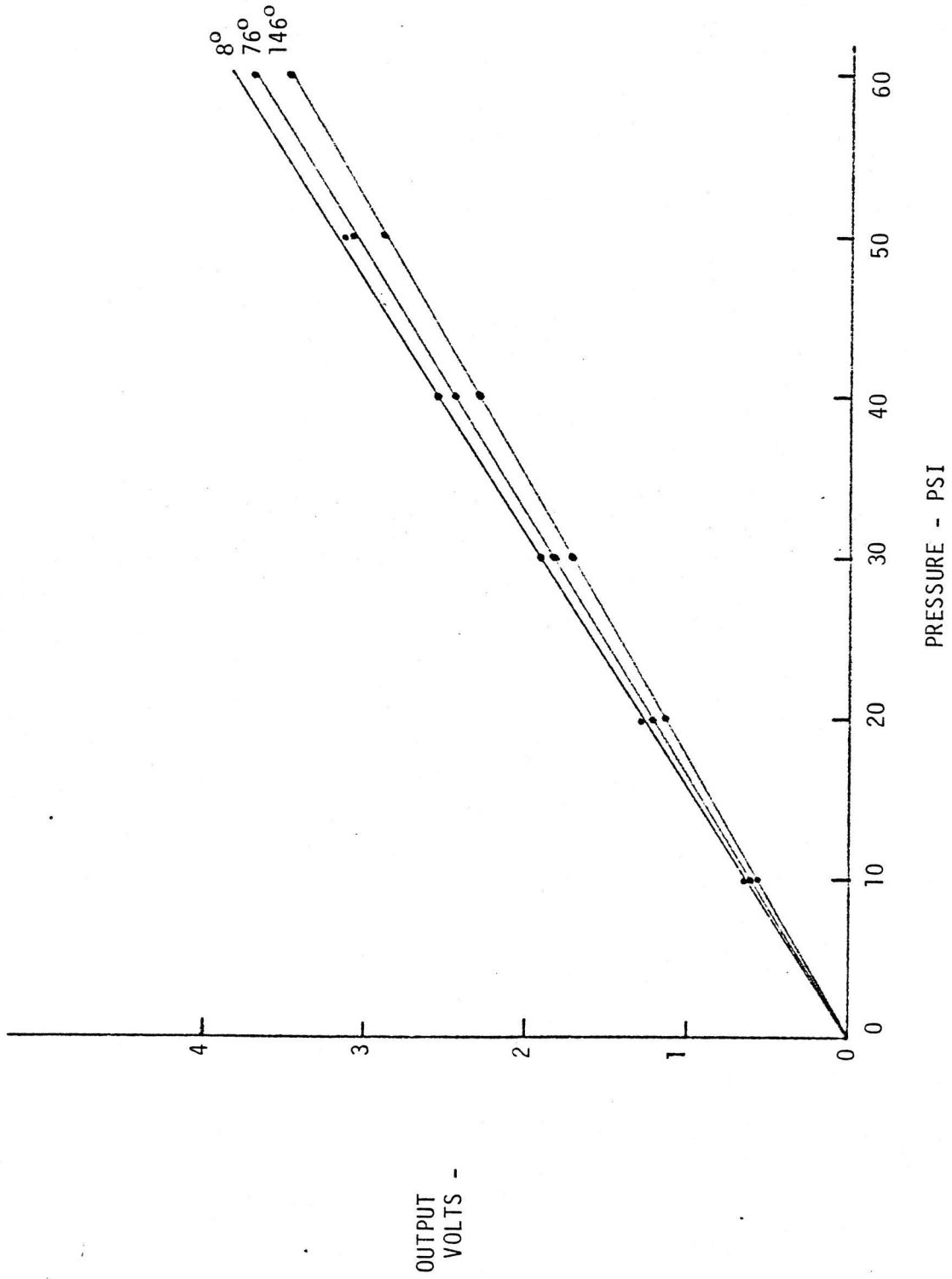


Figure 3.10 Typical Calibration Curve for Pressure Cell.

- 3) Recording of this data on one-half inch magnetic tape in IBM-compatible format;
- 4) Capability for plotting out any selected channel from a previously recorded run for verification of run data; and
- 5) Straightforward system operation requiring minimal operator training.

The above goals were achieved and resulted in the system henceforth described as the Pavement Data Acquisition System (PDAS).

1. THE PDAS HARDWARE - Physically, the PDAS instrumentation resides within a modified 1978 Ford long wheelbase van. The PDAS basically consists of three consoles, referred to below as left, right and center, with an operator's chair facing the center console and looking out the left side of the vehicle. Provision for external AC power was also installed. The van itself is equipped with dual air conditioning blowers and the engine with heavy duty cooling capacity so that the interior of the van can be kept at near room temperatures even on very hot days.

The left console consists of the following items:

- 1) A bank of 20 Validyne CD90 Carrier Demodulators for powering each transmitting coil and decoding the signal from each receiving coil. These units reside in a case with a common power supply. Each transmitter output and each receiver input is connected via a twisted wire pair to a BNC bulkhead connector located on the left rear quarter panel of the van. From outside the van, there appears two doors, approximately 8 in. square, each of which covers an array of 20 BNC connectors, with transmitting and receiving connectors grouped separately. In addition, there is also one BNC connector behind each door for

attachment of tape switches for signaling the beginning and end of a run.

- 2) A variable frequency pulse generator for controlling the input signal sample rate.
- 3) The magnetic tape formatter which controls the tape drive and provides the appropriate characters necessary for producing an IBM-compatible tape.

The center console is a self-contained microcomputer with the following components:

- 1) Intel SBC 80/10 single board computer with 13K byte assembly language program.
- 2) Video controller board and 9-inch CRT.
- 3) Tape controller board
- 4) ASCII keyboard
- 5) Switching power supply.
- 6) 25 channel multiplexer with 8 bit A/D converter. Full scale input voltage ± 2.5 volts.

The right console consists of the following:

- 1) 45 ips magnetic tape drive (DigiData MAXIDECK), capable of reading and writing 2400 foot tape reels.
- 2) AXIOM 820 printer-plotter for reproducing run headers and data previously recorded on tape.

For conditioning the input AC power, a SOLA CVN voltage regulator was installed inside the left rear door of the van. A covered AC receptacle on the outside left rear quarter allows power to be provided by a stationary or portable source.

2. THE PDAS SIGNAL PROCESSING - Connections are made between the van connector panels and the desired mix of buried transmitter and receiver coils. Each Validyne CD90 generates a 5 VRMS, 20 KHz signal for driving a transmitter (in phase for all 20 units). The output from a receiving coil is compared internally in the CD90 in magnitude and phase, resulting in a DC signal with a ± 10 volt swing. Since this magnitude was found to generate considerable crosstalk in the downstream multiplexer, the CD90 outputs were modified with Zener diode clipping to restrict the output swing to ± 4 volts. The CD90 has front panel controls for balancing (required for each change in initial coil spacing), zero offset and sensitivity (range 0.1 to 100 mv/v). The latter was set to the largest value which would not generate an output exceeding ± 2.5 volts, generally on the order of .25 mv/v.

The A/D converter produces an 8 bit digital equivalent of each signal on software selected channels. The sample rate can be varied by the pulse generator in the left console. The order in which input channels are sampled is controlled by software. The digitized signals are input to the tape controller, which writes the data to tape together with the IBM check characters. All data is written in 4K (4096) byte blocks. Recording format is ASCII for all text and 8 bit 2's complement for all data.

Following a run, any selected channel can be plotted out on the AXIOM 820 plotter. Run header information and calibration data are also included. Since the data on tape represent digital samples, they must be converted before plotting. This is done by extracting the stored CD90 sensitivity settings and using the fact that for the A/D converter ± 2.5 volts equals 256 counts. This results in the calculation of a

demodulated voltage at the receiver coil. Then using the stored values of initial coil spacing and installation mode (e.g., coaxial, coplanar, etc.) and the nonlinear curve of displacement vs. voltage stored in ROM, the actual coil displacement from the initial spacing can be determined and plotted.

3. THE PDAS SOFTWARE - From the operator's viewpoint, PDAS control is very straightforward. A menu of operations is made available from which a mode is selected. Listed below is the menu; following the menu list is a description of each of the modes. The "MENU" key may be pressed any time during operation of the system. If an action is being performed, it will be halted. The system then displays a menu which describes each of the functions that may be performed. The operator selects a function, enters the corresponding function number, and presses the "ESC" key. The selected function will then be started.

The menu functions are:

- 1) reset date and time
- 2) initialize new tape
- 3) define channel
- 4) define channel order
- 5) display channel summary
- 6) start new run
- 7) rerun previous run
- 8) scratch last run on tape
- 9) plot run
- 10) tape diagnostic.

1) Reset Date and Time (entered on automatically at powerup) - When power is applied to the system, certain information must be supplied by the operator before any other actions are taken. The date and time must be specified, along with a 40 character location name and the length of the test pavement. This information is entered via the keyboard as follows:

* DATE

The current date is specified in the form "MM/DD/YY", where "MM" is the numeric representation of the month, "DD" is the day of the month and "YY" is the last two digits of the current year. Slashes separate the month from the day and the day from the year. If the system is operated past midnight, the date will be automatically incremented.

* TIME

The current time is specified in the form "HH:MM", where "HH" is the number of hours since midnight and "MM" is the number of minutes into the hour. A colon separates the hour and minute. The system operates with a 24-hour clock. For example, 00:00 represents midnight, 10:00 is 10 AM, 12:00 is noon, and 20:00 is 8 PM. The date and time are written to tape each time a run is started and are also printed each time a channel is plotted.

* LOCATION NAME

This field allows the operator to describe the test location using the alphabetic and numeric buttons on the keyboard. Any combination of letters and numbers up to 40 characters in length may be entered. The location name is written to tape each time a run is started and is also reproduced each time a channel is plotted.

* DISTANCE BETWEEN START AND STOP SWITCHES

In order for the system to calculate the speed of the vehicle used in each run, the length of the pavement must be known. For this calculation to be valid, the run must be started and stopped with signals from tape switches lying on the pavement. The operator enters the number of feet and inches which separate the tape switches.

2) Initializing a New Tape - Before a new magnetic tape can be used by the system it must be initialized. This operation writes a tape header record at the beginning of the tape which includes a tape name, the location name, and the current date and time.

* TAPE NAME

Before the tape is initialized, the operator is requested to enter a tape name. The name may be any combination of letters and numbers up to 40 characters long. When the "ESC" key is pressed, the tape header record is written to the tape. If no error is detected, the "INITIALIZATION COMPLETE" message will be shown.

* TAPE ERRORS

If the tape drive is not on line or is malfunctioning, an error message will be displayed at the bottom of the screen.

3) Defining a Channel - The Pavement Data Acquisition System takes its input from up to 25 transducer channels. Each channel may be set up separately for different operating parameters which correspond to the transducer being used. The operator must define each of the channels which will be included in a test run. This information is written to tape when the run is started.

* CHANNEL NUMBER

This window allows the operator to select a channel number from one to 25.

* TRANSMITTER ID

This is a number from zero to 255 which identifies the transmitting coil attached to the selected channel number. This number may be matched against a list of transducers present at a given location.

* RECEIVER ID

A number from zero to 255 which identifies the receiving coil attached to the selected channel number.

* CONFIGURATION

There are four possible configurations which describe the placement of the transmitting and receiving coils:

<u>Configuration</u>	<u>Coil Placement</u>
Coaxial	Face to face
Coplanar	Edge to edge
1" extensometer	One inch coil transmitting
2" extensometer	Two inch coil transmitting

* INITIAL SPACING

This is the "AT REST" spacing between the two coils attached to the selected channel number. This distance may be specified in tenths or hundredths of an inch by using a decimal point.

* DEMODULATOR RANGE

The gain for each channel may be set by adjusting two knobs on the Validyne modulator/demodulator unit. One knob selects the range and the other selects a percentage of that range. The possible range settings are: 100, 50, 25, 10, 5, 2.5, 1, .5, .25, and .1 millivolts per volt. The demodulator range value should correspond to the setting of the middle knob for the selected channel on the Validyne unit.

* DEMODULATOR GAIN

This field allows the operator to specify a percentage (0.0 - 100.0) of the desired range. This number corresponds to the setting of the top knob for the selected channel on the Validyne unit.

Note: The gain knobs for all channels which are not connected to a transducer must be set to zero to avoid interference with the rest of the channels.

* COMMENTS

This window allows the operator to describe the setup for the selected channel. It may be any combination of letters and numbers up to 18 characters long.

4) Defining the Channel Order - The operator may select up to 25 channels to be scanned during a test run. The channel numbers may come in any order, and a channel may be repeated if necessary.

* CURRENT CHANNEL ORDER

Each time this display is selected, the current channel order is shown. If no channels are selected, a window will be opened and the operator will be requested to fill in the desired channel order.

* CHANGING THE CHANNEL ORDER

If the current channel order is to be changed, the operator presses the

"ESC" button on the keyboard. This causes the window to be blanked so the operator may enter the new channel order. The channel numbers are entered one after another, separated by commas. Pressing the "ESC" key causes the new order to be displayed. If there is an error in the specification, only those channels up to the error will be saved.

* CHANNEL DATA DISPLAY

Directly below each channel number, the current channel reading (-128 to 127) is continually displayed. This allows the operator to use this display for monitoring the channel activity during setup and testing.

5) Displaying the Channel Summary - This display shows a summary of each of the 25 channels. All of the information which was specified by the operator when defining the channels is displayed in a tabular format. This information is also reproduced each time a channel is plotted. The first 15 channels are initially displayed. Pressing the "RETURN" button on the keyboard causes the remainder of the channels to be shown. The "RETURN" key may be pressed any number of times to view both pages of channel information. An example of the information format is shown below.

<u>CHANNEL</u>	<u>TX ID</u>	<u>RX ID</u>	<u>CONFIG</u>	<u>SPACING</u>	<u>RANGE</u>	<u>GAIN</u>	<u>COMMENTS</u>
1	10	100	COPL	3.78	.25	75.3	Channel 1 comments

where:

CHANNEL = channel number (1-25)

TX ID = transmitter ID (0-255)

RX ID = receiver ID (0-255)
CONFIG = configuration: COAX = coaxial
 COPL = coplanar
 EXT1 = 1" extensometer
 EXT2 = 2" extensometer
SPACING = initial spacing (inches)
RANGE = demodulator range (mv/v)
GAIN = demodulator gain (0.0-100.0%)

6) Starting a New Run - Before starting a new run: a) define each channel to be scanned (see "Defining a Channel", 3) above), and b) define the channel scan order (see "Defining the Channel Order", 4) above).

When a new run is started, the system first searches for the end of tape record. When the tape has been positioned after the last set of data which was previously recorded, a sequential run number is assigned and the operator is requested to enter some information about the new plan.

* CHANNEL DEFINITION ERRORS

"NO CHANNELS DEFINED" indicates that the channel order was not specified. "CHANNEL X NOT DEFINED" means that the named channel number was included in the scan order but was not defined. In either case, the "MENU" key may be pressed so the operator may supply the required information.

* AXLE LOAD

This window allows the operator to specify the axle load (pounds) for the

new run. This information does not affect the operation of the system, but is recorded on the tape for reference. The axle load is also printed each time a channel is plotted.

* PAVEMENT LAYER TEMPERATURES

This line allows the operator to enter the temperature (degrees Fahrenheit) for each of four pavement layers. This information does not affect the operation of the system, but is recorded on the tape so it may be printed each time a channel is plotted.

* COMMENTS

This window allows the operator to describe the run using any combination of letters, numbers and special symbols. The window is 20 lines by 79 characters. The editing keys are especially useful when entering these comments. The comments are recorded on tape and printed each time a channel is plotted.

* WAITING FOR ZERO READING

At the bottom of the screen, the current channel scan order is shown along with a continuous display of the channel data values. The "RBAL" control on the Validyne unit is used to obtain a zero reading for each of the selected channels. The higher gain settings will make it hard to get a reading that is exactly zero. Any number near zero will do. When all channels are balanced, the operator presses the "ESC" button. This causes

the zero readings to be saved for future reference. These readings are written to the tape and are reproduced each time a channel is plotted. In addition, the zero reading is used to adjust the channel data during the plot operation. The plotted value equals the channel reading minus the zero reading.

* WAITING FOR POSITIVE CALIBRATION READING

This allows the operator to set up each channel for calibration in the positive direction. The "ESC" button causes the calibration readings to be saved. They are recorded on tape and reproduced each time a channel is plotted, but do not affect the plotted data values.

* WAITING FOR NEGATIVE CALIBRATION READING

This allows the operator to set up each channel for calibration in the negative direction. The "ESC" button causes the calibration readings to be saved. They are recorded on tape and reproduced each time a channel is plotted, but do not affect the plotted data values.

* ADJUST SCAN FREQUENCY

The scan frequency is determined by an external square wave signal from the adjustable signal generator on the left console. The system counts the incoming pulses and continually displays the frequency so the operator may adjust the signal to the desired rate. There is a maximum frequency which depends on the number of channels selected. This number is dis-

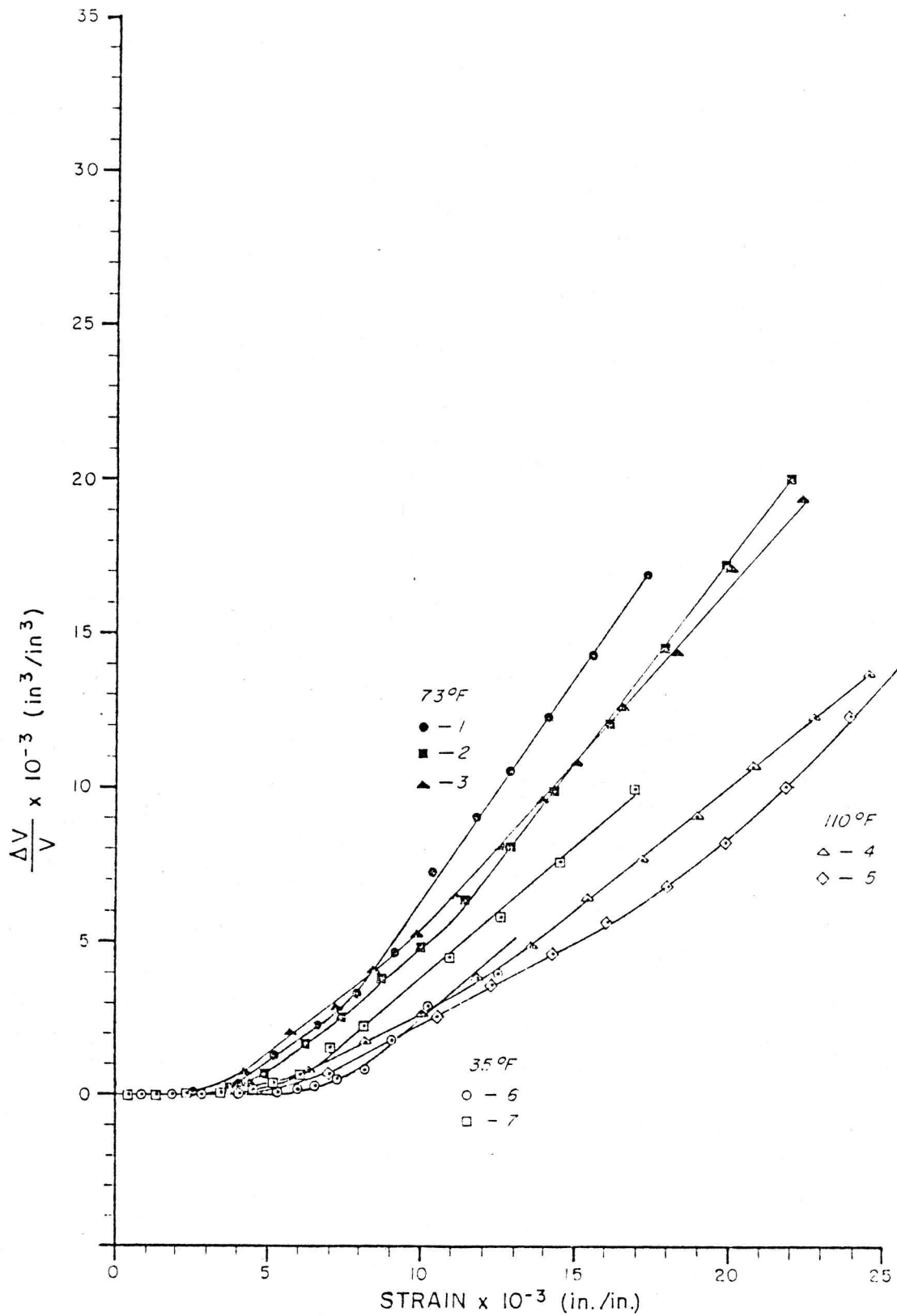


Figure 4.6 Change in Volume per Unit Volume vs. Strain at Various Temperatures
Asphaltic Concrete Open-Graded Course

of the modulus of elasticity computed at each test temperature are given in Table 4.3 and a modulus of elasticity versus temperature curve is plotted in Figure 4.15. Using the observed volume change readings, the changes in volume per unit volume were computed and plotted versus strains for each test sample. The results of those plots are shown in Figure 4.6.

2. BINDER COURSE - The asphaltic concrete binder course is a leveling course composed of a compacted mixture of mineral aggregate and asphalt cement constructed on the existing pavement or on an asphaltic concrete open-graded base course in accordance with the specifications in Appendix A. The mix is composed of 95.4% mineral aggregate and 4.6% AC-30 asphalt cement and meets the gradation requirements of a Type 2 ACHM Binder Course Mix (Table 4.2).

The binder course specimen obtained from the field was batched into 3600 gram samples. Each sample was heated to 250°F and then molded in a four inches diameter by eight inches high mold. The sample was compacted with a Hveem kneading compactor (Figure 4.7) to a compaction pressure of 2000 psi. The sample was unloaded, inverted and compacted from the opposite end. The sample was then removed from the mold and allowed to cool to room temperature (73°F).

All test samples were capped (Figure 4.8) and then allowed to cure for seven days prior to testing. The same testing procedure was used to test the binder samples as was used to test the open-graded samples (Figures 4.9 and 4.10). Tests on the binder samples were performed at five different temperatures. Three samples were tested at each of the following temperatures: 127°F, 73°F, and 35°F. Two samples were tested at each of the following temperatures: 73°F and 50°F. Stress-strain curves for each test sample at the five test temperatures for the

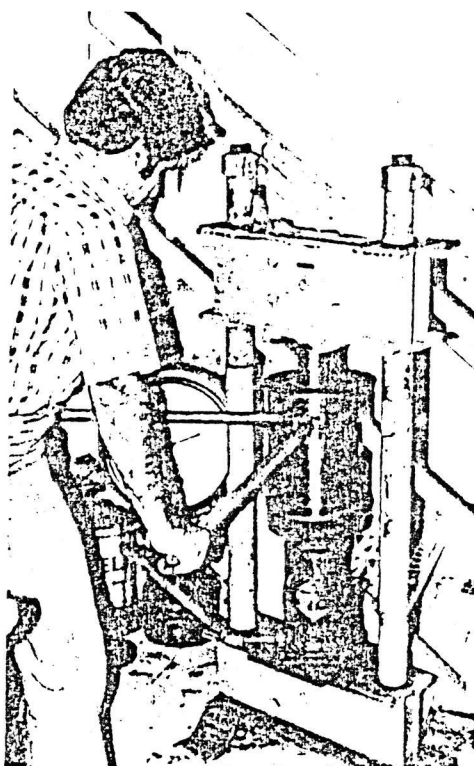


Figure 4.7 Binder sample being compacted in Hveem kneading compactor.

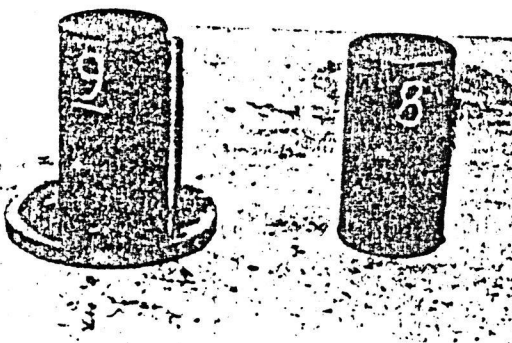


Figure 4.8 Binder sample being capped prior to testing.

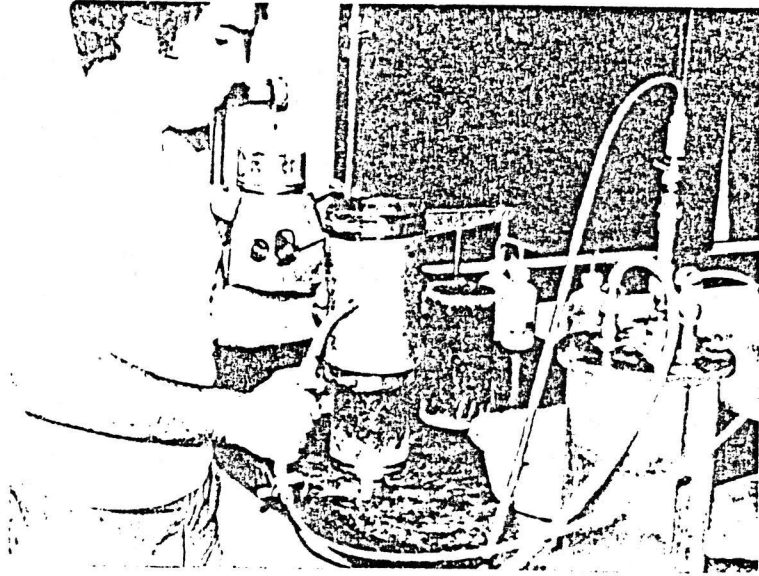


Figure 4.9 Inserting binder sample into Texas triaxial cylinder prior to testing.

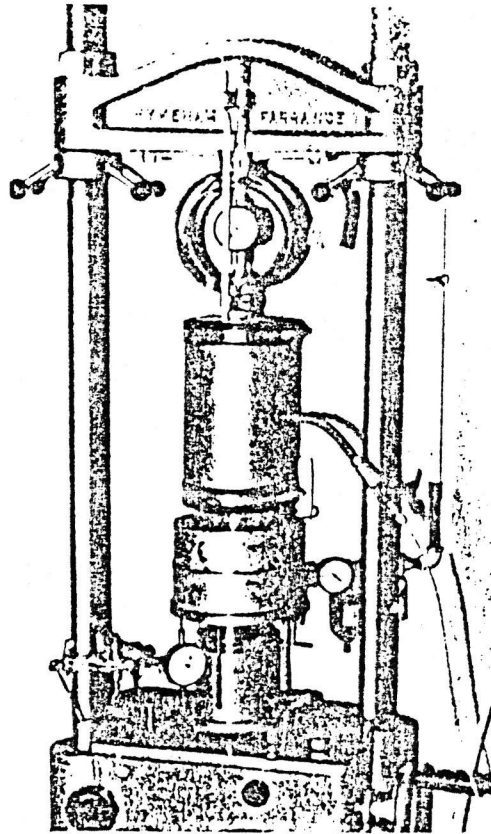


Figure 4.10 Binder sample in compression machine ready for testing.

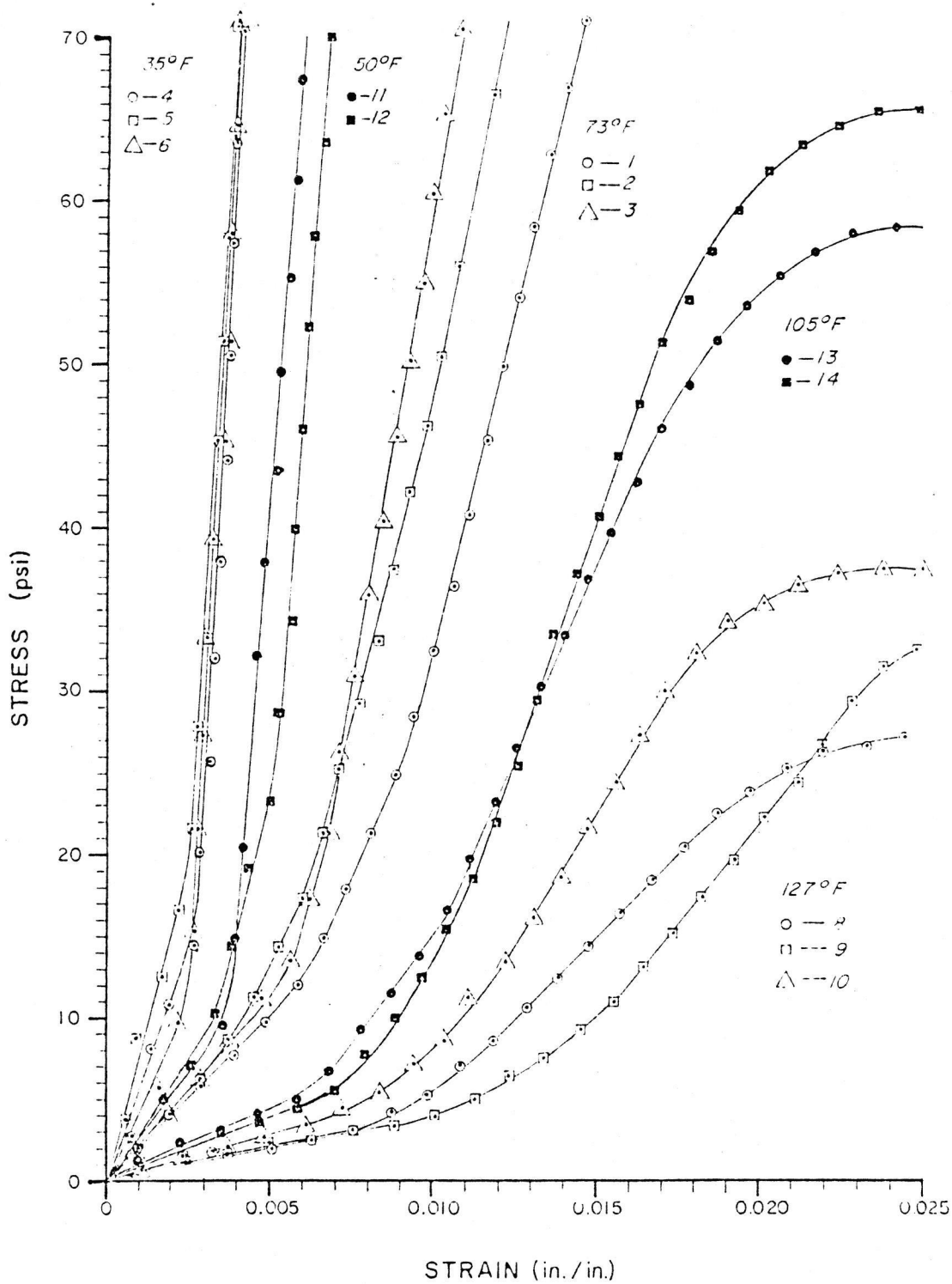


FIGURE 4.11 STRESS-STRAIN CURVES AT VARIOUS TEMPERATURES
 ASPHALTIC CONCRETE BINDER COURSE

asphaltic concrete binder course are shown in Figure 4.11. Averages of the modulus of elasticity computed at each test temperature are given in Table 4.3 and a modulus of elasticity versus temperature curve is plotted in Figure 4.15. Plots of changes in volume per unit volume versus strains are shown in Figure 4.12.

3. SURFACE COURSE - The asphaltic concrete surface course is a wearing course composed of a compacted mixture of mineral aggregate and asphalt cement constructed on the existing pavement or on an asphaltic concrete binder course in accordance with the specifications in Appendix A. The mix is composed of 94.4% mineral aggregates and 5.6% AC-20 asphalt cement and meets the gradation requirements of a Type 2 ACHM Surface Course Mix (Table 4.2).

The surface course specimen obtained from the field was batched into 4000 gram samples. The same procedures were used for molding and testing the surface course samples as were used for molding and testing the binder course samples. Three samples were tested at each of the following temperatures: 120⁰F, 105⁰F, 73⁰F and 50⁰F. Two samples were tested at 35⁰F. Stress-strain curves for each test sample at the five test temperatures for the asphaltic concrete surface course are shown in Figure 4.13. Averages of the modulus of elasticity computed at each test temperature are given in Table 4.3 and a modulus of elasticity versus temperature is plotted in Figure 4.15. Plots of changes in volume per unit volume versus strains are shown in Figure 4.14.

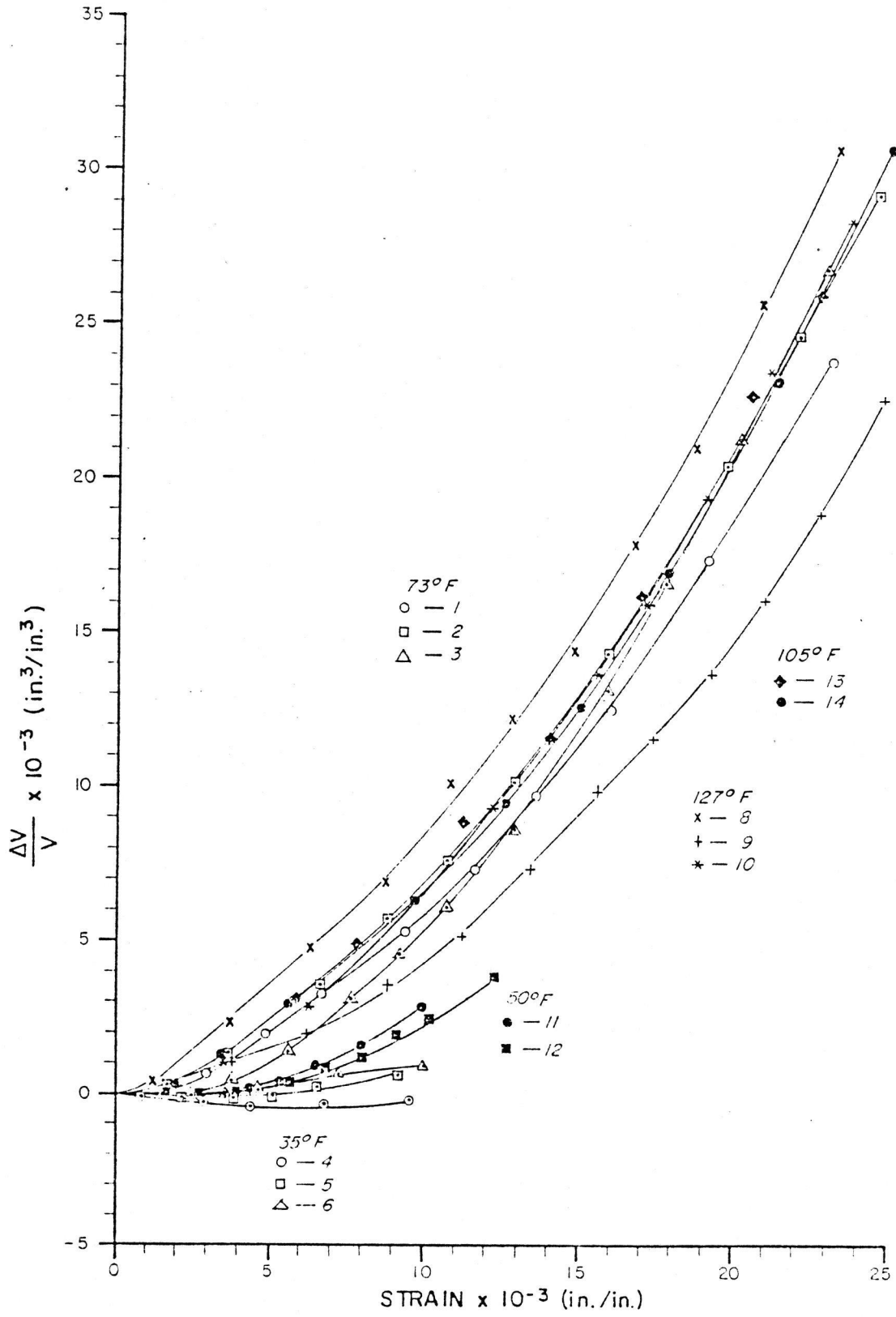


Figure 4.12 Change in Volume per Unit Volume vs. Strain at Various Temperature Asphaltic Concrete Binder Course

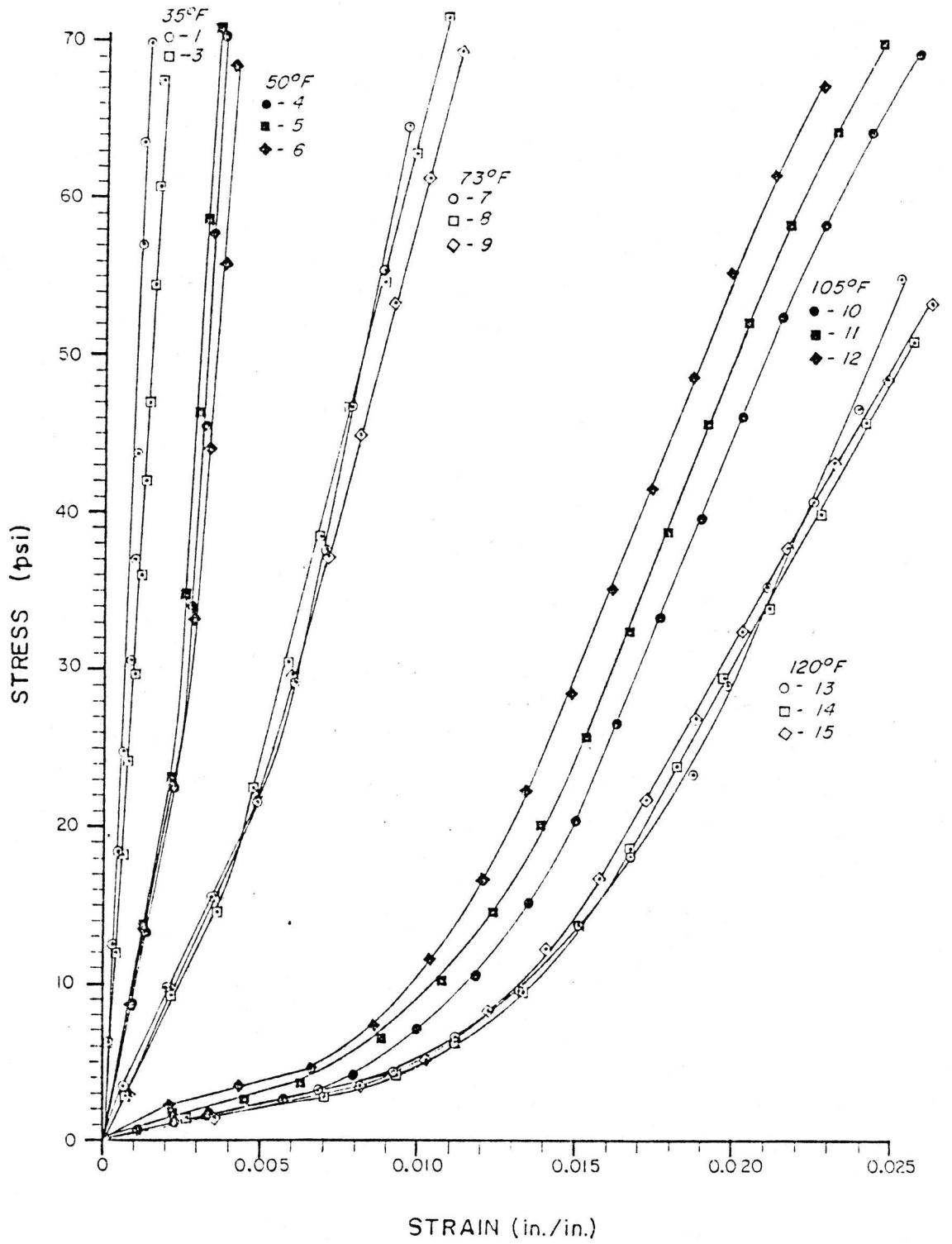


FIGURE 4.13 STRESS-STRAIN CURVES AT VARIOUS TEMPERATURES
ASPHALTIC CONCRETE, SURFACE COURSE

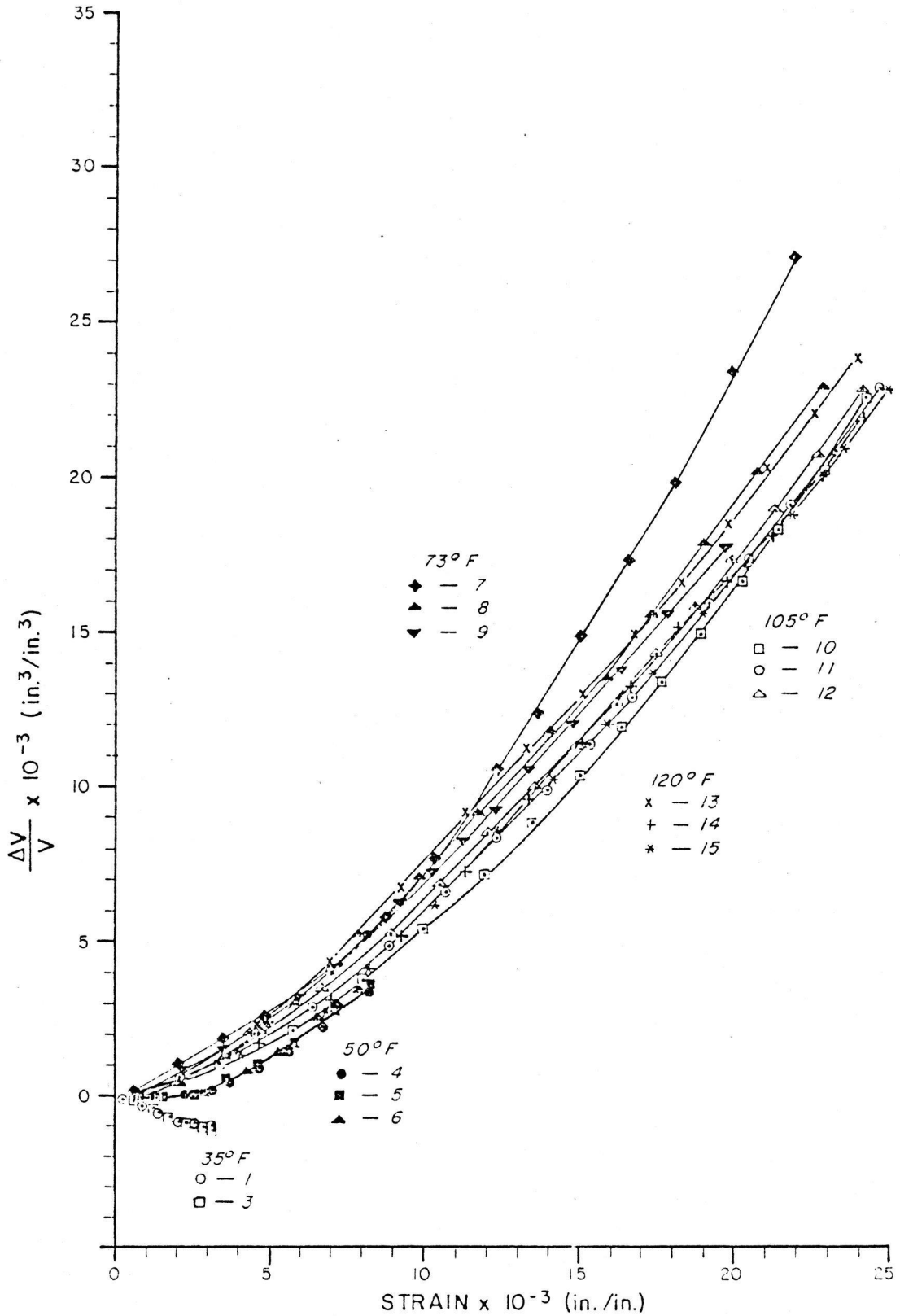


Figure 4.14 Change in Volume per Unit Volume vs. Strain at Various Temperature Asphaltic Concrete Surface Course

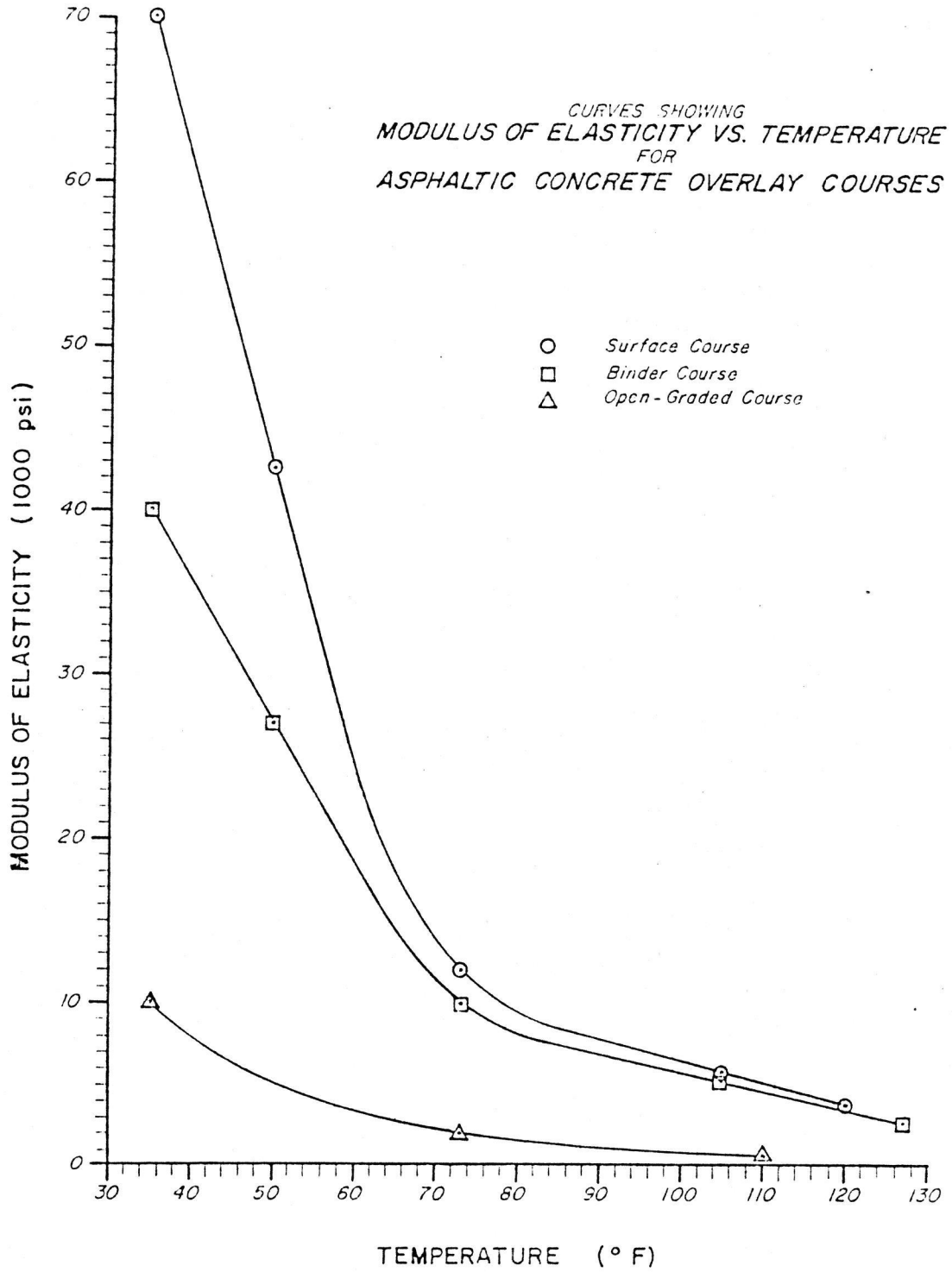


FIGURE 4.15 MODULUS OF ELASTICITY VS. TEMPERATURE CURVES
ASPHALTIC CONCRETE OVERLAY COURSES

TABLE 4.3
ASPHALTIC CONCRETE PROPERTIES

Temperature (°F)	Modulus of Elasticity (psi)		
	Surface ($\gamma=152$ pcf)	Binder ($\gamma=148$ pcf)	Open-graded ($\gamma=110$ pcf)
35	70,000	40,000	10,000
50	42,500	27,000	
73	12,000	10,000	2,000
105	5,800	5,000	
110			500
120	3,900		
127		2,600	

CHAPTER V

DATA ACQUISITION AND RESULTS

A. PROCEDURE - STATIC DATA ACQUISITION

Static measurements were begun as soon as each test section was completed. Initial measurements were observed and recorded. These measurements served two purposes: one, to check out the system, and two, to establish a data base from which magnitudes of movements could be determined.

The objectives of the static measurements were to measure the cumulative deformations due to traffic loads and the cyclic movements due to both daily and seasonal temperature variations of the asphaltic concrete overlay system in the vicinity of a joint in the overlaid pavement. Static readings were made approximately every two weeks for several months after construction was completed and then approximately once a month during the winter months. When weather permitted, readings were made twice a day, once in the early morning and once in the afternoon, for periods of two and three consecutive days so that daily movements as well as long term movements could be observed.

Static readings were accomplished by systematically connecting related coaxial, coplanar, or extensometer sensor pairs to a Bison strain gage meter and obtaining an amplitude dial reading by balancing the phase and amplitude on the meter for each sensor pair. Each amplitude dial reading was recorded and later reduced to a spacing between the corresponding sensor pair by extrapolation from previously compiled calibration data tables associating amplitude dial readings with sensor

spacings. Three sets of calibration data tables were required: one for coaxial sensor pairs, one for coplanar sensor pairs, and one for extensometer sensor pairs.

Movements were determined by computing the differences between successive spacings and the initial spacings. A negative difference between a coplanar sensor pair indicates that the joint in the PCC pavement closed relative to the initial spacing or that compression occurred in the asphalt overlay across the joint. A negative difference between a coaxial sensor pair indicates compression of the asphaltic concrete layer, or for the extensometer, settlement of the PCC pavement relative to the initial spacing. Similarly, a positive difference between a coplanar sensor pair indicates that the joint in the PCC pavement opened relative to the initial spacing or that expansion occurred in the asphalt overlay across the joint. A positive difference between a coaxial sensor pair indicates expansion of the asphaltic concrete layer, or for the extensometer, uplift of the PCC pavement relative to the initial spacing. The strain was computed for each sensor pair by dividing the movement by the initial spacing for each corresponding sensor pair.

Each time a set of static readings was made at one of the test sections, the temperature at each interface of the asphaltic concrete overlay was observed and recorded.

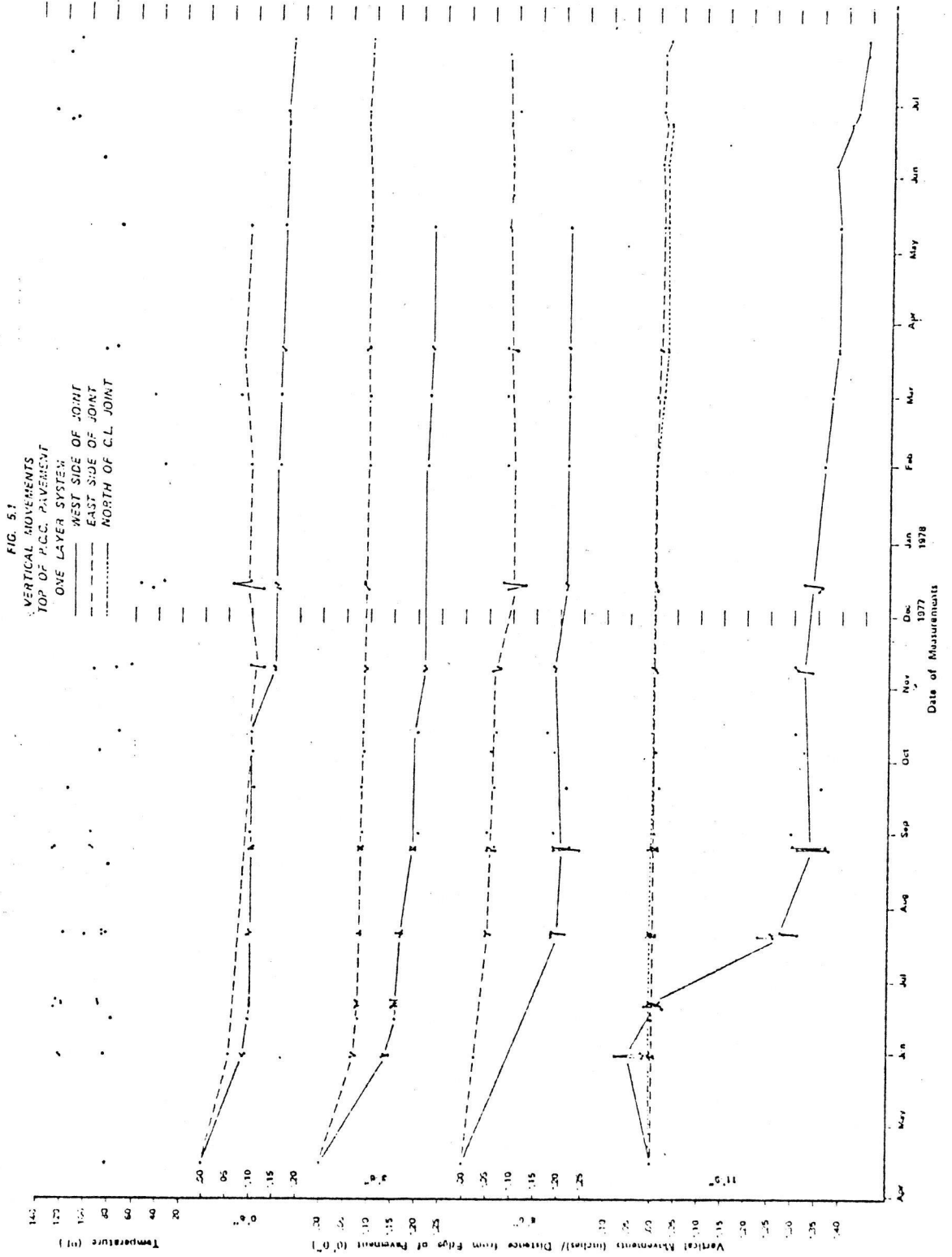
Various movement versus time plots and strain versus time plots have been drawn to graphically present the accumulative deformations and cyclic movements observed from the static measurements. This data is presented and discussed in the following sections.

B. VERTICAL MOVEMENTS - TOP OF PCC PAVEMENT

1. ONE LAYER SYSTEM - The one layer test site is located in the east end transition zone of the east bound lane approximately two hundred feet beyond the I-30 Congo exit ramp, which is located on the east side of the town of Benton. Approximately two inches of surface course overlays the PCC pavement at this test site. Static data acquisition was begun on April 15, 1977 and has been periodically maintained until the present time. Figure 5.1 shows a vertical movement of the PCC pavement versus time plot for each of the extensometer locations along the overlaid joint.

From Figure 5.1 it is seen that the majority of the vertical movement of the PCC pavement occurred within two to three months after the section was opened to traffic. Additional settlement occurred between October and December when the average temperature of the pavement dropped about forty degrees. It appears that since mid-December the vertical settlement has virtually ceased. At all locations along the joint the settlement is greater for the west side slab (the "up-stream" traffic side) than it is for the east side slab (the "down-stream" traffic side). On the west side of the joint, magnitudes of total settlements are approximately 0.16 inch at six inches from the edge of the pavement and approximately 0.22 inch at 3'-6" inch and 8'-6" from the edge of the pavement. However, the differential settlements with the adjacent east side slab are considerably smaller. The magnitudes of the total differential settlements are approximately 0.07 inch at six inches from the edge and approximately 0.13 inch at 3'-6" and 8'-6" from the edge of the pavement.

Measurements recorded for the west side slab at 11'-9" from the edge of the pavement indicate considerable settlement of approximately 0.34 inch from mid-June to late August. The total settlement recorded at this



location is approximately 0.45 inch. However, the adjacent east side slab across the contraction joint and the adjacent west side slab across the centerline joint show virtually no settlement. Since no visible surface distress has been observed at this location it is doubtful that this magnitude of settlement has occurred at this location. Although the exact cause of this sudden vertical movement is not known, the following two possibilities exist: (1) The friction course was placed and rolled during the latter part of June. The corner of the PCC pavement slab may have broken off and reseated during the laydown and rolling of the friction course. (2) Difficulties were encountered during the installation of the extensometer at this location. The stabilizing rod of the extensometer assembly could not be driven to its full depth. Therefore the top of the rod had to be cut with a torch. The one inch sensor and the aluminum cap, which were normally screwed to the top of the rod, were in this case glued. It is possible that the sensor and the aluminum cap became unglued and popped off the rod. Both possibilities would result in a closer sensor spacing as indicated by the movements.

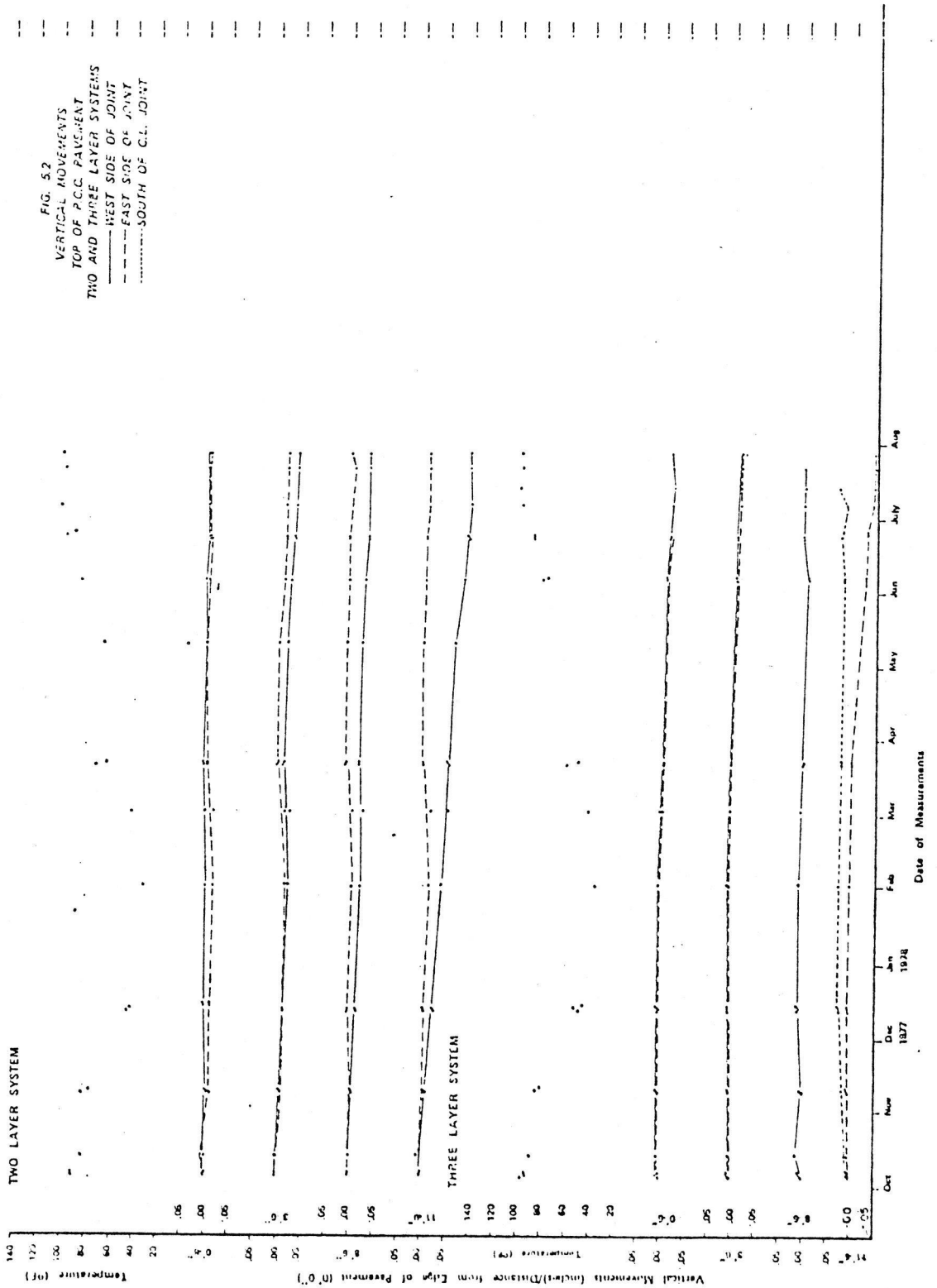
2. TWO LAYER SYSTEM - The two layer test site is located in the west end transition zone of the west bound lane which is located on the west side of the town of Benton. Approximately two and one-half inches of binder and one and one-half inches of surface course overlays the PCC pavement at this test site. Static data acquisition was begun on October 5, 1977 and has been periodically maintained since then. The top half of Figure 5.2 shows a vertical movement of the PCC pavement versus time plot for each of the extensometer locations along the overlaid joint.

Figure 5.2 shows a gradual increase in differential vertical movements between adjacent slabs from the edge of the pavement to the centerline joint. The total differential settlements are approximately 0.01 inch at six inches from the edge, 0.02 inch at 3'-6" from the edge, 0.04 inch at 8'-6" from the edge and 0.08 inch at 11'-9" from the edge of the PCC pavement.

3. THREE LAYER SYSTEM - The three layer test site is located in the west bound lane at approximately one thousand feet east of the two layer test site. Static data acquisition was begun on October 4, 1977 and has been periodically maintained since then. The bottom half of Figure 5.2 shows a vertical movement of the PCC pavement versus time plot for each of the extensometer locations along the joint.

Total settlement of only 0.02 inch and no differential settlement have been recorded at six inches and at 3'-6" from the edge of the pavement. There has been no settlement of the west side slab at 8'-6" and only 0.05 inch settlement of the east side slab at 11'-9" from the edge of the pavement. Differential settlements at these two locations are unobtainable because of inoperative sensors across the joint.

4. COMPARISON OF VERTICAL MOVEMENTS - The differential settlement between adjacent slabs at the two layer test site has a similar pattern as that of the one layer test site, i.e., the differential vertical movement between adjacent slabs increases from the edge to the centerline of the pavement and the west side slab settled more than the east side slab. However, the magnitudes of differential settlements at the two layer test site are much smaller than those at the one layer test site and, although the settlement of the west side slab is greater than the east



side slab at both test sites, traffic flows in opposite directions. Little or no settlement of the slabs occurred at the three layer test site.

Prior to overlay construction, pressure grouting under the existing pavement was performed along the length of the pavement that was to have the full depth three layer overlay. The transition zones, however, were not pressure grouted. Although the thickness of the three layer overlay would reduce the intensity of stresses at the top of the overlaid pavement due to a load at the surface of the overlay, it is more probable that the small settlements of the PCC pavement at the three layer test site are the positive results of pressure grouting.

Prior to the pressure grouting operation it was observed that at practically all of the contraction joints in the west bound lane from the two layer test site to several thousand feet beyond the three layer test site, the west side slabs had characteristically settled from one-eighth to one-fourth of an inch more than the east side slabs. From the measured vertical movements at the two layer test site after overlay construction, it is evident that this trend has continued, whereas at the three layer test site this trend has apparently been arrested. This, again, is probably due to the increase in stability of the overlaid pavement at the three layer test site by pressure grouting.

Tests performed on the subgrade material at the three layer test site confirmed the subgrade material classification indicated on the Arkansas Highway Department construction plans. The construction plans also indicate the same subgrade material classification at the one and two layer test sites, therefore, it has been assumed that the subgrade material at all three test sites are the same. This assumption seems to

be reasonable for the two and three layer sites because of their close proximity and because of the comparison of their vertical movements. However, the one layer test site is approximately two miles from the other two test sites and is located in the opposite direction traffic lane. Therefore, the comparatively large vertical movements between the one layer test site and the two and three layer test sites may be indicative of a different subgrade material. It may be desirable, then, to perform an analysis of the one layer test site subgrade material.

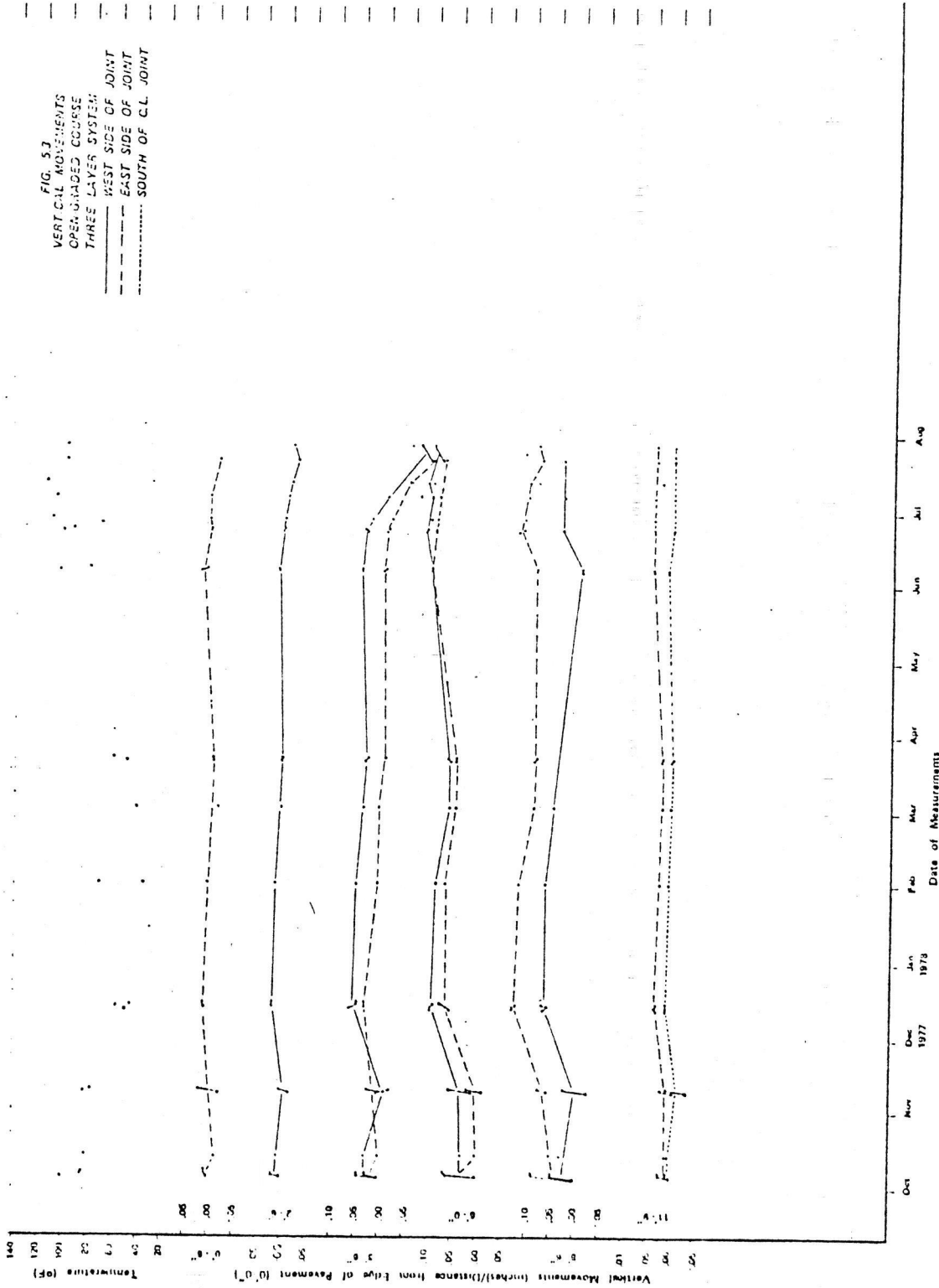
Traffic was detoured off of the Interstate for several months during overlay construction. The recorded movements, in particular at the one layer test site, indicate that a large majority of the settlement of the PCC pavement occurred during the first three months after the Interstate was reopened to traffic. It is believed that this settlement is primarily induced by traffic loads. The effects of moisture and moisture changes, however, should be investigated.

C. VERTICAL MOVEMENTS - TOP OF OPEN GRADE

1. THREE LAYER SYSTEM - Figure 5.3 is a vertical movement versus time plot for the open-graded course. Movements on each side of the joint are plotted for each sensor location along the joint.

Only one sensor each and on opposite sides of the joint are operative at locations six inches and 2'-6" from the edge of the pavement. Vertical movements at these two locations are small ranging from a +0.02 to -0.02 inch. At location 3'-6" the vertical movements ranges from +0.05 to -0.08 inch on the west side of the joint with approximately 0.04 inch differential vertical movement with the east side of the joint. At location 6'-0" an upward total movement of +0.10 inch occurred on the west

FIG. 5.7
 VERTICAL MOVEMENTS
 OPERGRADED COURSE
 THREE LAYER SYSTEM:
 — WEST SIDE OF JOINT
 - - - EAST SIDE OF JOINT
 ····· SOUTH OF C.L. JOINT



side of the joint with only about 0.02 inch differential movement with the east side of the joint. At location 8'-6" the east side of the joint has moved upward about 0.12 inch with about 0.05 differential movement with the west side of the joint. The total vertical movement at location 11'-9" is about 0.04 inch.

From Figure 5.3 it can be seen that most of the vertical movements are occurring between location 3'-6" and 8'-6" which are the approximate locations of the vehicular wheel paths, and only very small movements occurring away from the vehicular wheel paths. It seems apparent that the vertical movements in the open-graded course are at least partly related to vehicular induced loads. First consider the time interval from mid-December through mid-June. Vertical movements and differential vertical movements appear to have been reasonably stable with the exception of locations 6'-0" and 8'-6". From March to June at location 8'-6", which is the approximate location of the interior vehicular wheel path, the top of the open-graded course displaced downward approximately 0.06 inch while at location 6'-0", which is between the wheel paths at the center line of the outside lane, it displaced upward by approximately the same amount. This is probably due to open-graded material being shoved sideways under the application of repeated wheel loads and may be the first indication of rutting.

The stiffness of the asphalt reduces as the temperature increases. Therefore, some densification of the asphalt may be expected particularly in the wheel paths as is indicated from June through August at location 3'-6". Another point of interest is the upward movement or swelling which typically occurred at all locations along the joint from mid-November to mid-December as the average temperature of the pavement

dropped. Again, the movements are comparatively larger in the vicinity of the wheel path. One possibility which may create this type of movement would be the freezing of water trapped in the voids of the open-graded course. However, the aggregate gradation of the open-graded course creates a highly porous layer from which water should easily drain. The overlaid PCC pavement was initially constructed with a drainage slope toward the outside edge of the pavement. Side drains were installed all along the outside edge of the pavement prior to overlay. These facts make it improbable that water would be retained in the open-graded course. Another observation is that if the upward movement was due to the freezing of water, then similar magnitudes of upward movements may have been expected at all locations along the joint. Also, the larger movements in the vicinity of the wheel paths leads to the belief that the movements are related to the application of repeated wheel loads.

During the compression testing of the open-graded mix, it was observed that the test samples increased in volume when loaded in compression. It may be possible that, if the open-graded course was subjected to horizontal compressive stresses induced by the horizontal movement of the underlying pavement slabs, swelling of the open-graded course could occur. In that time period, from mid-November to mid-December, the concrete slabs contracted due to the decrease in temperature which caused the joint to open. (Horizontal movements will be discussed later in the chapter.) Because the open-graded course is bonded across the joints, it is more probable that tension stresses rather than compression stresses were induced near the joint. If, however, compressive stresses were induced and they produced the upward movement, again, similar magnitudes of these movements may have been expected at all locations along the

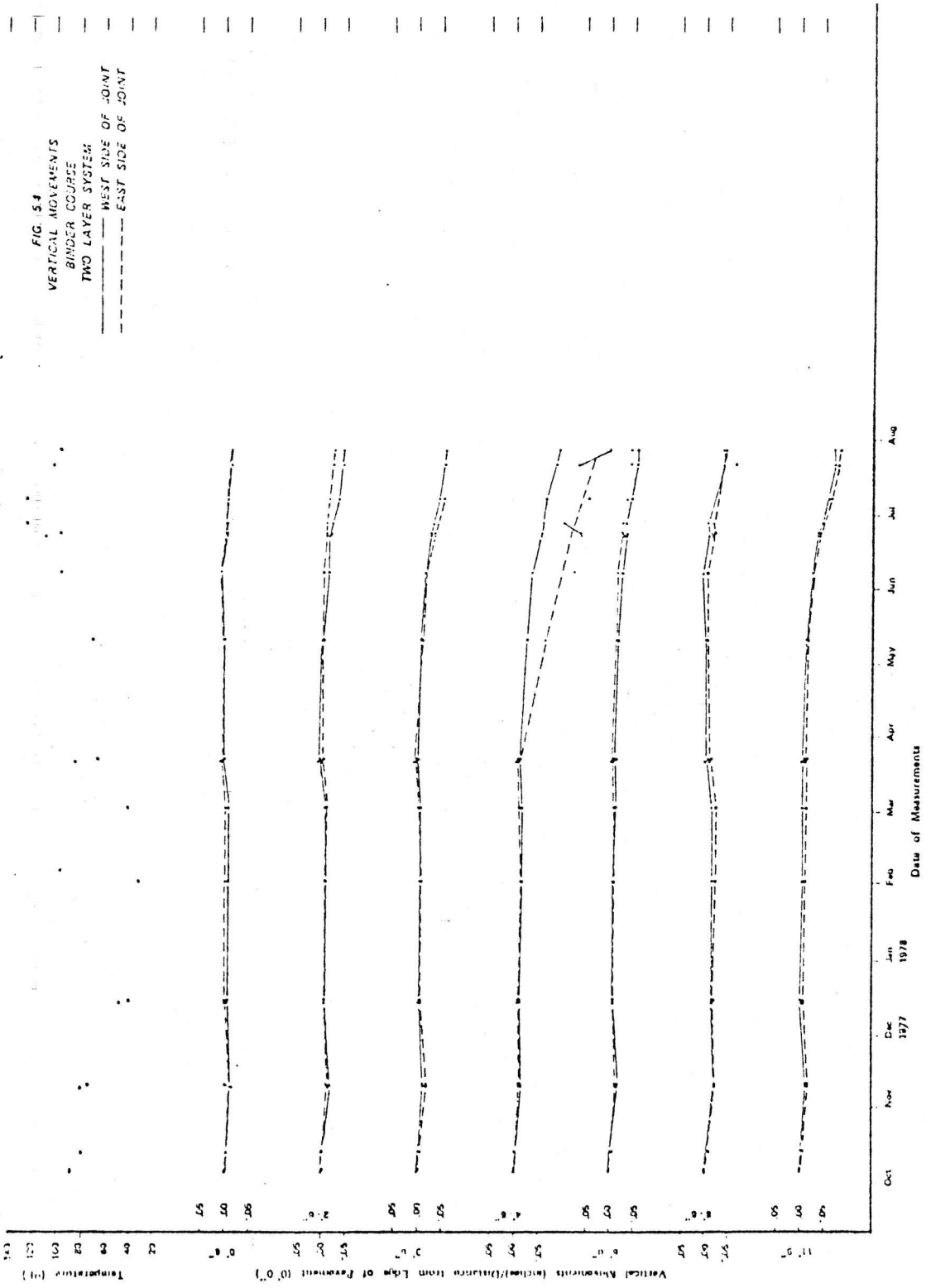
joint.

It seems more logical that the upward movement was caused by shoving of the material away from the wheel paths. The locations 3'-6" and 8'-6" from the edge of the pavements are approximate locations of the exterior and interior wheel paths. First, consider that the actual exterior wheel path is between locations 2'-6" and 3'-6". Locations 3'-6" and 6'-0" now fall between the wheel paths. As the wheel load depresses the material in the wheel path, the material is also shoved toward the opposite wheel path thereby creating an upheaval as indicated at 3'-6" and 6'-0". Similar upheavals should be occurring at locations 2'-6" and 8'-6" which are now just outside of their respective wheel paths. However, the upward movement at 8'-6" is much greater than that at 2'-6".

Now consider that the actual exterior wheel path is one foot away from location 3'-6", whereby now locations 6'-0" and 8'-6" fall between the wheel paths. Similar to the above, as the wheel load depresses the material in the wheel path, the material is also shoved toward the opposite wheel path, thereby creating an upheaval as indicated at 6'-0" and 8'-6". Location 3'-6", which is now just outside of the exterior wheel path, experiences a similar upheaval. Locations 2'-6" and 11'-9" are now approximately the same distance from their respective wheel paths and indicate very similar movements. This is believed to be the most logical explanation for the upward movements of the open-graded course.

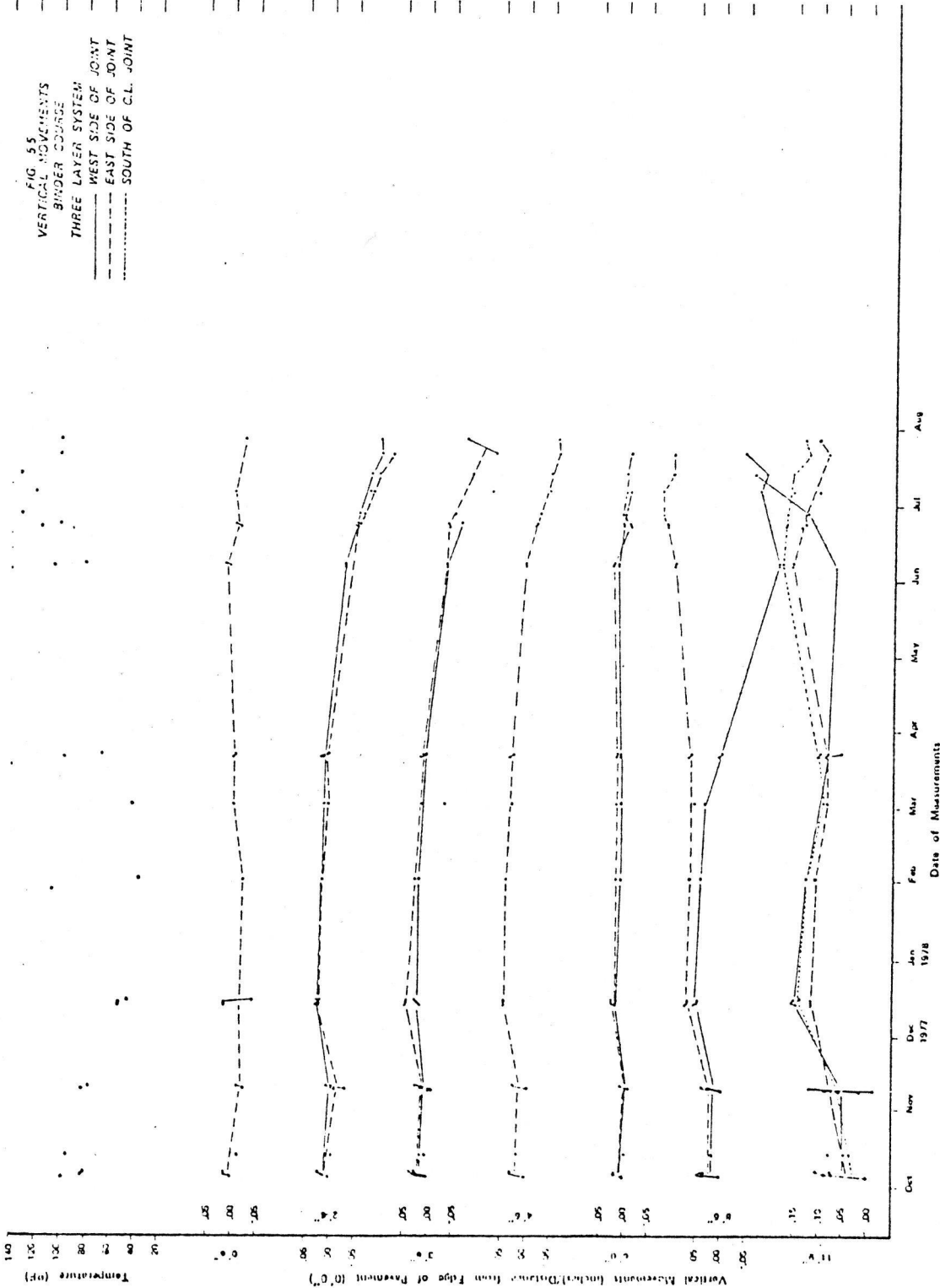
D. VERTICAL MOVEMENT - TOP OF BINDER

1. TWO LAYER SYSTEM - Figure 5.4 is a vertical movement versus time



plot for the binder course at each sensor location along the joint. The pattern of displacement is very similar at all locations with the exception of the east bound lane at location 4'-6". From late March to August the data points are scattered which leads to the belief that the sensor pair on the east side of the joint is not functioning properly. All other locations show small magnitudes of movement ranging from -0.02 to 0.01 inch from October through June. Differential movements across the joint are only about 0.01 inch. As the warming trend continues from June through August, the overlay loses stiffness and increases compaction. The top of the binder has settled from 0.01 to 0.08 inch with a maximum differential settlement of only 0.02 inch.

2. THREE LAYER SYSTEM - Figure 5.5 is a vertical movement versus time plot for the binder course at each sensor location along the joint. From October through March a very similar pattern of vertical movements has developed at all locations in the binder layer as has developed in the underlying open-graded layer (Figure 5.3). Total vertical movements at all locations except at 11'-9" range from -0.02 to +0.07 inch with maximum differential movements of only 0.02 inch during this time period. A similar upward movement or swelling is indicated between mid-November and mid-December and then relative stability through March with no appreciable changes in differential movements. It is believed that the upward movement is the result of the material being shoved away from the wheel paths in a similar manner as was discussed for the open-graded layer. The slow settlement trend from April through mid-June at locations 2'-6", 3'-6" and 4'-6" could be due to the binder material being slowly compacted into the surface voids of the open-graded course as the temperature increases and the stiffness of both layers decreases. The continu-



ing warm temperatures through July promote further densification of the binder course.

The total movement of 0.15 inch and differential movement of 0.20 inch as is indicated for June at location 8'-6" do not seem realistic in comparison to the movements at the other locations. This is also about three times the total movement and two times the differential movement indicated at the same location in the underlying open-graded course. It is doubtful that this magnitude of movement has occurred on the west side of the joint. The sensors may be malfunctioning or the top sensor may have been driven into the binder course.

Discrepancies are also apparent between the magnitudes of movement at location 11'-9" and those at the other locations. The order of magnitude is approximately three times greater at location 11'-9". Here, too, it is doubtful that this magnitude of upward movement occurred especially when comparison is made to the much smaller upward movements at the same location in the underlying open-graded layer (Figure 5.3). Because of the smaller aggregates and the greater density of the binder course, it would be expected that smaller movements would occur in the binder layer rather than the open-graded layer. This can be seen by comparing the movements of the binder layer to that of the open-graded layer at each of the other locations. The reason for the apparently large indication of upward movement at location 11'-9" is not known, however, one possibility will be discussed.

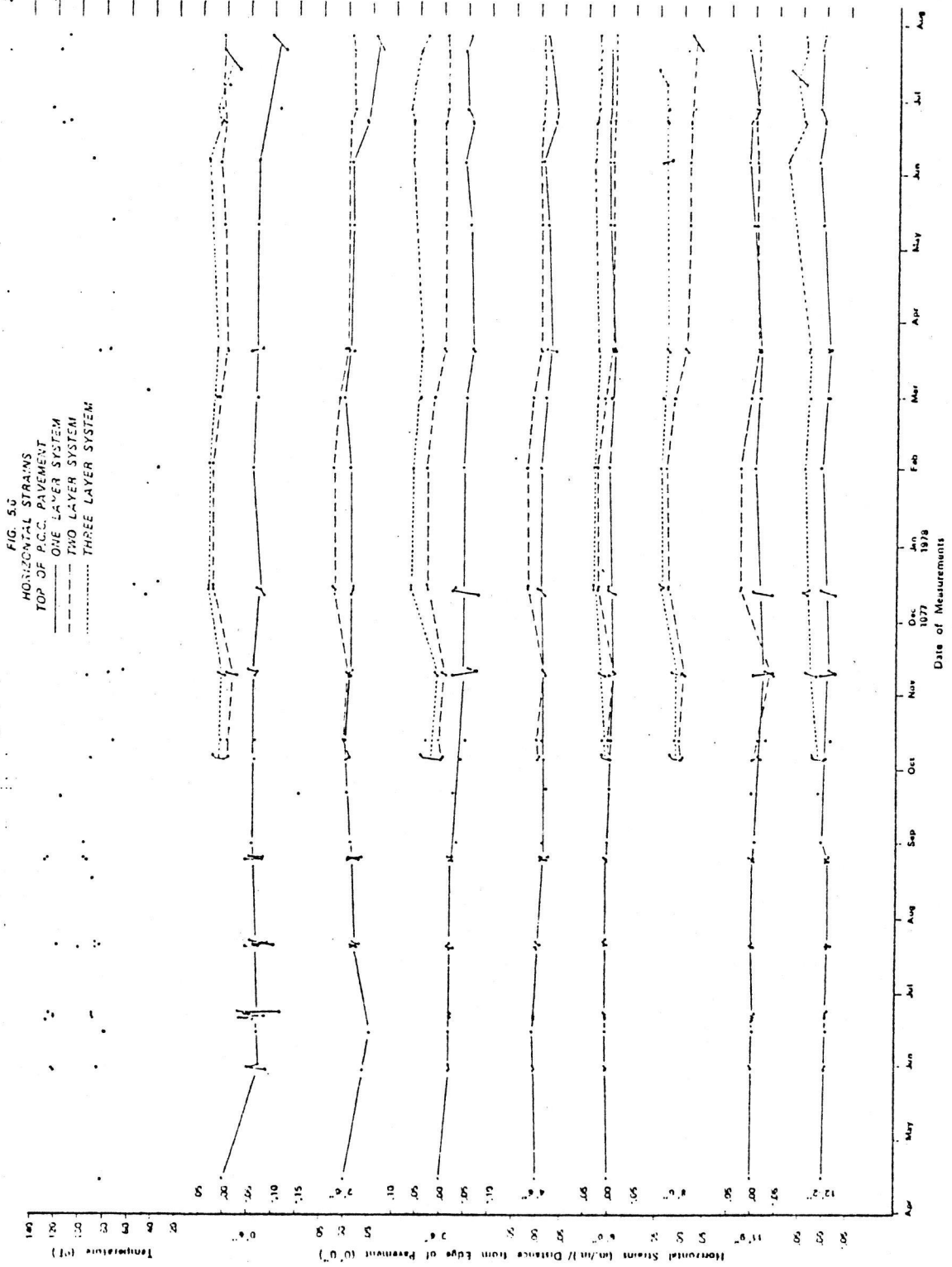
During overlay construction of the open-graded course the sensors at location 11'-9" were damaged and had to be replaced. A small area of the open-graded material had to be removed in order to replace the sensors. The open-graded material was replaced by hand and tamped

in place. This small area was not rolled until after the binder course had been placed. The sensors set on top of the open-graded layer may not have been stable and may have been subjected to rocking under small movements. This rocking may be the reason for the large variation in movements on consecutive days as indicated by the October and November readings. When the sensors did stabilize their orientations may have been in misalignment with their respective sensor pair. Large misalignments through rotation or lateral translation or a combination of both would result in observed movements being larger than the actual movements.

E. HORIZONTAL STRAINS - TOP OF PCC PAVEMENT

In Figures 5.6, 5.7, and 5.8, various horizontal strain versus time plots are presented. Horizontal strains were plotted rather than horizontal movements because of the different gage lengths between the various coplanar sensor pairs. The differences in gage lengths were due to the difficulty in placing the coring rig exactly over the locations marked for the extensometers. The two inches in diameter sensor which is part of the top half assembly of the extensometer is also one of the coplanar sensor pair across the joint on top of the PCC pavement. Consequently, the distances between coplanar pairs vary from about four and one-half inches to six and one-half inches. Therefore, the strains provide a better representative value for comparison.

Figure 5.6 shows horizontal strain versus time plots for the one, two, and three layer test sites at each location along the joint on top of the PCC pavement. Since the joints at each of the three locations were initially approximately one inch wide, the strains can be inter-



preted as opening and closing movements of the joint in the PCC pavement. Positive and negative strains, respectively, indicate opening and closing of the joint relative to the data base.

1. ONE LAYER SYSTEM - From April through mid-June, 1977, the movements at locations 0'-6", 2'-6", and 3'-6" indicate that the joint was closing. This would be expected for that time period because the increase in the average temperature of the pavement would cause expansion of the slabs on each side of the joint and thereby cause closing of the joint. However, the magnitude of closing is largest at location 0'-6" and becomes progressively smaller as the distance from the edge increases until beyond location 3'-6", where there was virtually no movement. At location 0'-6", the magnitude of movement was approximately -0.10 inch, at location 2'-6" approximately -0.05 inch, and at location 3'-6" approximately -0.02 inch. The magnitudes of movements at all the other locations were less than 0.01 inch. As the warming trend continued through August of 1977, the movements indicate that the joint began reopening at locations 0'-6" and 2'-6", contrary to what would be expected. Other than the joint closing 0.01 inch at location 4'-6", no movements occurred at the other locations. From September of 1977 through June of 1978 all of the locations indicate very little movement with the maximum being about 0.02 inch. From June through August of 1978, the joint at locations 0'-6" and 2'-6" were closed back to their approximate magnitudes of the June 1977 closings. They now show magnitudes of -0.11 inch at location 0'-6" and -0.06 inch at location 2'-6". The magnitude of movement still decreases away from the edge. At location 3'-6" the movement is approximately -0.05 inch, at location 4'-6" approximately -0.02 inch, at loca-

tion 6'-0" none, and at 11'-9" approximately +0.01 inch.

2. TWO LAYER SYSTEM - The reaction of closing and opening of the joint due to seasonal changes in temperature was consistent in pattern and magnitude at all locations along the joint. As the temperature decreased from November through December the joint opened due to the contraction of the pavement slabs. The magnitudes of opening at all locations were between 0.02 and 0.04 inch. Then as the temperature began increasing in March, the joint slowly closed to its approximate original spacing.

3. THREE LAYER SYSTEM - The pattern of the joint movements was similar at all locations along the joint. From November through December the joint expanded from 0.03 to 0.05 inch at all locations due to the contraction of the pavement slabs as the temperature decreased. But during the warming trend from March through July, the pavement apparently did not expand and the joint has remained opened. Since the three layer test site is overlaid with the open-graded course, it is believed that due to rolling of each overlay course and due to repeated traffic loads, some of the large aggregates have been forced into the joint, and thereby prevented the slabs from expanding and closing the joint.

4. COMPARISON OF HORIZONTAL STRAINS - The horizontal strains, or movements in this case, across the joint on top of the PCC pavement were consistently greatest for the three layer system and consistently smallest for the one layer system. Perhaps the greater thicknesses of overlay allow the overlaid pavement to retain maximum high or cold temperatures for longer periods of time, which, in turn, would allow more time for the slab to expand or contract at that temperature.

F. HORIZONTAL STRAINS - TOP OF OPEN-GRADE

1. THREE LAYER SYSTEM - In Figure 5.7 it can be seen that expansion strains developed over the joint at the top of the open-graded layer as the temperature decreased from November through December. Magnitudes of strains varied along the joint from 0.02 to 0.05 inch per inch. These expansion strains were probably induced by the contraction of the underlying pavement. Although some reversal in strain occurred as the temperature increased in March, by July most of the locations along the joint had retained expansion strains. This would be expected since it was observed in Figure 5.6 that the joint in the underlying pavement remained opened.

G. HORIZONTAL STRAINS - TOP OF BINDER

1. TWO LAYER SYSTEM - Figure 5.8 shows a similar pattern of strains on top of the binder layer as was observed in Figure 5.6 for the top of the PCC pavement. As the temperature decreased from November to December, expansion strains developed at all locations along the joint. The magnitudes of expansion strains were approximately +0.02 inch per inch at all locations. As the temperature increased in March, reversals in strains of magnitudes slightly less than -0.02 inch per inch occurred. But then, from April through July all locations along the joint, except at 4'-6" show the development of gradual expansion strains while the temperature continues its warming trend. It appears evident that other factors, not known at this time, other than temperature changes are creating movements in the overlay structure.

2. THREE LAYER SYSTEM - The discontinued curves for the three layer system in Figure 5.8 are the result of the sensors at those locations

FIG. 57
HORIZONTAL STRAINS
TCP OF OPEN-GRADED COURSE,
THREE LAYER SYSTEM

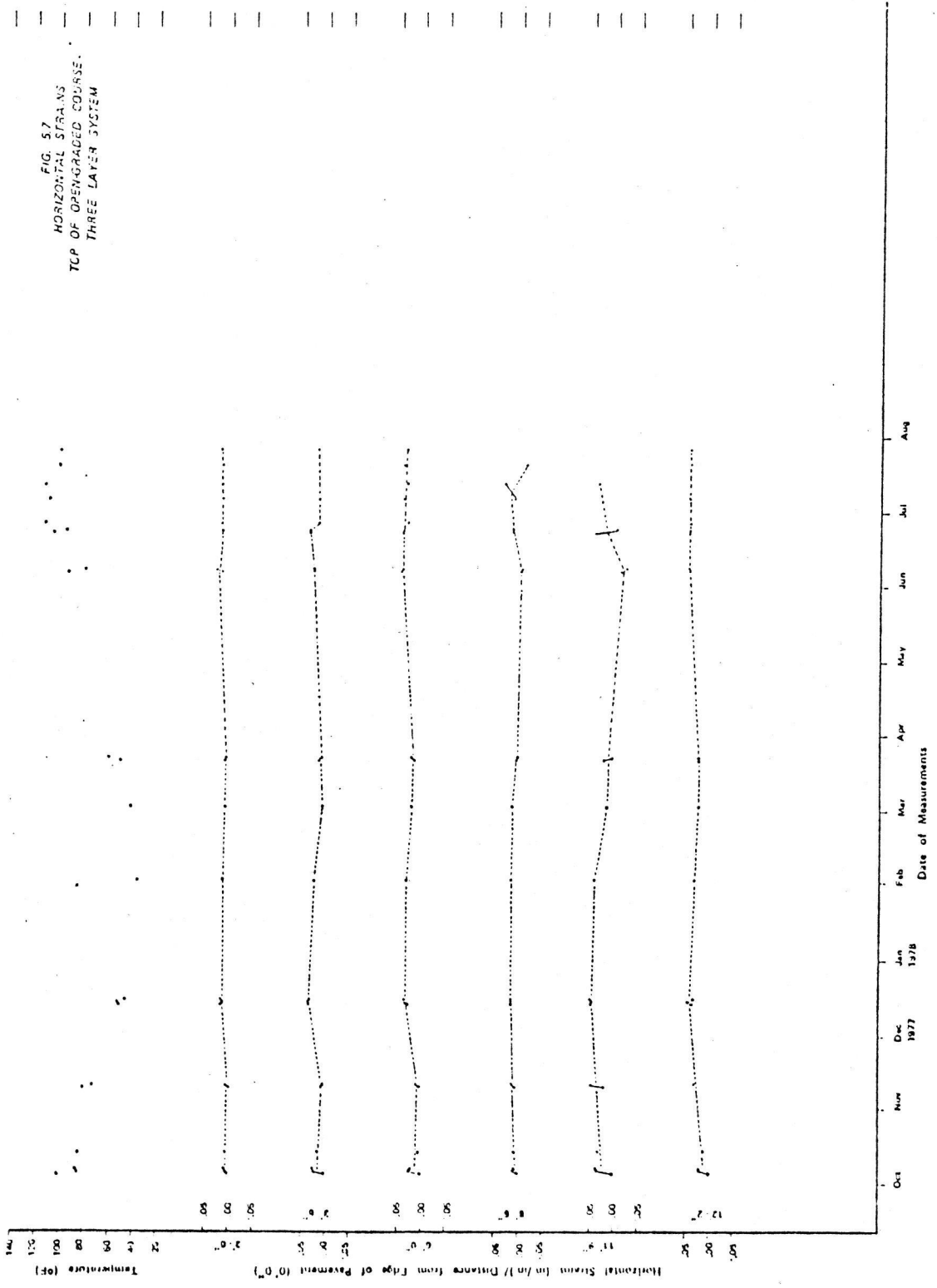
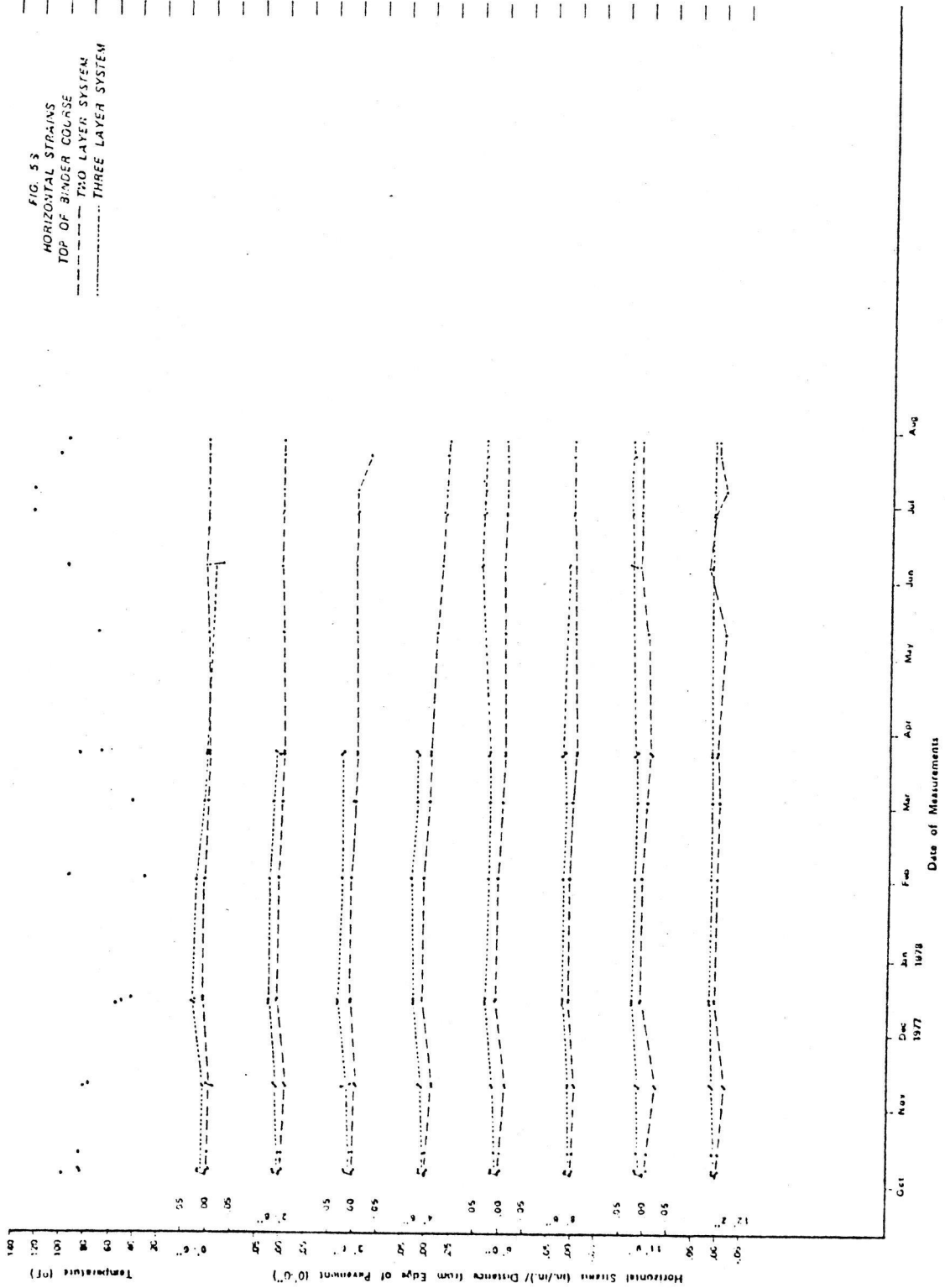


FIG. 53
HORIZONTAL STRAINS
TOP OF BINDER COURSE
--- TWO LAYER SYSTEM
- - - THREE LAYER SYSTEM



becoming inoperative. The basic pattern of strains which developed across the joint on top of the pavement and on top of the open-graded layer are again present on top of the binder. Expansion strains occurred as the temperature decreased from November through December. As the temperature increased from March through July, only at location 0'-6" from the edge is there indication of a reversal in the strains. All other locations indicate a retention of the expansion strains. Similar to the top of the open-graded layer, since the overlaid joint in the pavement remained opened when temperatures increased, then it would be expected that the top of the binder layer would retain expansion strains.

3. COMPARISON OF HORIZONTAL STRAINS - The horizontal strains across the joint on top of the binder layer were larger for the three layer system than they were for the two layer system. The same observation was made across the joint on top of the PCC pavement. It is evident from the data that the movements on top of the binder course of the two layer system and that the movements on top of the binder and open-graded courses of the three layer system are related to the movements of the overlaid joints in the PCC pavement.

H. PROCEDURE - DYNAMIC DATA ACQUISITION

Dynamic data were taken using the PDAS to record pavement deformations as vehicles with various axle loadings passed over the instrumented sections. Several passes at different speeds were made by each vehicle. It was necessary to block off the outside lane of Interstate 30 during the data acquisition.

1. VEHICLES AND AXLE LOADS - Several different vehicle configurations and weights were selected in cooperation with the Design Division of the Arkansas State Highway and Transportation Department. These are as follows:

1. Trucks with two single axles, with axle loads as follows:

	<u>Steering Axle</u>	<u>Drive Axle</u>
a.	8 kips	14 kips
b.	12 "	18 "
c.	12 "	20 "

2. Trucks with a single steering axle and a tandem drive axle, with axle loads as follows:

	<u>Steering Axle</u>	<u>Drive Axle</u>
a.	12 kips	28 kips
b.	12 "	32 "
c.	12 "	34 "

3. Tractor-trailor with single axles, with axle loads as follows:

	<u>Steering Axle</u>	<u>Drive Axle</u>	<u>Rear Axle</u>
a.	8 kips	16 kips	16 kips
b.	12 "	18 "	18 "
c.	12 "	20 "	20 "

4. Tractor-trailor with tandem drive and rear axles, with axle loads as follows:

	<u>Steering Axle</u>	<u>Drive Axle</u>	<u>Rear Axle</u>
a.	12 kips	28 kips	28 kips
b.	9 "	32 "	32 "
c.	12 "	34 "	34 "

5. A small truck with a gross weight of about 10 kips.
6. A full-size automobile with a gross weight of about 5 kips.

2. VEHICLE SPEEDS - It was planned that each vehicle configuration and weight would pass over the test section at 70 mph, 55 mph, 30 mph, and 5 mph. Due to the location of entrance ramps and the undesirability of blocking entrance ramps and the presence of uphill grades near some test sections, it was not possible to achieve the higher speeds with the more heavily loaded trucks.

3. FOIL SHIELDING - Preliminary tests on the instrumented sections showed a significant amount of interference with signals from the induction coils due to the ignition systems of gasoline engines. Diesel engines did not produce measurable interference. Experimentation showed that aluminum foil was effective in preventing ignition interference and a three-foot wide strip was placed across the traffic lane above the sensors prior to each series of tests.

4. TAPE SWITCHES - The starting and stopping of the data acquisition was controlled by tapeswitches placed across the roadway. Preliminary tests indicated the optimum location of the start tapeswitch was 20 feet from the instrumented section and a spacing of 100 feet between tapeswitches was adequate to gather the required data. The spacing was input through the keyboard of the PDAS and was used along with the elapsed time between start and stop to compute actual vehicle speed.

5. TEMPERATURE - Temperature readings were taken periodically with a battery-operated analog meter and entered through the keyboard of the PDAS. This data was displayed and recorded for information only and did not enter into the computations of deformations.

6. INITIAL SPACING - Each time the PDAS was set up to acquire dynamic data, the initial spacings, both coaxial and coplanar, were determined for all adjacent pairs of induction coils. The initial spacing data was obtained with the Bison single channel battery-operated meter. This data was entered through the keyboard of the PDAS and was used along with stored calibration data to determine the dynamic deformations. The calibration data was a table of change in spacing per unit change in voltage as a function of distance between coils.

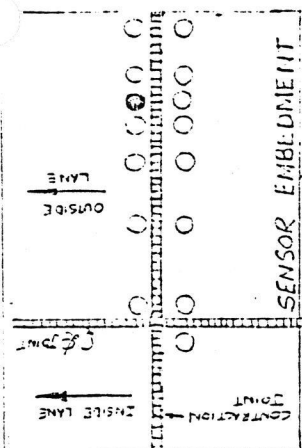
7. SENSOR CONNECTIONS - The leads from the sensors were connected by coaxial cable to a terminal block on the outside of the van housing the PDAS. All of the coil pairs could not be energized simultaneously because of interference between adjacent pairs. It was therefore necessary for the vehicles to make multiple passes at the same speed and weight with different pairs of coils energized on each pass in order to gather all of the desired data.

I. DATA REDUCTION

A complete guide to data reduction using PDRS (Pavement Data Reduction System) has been furnished to the Research Section, Arkansas State Highway and Transportation Department. This 181 page guide documents the programs and JCL statements required to take the field data tapes and process them to obtain printed and plotted output. No further discussion of this topic is required here.

J. RESULTS OF DYNAMIC DATA ACQUISITION

During the period of July 9, 1983, through July 24, 1980, 307 passes of vehicles across the instrumented sections were recorded. On each pass, data was recorded from approximately sixteen pairs of induction coils at the rate of 2,000 data points per second. During subsequent test periods, less data was obtained because fewer different axle loads were used and because some sensors had ceased to function. Between January 27, 1981, and January 29, 1981, 135 passes were recorded and 58 passes were recorded on August 17 and 18, 1981. Because of the large amount of data, only typical results will be presented. The data tapes are available for use upon request by the Arkansas State Highway and Transportation Department. Figures 5.1 through 5.35 show the results of the dynamic data acquisition without any smoothing or enhancement of the data.



SENTON ONE LAYER DATE-7 /23/80
 TRUCK WITH TWO SINGLE AXLES
 VEHICLE SPEED =22MPH
 PAVEMENT TEMPERATURES (F) ---LAYER 1= , LAYER 2= , LAYER 3= , LAYER 4=
 EXTENSOMETER SETUP WITH 1 INCH COIL TRANSMITTING
 TRANSMITTING SENSOR IS #20 RECEIVING SENSOR IS #19 RUN 87 CHANNEL 4
 PORS3

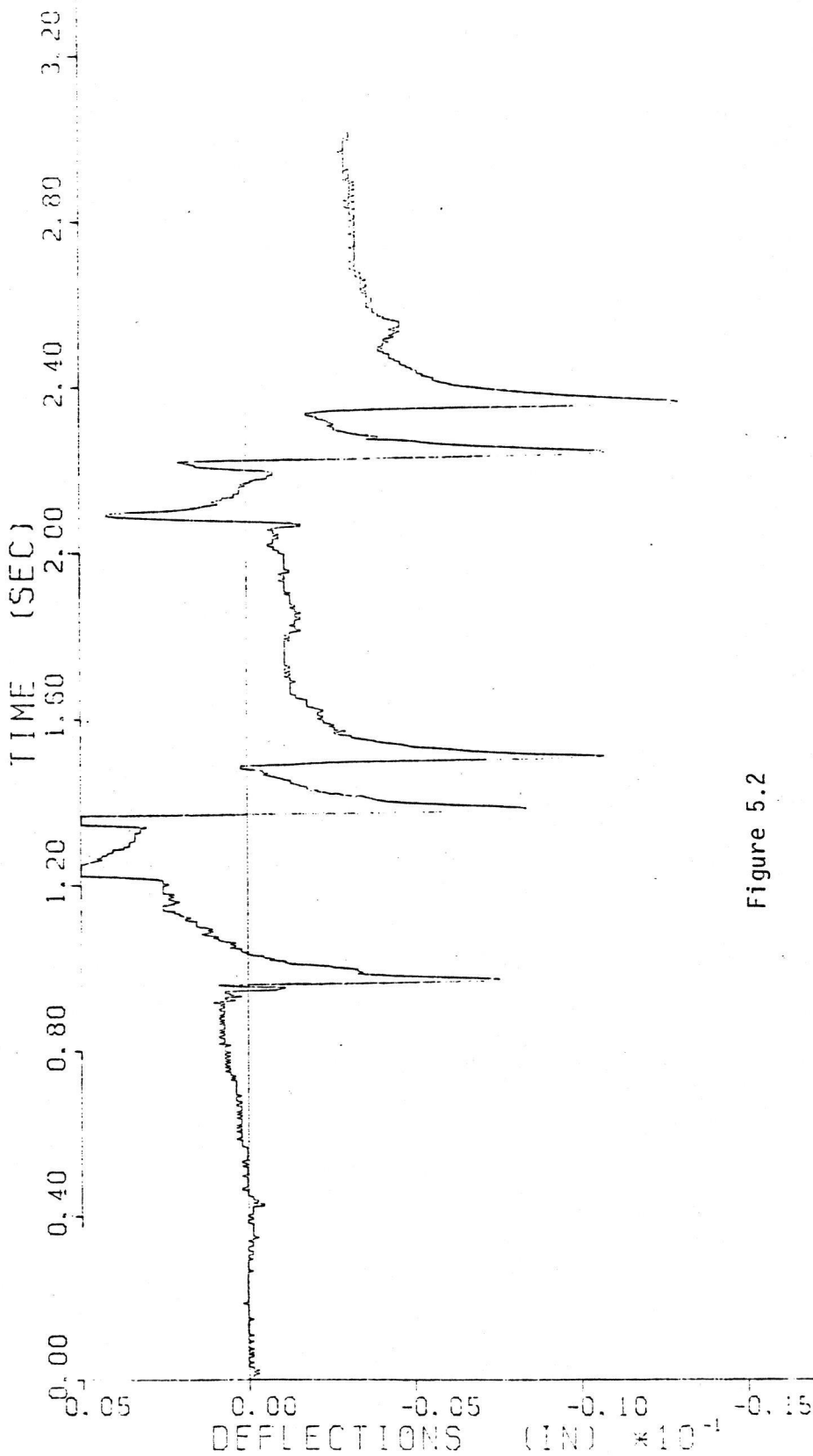


Figure 5.2

BENTON ONE LAYER
 TRUCK WITH TWO SINGLE AXLES
 DATE-7 /23/80
 VEHICLE SPEED =22MPH
 AXLE LOADS (KIPS) ---7/14
 PAVEMENT TEMPERATURES (F) ---LAYER 1= . LAYER 2= . LAYER 3= . LAYER 4=
 EXTENSOMETER SETUP WITH 2 INCH COIL TRANSMITTING
 TRANSMITTING SENSOR IS #24 RECEIVING SENSOR IS #25

RUN 87 CHANNEL 6
 POPS3

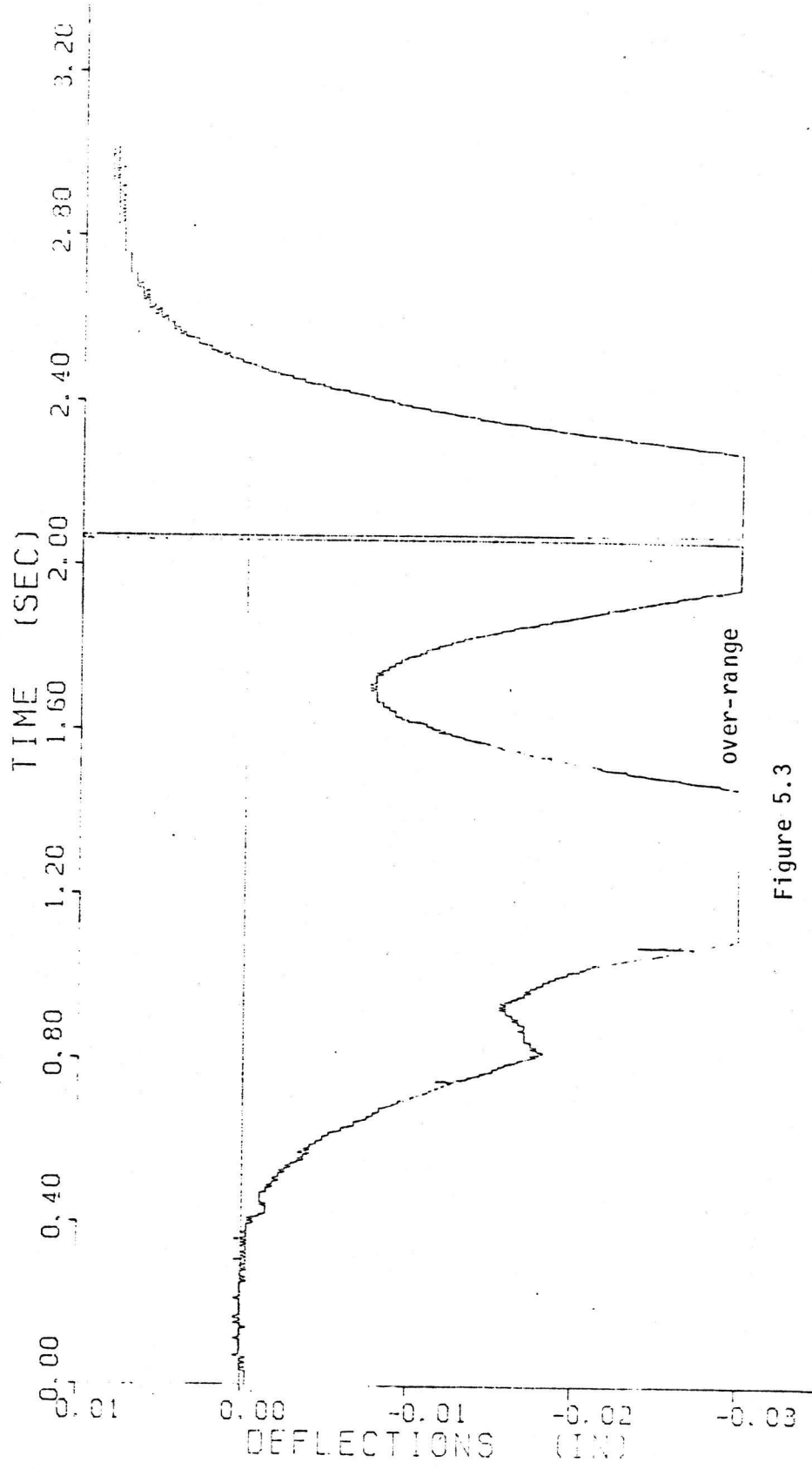
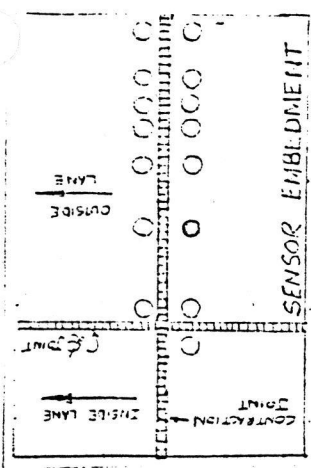


Figure 5.3

SECTION ONE LAYER
 TRACTOR-TRAILER WITH TANDEM DRIVE AND REAR AXLES
 VEHICLE SPEED =21MPH
 AXLE LOADS (KIPS) ---7/32/32
 PAVEMENT TEMPERATURES (F) ---LAYER 1= . LAYER 2= . LAYER 3= . LAYER 4=
 EXTENSOMETER SETUP WITH 2 INCH COIL TRANSMITTING
 TRANSMITTING SENSOR IS #24 RECEIVING SENSOR IS #25

RUN 71 CHANNEL 6
 15 PDAS3

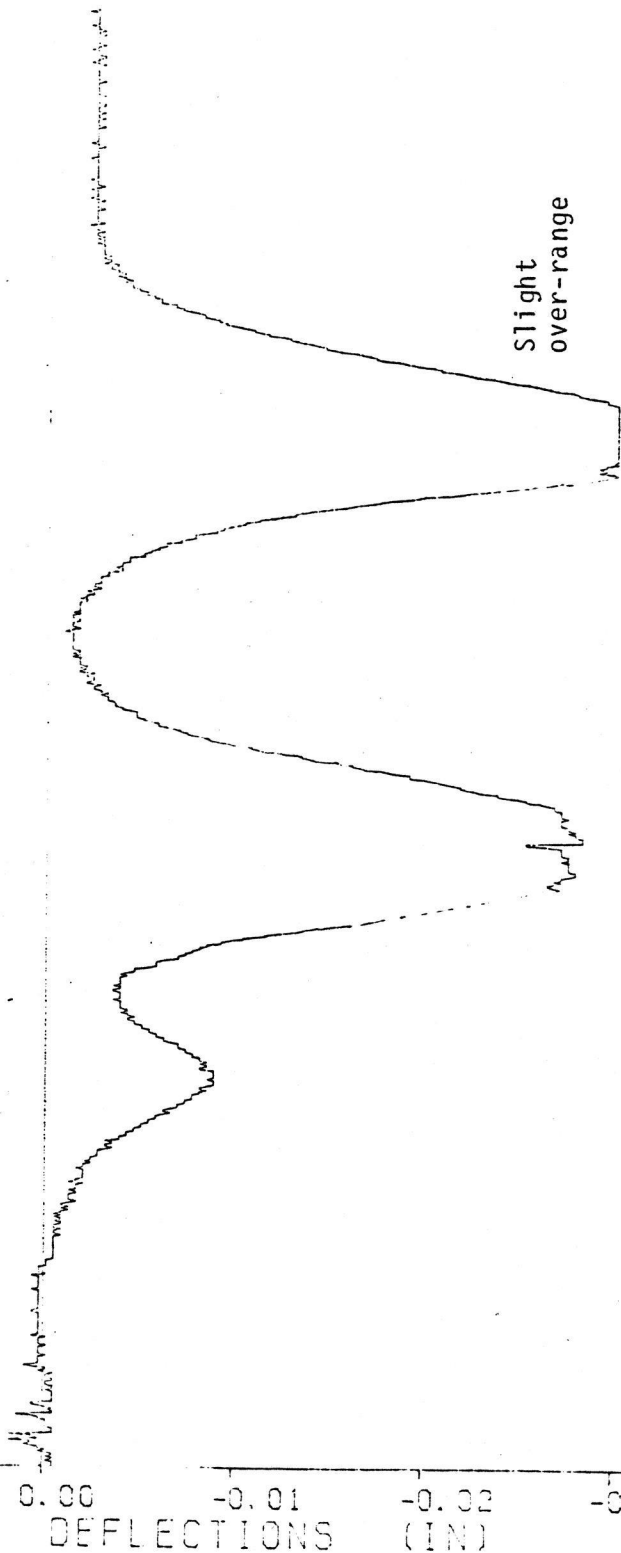
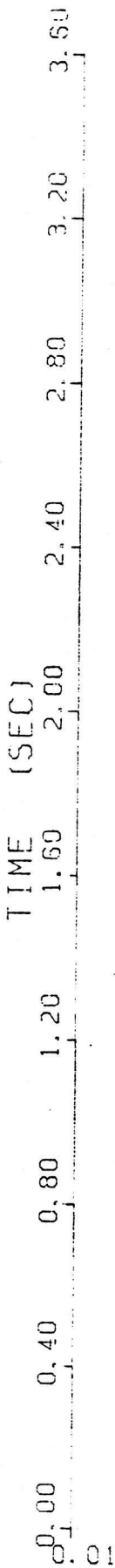
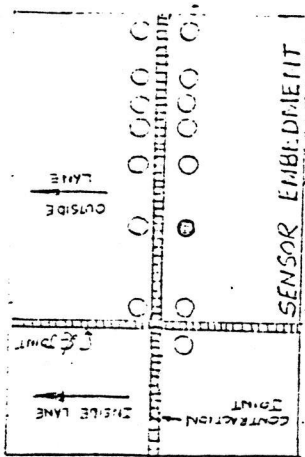


Figure 5.4

BENTON ONE LAYER

TRACTOR-TRAILER WITH TANDEM DRIVE AND REAR AXLES

VEHICLE SPEED =20MPH

AXLE LOADS (KIPS) ---7/34/34

PAVEMENT TEMPERATURES (F) ---LAYER 1= , LAYER 2= , LAYER 3= , LAYER 4=

EXTENSOMETER SETUP WITH 2 INCH COIL TRANSMITTING

TRANSMITTING SENSOR IS #24

RECEIVING SENSOR IS #25

RUN 31 CHANNEL 6

25 P0AS3

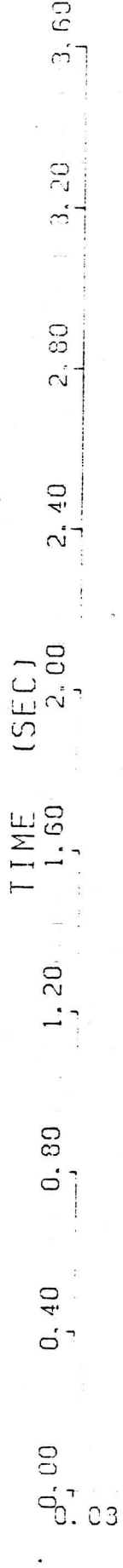
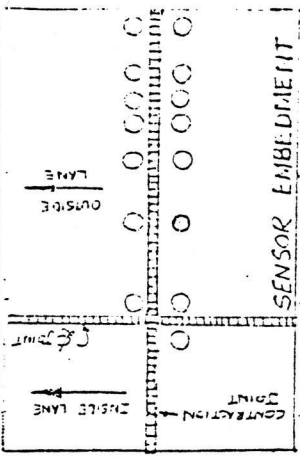


Figure 5.5

BEITON TWO LAYER DATE -7 /10/80
 A FULL-SIZE AUTOMOBILE WITH A GROSS WEIGHT OF ABOUT 5 KIPS
 VEHICLE SPEED =8 MPH AXLE LOADS (KIPS) ---1620/1570
 PAYEMENT TEMPERATURES (F) ---LAYER 1= , LAYER 2= , LAYER 3= , LAYER 4=
 EXTENSOMETER SETUP WITH 2 INCH COIL TRANSMITTING
 TRANSMITTING SENSOR IS #19 RECEIVING SENSOR IS #20 RUN 46 CHANNEL 5

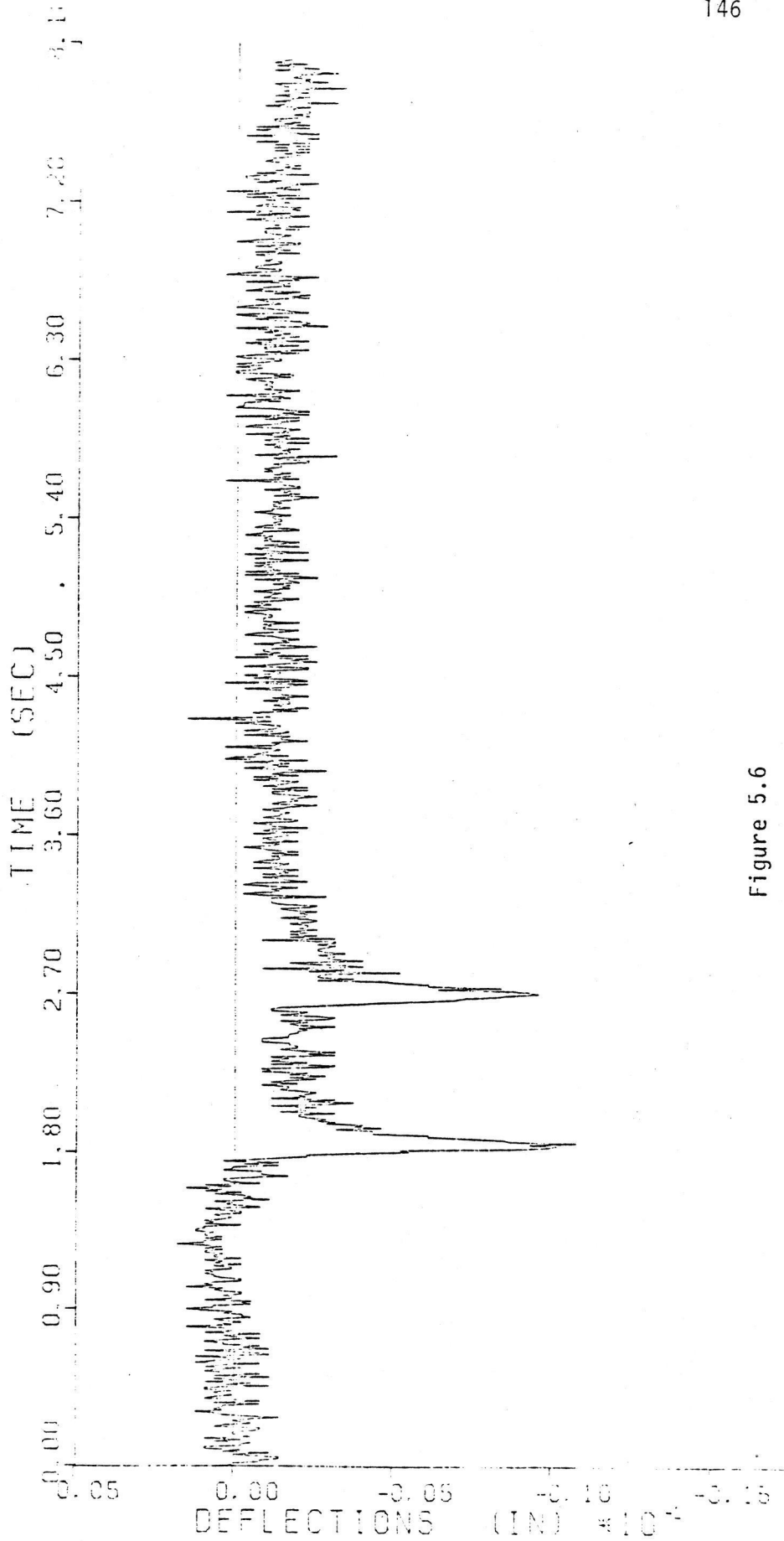
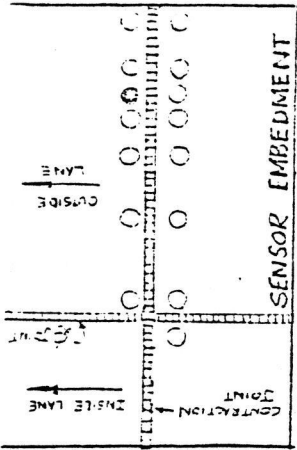


Figure 5.6

BEHTON TWO LAYER DATE -7 /10/80
 A FULL-SIZE AUTOMOBILE WITH A GROSS WEIGHT OF ABOUT 5 KIPS
 VEHICLE SPEED =8 MPH AXLE LOADS (KIPS) ---1620/1570
 PAYEMENT TEMPERATURES (F) ---LAYER 1= .LAYER 2= .LAYER 3= .LAYER 4=
 EXTENSOMETER SETUP WITH 2 INCH COIL TRANSMITTING
 TRANSMITTING SENSOR IS #29 RECEIVING SENSOR IS #30 RUN 46 CHANNEL 13

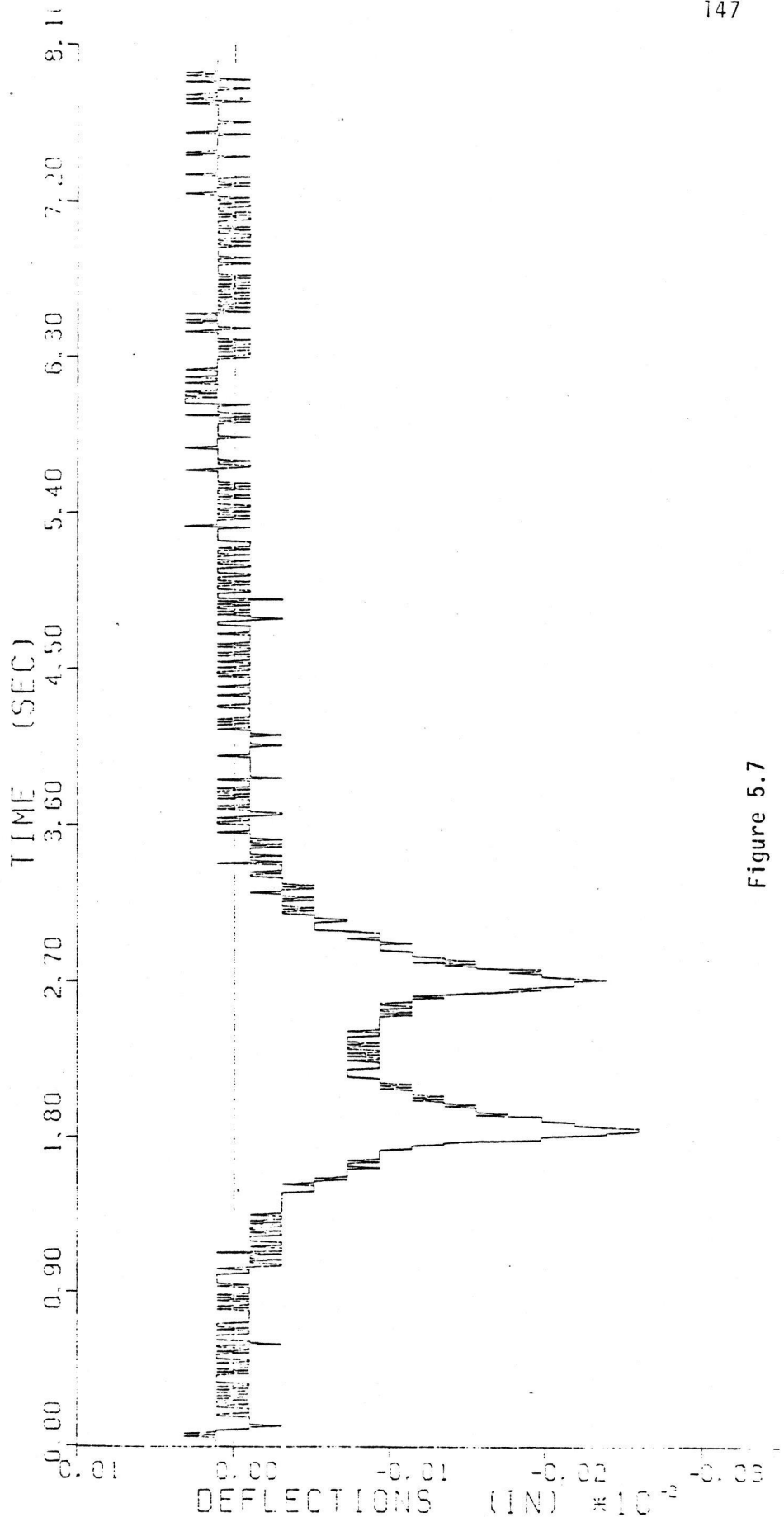
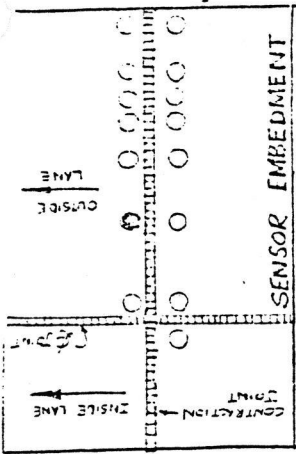


Figure 5.7

SENTON TWO LAYER DATE-7 /10/80
 A FULL-SIZE AUTOMOBILE WITH A GROSS WEIGHT OF ABOUT 5 KIPS
 VEHICLE SPEED =30MPH AXLE LOADS (KIPS) ---1620/1570
 PAVEMENT TEMPERATURES (F) ---LAYER 1= .LAYER 2= .LAYER 3= .LAYER 4=
 EXTENSOMETER SETUP WITH 2 INCH COIL TRANSMITTING
 TRANSMITTING SENSOR IS #29 RECEIVING SENSOR IS #30 RUN 48 CHANNEL 13

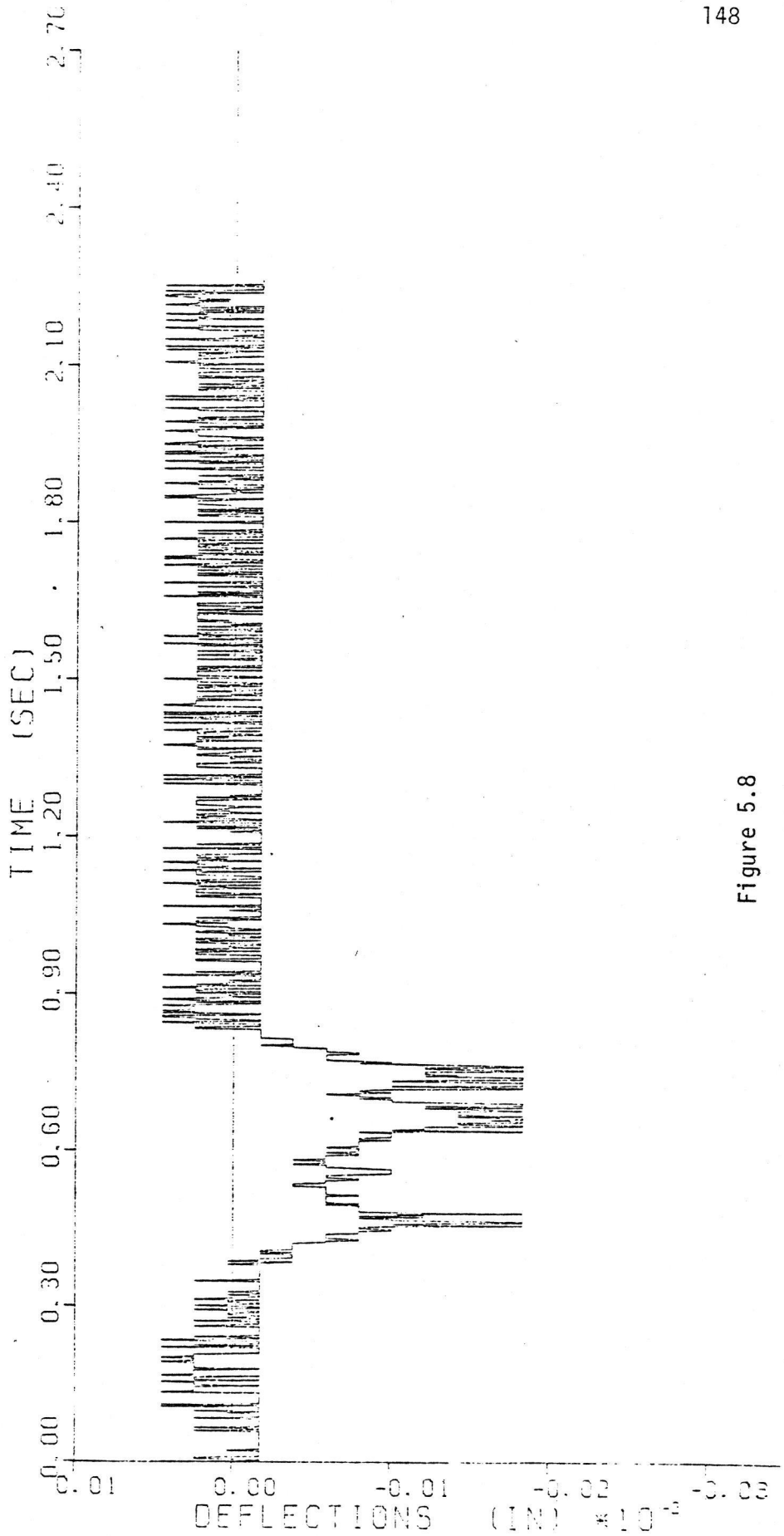
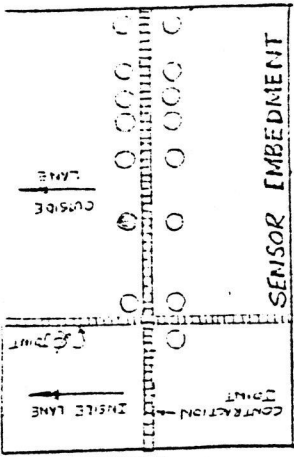


Figure 5.8

BENTON TWO LAYER DATE -7 /10/80
 A SMALL TRUCK WITH A GROSS WEIGHT OF ABOUT 10 KIPS
 VEHICLE SPEED =7 MPH AXLE LOADS (KIPS) ---2550/5200
 PAVEMENT TEMPERATURES (F) ---LAYER 1= .LAYER 2= .LAYER 3= .LAYER 4=
 EXTENSOMETER SETUP WITH 2 INCH COIL TRANSMITTING
 TRANSMITTING SENSOR IS #14 RECEIVING SENSOR IS #15 RUN 59 CHANNEL 7

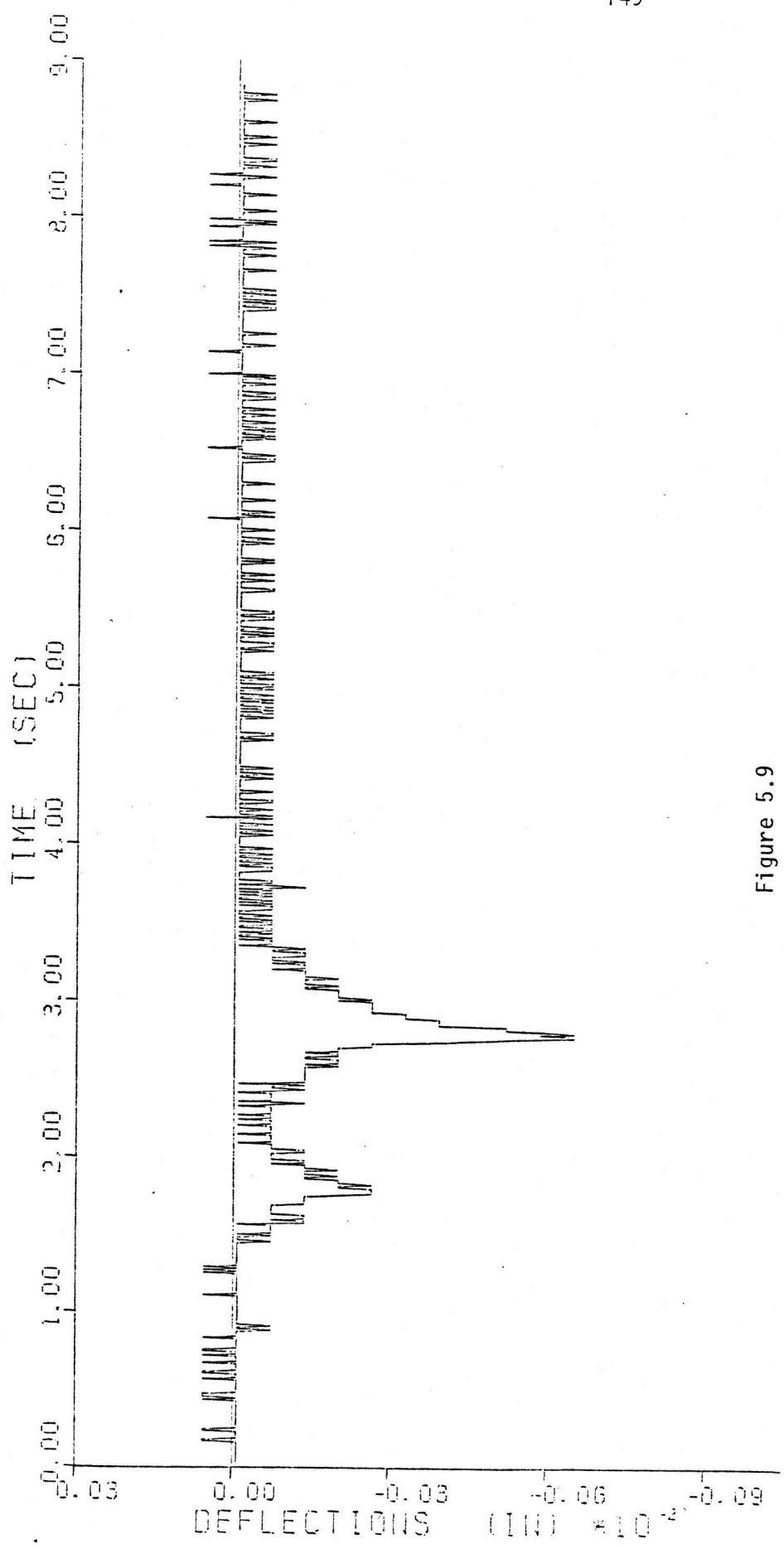
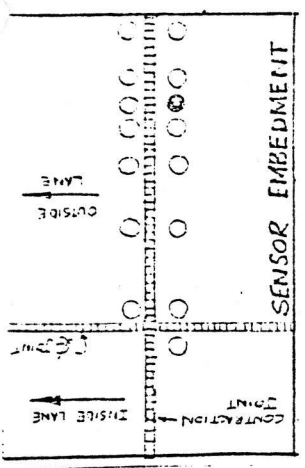
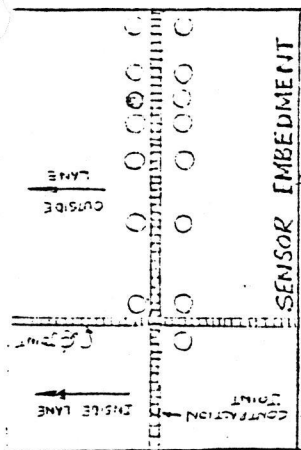


Figure 5.9

BENTON TWO LAYER DATE-7 /10/80
 A SMALL TRUCK WITH A GROSS WEIGHT OF ABOUT 10 KIPS
 VEHICLE SPEED =7 MPH AXLE LOADS (KIPS) ----2550/5200
 PAVEMENT TEMPERATURES (F) --LAYER 1= . LAYER 2= . LAYER 3= . LAYER 4=
 EXTENSOMETER SETUP WITH 2 INCH COIL TRANSMITTING
 TRANSMITTING SENSOR IS #19 RECEIVING SENSOR IS #20 RUN 38 CHANNEL 6
 PDASI



TIME (SEC)	DEFLECTIONS (IN) $\times 10^{-2}$
0.00	0.00
1.20	0.00
2.40	0.00
3.60	-0.03
4.80	-0.06
6.00	-0.06
7.20	-0.06
8.40	-0.06
9.60	-0.06
10.80	-0.06

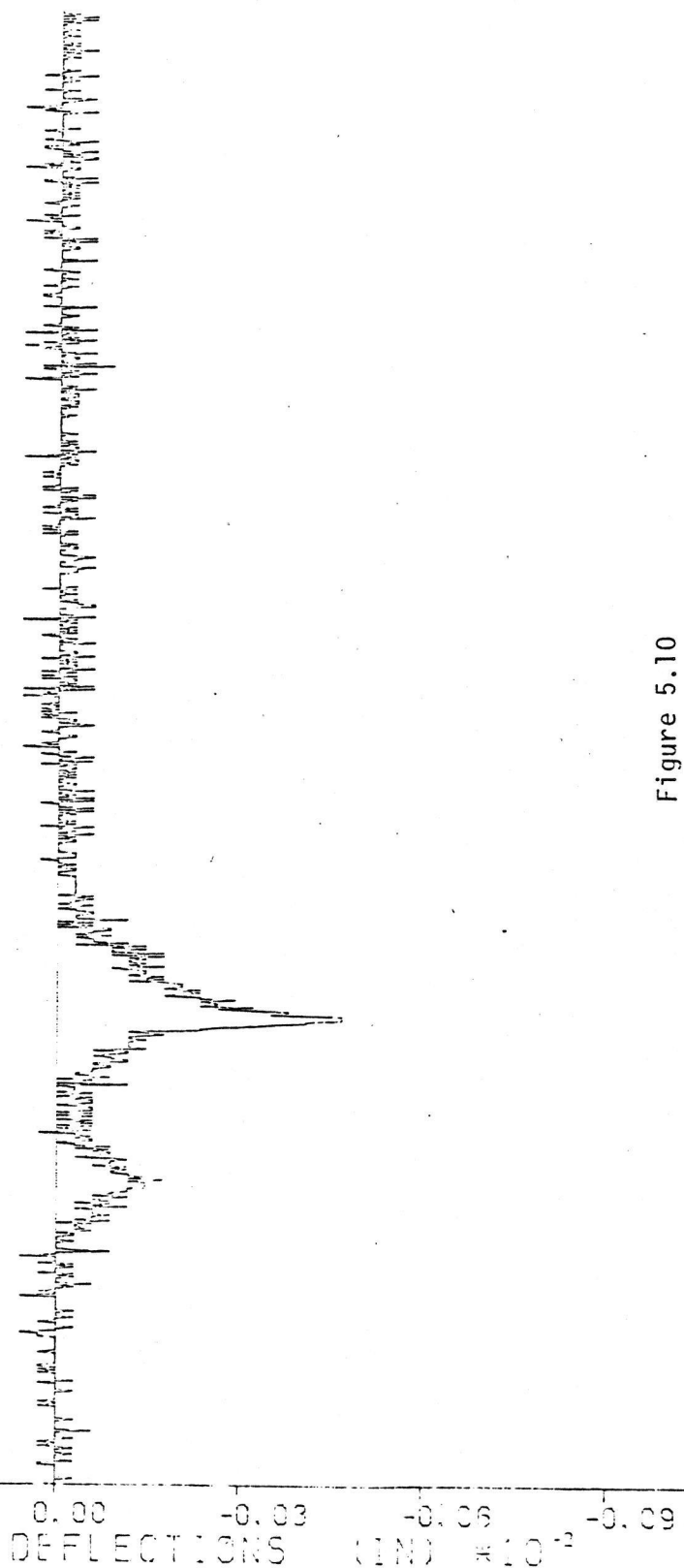
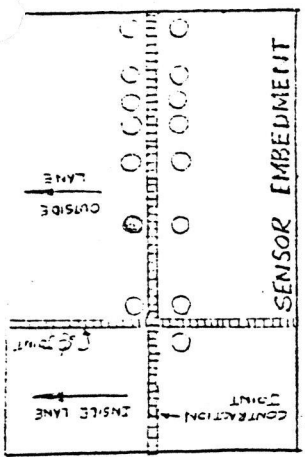


Figure 5.10



BENTON TWO LAYER DATE -7 /10/80
 A SMALL TRUCK WITH A GROSS WEIGHT OF ABOUT 10 KIPS
 VEHICLE SPEED =7 MPH AXLE LOADS (KIPS) ---2550/5200
 PAYEMENT TEMPERATURES (F) ---LAYER 1= .LAYER 2= .LAYER 3= .LAYER 4=
 EXTENSOMETER SETUP WITH 2 INCH COIL TRANSMITTING
 TRANSMITTING SENSOR IS #29 RECEIVING SENSOR IS #30 RUN 38 CHANNEL 13

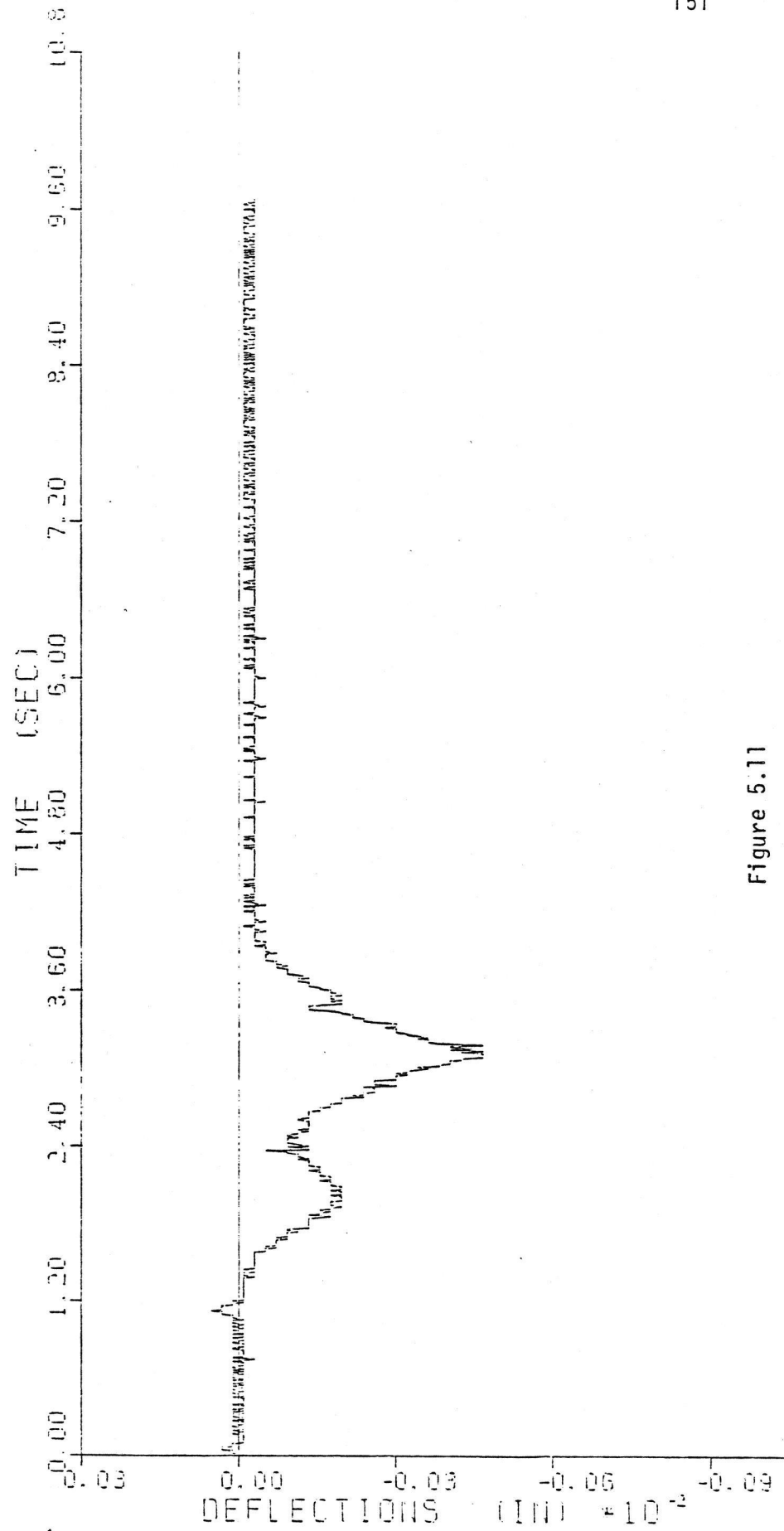


Figure 5.11

SECTION TWO LAYER
A SMALL TRUCK WITH A GROSS WEIGHT OF ABOUT 10,000 LBS

DATE-7 /10/80

TRANSMITTING SENSOR IS #19 RECEIVING SENSOR IS #20 RUN 40 CHANNEL 6
LAYER 2= , LAYER 3= , LAYER 4=

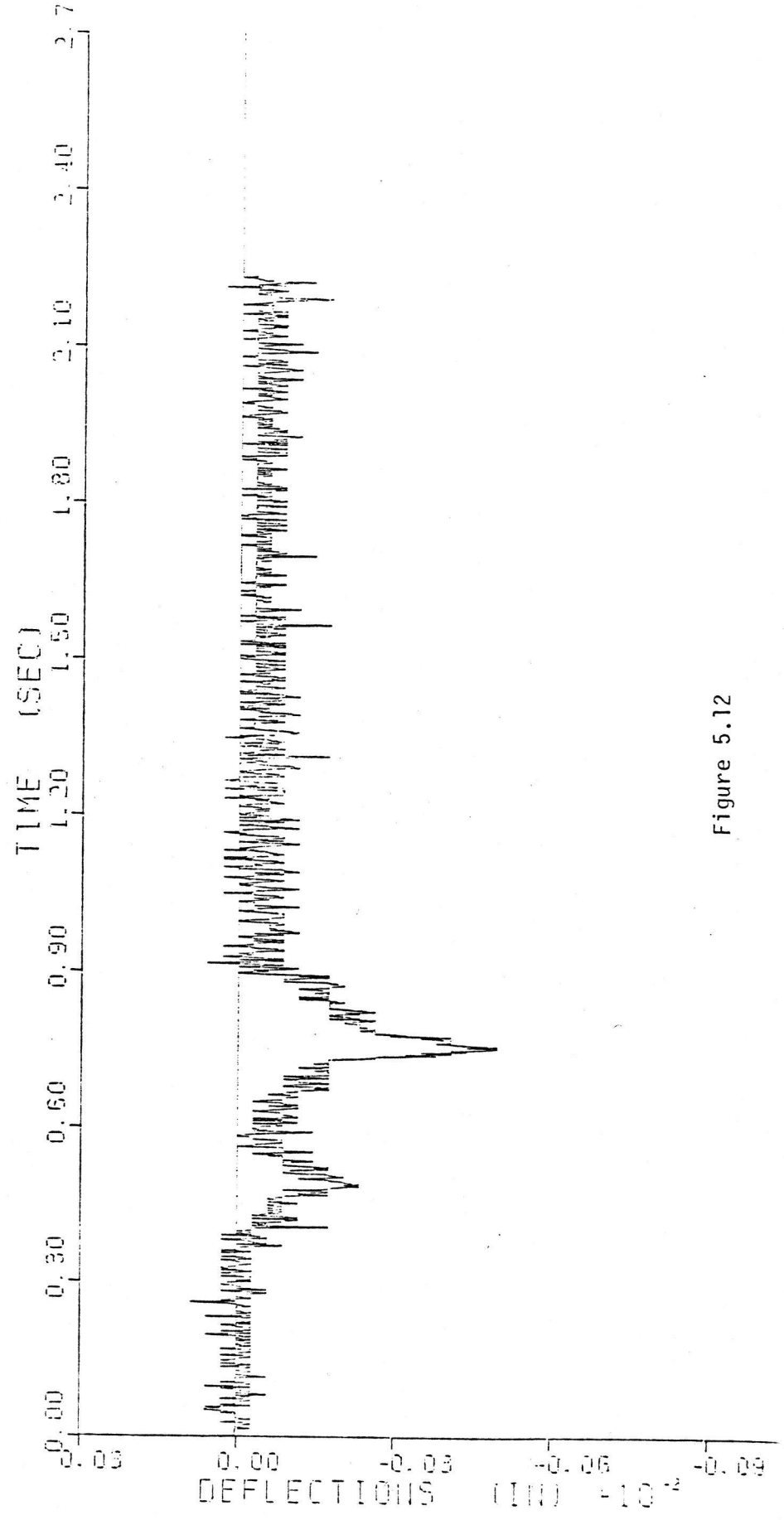
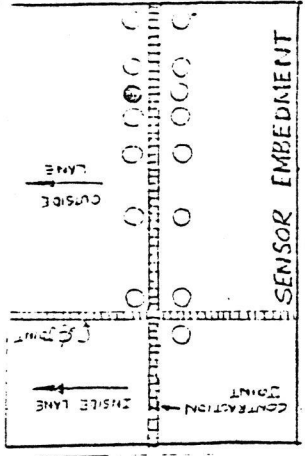


Figure 5.12

BEHION TWO LAYER
 A SMALL TRUCK WITH A GROSS WEIGHT OF ABOUT 10 KIPS
 VEHICLE SPEED =29MPH
 AXLE LOADS (KIPS) ---2550/5200
 PAVEMENT TEMPERATURES (F) ---LAYER 1= . LAYER 2= . LAYER 3= . LAYER 4= .
 EXTENSOMETER SETUP WITH 2 INCH COIL TRANSMITTING
 TRANSMITTING SENSOR IS #29 RECEIVING SENSOR IS #30 RUN 40 CHANNEL 13

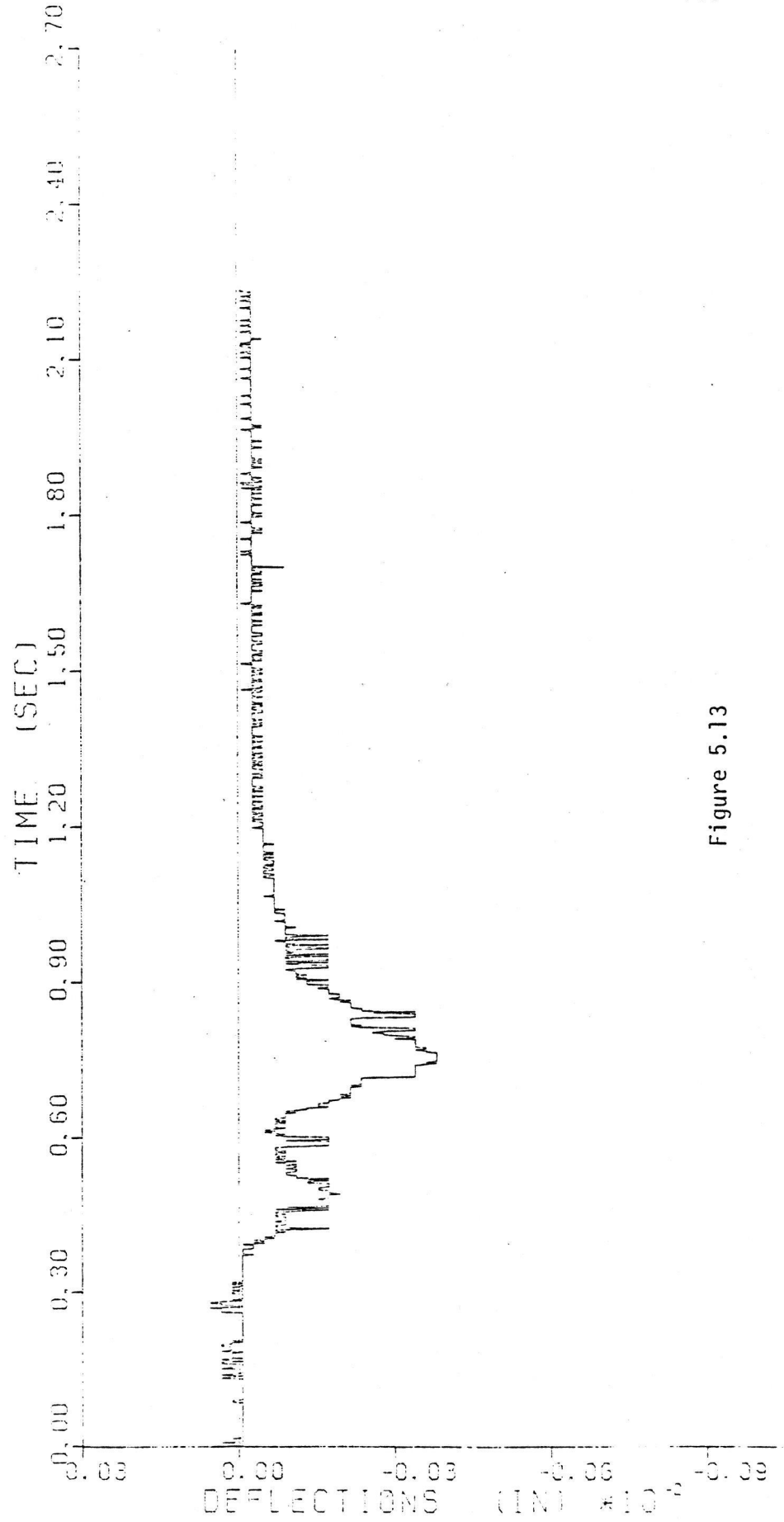
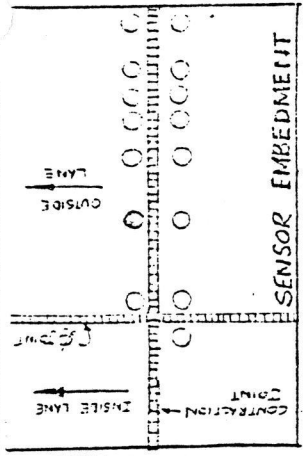


Figure 5.13

BENTON TWO LAYER
 A SMALL TRUCK WITH A GROSS WEIGHT OF ABOUT 10 KIPS
 VEHICLE SPEED = 53MPH
 AXLE LOADS (KIPS) ---2550/5200
 PAVEMENT TEMPERATURES (F) ---LAYER 1= . LAYER 2= . LAYER 3= . LAYER 4=
 EXTENSOMETER SETUP WITH 2 INCH COIL TRANSMITTING
 TRANSMITTING SENSOR IS #29 RECEIVING SENSOR IS #30 RUN 42 CHANNEL 13

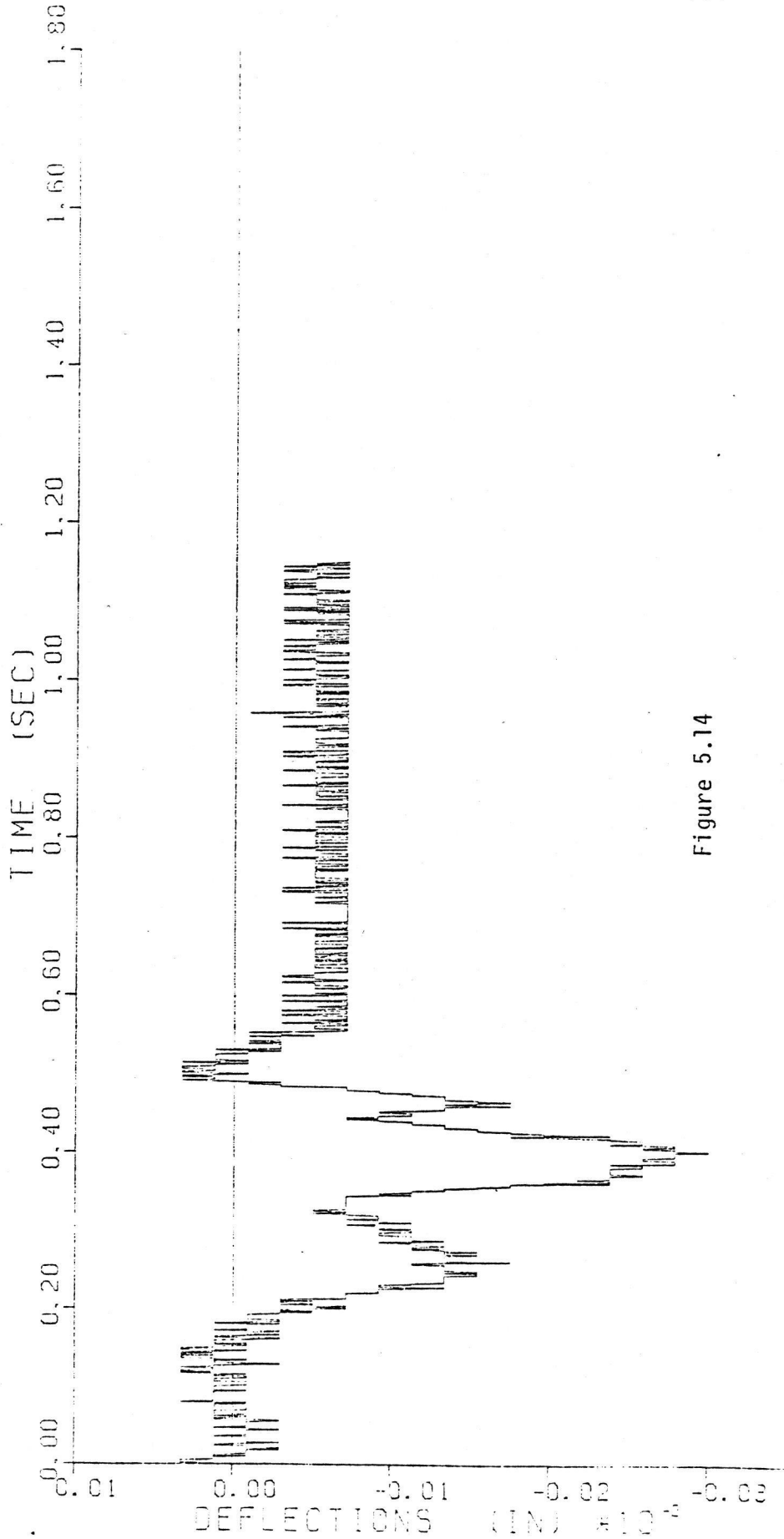
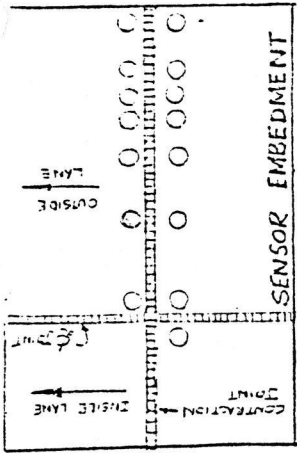


Figure 5.14

BENTON TWO LAYER DATE - 7 / 10 / 80
 A SMALL TRUCK WITH A CROSS WEIGHT OF ABOUT 10 KIPS
 VEHICLE SPEED = 54MPH AXLE LOADS (KIPS) ---2550/5200
 PAVEMENT TEMPERATURES (F) ---LAYER 1= . LAYER 2= . LAYER 3= . LAYER 4=
 EXTENSOMETER SETUP WITH 2 INCH COIL TRANSMITTING
 TRANSMITTING SENSOR IS #14 RECEIVING SENSOR IS #15 RUN 63 CHANNEL 7

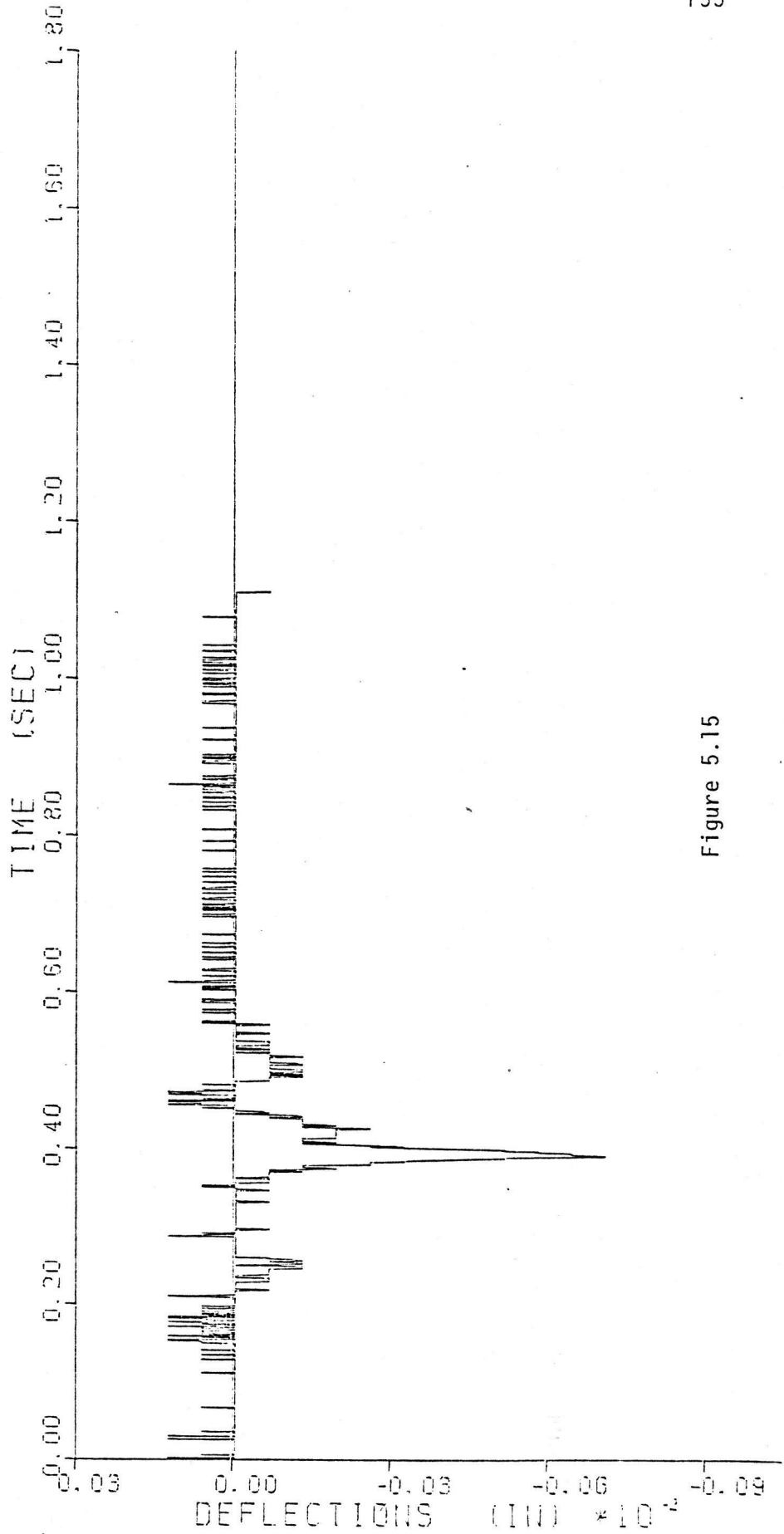
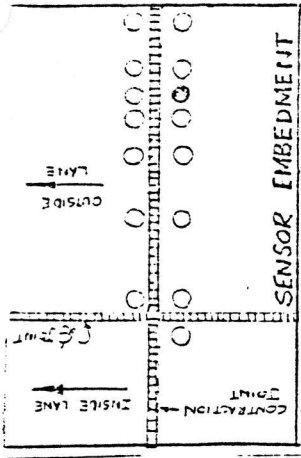


Figure 5.15

BENTON TWO LAYER DATE-7 /10/80
 A SMALL TRUCK WITH A GROSS WEIGHT OF ABOUT 10 KIPS
 VEHICLE SPEED =70MPH AXLE LOADS (KIPS) --2550/5200
 PAVEMENT TEMPERATURES (F) ---LAYER 1= . LAYER 2= . LAYER 3= . LAYER 4=
 EXTENSOMETER SETUP WITH 2 INCH COIL TRANSMITTING
 TRANSMITTING SENSOR IS #19 RECEIVING SENSOR IS #20 RUN 44 CHANNEL 6

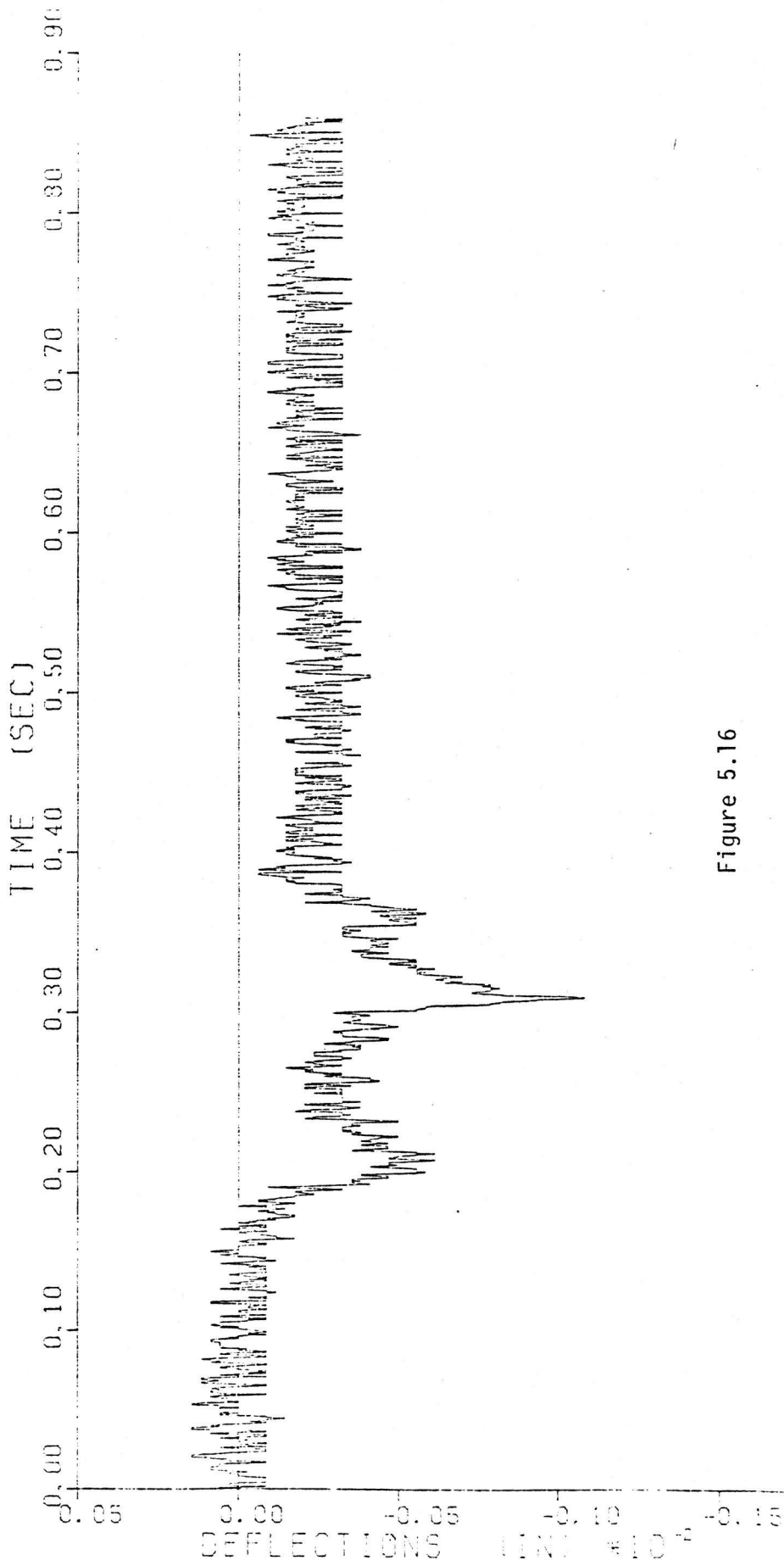
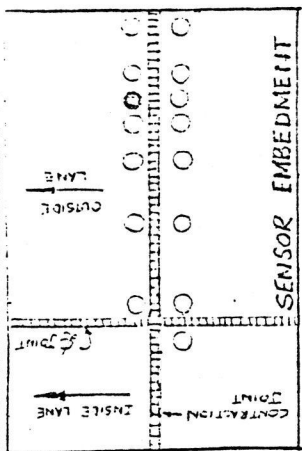


Figure 5.16

BENTON TWO LAYER DATE - 7 / 10 / 80
 A SMALL TRUCK WITH A GROSS WEIGHT OF ABOUT 10 KIPS
 VEHICLE SPEED = 70MPH AXLE LOADS (KIPS) --- 2550 / 5200
 PAVEMENT TEMPERATURES (F) --- LAYER 1 = LAYER 2 = LAYER 3 = LAYER 4 =
 EXTENSOMETER SETUP WITH 2 INCH COIL TRANSMITTING
 TRANSMITTING SENSOR IS #29 RECEIVING SENSOR IS #30 RUN 44 CHANNEL 13

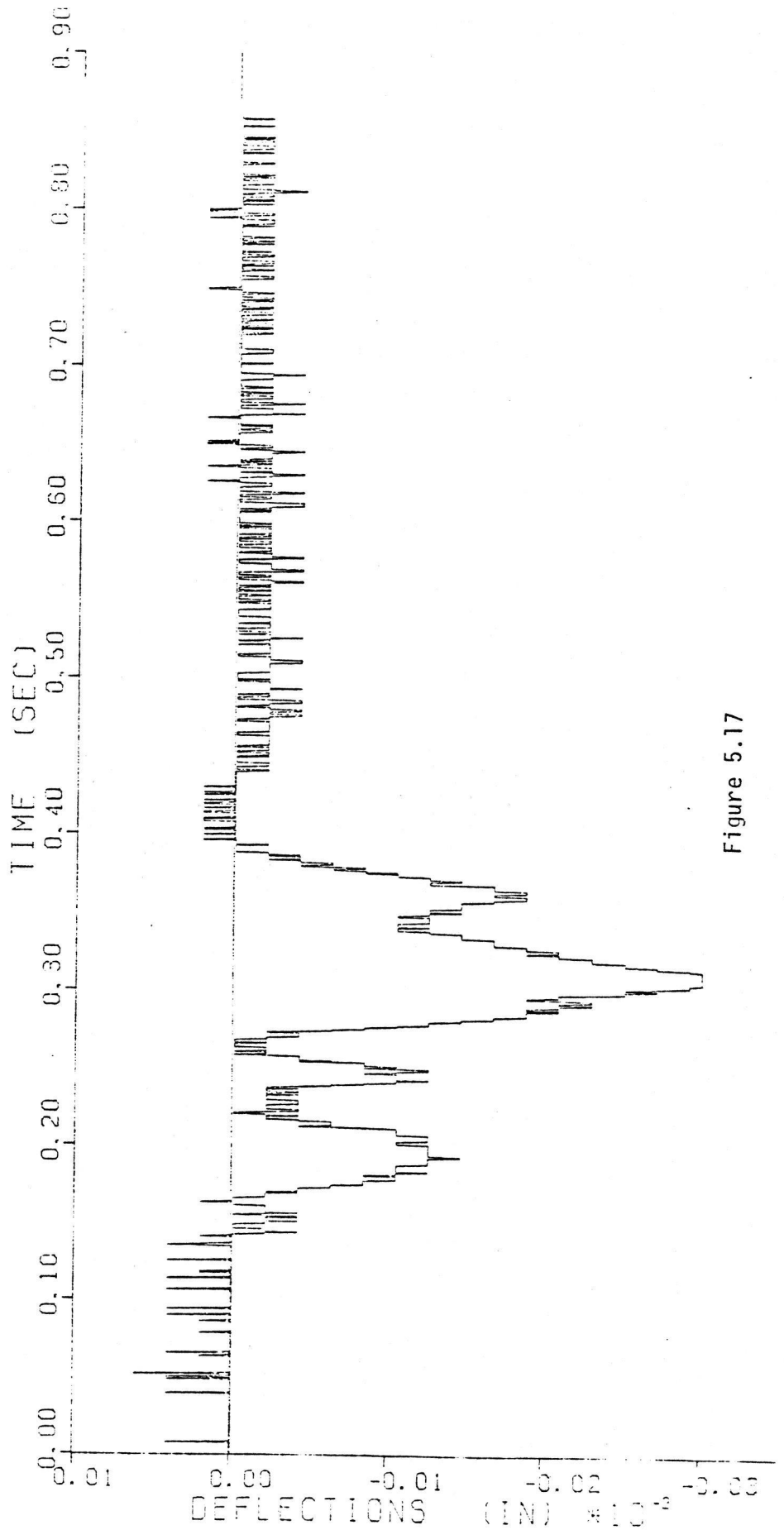
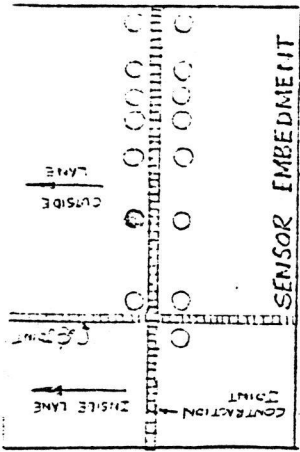


Figure 5.17

DATE -7 /15/80

SENTEC TWO LAYER
TRUCK WITH TWO SINGLE AXLES

VEHICLE SPEED =6 MPH

AXLE LOADS (KIPS) ---6/18

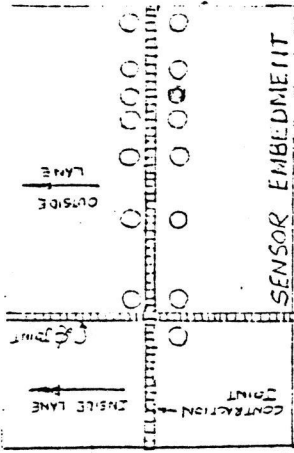
PAVEMENT TEMPERATURES (F) ---LAYER 1= , LAYER 2= , LAYER 3= , LAYER 4=

EXTENSOMETER SETUP WITH 2 INCH COIL TRANSMITTING

TRANSMITTING SENSOR IS #14 RECEIVING SENSOR IS #15

RUN 26 CHANNEL 7

PGPS2



TIME (SEC)	DEFLECTIONS (IN) $\times 10^{-1}$
0.00	0.00
1.20	-0.015
2.40	-0.025
3.60	-0.025
4.80	-0.025
6.00	-0.025
7.20	-0.025
8.40	-0.025

0.01

DEFLECTIONS (IN) $\times 10^{-1}$

0.00

-0.01

-0.02

-0.03

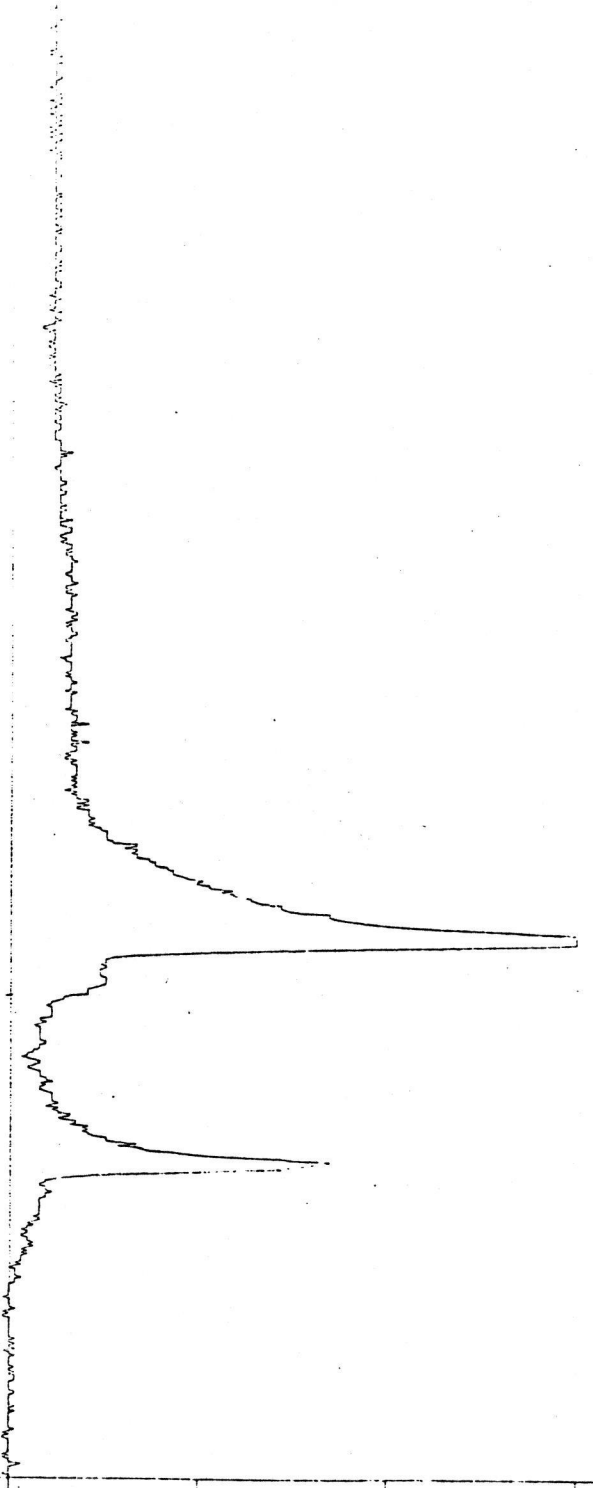


Figure 5.18

BATCH TWO LAYER DATE-7 /15/80
 TRACTOR-TRAILER WITH TANDEM DRIVE AND REAR AXLES
 VEHICLE SPEED =30MPH AXLE LOADS (KIPS) ---7/32/33
 PAVEMENT TEMPERATURES (F) ---LAYER 1= , LAYER 2= , LAYER 3= , LAYER 4=
 EXTENSOMETER SETUP WITH 2 INCH COIL TRANSMITTING
 TRANSMITTING SENSOR IS #14 RECEIVING SENSOR IS #15 RUN 10 CHANNEL 7
 POPS2

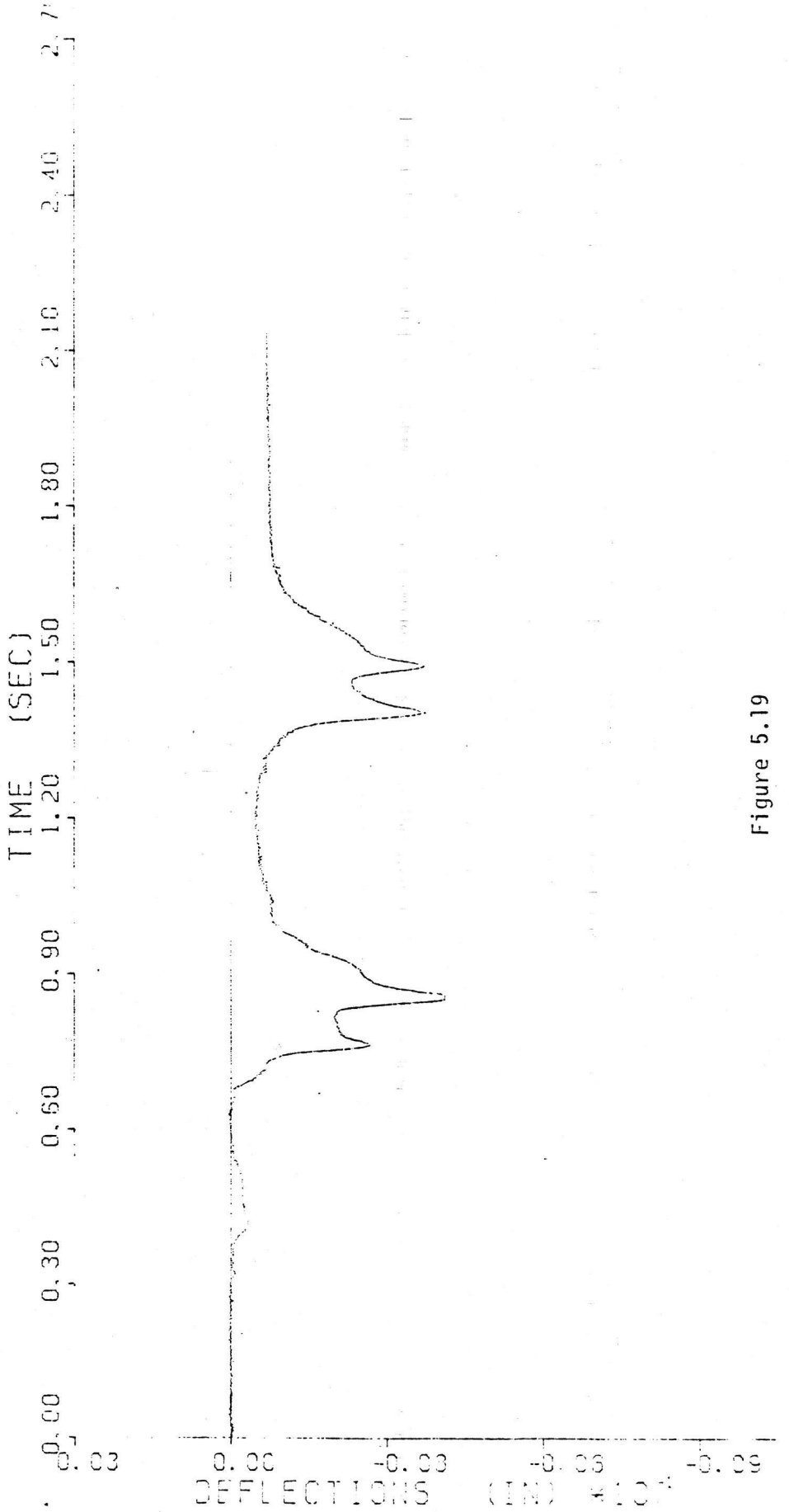
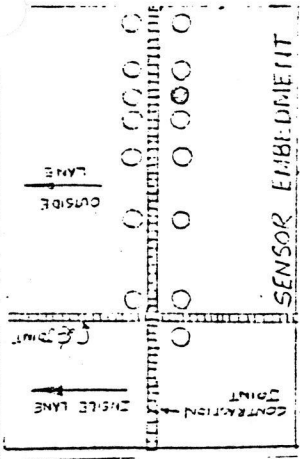


Figure 5.19

BENTON TWO LAYER DATE -7 /15/80
 TRACTOR-TRAILER WITH TANDEN DRIVE AND REAR AXLES
 VEHICLE SPEED =54MPH AXLE LOADS (KIPS) ---7/32/33
 PAVEMENT TEMPERATURES (F) ---LAYER 1= . LAYER 2= . LAYER 3= . LAYER 4= .
 EXTENSOMETER SETUP WITH 2 INCH COIL TRANSMITTING
 TRANSMITTING SENSOR IS #14 RECEIVING SENSOR IS #15 RUN 13 CHANNEL 7

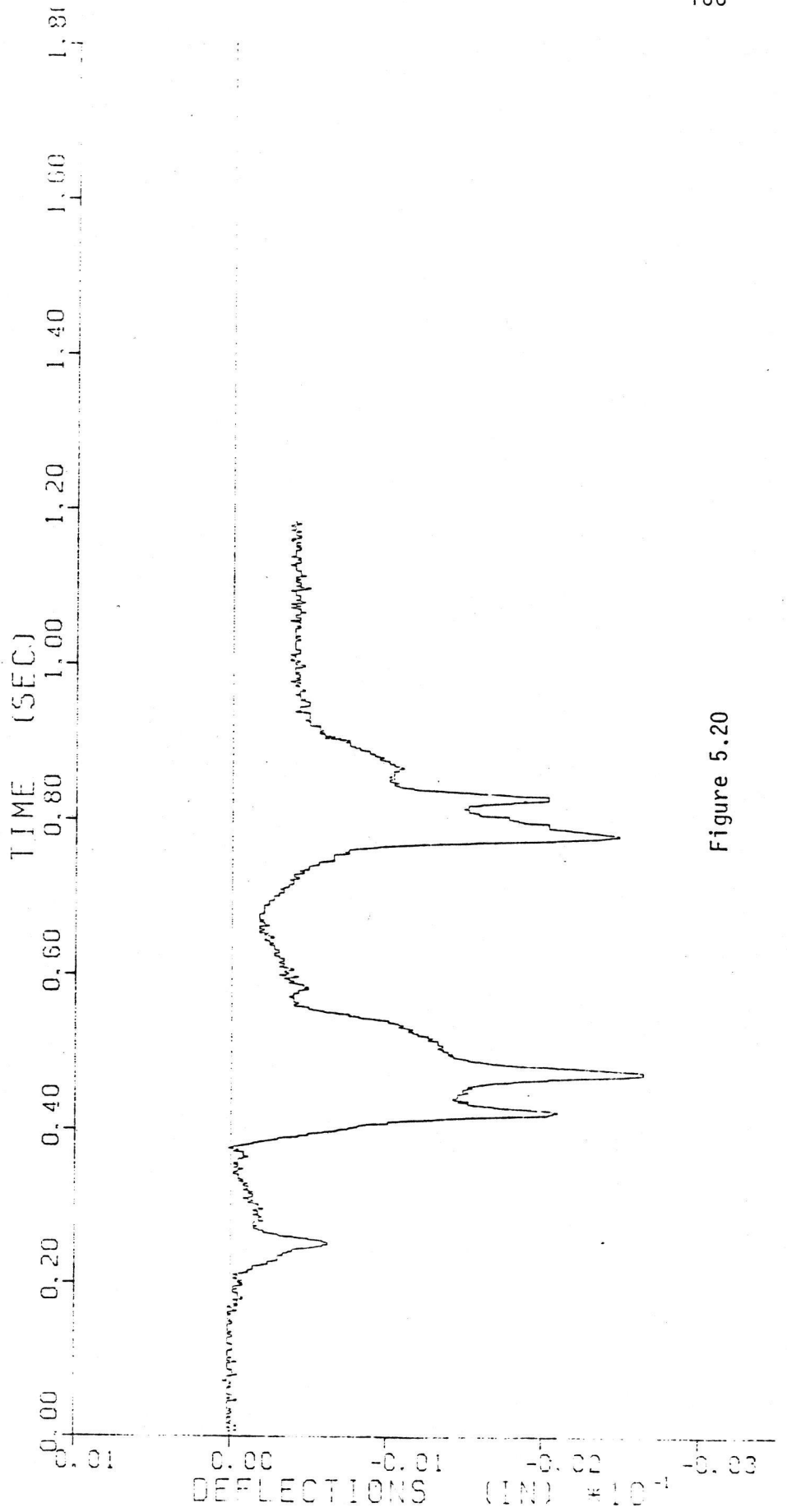
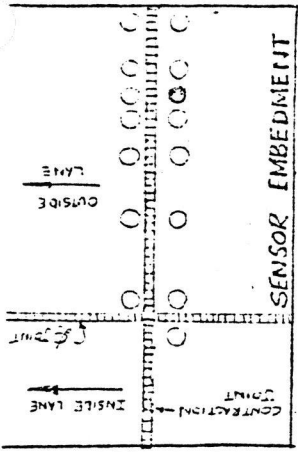


Figure 5.20

PENTON TWO LAYER
 TRACTOR-TRAILER WITH TANDEM DRIVE AND REAR AXLES
 VEHICLE SPEED = 7 MPH
 PAVEMENT TEMPERATURES (F) ---LAYER 1= , LAYER 2= , LAYER 3= , LAYER 4=
 EXTENSOMETER SETUP WITH 2 INCH COIL TRANSMITTING
 TRANSMITTING SENSOR IS #19 RECEIVING SENSOR IS #20 RUN 36 CHANNEL 6

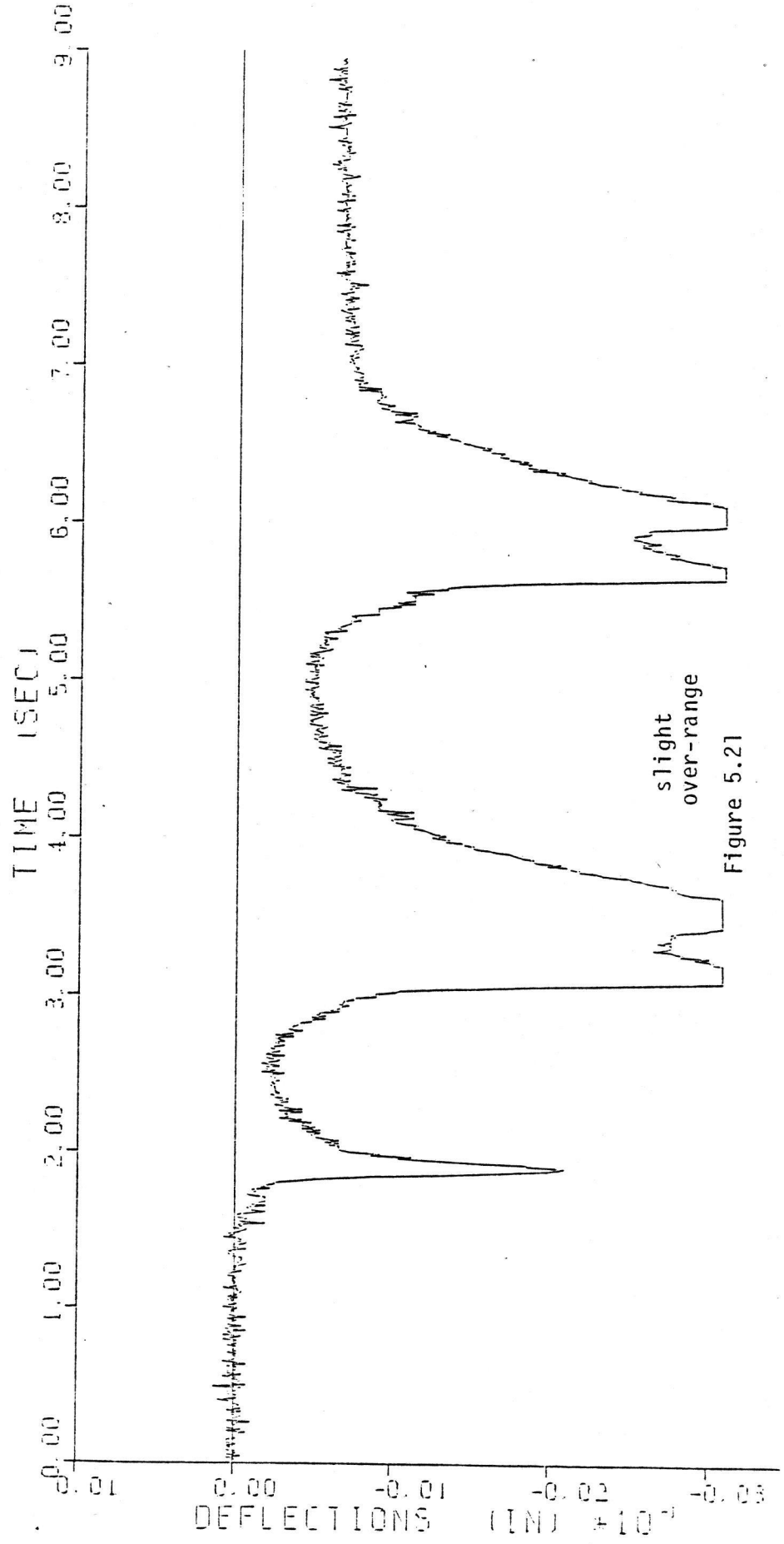
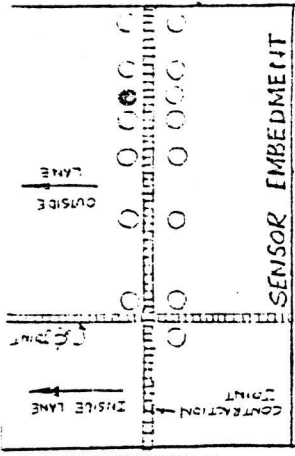


Figure 5.21

BENTON INO LAYER DATE -7 /10/80
 TRACTOR-TRAILER WITH TANDEM DRIVE AND REAR AXLES
 VEHICLE SPEED =7 MPH AXLE LOADS (KIPSI) ---7.735/37
 PAVEMENT TEMPERATURES (F) ---LAYER 1= , LAYER 2= , LAYER 3= , LAYER 4=
 EXTENSOMETER SETUP WITH 2 INCH COIL TRANSMITTING
 TRANSMITTING SENSOR IS #29 RECEIVING SENSOR IS #30 RUN 30 CHANNEL 13

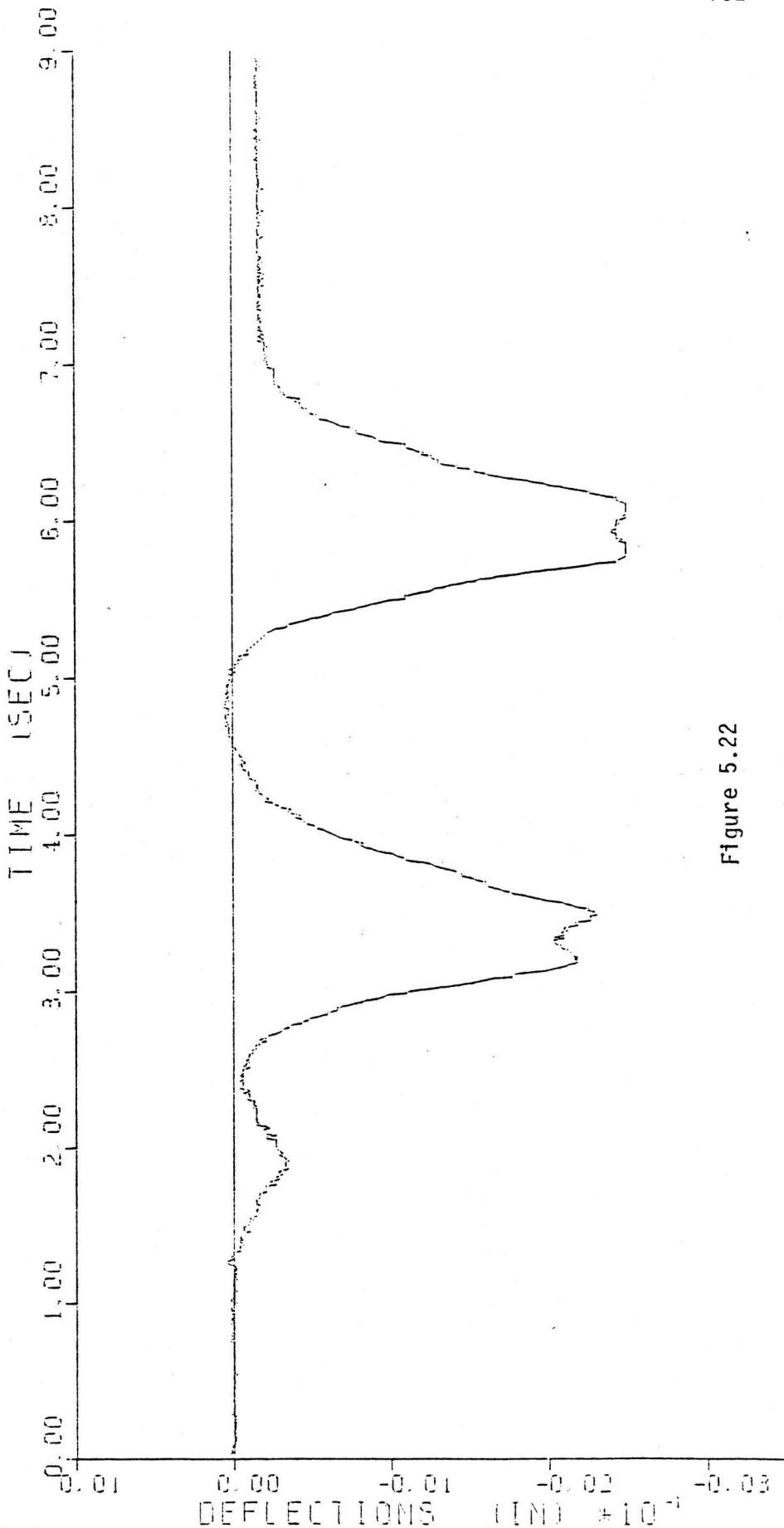
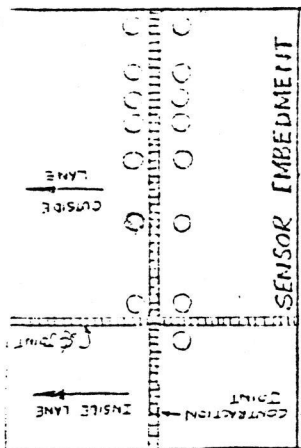


Figure 5.22

BENTON TWO LAYER
 TRACTOR-TRAILER WITH TANDEM DRIVE AND REAR AXLES
 DATE-7 /10/80
 VEHICLE SPEED =30MPH
 AXLE LOADS (KIPS) ---7/35/37
 PAYEMENT TEMPERATURES (F) ---LAYER 1= , LAYER 2= , LAYER 3= , LAYER 4=
 EXTENSOMETER SETUP WITH 2 INCH COIL TRANSMITTING
 TRANSMITTING SENSOR IS #14 RECEIVING SENSOR IS #15 RUN 54 CHANNEL 7

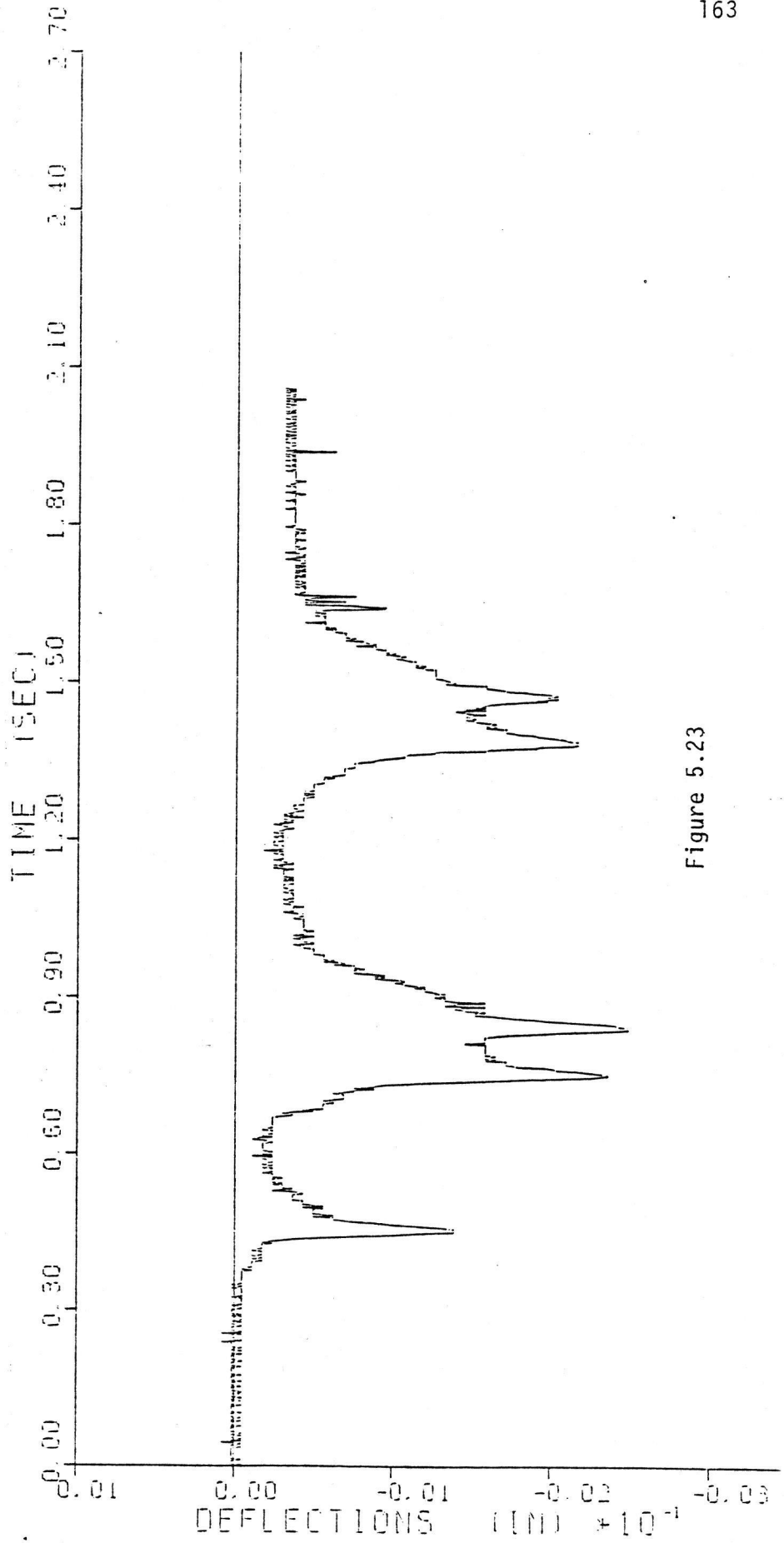
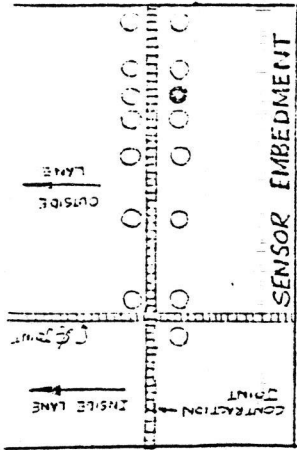


Figure 5.23

SECTION THREE LAYER
 A FULL-SIZE AUTOMOBILE WITH A GROSS WEIGHT OF ABOUT 5 KIPS
 VEHICLE SPEED = 9 MPH
 AXLE LOADS (KIPS) ---1620/1570
 PAVEMENT TEMPERATURES (F) ---LAYER 1= , LAYER 2= , LAYER 3= , LAYER 4=
 EXTENSOMETER SETUP WITH 2 INCH COIL TRANSMITTING
 TRANSMITTING SENSOR IS #14 RECEIVING SENSOR IS #15 RUN 12 CHANNEL 5
 PGAS4

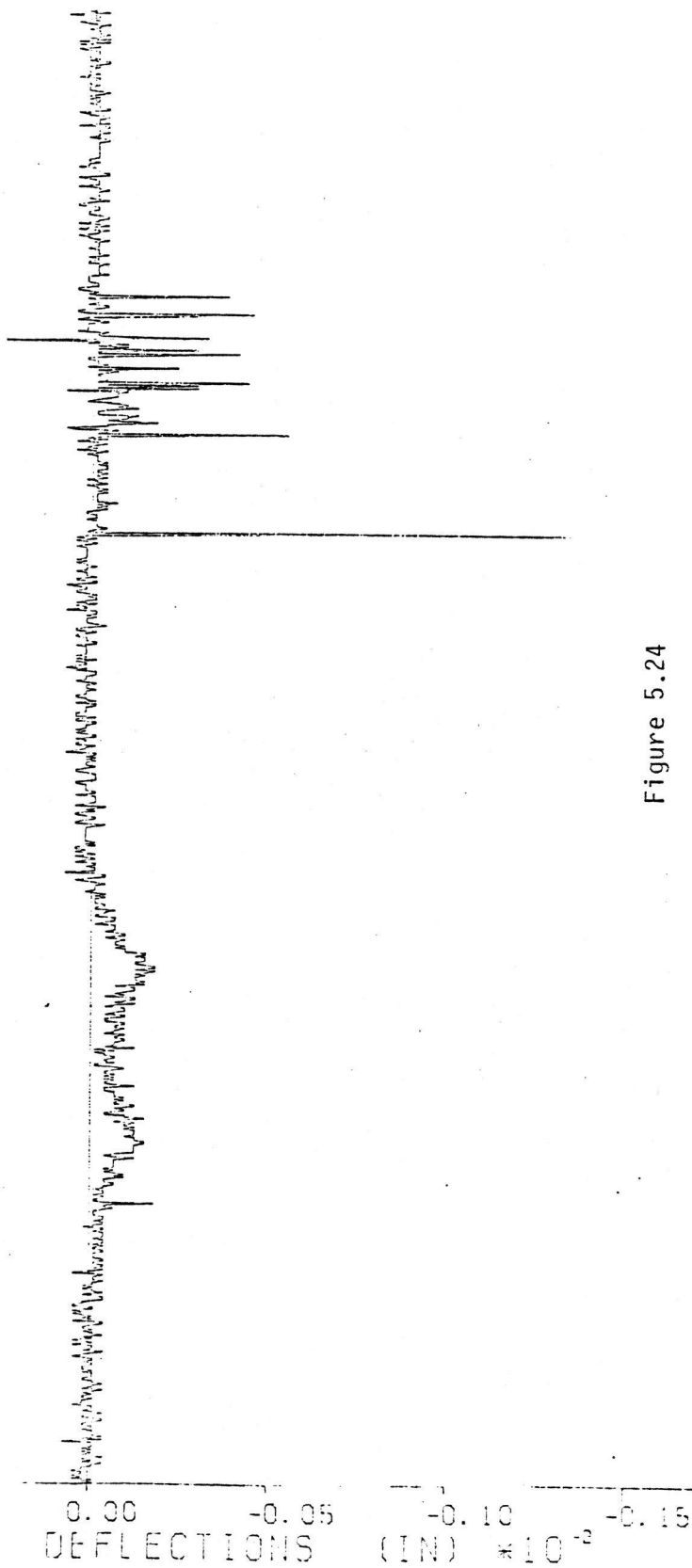
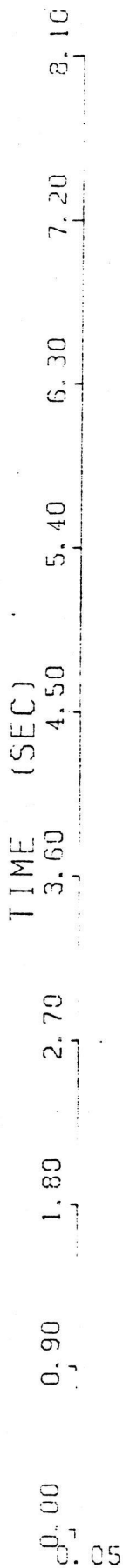
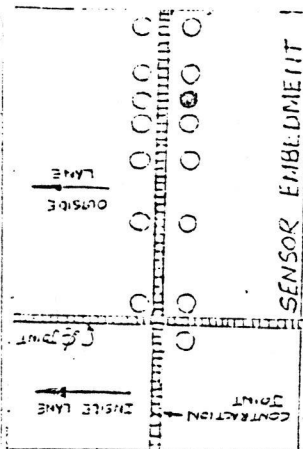


Figure 5.24

SECTION THREE LAYER

TRUCK WITH TWO SINGLE AXLES

VEHICLE SPEED = 7 MPH

PAVEMENT TEMPERATURES (F) ---LAYER 1= , LAYER 2= , LAYER 3= , LAYER 4=

EXTENSOMETER SETUP WITH 2 INCH COIL TRANSMITTING

TRANSMITTING SENSOR IS #9

RECEIVING SENSOR IS #10

RUN 70

CHANNEL 2

TIME (SEC)

0.00 1.00 2.00 3.00 4.00 5.00 6.00 7.00 8.00 9.00

DEFLECTIONS (IN) *10⁻¹

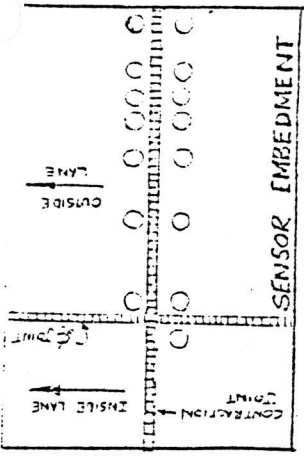
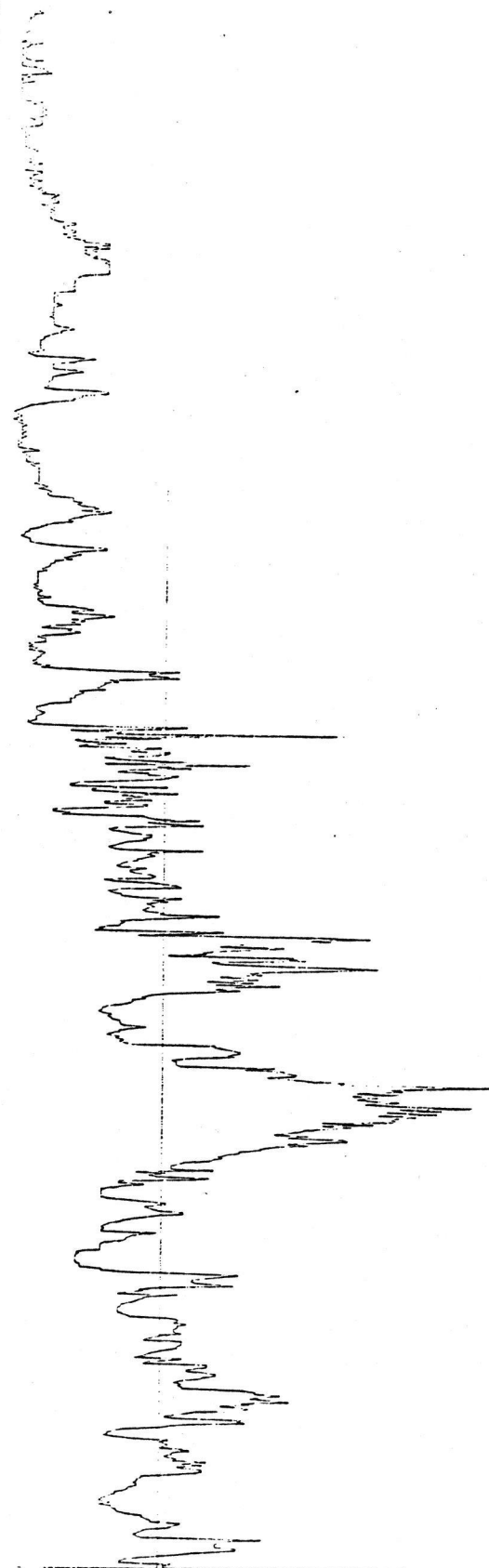


Figure 5.25

BENTON THREE LAYER DATE -7 /16/80
 TRUCK WITH TWO SINGLE AXLES
 VEHICLE SPEED =6 MPH
 AXLE LOADS (KIPS) ---6/18
 PAVEMENT TEMPERATURES (F) ---LAYER 1= , LAYER 2= , LAYER 3= , LAYER 4=
 EXTENSOMETER SETUP WITH 2 INCH COIL TRANSMITTING
 TRANSMITTING SENSOR IS #14 RECEIVING SENSOR 1

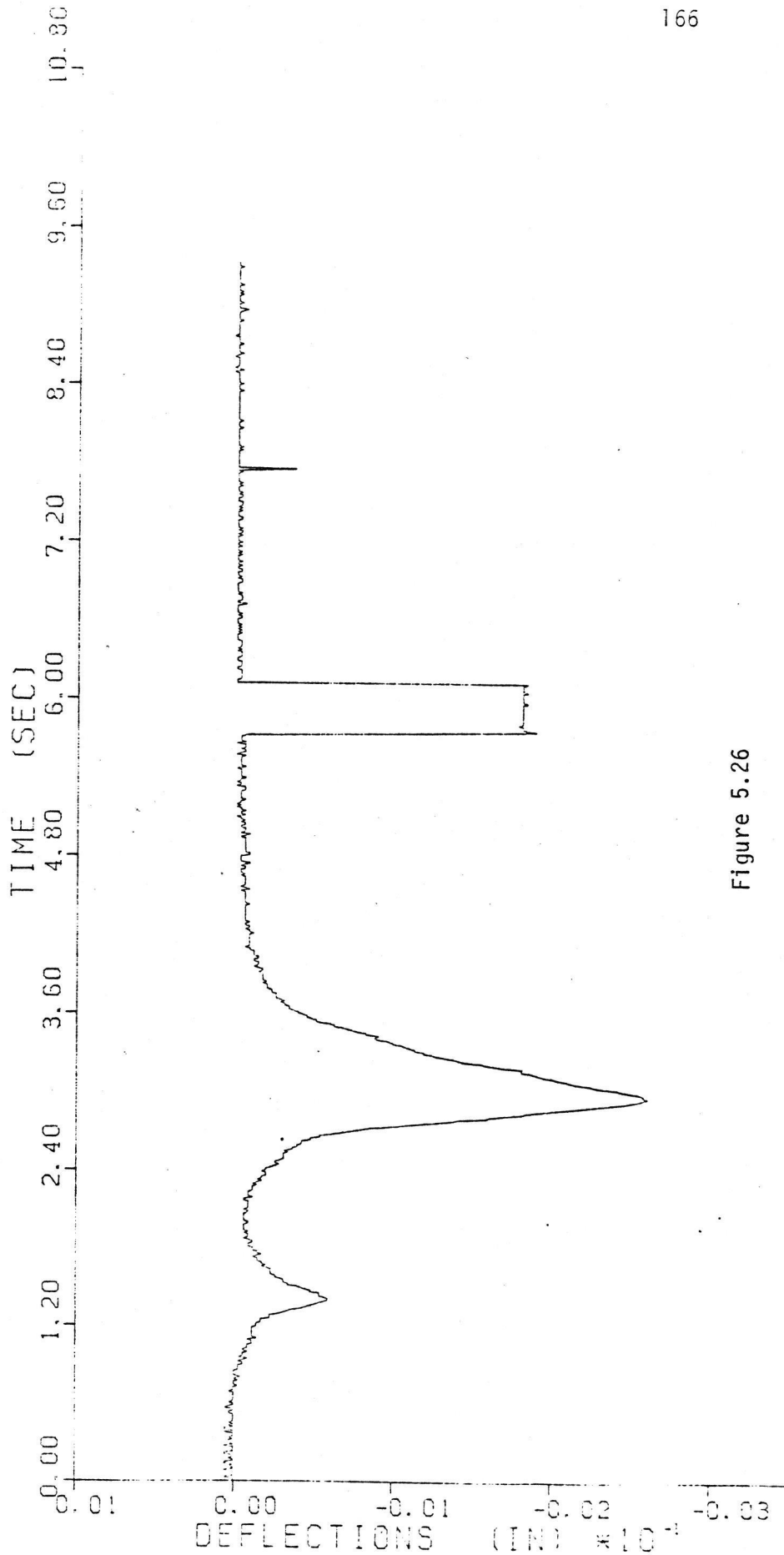
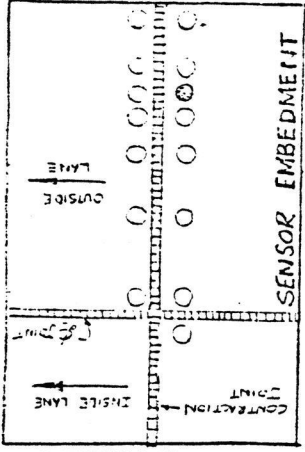


Figure 5.26

BENTON THREE LAYER DATE-7/9/80
 TRACTOR-TRAILER WITH TANDEM DRIVE AND REAR AXLES
 VEHICLE SPEED =6 MPH AXLE LOADS (KIPS) ---7.35/37
 PAVEMENT TEMPERATURES (F) ---LAYER 1= .LAYER 2= .LAYER 3= .LAYER 4=
 EXTENSOMETER SETUP WITH 2 INCH COIL TRANSMITTING
 TRANSMITTING SENSOR IS #9 RECEIVING SENSOR IS #10 RUN 6 CHANNEL 2

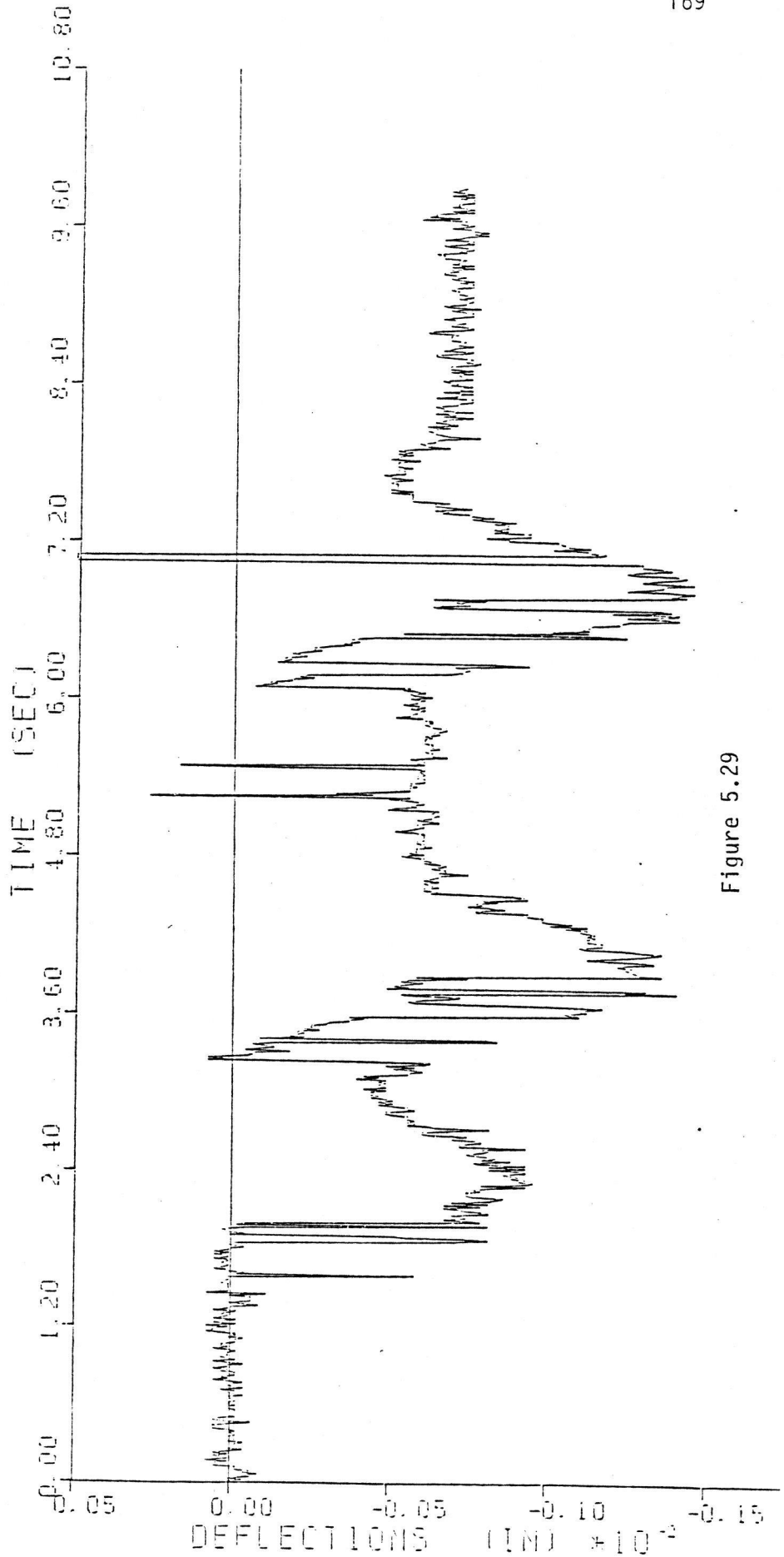
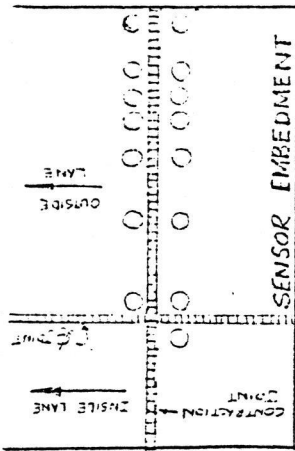


Figure 5.29

BENTON THREE LAYER
 TRACTOR-TRAILER WITH TANDEM DRIVE AND REAR AXLES
 VEHICLE SPEED = 6 MPH
 AXLE LOADS (KIPS) ---7.35/37
 PAVEMENT TEMPERATURES (F) ---LAYER 1= , LAYER 2= , LAYER 3= , LAYER 4=
 EXTENSOMETER SETUP WITH 2 INCH COIL TRANSMITTING
 TRANSMITTING SENSOR IS #14 RECEIVING SENSOR IS #15 RUN 6 CHANNEL 5

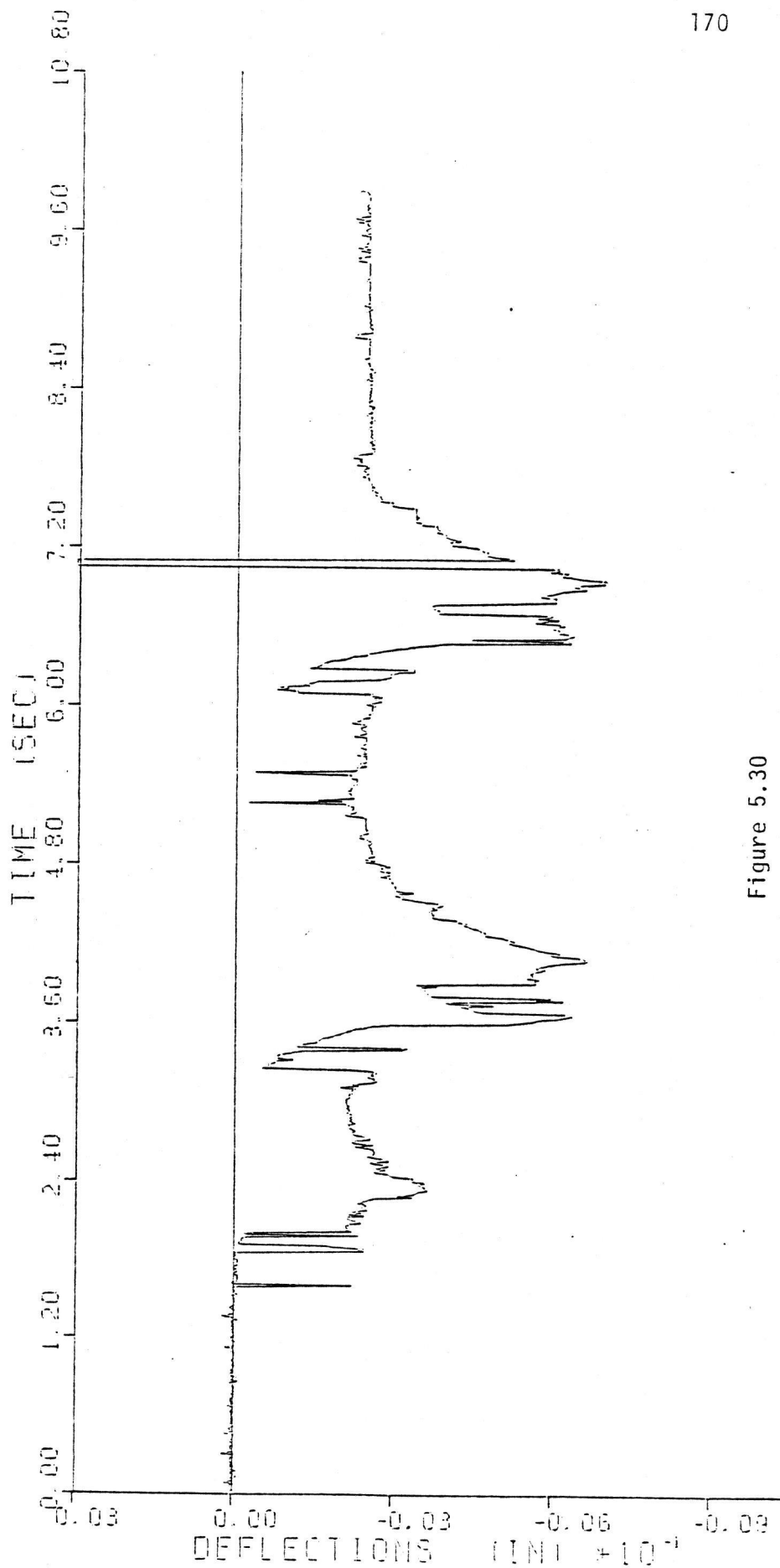
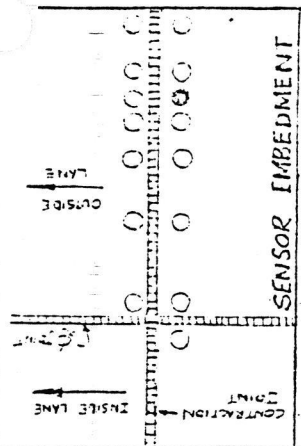


Figure 5.30

BENTON THREE LAYER
 TRACTOR-TRAILER WITH TANDEM DRIVE AND REAR AXLES
 DATE-7 19 780
 VEHICLE SPEED =7 MPH
 AXLE LOADS (KIPS) ---7/35/37
 PAVEMENT TEMPERATURES (F)---LAYER 1= , LAYER 2= , LAYER 3= , LAYER 4=
 EXTENSOMETER SETUP WITH 1 INCH COIL TRANSMITTING
 TRANSMITTING SENSOR IS #10 RECEIVING SENSOR IS #9 RUN 14 CHANNEL 2

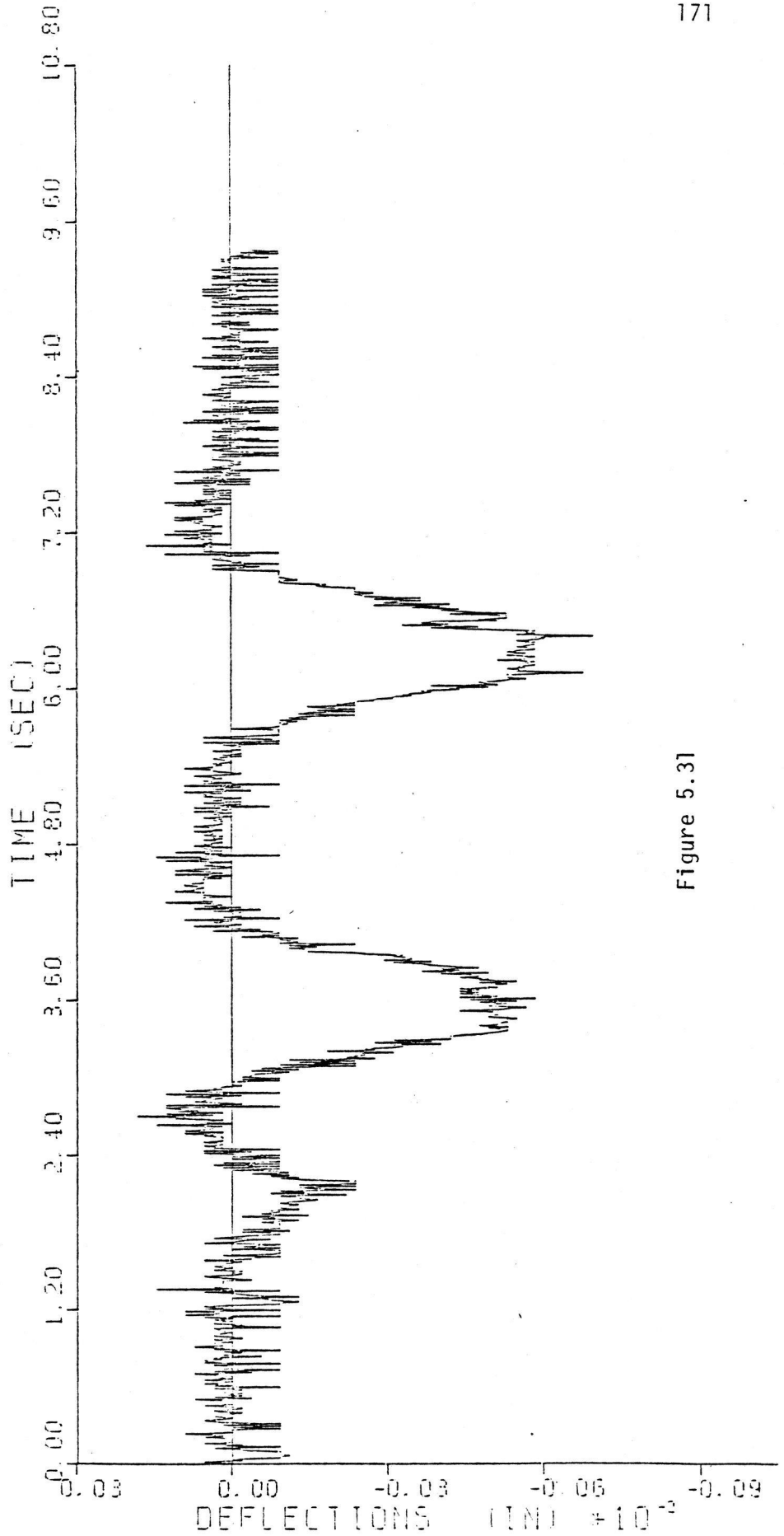
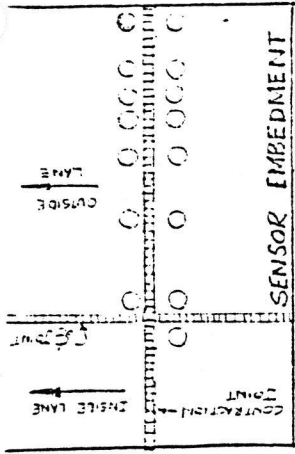


Figure 5.31

BENTON THREE LAYER DATE-7 /11/80
 TRACTOR-TRAILER WITH TANDEM DRIVE AND REAR AXLES
 VEHICLE SPEED =6 MPH AXLE LOADS (KIPS) ----7/32/33
 PAVEMENT TEMPERATURES (F) ---LAYER 1= , LAYER 2= , LAYER 3= , LAYER 4=
 EXTENSOMETER SETUP WITH 2 INCH COIL TRANSMITTING
 TRANSMITTING SENSOR IS #14 RECEIVING SENSOR IS #15 RUN 76 CHANNEL 5

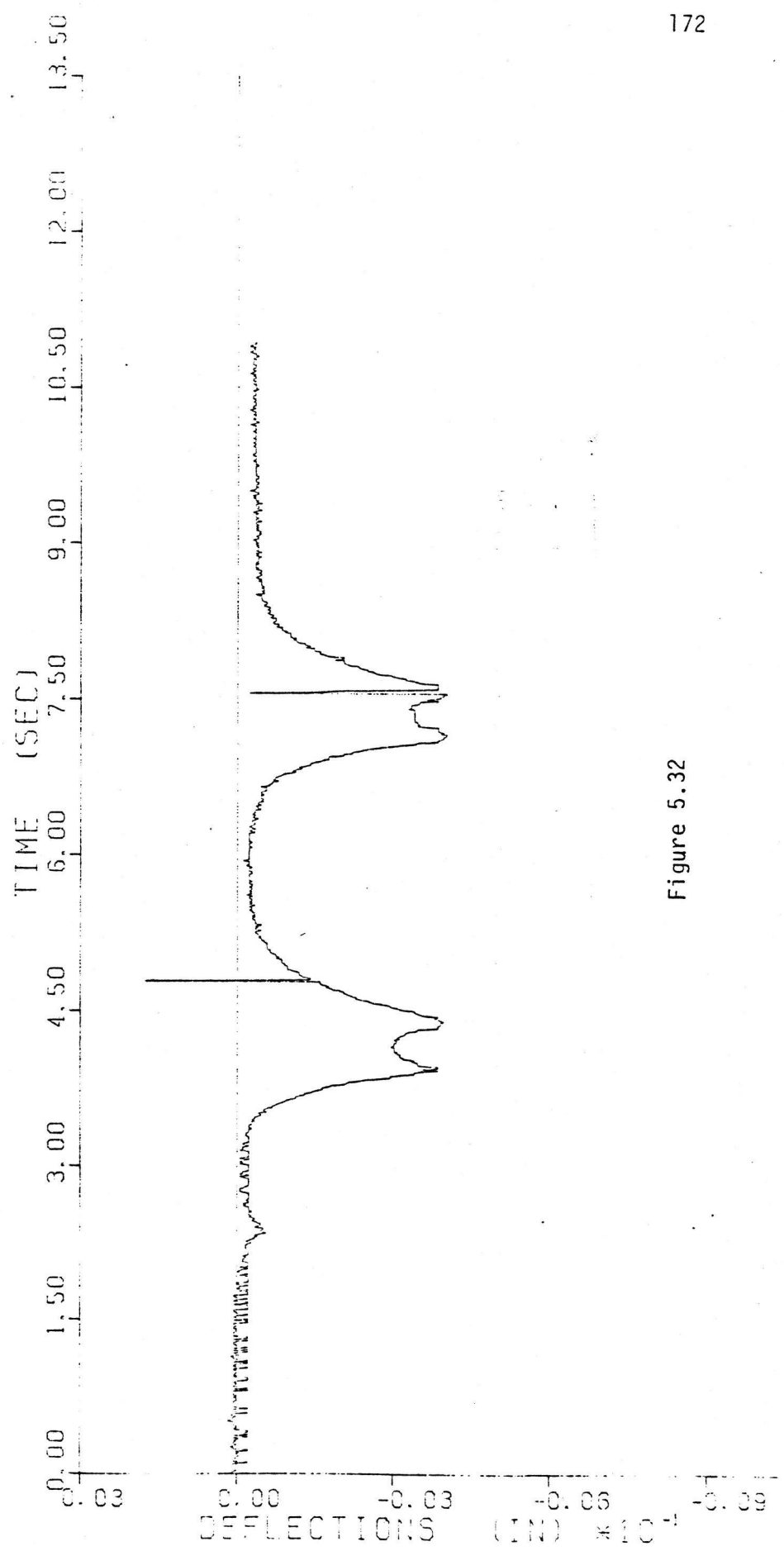
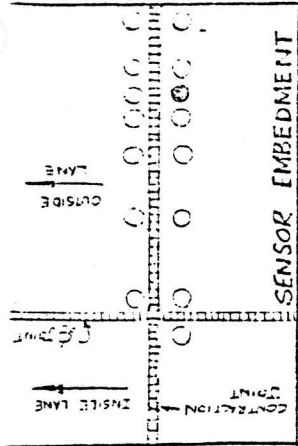


Figure 5.32

BENTON THREE LAYER DATE-7 /9 /80
 TRACTOR-TRAILER WITH TANDEM DRIVE AND REAR AXLES
 VEHICLE SPEED =26MPH AXLE LOADS (KIPS) ---7/35/37
 PAVEMENT TEMPERATURES (F) ---LAYER 1= .LAYER 2= .LAYER 3= .LAYER 4=
 EXTENSOMETER SETUP WITH 2 INCH COIL TRANSMITTING
 TRANSMITTING SENSOR IS #9 RECEIVING SENSOR IS #10 RUN 8 CHANNEL 2

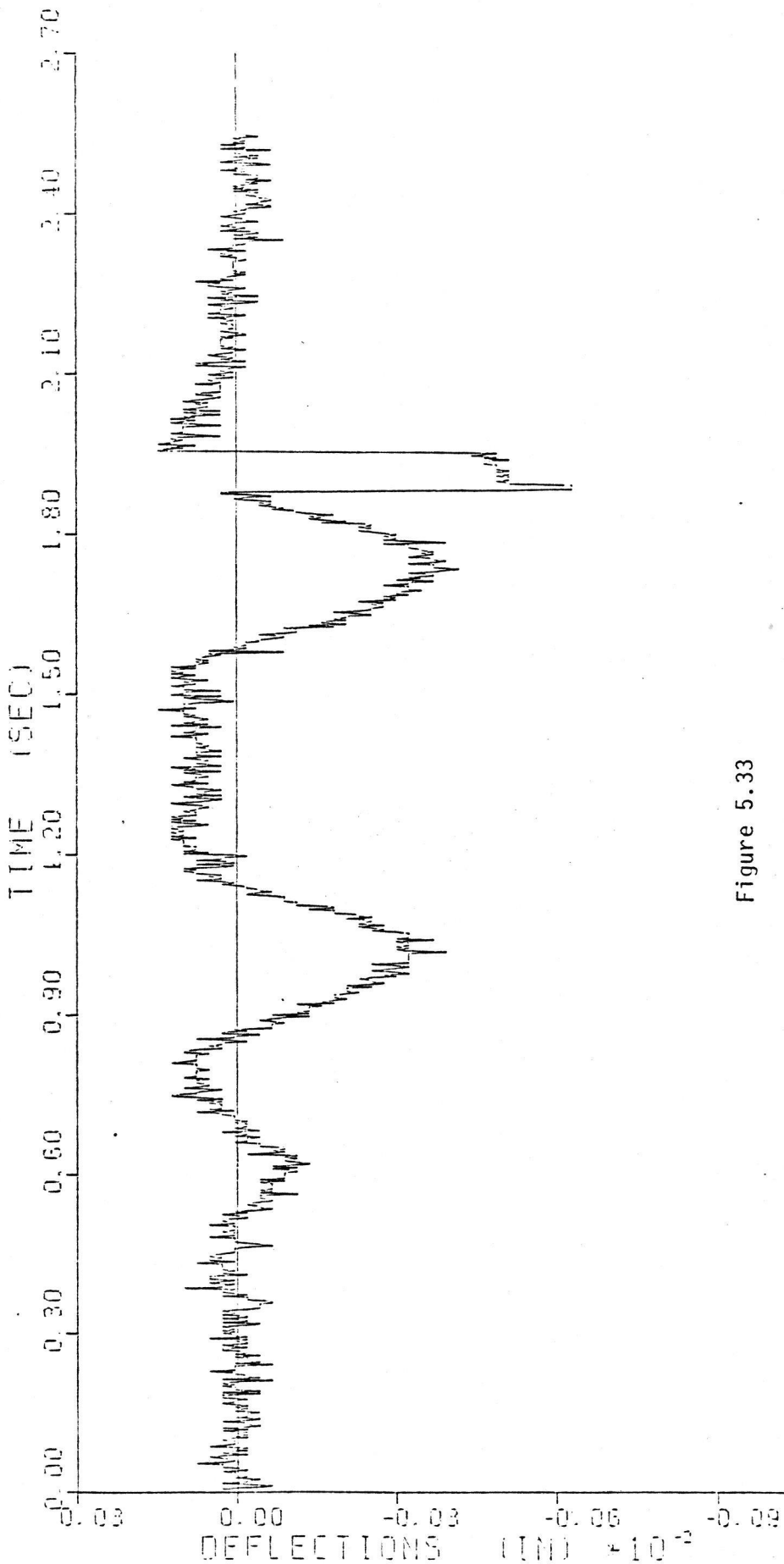
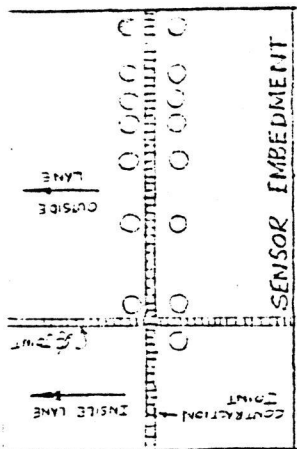


Figure 5.33

BENTON THREE LAYER
 TRACTOR-TRAILER WITH TANDEM DRIVE AND REAR AXLES
 VEHICLE SPEED = 26MPH
 AXLE LOADS (KIPS) ---7.35/37
 PAVEMENT TEMPERATURES (F) ---LAYER 1= , LAYER 2= , LAYER 3= , LAYER 4=
 EXTENSOMETER SETUP WITH 2 INCH COIL TRANSMITTING
 TRANSMITTING SENSOR IS #14 RECEIVING SENSOR IS #15 RUN 8 CHANNEL 5

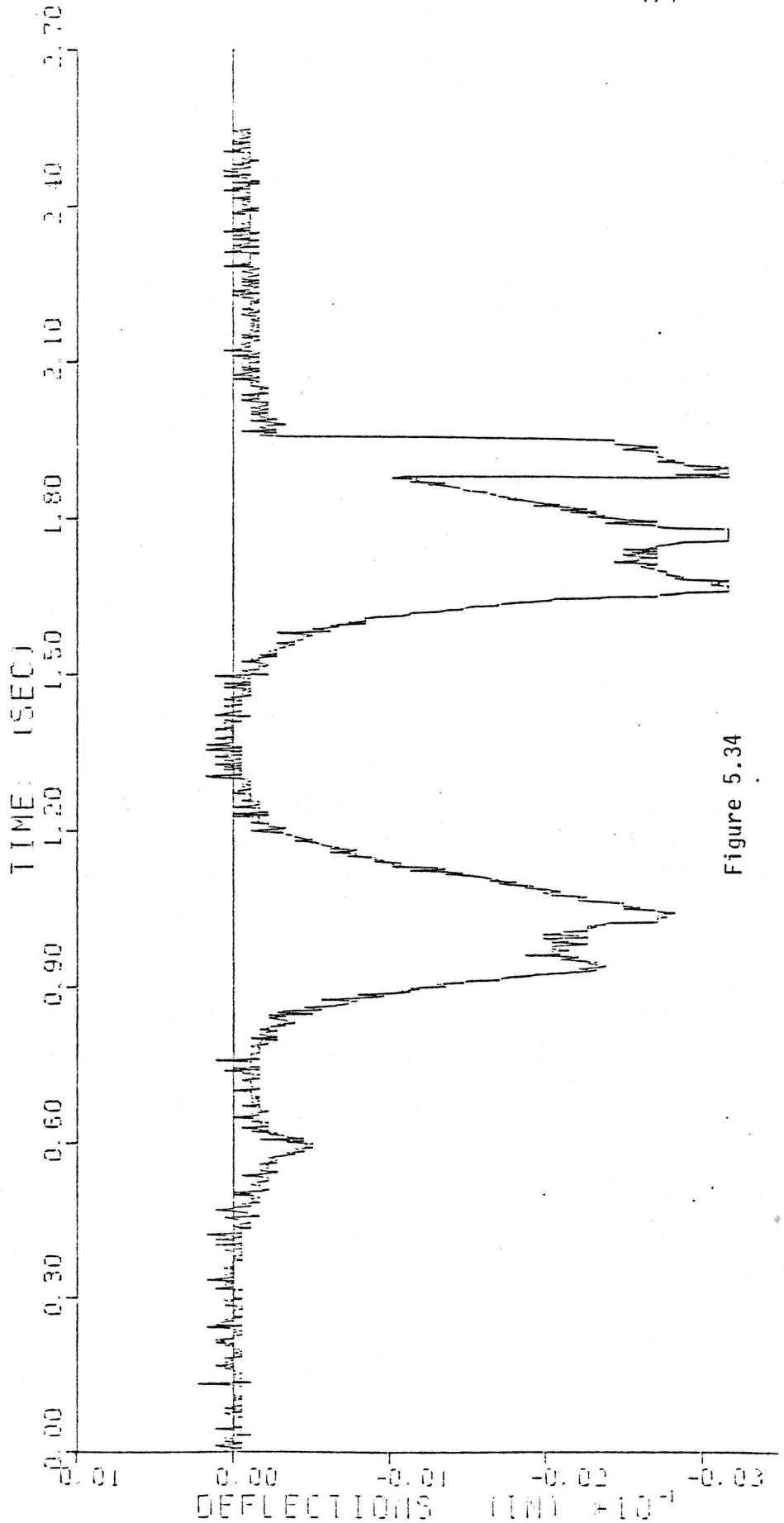
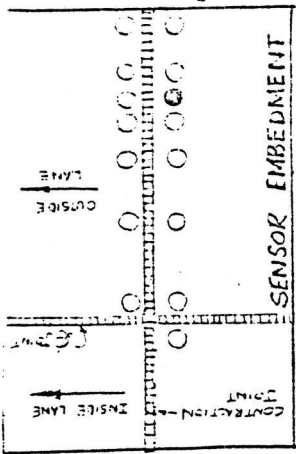


Figure 5.34

SECTION THREE LAYER
 TRACTOR-TRAILER WITH TANDEM DRIVE AND REAR AXLES
 VEHICLE SPEED = 28MPH
 AXLE LOADS (KIPS) ---7.35/37
 PAYEMENT TEMPERATURES (F) ---LAYER 1= . LAYER 2= . LAYER 3= . LAYER 4=
 EXTENSOMETER SETUP WITH 1 INCH COIL TRANSMITTING
 TRANSMITTING SENSOR IS #10 RECEIVING SENSOR IS #9 RUN 12 CHANNEL 2

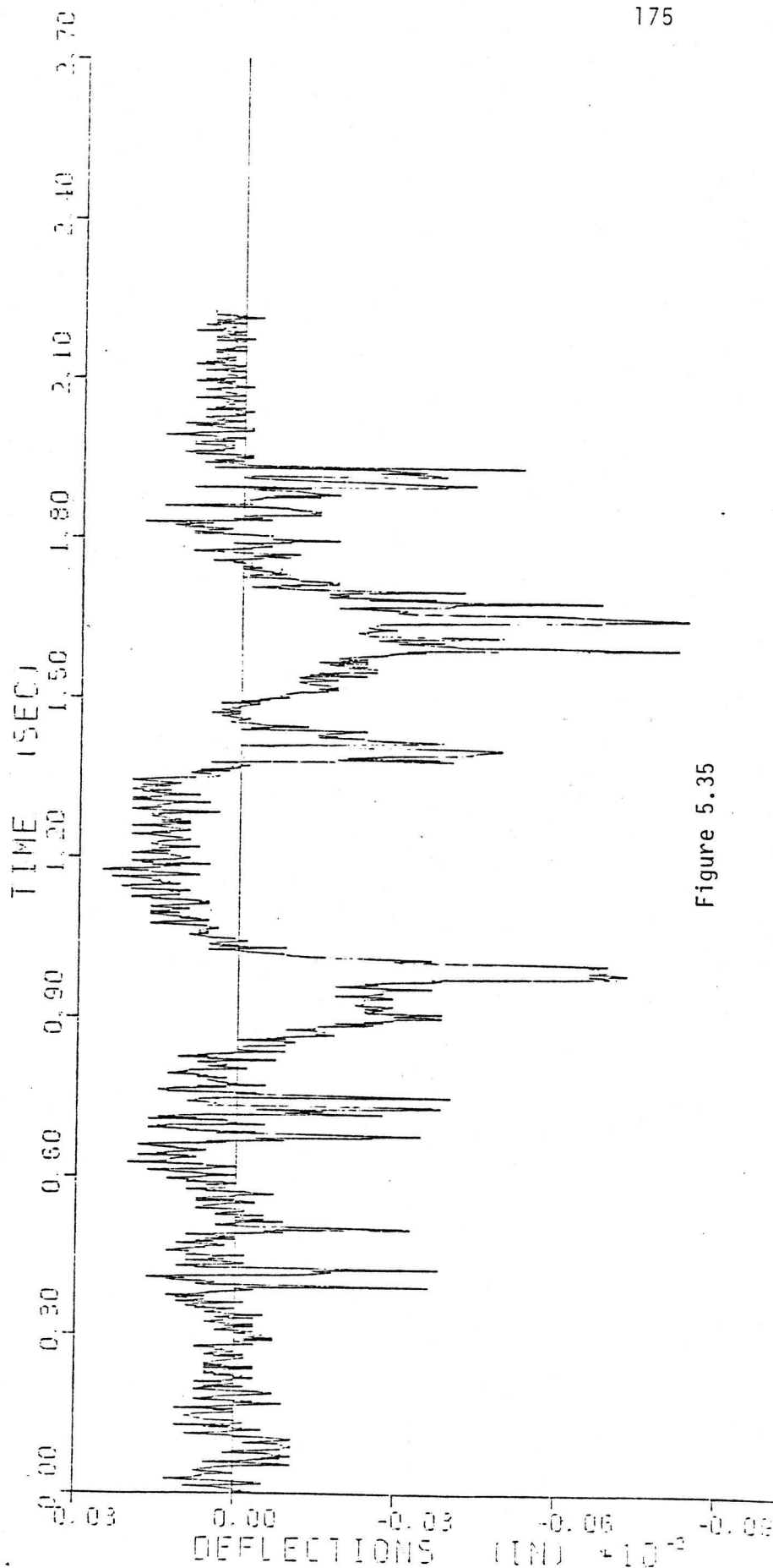
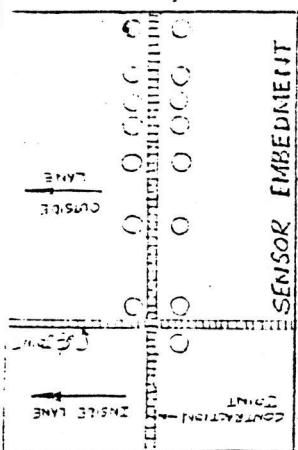


Figure 5.35

CHAPTER VI

CONCLUSIONS AND RECOMMENDATIONS

As a result of this research effort, the following conclusions and recommendations are stated:

1. A system capable of measuring the dynamic behavior of pavement systems has been developed. The components of this system are:
 - a. Sensors and installation procedures
 - b. Data acquisition system
 - c. Data reduction procedures.
2. The horizontal movements under dynamic loading were very small and probably of no significance.
3. The sampling frequency could be reduced without losing significant data.
4. Signal processing or enhancement would improve the usability of the data.
5. Although protection against voltage surges or drops is incorporated in the PDAS, additional protection should be provided.
6. The portable generator used was subject to voltage and frequency fluctuations which caused problems in data acquisition, especially with the magnetic tape drive.
7. The temperature sensors should have a range at least equal to the laydown temperature of the asphalt pavement. Adequate protection of the leadwires is essential.
8. The temperature data should be taken by the PDAS, with the instantaneous temperature profile recorded for each vehicle pass.
9. Waterproof connectors should be used to protect the leadwires and connections from moisture damage and corrosion. BNC connectors are acceptable for connection to the terminal block on the PDAS but are not acceptable for the leads from the sensors.

BIBLIOGRAPHY

- "Asphalt in Pavement Maintenance", First Ed., Manual Series No. 16, The Asphalt Institute (1967) pp. 2.
- Billingsley, N.A., Jr., "Salvaging Old Pavements by Resurfacing," Hwy Res. Circ. 34 (1966) pp. 1-12.
- Bone, A.J., and Crump, L.W., "Current Practices and Research on Controlling Reflection Cracking," HRB Bull. 123 (1956) pp. 33-39.
- Bone, A.J., Crump, L.W., and Roggeveen, V.J., "Control of Reflection Cracking in Bituminous Resurfacing Over Old Cement-Concrete Pavements," Proc. HRP, Vol. 33 (1954) pp. 345-354.
- Burgess, R.A., Kopvillem, O., and Young, F.D., "St. Anne Test Road-Relationships Between Predicted Fracture Temperatures and Low Temperature Field Performance," Proc. AAPT, Vol. 40 (1971) pp. 148-193.
- Busching, H.W., Elliott, E.H. and Reyneveld, N.G., "A State-of-the-Art Survey of Reinforced Asphalt Paving," Proc. AAPT, Vol. 39 (1970) pp. 766-798.
- Chan, C.K. and Duncan, J.M., "A New Device for Measuring Volume Changes and Pressures in Triaxial Tests on Soils," Materials Research and Standards, Vol. 7, No. 7 (July 1967) pp. 312-314.
- Chastain, W.E., Sr. and Mitchell, R.H., "Evaluation of Welded Wire Fabric in Bituminous Concrete Resurfacing," Hwy. Res. Record No. 61, (1964) pp. 48-55.
- Copple, F. and L.T. Ochler, "Michigan Investigation of Soil-Aggregate Cushions and Reinforced Asphaltic Concrete for Preventing or Reducing Reflection Cracking of Resurfaced Pavements," HRB Record 239 (1968) pp. 120-131.
- Erickson, L.F. and March, P.A., "Pavement Widening and Resurfacing in Idaho," HRB Bulletin 131 (1956) pp. 19-25.
- Gould, V.G., "Summarized Committee Report 1948-1960: Salvaging Old Pavements by Resurfacing," HRB Bull. 290 (1961) pp. 1-14.
- Griffith, A.A., "The Phenomena of Rupture and Flow in Solids," Phil. Trans. Roy. Soc. London, Ser. A221 (1921) pp. 163-198.
- Haas, R.C.G. et al., "Low Temperature Pavement Cracking in Canada-The Problem and Its Treatment," Canadian Good Roads Assn. Proc. (1970) pp. 69-96.

- Hensley, M.J., "Open Graded Base Course for Control of Reflective Cracking", Presentation of SASHTO conference, Myrtle Beach, South Carolina.(Oct. 13, 1975).
- Irwin, G.R., "Fracture Mechanics," Proceedings, First Symposium on Naval Structural Mechanics, Macmillan Press (1958).
- Irwin, G.R. and Kies, J., "Fracturing and Fracture Dynamics," Welding Journal Research Supplement (Feb. 1952).
- Kauffmann, E.M., "The Application of Fracture Mechanics Concepts to Predict Cracking of Flexible Pavements," Ph.D. Dissertation, The Ohio State University (1973).
- Kobayashi, A.S., "Experimental Techniques in Fracture Mechanics," SESA Monograph No. 1, The Iowa State University Press (1973).
- Korfhage, G.R., "Effect of Pavement Breaker-Rolling on the Crack Reflectance of Bituminous Overlays," Hwy. Res. Record No. 327 (1970) pp. 50-63.
- Luther, M.S., "The Fracture Mechanics Approach to Reflection Cracking," Master's Thesis, The Ohio State University (1973).
- Luther, M.S., Jamidzadeh, K. and Chang, Che-Wei, "Mechanistic Investigation of Reflection Cracking of Asphalt Overlays," TRB Record No. 572 (1976) pp. 111-122.
- Lyon, J.W., "Heavy Pneumatic Rolling Prior to Overlaying: A 10-Year Project Report," HRB Record 327 (1970) pp. 45-49.
- Majidzadeh, K., Kauffmann, E.M. and Ramsamooj, D.V., "Application of Fracture Mechanics in the Analysis of Pavement Fatigue," AAPT, Vol. 40 (1971) pp. 227-246.
- Majidzadeh, K. and Ramsamooj, D.V., "Mechanistic Approach to the Solution of Cracking in Pavements," HRB Special Report No. 140 (1973) pp. 143-157.
- Majidzadeh, K., Talbert, L.O., and Karakouzian, "Development and Field Verification of a Mechanistic Structural Design System in Ohio," Proceedings, The University of Michigan - Fourth International Conference - Structural Design of Asphalt Pavements, Vol. 1, Ann Arbor, Michigan (1977) pp. 402-408.
- "Pavement Rehabilitation - Materials and Techniques," National Cooperative Highway Research Program, Synthesis of Highway Practice 9, HRB (1972).
- Ramsamooj, D.V., "The Design and Analysis of the Flexibility of Pavements," Ph.D. Dissertation, The Ohio State University (1970).

- Ramsamooj, D.V., "Prediction of Reflection Cracking in Pavement Overlays," HRB Record 434 (1973) pp. 34-42.
- Roberts, S.E., "Cracks in Asphalt Resurfacing Affected by Cracks in Rigid Bases," Proc. HRB, Vol. 33 (1954) pp. 341-345.
- Roggeveen, V.J. and Tons, E., "Progress of Reflection Cracking in Bituminous Concrete Resurfacings," HRB Bull. 131 (1956) pp. 31-46.
- Selig, E.T. and Grangaard, O.H., Jr., "A New Technique for Soil Strain Measurements," Materials Research and Standards, MTRSA, Vol. 10, No. 10 (1970) pp. 19-22.
- Sih, G.C., "A Special Theory of Crack Propagation, Methods of Analysis and Solutions to Crack Problems," Walters-Noordhoff (1973).
- Sih, G.C. and Kassir, M.K., "Mechanics of Fracture, Three-Dimensional Crack Problems," Vol. 2, Noordhoff International Publishing, Leyden, The Netherlands (1975).
- Smith, L.L. and Gartner, W., Jr., "Welded Wire Fabric Reinforcement for Asphaltic Concrete," HRB Bull. 322, (1962) pp. 1-20.
- Tons, E., Bone, A.J. and Roggeveen, V.J., "Five-Year Performance of Welded Wire Fabric in Bituminous Resurfacing," HRB Bull. 290 (1961) pp. 15-38.
- Vicelja, J.L., "Methods to Eliminate Reflection Cracking in Asphalt Concrete Resurfacing Over Portland Cement Concrete Pavements," Proceedings of the Association of Asphalt Paving Technologists, Vol. 32 (1963) pp. 200-227.
- Wilson, J.O., "Crack Control Joints in Bituminous Overlays on Rigid Pavements," HRB Bull. 322 (1962) pp. 21-29.
- Zube, E., "Wire Mesh Reinforcement in Bituminous Resurfacing," HRB Bull. 131 (1956) pp. 1-18.

APPENDIX

Tabulated Data of Vertical and Horizontal
Spacings, Movements and Strains in the
Vicinity of an Overlaid Joint in a PCC
Pavement for a One, Two and Three
Layered Overlay Systems

ONE LAYERED SYSTEM

Vertical Spacings, Movements and Strains

VERTICAL SPACINGS, MOVEMENTS, & STRAINS
 INTERSTATE HIGHWAY I-30 BENTON, ARKANSAS
ONE LAYERED SYSTEM - TOP OF CONCRETE
0'-6" FROM EDGE OF PAVEMENT

DATE	temp	WEST SIDE OF JOINT			EAST SIDE OF JOINT		
		spacing	movement	strain	spacing	movement	strain
1977 4/15	82	0.9874			1.3124		
5/30	120	0.9039	-0.0835	-0.0846			
5/31	84	0.9065	-0.0809	-0.0819	1.2577	-0.0547	-0.0417
5/31	122	0.8987	-0.0887	-0.0898			
6/15	78	0.8927	-0.0947	-0.0959			
6/20	126	0.8876	-0.0998	-0.1011			
6/21	88	0.8909	-0.0965	-0.0977			
6/21	120	0.8871	-0.1003	-0.1016			
6/22	89	0.8916	-0.0958	-0.0970			
6/22	120	0.8873	-0.1001	-0.1014			
6/23	89	0.8911	-0.0963	-0.0975			
6/23	124	0.8876	-0.0998	-0.1011			
7/20	86	0.8958	-0.0916	-0.0928			
7/20	100	0.8878	-0.0996	-0.1009			
7/21	82	0.8927	-0.0947	-0.0959			
7/21	118	0.8873	-0.1001	-0.1014			
7/22	86	0.8921	-0.0953	-0.0965			
8/25	94	0.8921	-0.0953	-0.0965			
8/25	128	0.8842	-0.1032	-0.1045			
8/26	96	0.8891	-0.0983	-0.0996			
8/26	126	0.8839	-0.1035	-0.1048			
9/1	96	0.8909	-0.0965	-0.0977			
9/20	115	0.8820	-0.1054	-0.1067			
10/5	89	0.8873	-0.1001	-0.1014	1.2008	-0.1116	-0.0850
10/13	73	0.8919	-0.0955	-0.0967	1.2173	-0.0951	-0.0725
11/8	94	0.8381	-0.1493	-0.1512			
11/9	76	0.8392	-0.1482	-0.1501	1.1861	-0.1263	-0.0962
11/10	64	0.8451	-0.1423	-0.1441	1.2173	-0.0951	-0.0725
12/12	46	0.8305	-0.1569	-0.1589	1.1894	-0.1230	-0.0937
12/14	56	0.8335	-0.1539	-0.1559	1.2595	-0.0529	-0.0403
12/15	36	0.8395	-0.1479	-0.1498	1.2193	-0.0931	-0.0709
1978 2/2	36	0.8305	-0.1569	-0.1589	1.2485	-0.0639	-0.0487
3/3	45	0.8296	-0.1578	-0.1598	1.2407	-0.0717	-0.0055
3/22	85	0.8249	-0.1625	-0.1646	1.2328	-0.0796	-0.0607

VERTICAL SPACINGS, MOVEMENTS, & STRAINS
 INTERSTATE HIGHWAY I-30 BENTON, ARKANSAS
ONE LAYERED SYSTEM - TOP OF CONCRETE
3'-6" FROM EDGE OF PAVEMENT

DATE	temp	WEST SIDE OF JOINT			EAST SIDE OF JOINT		
		spacing	movement	strain	spacing	movement	strain
1977 4/15	82	1.0574			0.8729		
5/30	120	0.9286	-0.1288	-0.1218	0.8118	-0.0611	-0.0700
5/31	84	0.9127	-0.1447	-0.1368	0.8003	-0.0726	-0.0832
5/31	122	0.9248	-0.1326	-0.1254	0.8093	-0.0636	-0.0729
6/15	78	0.9017	-0.1557	-0.1472	0.7944	-0.0785	-0.0899
6/20	126	0.9090	-0.1484	-0.1403	0.8012	-0.0717	-0.0821
6/21	88	0.8976	-0.1598	-0.1511	0.7944	-0.0785	-0.0899
6/21	120	0.9096	-0.1478	-0.1398	0.8003	-0.0726	-0.0832
6/22	89	0.8976	-0.1598	-0.1511	0.7936	-0.0793	-0.0908
6/22	120	0.9073	-0.1501	-0.1420	0.7995	-0.0734	-0.0841
6/23	89	0.8974	-0.1600	-0.1513	0.7936	-0.0793	-0.0908
6/23	124	0.9113	-0.1461	-0.1382	0.8012	-0.0717	-0.0821
7/20	86	0.8911	-0.1663	-0.1573	0.7919	-0.0810	-0.0928
7/20	100	0.8911	-0.1663	-0.1573	0.7928	-0.0801	-0.0918
7/21	82	0.8886	-0.1688	-0.1569	0.7894	-0.0835	-0.0957
7/21	118	0.8998	-0.1576	-0.1490	0.7969	-0.0760	-0.0871
7/22	86	0.8889	-0.1691	-0.1599	0.7919	-0.0810	-0.0928
8/25	94	0.8601	-0.1973	-0.1866	0.7894	-0.0835	-0.0957
8/25	128	0.8724	-0.1850	-0.1750	0.7969	-0.0760	-0.0871
8/26	96	0.8597	-0.1977	-0.1870	0.7870	-0.0859	-0.0984
8/26	126	0.8695	-0.1879	-0.1777	0.7953	-0.0776	-0.0889
9/1	96	0.8570	-0.2004	-0.1895	0.7878	-0.0851	-0.0975
9/20	115				0.7911	-0.0818	-0.0937
10/5	89				0.7845	-0.0884	-0.1013
10/13	73	0.8570	-0.2004	-0.1895	0.7853	-0.0876	-0.1004
11/8	94	0.8471	-0.2103	-0.1989	0.7853	-0.0876	-0.1004
11/9	76	0.8395	-0.2179	-0.2061	0.7820	-0.0909	-0.1041
11/10	64	0.8436	-0.2138	-0.2022	0.7845	-0.0884	-0.1013
12/12	46				0.7812	-0.0917	-0.1051
12/14	56				0.7845	-0.0884	-0.1013
12/15	36				0.7853	-0.0876	-0.1004
1978 2/2	36	0.8395	-0.2179	-0.2061	0.7804	-0.0925	-0.1060
3/3	45	0.8365	-0.2209	-0.2089	0.7788	-0.0941	-0.1078
3/22	85				0.7845	-0.0884	-0.1013

VERTICAL SPACINGS, MOVEMENTS, & STRAINS
 INTERSTATE HIGHWAY I-30 BENTON, ARKANSAS
ONE LAYERED SYSTEM - TOP OF CONCRETE
8'-6" FROM EDGE OF PAVEMENT

DATE	temp	WEST SIDE OF JOINT			EAST SIDE OF JOINT		
		spacing	movement	strain	spacing	movement	strain
1977 4/15	82	1.2397			1.2401		
5/30	120						
5/31	84				1.2173	-0.0288	-0.0187
5/31	122						
6/15	78						
6/20	126						
6/21	88						
6/21	120						
6/22	89						
6/22	120						
6/23	89						
6/23	124						
7/20	86	1.0547	-0.1850	-0.1492	1.1018	-0.0483	-0.0389
7/20	100	1.0538	-0.1859	-0.1500	1.1963	-0.0438	-0.0353
7/21	82	1.0579	-0.1818	-0.1466	1.1942	-0.0459	-0.0370
7/21	118	1.0276	-0.2121	-0.1711	1.1837	-0.0564	-0.0455
7/22	86	1.0565	-0.1832	-0.1478	1.1954	-0.0447	-0.0360
8/25	94	1.0511	-0.1886	-0.1521	1.1930	-0.0471	-0.0380
8/25	128	0.9968	-0.2429	-0.1959	1.1722	-0.0679	-0.0548
8/26	96	1.0524	-0.1873	-0.1511	1.1927	-0.0474	-0.0382
8/26	126	1.0194	-0.2203	-0.1777	1.1780	-0.0621	-0.0501
9/1	96	1.0506	-0.1891	-0.1525	1.1921	-0.0480	-0.0387
9/20	115	1.0248	-0.2149	-0.1733	1.1777	-0.0624	-0.0503
10/5	89	1.0511	-0.1886	-0.1521	1.1852	-0.0549	-0.0443
10/13	73	1.0670	-0.1727	-0.1393	1.1736	-0.0665	-0.0536
11/8	94	1.0497	-0.1900	-0.1533	1.1813	-0.0588	-0.0474
11/9	76	1.0497	-0.1900	-0.1533	1.1682	-0.0719	-0.0580
11/10	64	1.0529	-0.1868	-0.1507	1.1716	-0.0685	-0.0552
12/12	46	1.0280	-0.2117	-0.1703	1.1514	-0.0887	-0.0715
12/14	56	1.0262	-0.2135	-0.1722	1.1146	-0.1255	-0.1012
12/15	36	1.0385	-0.2012	-0.1623	1.1626	-0.0775	-0.0625
1978 2/2	36	1.0262	-0.2135	-0.1722	1.1545	-0.0856	-0.0690
3/3	45	1.0239	-0.2158	-0.1741	1.1553	-0.0848	-0.0744
3/22	85				1.1366	-0.1035	-0.0835

VERTICAL SPACINGS, MOVEMENTS, & STRAINS
 INTERSTATE HIGHWAY I-30 BENTON, ARKANSAS
ONE LAYERED SYSTEM - TOP OF CONCRETE
11'-9" FROM EDGE OF PAVEMENT

DATE	temp	WEST SIDE OF JOINT			EAST SIDE OF JOINT		
		spacing	movement	strain	spacing	movement	strain
1977 4/15	82	0.7458			0.7894		
5/30	120	0.7635	+0.0177	+0.0237	0.7828	-0.0066	-0.0084
5/31	84	0.8262	0.0804	0.1078	0.7969	+0.0075	+0.0095
5/31	122	0.7659	0.0201	0.0270	0.7861	-0.0033	-0.0042
6/15	78	0.7511	0.0053	0.0071	0.7894	0.0000	0.0000
6/20	126	0.7230	-0.0228	-0.0306	0.7820	-0.0074	-0.0094
6/21	88	0.7643	+0.0185	+0.0248	0.7911	+0.0017	+0.0022
6/21	120	0.7259	-0.0199	-0.0267	0.7820	-0.0074	-0.0094
6/22	89	0.7573	+0.0115	+0.0154	0.7911	+0.0017	+0.0022
6/22	120	0.7310	-0.0148	-0.0198	0.7828	-0.0066	-0.0084
6/23	89	0.7526	+0.0068	+0.0091	0.7911	+0.0017	+0.0022
6/23	124	0.7288	-0.0170	-0.0228	0.7820	-0.0074	-0.0094
7/20	86	0.5185	-0.2273	-0.3048	0.7944	+0.0050	+0.0063
7/20	100	0.4862	-0.2596	-0.3481	0.7870	-0.0024	-0.0030
7/21	82	0.4892	-0.2566	-0.3441	0.7911	+0.0017	+0.0022
7/21	118	0.4348	-0.3110	-0.4170	0.7812	-0.0082	-0.0104
7/22	86	0.4753	-0.2705	-0.3627	0.7936	+0.0042	+0.0053
8/25	94	0.4376	-0.3082	-0.4132	0.7919	0.0025	0.0032
8/25	128	0.3710	-0.3748	-0.5025	0.7812	-0.0082	-0.0104
8/26	96	0.4497	-0.2961	-0.3970	0.7878	-0.0016	-0.0020
8/26	126	0.3761	-0.3697	-0.4957	0.7820	-0.0074	-0.0094
9/1	96	0.4510	-0.2948	-0.3953	0.7878	-0.0016	-0.0020
9/20	115	0.3877	-0.3581	-0.4802	0.7779	-0.0115	-0.0146
10/5	89	0.4248	-0.3210	-0.4304	0.7845	-0.0049	-0.0062
10/13	73	0.4404	-0.3054	-0.4095	0.7928	+0.0034	-0.0043
11/8	94	0.4068	-0.3390	-0.4545	0.7845	-0.0049	-0.0062
11/9	76	0.4376	-0.3082	-0.4132	0.7903	+0.0009	+0.0011
11/10	64	0.4431	-0.3027	-0.4059	0.7969	0.0075	0.0095
12/12	46	0.3957	-0.3501	-0.4694	0.7853	-0.0041	-0.0052
12/14	56	0.3909	-0.3549	-0.4759	0.7870	-0.0024	-0.0030
12/15	36	0.4277	-0.3181	-0.4265	0.7886	-0.0008	-0.0010
1978 2/2	36	0.3860	-0.3598	-0.4824	0.7878	-0.0016	-0.0020
3/3	45	0.3727	-0.3731	-0.5003	0.7853	-0.0041	-0.0052
3/22	85	0.3590	-0.3868	-0.5186	0.7771	-0.0123	-0.0156

VERTICAL SPACINGS, MOVEMENTS, & STRAINS
 INTERSTATE HIGHWAY 1-30 BENTON, ARKANSAS
 ONE LAYERED SYSTEM 12'-2" FROM EDGE OF PAVEMENT
 NORTH OF C. L. JOINT

DATE	TOP OF CONCRETE			DATE	TOP OF CONCRETE			
	temp	spacing	movement		strain	temp	spacing	movement
4/15/77	82	0.6914		10/13	73	0.7005	+0.0091	+0.0132
5/30	120	0.6914	0.0000	11/8	94	0.6825	-0.0089	-0.0129
5/31	84	0.7075	+0.0161	11/9	76	0.6866	-0.0048	-0.0069
5/31	122	0.6935	0.0021	11/10	64	0.6928	+0.0014	+0.0020
6/15	78	0.6977	0.0063	12/12	46	0.6852	-0.0062	-0.0090
6/20	126	0.6907	-0.0007	12/14	56	0.6873	-0.0041	-0.0059
6/21	88	0.7012	+0.0098	12/15	36	0.6845	-0.0069	-0.0100
6/21	120	0.6887	-0.0027	2/2/78	36	0.6756	-0.0158	-0.0229
6/22	89	0.7012	+0.0098	3/3	45	0.6729	-0.0185	-0.0268
6/22	120	0.6407	-0.0007	3/22	85	0.6689	-0.0225	-0.0363
6/23	89	0.7005	+0.0091	3/23	76	0.6703	-0.0211	-0.0305
6/23	124	0.6907	-0.0007	5/10	74	0.6716	-0.0198	-0.0286
7/20	86	0.7047	+0.0133	6/6	89	0.6736	-0.0178	-0.0257
7/20	100	0.6942	0.0028	6/22	116	0.6669	-0.0245	-0.0354
7/21	82	0.7012	0.0098	6/23	110	0.6669	-0.0245	-0.0354
7/21	118	0.6928	0.0014	6/27	128	0.6630	-0.0284	-0.0411
7/22	86	0.7005	0.0091	7/20	118	0.6676	-0.0238	-0.0344
8/25	94	0.6984	0.0070	7/26	110	0.6696	-0.0218	-0.0315
8/25	128	0.6859	-0.0055					
8/26	96	0.6991	+0.0077					
8/26	126	0.6887	-0.0027					
9/1	96	0.6970	+0.0056					
9/20	115	0.6845	-0.0069					
10/5	89	0.6949	+0.0035					

ONE LAYERED SYSTEM

Horizontal Spacings, Movements and Strains

HORIZONTAL SPACINGS, MOVEMENTS, & STRAINS
 INTERSTATE HIGHWAY I-30 BENTON, ARKANSAS
 ONE LAYERED SYSTEM 0'-6" FROM EDGE OF PAVEMENT

DATE	TOP OF CONCRETE			DATE	TOP OF CONCRETE			
	temp	spacing	movement		temp	spacing	movement	strain
4-15-77	82	5.8735		10-13	73	5.5002	-0.3733	-0.0636
5-30	120	5.3421	-0.5314	11-8	94	5.4974	-0.3761	-0.0640
5-31	84	5.5960	-0.2775	11-9	76	5.4861	-0.3874	-0.0660
5-31	122	5.4504	-0.4233	11-10	64	5.5804	-0.2931	-0.0499
6-15	78	5.4639	-0.4096	12-12	46	5.3902	-0.4833	-0.0823
6-20	126	5.5117	-0.3618	12-14	56	5.4529	-0.4206	-0.0716
6-21	88	5.6907	-0.1828	12-15	36	5.4917	-0.3818	-0.0650
6-21	120	5.3446	-0.5289	2-2-78	36	5.5350	-0.3385	-0.0576
6-22	89	5.6474	-0.2261	3-3	45	5.4666	-0.4069	-0.0693
6-22	120	5.3818	-0.7117	3-22	85	5.5529	-0.3206	-0.0546
6-23	89	5.6907	-0.1828	3-23	76	5.4068	-0.4667	-0.0795
6-23	124	5.7009	-0.1726	5-10	74	5.4917	-0.3818	-0.0650
7-20	86	5.6151	-0.2584	6-6	89	5.4722	-0.4013	-0.0683
7-20	100	5.4611	-0.4124	6-22	116	5.5262	-0.3473	-0.0592
7-21	82	5.5743	-0.2992	6-23	110	5.5291	-0.3444	-0.0586
7-21	118	5.2616	-0.6119	6-27	114	5.2324	-0.6411	-0.1092
7-22	86	5.5590	-0.3145	7-20	118	5.1597	-0.7138	-0.1215
8-25	94	5.6055	-0.2680	7-26	110	5.3221	-0.5514	-0.0939
8-25	128	5.3902	-0.4833					
8-26	96	5.5866	-0.2869					
8-26	126	5.3789	-0.4946					
9-1	96	5.5439	-0.3296					
9-20	115	5.2112	-0.0918					
10-5	89	5.5117	-0.3618					

HORIZONTAL SPACINGS, MOVEMENTS, & STRAINS
 INTERSTATE HIGHWAY 1-30 BENTON, ARKANSAS
 ONE LAYERED SYSTEM 2'-6" FROM EDGE OF PAVEMENT

DATE	TOP OF CONCRETE			DATE	TOP OF CONCRETE			
	temp	spacing	movement		strain	temp	spacing	movement
4-15-77	82	4.8617		10-13	73	4.8668	+0.0051	+0.0010
5-30	120			11-8	94	4.9144	0.0527	0.0108
5-31	84			11-9	76	4.8154	-0.0463	-0.0095
5-31	122			11-10	64	4.8685	+0.0068	+0.0014
6-15	78	4.6082	-0.2535	12-12	46	4.8061	-0.0556	-0.0114
6-20	126			12-14	56	4.9202	+0.0595	+0.0122
6-21	88			12-15	36	4.9202	0.0595	0.0122
6-21	120			2-2-78	36	4.9038	0.0421	0.0087
6-22	89			3-3	45	4.8772	0.0155	0.0032
6-22	120			3-22	85	4.7770	-0.0847	-0.0174
6-23	89			3-23	76	4.8667	+0.0050	+0.0010
6-23	124			5-10	74	4.8012	-0.0605	-0.0124
7-20	86	4.7898	-0.0719	6-6	89	4.8110	-0.0507	-0.0104
7-20	100	4.7301	-0.1316	6-22	116	4.6677	-0.1940	-0.0399
7-21	82	4.8106	-0.0511	6-23	110	4.6765	-0.1852	-0.0381
7-21	118	4.7056	-0.1561	6-27	114			
7-22	86	4.7945	-0.0672	7-20	118	4.5132	-0.3485	-0.0717
8-25	94	4.8284	-0.0333	7-26	110	4.5839	-0.2778	-0.0571
8-25	128	4.6891	-0.1726					
8-26	96	4.8251	-0.0366					
8-26	126	4.6956	-0.1661					
9-1	96	4.8106	-0.0511					
9-20	115	4.8736	-0.0119					
10-5	89	4.8702	+0.0085					

HORIZONTAL SPACINGS, MOVEMENTS, & STRAINS
 INTERSTATE HIGHWAY I-30 BENTON, ARKANSAS
 ONE LAYERED SYSTEM 3'-6" FROM EDGE OF PAVEMENT

DATE	TOP OF CONCRETE			DATE	TOP OF CONCRETE			
	temp	spacing	movement		strain	temp	spacing	movement
4-15-77	82	6.3992		10-13	73	6.0711	-0.3281	-0.0513
5-30	120	6.2669	-0.1323	11-8	94	6.2416	-0.1576	-0.0246
5-31	84			11-9	76	5.9201	-0.4791	-0.0749
5-31	122	6.2720	-0.1272	11-10	64	6.0578	-0.3414	-0.0534
6-15	78	6.2771	-0.1221	12-12	46	5.9240	-0.4752	-0.0743
6-20	126	6.2720	-0.1272	12-14	56	6.2366	-0.1626	-0.0254
6-21	88	6.2618	-0.1374	12-15	36	6.2266	-0.1726	-0.0270
6-21	120	6.2720	-0.1272	2-2-78	35	6.1303	-0.2689	-0.0420
6-22	89	6.2669	-0.1323	3-3	45	6.0756	-0.3236	-0.0506
6-22	120	6.2720	-0.1272	3-22	85	5.9643	-0.4349	-0.0680
6-23	89	6.2567	-0.1425	3-23	76	5.9933	-0.4059	-0.0634
6-23	124	6.2720	-0.1272	5-10	74	6.0446	-0.3546	-0.0554
7-20	86	6.2720	-0.1272	6-6	89	6.1257	-0.2735	-0.0427
7-20	100	6.2669	-0.1323	6-22	116	6.0102	-0.3890	-0.0608
7-21	82	6.2822	-0.1170	6-23	110	6.0102	-0.3890	-0.0608
7-21	118	6.3239	-0.0753	6-27	114	6.0936	-0.3056	-0.0478
7-22	86	6.2822	-0.1170	7-20	118	6.1303	-0.2689	-0.0420
8-25	94	6.2517	-0.1475	7-26	110	6.0446	-0.3546	-0.0554
8-25	128	6.2822	-0.1170					
8-26	96	6.2618	-0.1374					
8-26	126	6.2977	-0.1015					
9-1	96	6.1917	-0.2021					
9-20	115	6.2366	-0.1626					
10-5	89	6.1350	-0.2642					

HORIZONTAL SPACINGS, MOVEMENTS, & STRAINS
 INTERSTATE HIGHWAY I-30 BENTON, ARKANSAS
 ONE LAYERED SYSTEM 4'-6" FROM EDGE OF PAVEMENT

DATE	TOP OF CONCRETE			DATE	TOP OF CONCRETE				
	temp	spacing	movement		strain	temp	spacing	movement	strain
4-15-77	82	4.4469			10-13	73	4.4046	-0.0423	-0.0095
5-30	120	4.4733	+0.0264	+0.0059	11-8	94	4.3842	-0.0627	-0.0141
5-31	84	4.4660	0.0191	0.0043	11-9	76	4.3875	-0.0594	-0.0134
5-31	122	4.4769	0.0300	0.0067	11-10	64	4.4046	-0.0423	-0.0095
6-15	78	4.4733	0.0264	0.0059	12-12	46	4.3842	-0.0627	-0.0141
6-20	126	4.4685	0.0216	0.0049	12-14	56	4.4219	-0.0250	-0.0056
6-21	88	4.4648	0.0179	0.0040	12-15	35	4.4539	+0.0070	+0.0016
6-21	120	4.4745	0.0276	0.0062	2-2-78	35	4.4325	-0.0144	-0.0032
6-22	89	4.4708	0.0239	0.0054	3-3	45	4.3842	-0.0627	-0.0141
6-22	120	4.4769	0.0300	0.0067	3-22	85	4.2821	-0.1648	-0.0371
6-23	89	4.4708	0.0239	0.0054	3-23	76	4.3609	-0.0860	-0.0193
6-23	124	4.4708	0.0239	0.0054	5-10	84	4.3609	-0.0860	-0.0193
7-20	86	4.4516	0.0047	0.0011	6-6	89	4.4080	-0.0389	-0.0087
7-20	100	4.4353	0.0116	0.0026	6-22	116	4.3065	-0.1404	-0.0316
7-21	82	4.4516	0.0047	0.0011	6-23	110	4.3096	-0.1373	-0.0308
7-21	118	4.4147	-0.0322	-0.0072	6-27	114	4.3004	-0.1465	-0.0329
7-22	86	4.4516	+0.0047	+0.0011	7-20	118	4.3609	-0.0860	-0.0193
8-25	94	4.4238	-0.0231	-0.0052	7-26	110	4.3808	-0.0661	-0.0149
8-25	128	4.3501	-0.0968	-0.0218					
8-26	96	4.4227	-0.0242	-0.0054					
8-26	126	4.3524	-0.0945	-0.0213					
9-1	96	4.4022	-0.0447	-0.0101					
9-20	115	4.3630	-0.0839	-0.0189					
10-5	89	4.3808	-0.0661	-0.0149					

HORIZONTAL SPACINGS, MOVEMENTS, & STRAINS
INTERSTATE HIGHWAY 1-30 BENTON, ARKANSAS
ONE LAYERED SYSTEM 6'-0" FROM EDGE OF PAVEMENT

DATE	TOP OF CONCRETE			DATE	TOP OF CONCRETE			
	temp	spacing	movement		temp	spacing	movement	strain
4-15-77	82	4.6110		10-13	73	4.5920	-0.0190	-0.0041
5-30	120	4.6458	0.0348	11-8	94	4.6280	+0.0170	+0.0037
5-31	84	4.6353	0.0243	11-9	76	4.5503	-0.0607	-0.0132
5-31	122	4.6473	0.0363	11-10	64	4.5814	-0.0296	-0.0064
6-15	78	4.6377	0.0267	12-12	46	4.5480	-0.0630	+0.0137
6-20	126	4.6377	0.0267	12-14	56	4.6377	+0.0267	+0.0058
6-21	88	4.6335	0.0225	12-15	36	4.6335	0.0225	0.0049
6-21	120	4.6413	0.0303	2-2-78	35	4.6209	0.0099	-0.0021
6-22	89	4.6353	0.0243	3-3	45	4.6084	-0.0026	-0.0006
6-22	120	4.6413	0.0303	3-22	85	4.5961	-0.0149	-0.0032
6-23	89	4.6324	0.0214	3-23	76	4.6002	-0.0108	+0.0023
6-23	124	4.6458	0.0348	5-10	74	4.6335	+0.0225	+0.0049
7-20	86	4.6383	0.0273	6-6	89	4.6505	0.0395	0.0086
7-20	100	4.6383	0.0273	6-22	116	4.6420	0.0310	0.0067
7-21	82	4.6353	0.0243	6-23	110	4.6420	0.0310	0.0067
7-21	118	4.6582	0.0472	6-27	114	4.6293	0.0183	0.0040
7-22	36	4.6443	0.0333	7-20	118	4.6167	0.0057	0.0012
8-25	94	4.6383	0.0273	7-26	110			
8-25	128	4.6489	0.0379					
8-26	96	4.6383	0.0273					
8-26	126	4.6473	0.0363					
9-1	96	4.6251	0.0141					
9-20	115	4.6041	-0.0069					
10-5	89	4.5961	-0.0149					

HORIZONTAL SPACINGS, MOVEMENTS, & STRAINS
 INTERSTATE HIGHWAY I-30 BENTON, ARKANSAS
 ONE LAYERED SYSTEM 11'-9" FROM EDGE OF PAVEMENT

DATE	TOP OF CONCRETE			DATE	TOP OF CONCRETE			
	temp	spacing	movement		strain	temp	spacing	movement
4-15-77	82	6.2567		10-13	73	6.0800	-0.1767	-0.0282
5-30	120	6.2416	-0.0151	11-8	94	6.2466	-0.0101	-0.0016
5-31	84	6.2266	-0.0301	11-9	76	5.9725	-0.2842	-0.0454
5-31	122	6.2366	-0.0201	11-10	64	6.0845	-0.1722	-0.0275
6-15	78	6.2266	-0.0301	12-12	46	5.9933	-0.2634	-0.0421
6-20	126	6.2416	-0.0151	12-14	56	6.2618	+0.0051	+0.0008
6-21	88	6.2266	-0.0301	12-15	36	6.2618	0.0051	0.0008
6-21	120	6.2466	-0.0101	2-2-78	35	6.2366	-0.0201	-0.0032
6-22	89	6.2266	-0.0301	3-3	45	6.1586	-0.0981	-0.0157
6-22	120	6.2416	-0.0151	3-22	85	6.1586	-0.0981	-0.0157
6-23	99	6.2118	-0.0449	3-23	76	6.1633	-0.0934	-0.0149
6-23	124	6.2366	-0.0201	5-10	74	6.2720	+0.0153	+0.0024
7-20	86	6.2517	-0.0050	6-6	89	6.3398	0.0831	0.0132
7-20	100	6.2466	-0.0101	6-22	116	6.3239	0.0642	0.0102
7-21	82	6.2567	0.0000	6-23	110	6.3082	0.0485	0.0077
7-21	118	6.2771	+0.0204	6-27	114	6.2266	-0.0301	-0.0048
7-22	86	6.2517	-0.0050	7-20	118	6.2316	+0.0749	+0.0120
8-25	94	6.2366	-0.0201	7-26	110			
8-25	128	6.2771	+0.0204					
8-26	96	6.2466	-0.0101					
8-26	126	6.2771	+0.0204					
9-1	96	6.2167	-0.0400					
9-20	115	6.2720	+0.0153					
10-5	89	6.1350	-0.1217					

HORIZONTAL SPACINGS, MOVEMENTS, & STRAINS
 INTERSTATE HIGHWAY I-30 BENTON, ARKANSAS
 ONE LAYERED SYSTEM 12'-2" FROM EDGE OF PAVEMENT

DATE	TOP OF CONCRETE			DATE	TOP OF CONCRETE			
	temp	spacing	movement		strain	temp	spacing	movement
4-15-77	82	5.5030		10-13	73	5.4258	-0.0772	-0.0140
5-30	120	5.5499	+0.0469	11-8	94	5.5350	+0.0320	+0.0058
5-31	84	5.5439	0.0409	11-9	76	5.3543	-0.1487	-0.0270
5-31	122	5.5529	0.0499	11-10	64	5.4502	-0.0528	-0.0096
6-15	78	5.5499	0.0469	12-12	46	5.3818	-0.1212	-0.0220
6-20	126	5.5499	0.0569	12-14	56	5.5529	+0.0499	+0.0091
6-21	88	5.5439	0.0409	12-15	36	5.5499	0.0469	0.0085
6-21	120	5.5499	0.0469	2-2-78	35	5.5559	0.0529	0.0096
6-22	89	5.5469	0.0439	3-3	45	5.4777	-0.0253	-0.0046
6-22	120	5.5499	0.0469	3-22	85	5.4611	-0.0419	-0.0076
6-23	89	5.5439	0.0409	3-23	76	5.4367	-0.0663	-0.0120
6-23	124	5.5529	0.0499	5-10	74	5.5439	+0.0409	+0.0074
7-20	86	5.5559	0.0529	6-6	89	5.5960	0.0930	0.0169
7-20	100	5.5590	0.0560	6-22	116	5.5835	0.0805	0.0146
7-21	82	5.5559	0.0529	6-23	110	5.5743	0.0713	0.0129
7-21	118	5.5804	0.0774	6-27	114	5.5773	0.0743	0.0135
7-22	86	5.5559	0.0529	7-20	118	5.5529	0.0499	0.0091
8-25	94	5.5439	0.0409	7-26	110	5.5262	0.0232	0.0042
8-25	128	5.5712	0.0682					
8-26	96	5.5409	0.0379					
8-26	126	5.5681	0.0651					
9-1	96	5.5203	0.0173					
9-20	115	5.5590	0.0560					
10-5	89	5.4666	-0.0364					

TWO LAYERED SYSTEM

Vertical Spacings, Movements and Strains

VERTICAL MOVEMENTS WITH RESPECT TO
STABLE REFERENCE POINT
INTERSTATE HIGHWAY I-30 BENTON, ARKANSAS
TWO LAYERED SYSTEM-TOPOF CONCRETE

DATE	TEMP	DISTANCE FROM EDGE OF PAVEMENT									
		WEST SIDE OF JOINT					EAST SIDE OF JOINT				
		0'-6"	3'-6"	8'-6"	11'-9"	0'-6"	3'-6"	8'-6"	11'-9"	8'-6"	11'-9"
1977	10/5	90	0.0000	0.0000	0.0000	0.0000	0.0000	0.0000	0.0000	0.0000	0.0000
	10/6	90	-0.0008	-0.0003	-0.0008	-0.0011	0.0000	+0.0005	0.0000	0.0000	-0.0011
	10/13	82	-0.0008	-0.0006	+0.0017	+0.0066	+0.0012	-0.0014	-0.0014	-0.0027	-0.0014
	11/9	82	-0.0072	-0.0109	-0.0085	-0.0119	-0.0110	-0.0091	-0.0074	-0.0074	-0.0088
	11/10	76	-0.0039	-0.0087	-0.0042	-0.0048	-0.0005	-0.0045	-0.0062	-0.0062	-0.0028
	12/14	45	0.0000	-0.0154	-0.0151	-0.0277	-0.0110	-0.0107	+0.0030	+0.0030	-0.0069
	12/15	42	+0.0005	-0.0149	-0.0143	-0.0246	-0.0107	-0.0114	+0.0026	+0.0026	-0.0069
1978	2/2	32	0.0000	-0.0203	-0.0209	-0.0402	-0.0153	-0.0165	-0.0033	-0.0033	-0.0156
	3/3	42	0.0000	-0.0263	-0.0258	-0.0525	-0.0185	-0.0179	-0.0045	-0.0045	-0.0176
	3/22	72	+0.0040	-0.0109	-0.0184	-0.0575	-0.0025	+0.0025	+0.0111	+0.0111	-0.0014
	3/23	63	0.0043	-0.0130	-0.0184	-0.0502	-0.0020	-0.0022	0.0089	0.0089	-0.0007
	5/10	66	-0.0017	-0.0193	-0.0234	-0.0663	-0.0015	-0.0062			-0.0060
	6/6	84	+0.0025	-0.0273	-0.0299	-0.0844	-0.0070	-0.0129	0.0079	0.0079	-0.0037
	6/22	96	-0.0047	-0.0335	-0.0335	-0.0935	-0.0105	-0.0169	0.0053	0.0053	-0.0085
	6/23	90	-0.0011	-0.0325	-0.0339	-0.0890	-0.0090	-0.0165	0.0045	0.0045	-0.0072
	6/27	110	-0.0003	-0.0372	-0.0395	-0.1022	-0.0110	-0.0160	0.0022	0.0022	-0.0147
	7/6	100	-0.0039	-0.0385		-0.0997	+0.2304	-0.0172			-0.0127
	7/20	98	-0.0064	-0.0399	-0.0371	-0.0963	-0.0065	-0.0193	-0.0078	-0.0078	-0.0127
	7/26	100	-0.0064	-0.0408	-0.0379	-0.0985	-0.0090	-0.0211	0.0009	0.0009	-0.0127

TWO LAYERED SYSTEM
Horizontal Spacings, Movements and Strains

THREE LAYERED SYSTEM

Vertical Spacings, Movements and Strains

VERTICAL MOVEMENTS WITH RESPECT TO
STABLE REFERENCE POINT
INTERSTATE HIGHWAY I-30 BENTON, ARKANSAS
THREE LAYERED SYSTEM-TOP OF CONCRETE

DATE	TEMP	DISTANCE FROM EDGE OF PAVEMENT									
		WEST SIDE OF JOINT					EAST SIDE OF JOINT				
		0'-6"	3'-6"	8'-6"	11'-9"	0'-6"	3'-6"	8'-6"	11'-9"		
10/4	96	0.0000	0.0000	0.0000		0.0000	0.0000			0.0000	0.0000
10/5	92	+0.0027	+0.0052	+0.0055		+0.0017	+0.0029			+0.0046	+0.0046
10/6	93	0.0018	0.0052	0.0074		0.0022	0.0032			0.0046	0.0046
10/13	88	0.0055	0.0031	0.0118		0.0025	0.0044			0.0026	0.0026
11/9	84	0.0018	0.0026	-0.0015		-0.0015	0.0017			0.0026	0.0026
11/10	80	0.0055	0.0036	+0.0045		+0.0053	0.0049			0.0060	0.0060
12/13	49	0.0059	0.0073	0.0104		0.0025	0.0073			0.0046	0.0046
12/14	52	0.0057	0.0080	0.0091		0.0020	0.0060			0.0046	0.0046
12/15	46	0.0075	0.0082	0.0104		0.0030	0.0062			0.0052	0.0052
2/2	36	0.0086	0.0101	0.0108		0.0025	0.0088			0.0046	0.0046
3/3	42	0.0050	0.0066	0.0088		-0.0017	0.0060			0.0018	0.0018
3/22	60	-0.0028	0.0017	0.0068		-0.0054	0.0022			-0.0005	-0.0005
3/23	50	-0.0038	0.0010	-0.0012		-0.0057	0.0015			-0.0002	-0.0002
6/6	79	-0.0093	-0.0039	+0.0088		-0.0087	-0.0016			-0.0260	-0.0260
6/7	76	-0.0093	-0.0039	0.0052		-0.0094	-0.0026			-0.0257	-0.0257
6/22	87	-0.0132	-0.0079	0.0058		-0.0119				-0.0295	-0.0295
6/23	88	-0.0140	-0.0079	0.0052		-0.0128	-0.0051			-0.0302	-0.0302
6/27	94	-0.0157	-0.0114	0.0045		-0.0180	-0.0094			-0.0351	-0.0351
7/6	98	-0.0200	-0.0168	0.0045			-0.0140			-0.0388	-0.0388
7/12	100	-0.0225	-0.0182	0.0065			-0.0150			-0.0431	-0.0431
7/20	98	-0.0200	-0.0182	-0.0049						-0.0458	-0.0458
7/26	98	-0.0191	-0.0262				-0.0167			-0.0450	-0.0450

1977

1978

VERTICAL MOVEMENTS WITH RESPECT TO
STABLE REFERENCE POINT
INTERSTATE HIGHWAY I-30 BENTON, ARKANSAS
THREE LAYERED SYSTEM-TOP OF OPEN GRADE

DATE	TEMP	DISTANCE FROM EDGE OF PAVEMENT									
		WEST SIDE OF JOINT					EAST SIDE OF JOINT				
		0'-6"	3'-6"	8'-6"	11'-9"	0'-6"	3'-6"	8'-6"	11'-9"		
1977	10/4		0.0000	0.0000		0.0000	0.0000				
	10/5		+0.0485	+0.0529		+0.0078	+0.0293			+0.0267	
	10/6		0.0485	0.0548		0.0103	0.0296			0.0267	
	10/13		0.0329	0.0410		-0.0135	0.0044			0.0136	
	11/9		0.0059	-0.0241		-0.0215	-0.0083			-0.0006	
	11/10		-0.0190	+0.0248		+0.0253	+0.0290			+0.0265	
	12/13		+0.0676	0.0765		0.0126	0.0382			0.0362	
	12/14		0.0649	0.0689		0.0142	0.0369			0.0378	
	12/15		0.0651	0.0796		0.0152	0.0371			0.0373	
1978	2/2		0.0601	0.0737		0.0066	0.0162			0.0330	
	3/3		0.0431	0.0562		-0.0177	0.0110			0.0239	
	3/22		0.0349	-0.0240		-0.0114				0.0232	
	3/23		0.0308	-0.0642		-0.0117	-0.0060			0.0219	
	6/6		0.0428	+0.0031		+0.0158	-0.0016			0.0183	
	6/7		0.0428	-0.0005		0.0007	-0.0051			0.0186	
	6/22		0.0253			-0.0078				0.0132	
	6/23		0.0320	+0.0322		-0.0078	-0.0151			0.0125	
	6/27		0.0151			-0.0099	-0.0245			0.0092	
	7/6		-0.0230	0.0337			-0.0879			0.0071	
	7/12		-0.0691	0.0961			-0.0686			-0.0147	
	7/20		-0.1141	-0.0384						-0.0063	
	7/26		-0.9850				-0.0728			-0.0039	

VERTICAL SPACINGS, MOVEMENTS, & STRAINS
 INTERSTATE HIGHWAY I-30 BENTON, ARKANSAS
 THREE LAYERED SYSTEM 12'-2" FROM EDGE OF PAVEMENT
 SOUTH OF C.L. JOINT

DATE	TOP OF CONCRETE			TOP OF OPEN GRADE			TOP OF BINDER					
	temp	spacing	movement	strain	temp	spacing	movement	strain	temp	spacing	movement	strain
1977												
10/4	96	1.1159			101	3.0382			98	5.3763		
10/5	92	1.1252	+0.0093	+0.0083	85	3.0463	+0.0081	+0.0027	82	5.4663	+0.0900	+0.0167
10/6	93	1.1252	0.0093	0.0083	86	3.0463	0.0081	0.0027	80	5.4663	0.0900	0.0167
10/13	88	1.1209	0.0050	0.0045	78	3.0422	0.0040	0.0013	88	5.4206	0.0343	0.0064
11/9	84				80	3.0067	-0.0315	-0.0104	83	5.3888	0.0125	0.0023
11/10	80	1.1336	0.0177	0.0159	73	3.0503	+0.0121	+0.0040	81	5.4931	0.1168	0.0217
12/13	49	1.1403	0.0244	0.0219	51	3.0503	0.0121	0.0040	55	5.5169	0.1406	0.0262
12/14	52	1.1403	0.0244	0.0219	52	3.0503	0.0121	0.0040	52	5.5169	0.1406	0.0262
12/15	46	1.1410	0.0251	0.0225	46	3.0503	0.0121	0.0040	45	5.5068	0.1305	0.0243
2/2	36	1.1415	0.0256	0.0229	36	3.0463	0.0081	0.0027	36	5.5000	0.1237	0.0230
3/3	42	1.1413	0.0254	0.0228	42	3.0422	0.0040	0.0013	42	5.4663	0.0900	0.0167
3/22	60	1.1377	0.0218	0.0195	50	3.0422	0.0040	0.0013	97	5.4796	0.1033	0.0192
3/23	50	1.1372	0.0213	0.0191	60	3.0382	0.0000	0.0000	68	5.4729	0.0966	0.0180
6/6	79	1.1341	0.0182	0.0163	105	3.0544	0.0162	0.0053	105	5.5562	0.1799	0.0335
6/7	76	1.1339	0.0180	0.0161	81	3.0544	0.0162	0.0053	81	5.5562	0.1799	0.0335
6/22	87				102				116	5.5477	0.1714	0.0319
6/23	88	1.1390	0.0231	0.0207	94	3.0422	0.0040	0.0013	100	5.5429	0.1666	0.0319
6/27	94				113	3.0422	0.0040	0.0013	132	5.5453	0.1690	0.0314
7/6	98	1.1306	0.0147	0.0132	109	3.0422	0.0040	0.0013	120	5.5310	0.1547	0.0278
7/12	100	1.1458	0.0299	0.0268	116				132	5.5334	0.1571	0.0292
7/20	98	1.1288	0.0129	0.0115	99	3.0342	-0.0040	-0.0013	100	5.4982	0.1219	0.0226
7/26	98				99	3.0342	-0.0040	-0.0013	100	5.5075	0.1312	0.0244

THREE LAYERED SYSTEM

Horizontal Spacings, Movements and Strains

HORIZONTAL SPACINGS, MOVEMENTS, & STRAINS
 INTERSTATE HIGHWAY I-30 BENTON, ARKANSAS
 THREE LAYERED SYSTEM 0'-6" FROM EDGE OF PAVEMENT

DATE	TOP OF CONCRETE			TOP OF OPEN GRADE			TOP OF BINDER			
	temp	spacing	movement	temp	spacing	movement	temp	spacing	movement	strain
10/4	96	6.1210					98	6.5785		
10/5	92	6.2416	+0.1206				82	6.6946	+0.1161	+0.0176
10/6	93	6.2618	0.1408				83	6.7014	0.1229	0.0187
10/13	88	6.1729	0.0519				100	6.5126	-0.0659	-0.0100
11/9	84	6.1072	-0.0138				83	6.6287	0.0502	0.0076
11/10	80	6.1922	0.0712				81	6.6351	0.0566	0.0086
12/13	49	6.3344	0.2134				55	6.7580	0.1795	0.0273
12/14	52	6.3292	0.2082				52	6.7802	0.2017	0.0307
12/15	46	6.3292	0.2082				45	6.7364	0.1579	0.0240
2/2	36	6.3239	0.2029				30	6.7435	0.1650	0.0251
3/3	42	6.2167	0.0957				42	6.6415	0.0630	0.0096
3/22	50	6.2416	0.1206				97	6.5971	0.0186	0.0028
3/23	60	6.2316	0.1106				68	6.5847	0.0062	0.0009
6/6	76	6.3558	0.2348				105	6.5971	0.0186	0.0028
6/7	79	6.3611	0.2401				81	6.3992	-0.1793	-0.0273
6/22	87	6.2020	0.0810							
6/23	88	6.1825	0.0615							
6/27	94	6.2416	0.1206							
7/6	98	6.1072	-0.0138							
7/12	100	5.9562	-0.1648							
7/20	98	6.1491	0.0281							
7/26	98									

1977

1978

HORIZONTAL SPACINGS, MOVEMENTS, & STRAINS
 INTERSTATE HIGHWAY I-30 BENTON, ARKANSAS
 THREE LAYERED SYSTEM 2'-6" FROM EDGE OF PAVEMENT

DATE	TOP OF CONCRETE			TOP OF OPEN GRADE			TOP OF BINDER					
	temp	spacing	movement	strain	temp	spacing	movement	strain	temp	spacing	movement	strain
10/4					98	4.6462			98	4.7722		
10/5					82	4.6721	+0.0259	+0.0056	82	4.8209	+0.0487	+0.0102
10/6					83	4.6809	0.0347	0.0075	83	4.8259	0.0537	0.0113
10/13					84	4.6677	0.0215	0.0046	100	4.7866	0.0144	0.0030
11/9					80	4.6377	-0.0085	-0.0018	83	4.8159	0.0437	0.0092
11/10					73	4.6634	0.0172	0.0037	81	4.8309	0.0587	0.0123
12/13					51	4.7075	0.0613	0.0132	55	4.8824	0.1102	0.0231
12/14					52	4.7030	0.0568	0.0122	52	4.8824	0.1102	0.0231
12/15					46	4.7075	0.0613	0.0132	45	4.8824	0.1102	0.0231
2/2					36	4.7030	0.0568	0.0122	30	4.8877	0.1155	0.0242
3/3					42	4.6853	0.0391	0.0084	42	4.8615	0.0893	0.0187
3/22					50	4.6853	0.0391	0.0084	97	4.7818	0.0096	0.0020
3/23					60	4.6809	0.0347	0.0075	68	4.8309	0.0587	0.0123
6/6					92	4.7126	0.0664	0.0143				
6/7					79	4.7628	0.1166	0.0251				
6/22					104	4.7241	0.0779	0.0168				
6/23					94	4.7226	0.0764	0.0164				
6/27					113	4.7226	0.0764	0.0164				
7/6					109	4.7182	0.0720	0.0155				
7/12					116	4.7241	0.0779	0.0167				
7/20					99	4.7056	0.0594	0.0128				
7/26					99	4.7196	0.0734	0.0158				

1977

1978

HORIZONTAL SPACINGS, MOVEMENTS, & STRAINS
 INTERSTATE HIGHWAY I-30 BENTON, ARKANSAS
 THREE LAYERED SYSTEM 3'-6" FROM EDGE OF PAVEMENT

DATE	TOP OF CONCRETE			TOP OF OPEN GRADE			TOP OF BINDER					
	temp	spacing	movement	strain	temp	spacing	movement	strain	temp	spacing	movement	strain
10/4	96	6.4606			98	5.5651			98	5.4611		
10/5	92	6.7014	+0.2408	+0.0373	82	5.6806	+0.1155	+0.0208	82	5.5529	+0.0918	+0.0168
10/6	93	6.7222	0.2616	0.0405	83	5.6907	0.1256	0.0226	83	5.5651	0.1040	0.0190
10/13	88	6.6611	0.2005	0.0310	84	5.6376	0.0725	0.0130	100	5.4945	0.0334	0.0061
11/9	84	6.5067	0.0461	0.0071	80	5.5992	0.0341	0.0061	83	5.5929	0.1318	0.0241
11/10	80	6.5971	0.1365	0.0211	73	5.6409	0.0758	0.0136	81	5.6376	0.1765	0.0323
12/13	49	6.8844	0.4238	0.0656	51	5.7387	0.01736	0.0312	55	5.6474	0.1863	0.0341
12/14	52	6.8844	0.4238	0.0656	52	5.7387	0.1736	0.0312	52	5.6344	0.1733	0.0317
12/15	46	6.8844	0.4238	0.0656	46	5.7353	0.1702	0.0306	45	5.6442	0.1831	0.0335
2/2	36	6.8590	0.3984	0.0617	36	5.7009	0.1358	0.0244	30	5.6119	0.1508	0.0276
3/3	42	6.7580	0.2974	0.0460	42	6.6023	0.0372	0.0067	42	5.4584	-0.0027	-0.0005
3/22	50	6.7653	0.3047	0.0472	50	5.6279	0.0628	0.0113	97	5.6151	0.1540	0.0282
3/23	60	6.7435	0.2829	0.0438	60	5.6183	0.0532	0.0096	68	5.5992	0.1381	0.0253
6/6	76	6.8844	0.4238	0.0656	92	5.7145	0.1494	0.0268				
6/7	79	6.8844	0.4238	0.0656	79	5.6873	0.1222	0.0220				
6/22	87	6.8844	0.4238	0.0656	104	5.7492	0.1841	0.0331				
6/23	88	6.8844	0.4238	0.0656	94	5.7422	0.1771	0.0318				
6/27	94	6.9188	0.4582	0.0709	113	5.6606	0.0955	0.0172				
7/6	98	6.8590	0.3984	0.0617	109	5.6474	0.0823	0.0148				
7/12	100	6.8186	0.3580	0.0554	116	5.5145	-0.0506	-0.0091				
7/20	98	6.7727	0.3121	0.0483	99	5.2616	-0.3035	-0.0545				
7/26	98	6.6744	0.2138	0.0331	99	5.6672	0.1021	0.0183				

1977

1978

HORIZONTAL SPACINGS, MOVEMENTS, & STRAINS
 INTERSTATE HIGHWAY 1-30 BENTON, ARKANSAS
 THREE LAYERED SYSTEM 4'-6" FROM EDGE OF PAVEMENT

DATE	TOP OF CONCRETE			TOP OF OPEN GRADE			TOP OF BINDER				
	temp	spacing	movement	temp	spacing	movement	temp	spacing	movement	strain	
1977											
10/4							98	4.7850			
10/5							82	4.8360	+0.0510		+0.0107
10/6							83	4.8360	0.0510		0.0107
10/13							100	4.8025	0.0175		0.0037
11/9							83	4.8284	0.0434		0.0091
11/10							81	4.8583	0.0733		0.0153
12/13							55	4.9092	0.1242		0.0260
12/14							52	4.9092	0.1242		0.0260
12/15							45	4.9147	0.1297		0.0271
1978							30	4.9312	0.1462		0.0306
3/3							42	4.8824	0.0974		0.0204
3/22							97	4.8719	0.0869		0.0182
3/23							68	4.8877	0.1027		0.0215
6/6											
6/7											
6/22											
6/23											
6/27											
7/6											
7/12											
7/20											
7/26											

HORIZONTAL SPACINGS, MOVEMENTS, & STRAINS
 INTERSTATE HIGHWAY I-30 BENTON, ARKANSAS
 THREE LAYERED SYSTEM 8'-6" FROM EDGE OF PAVEMENT

DATE	TOP OF CONCRETE			TOP OF OPEN GRADE			TOP OF BINDER			
	temp	spacing	movement	temp	spacing	movement	temp	spacing	movement	strain
10/4	96	4.8461		101	4.2181		98	4.4150		
10/5	92	4.9368	+0.0907	85	4.2583	+0.0402	82	4.4648	+0.0498	+0.0113
10/6	93	4.9537	0.1076	86	4.2524	0.0343	83	4.4612	0.0462	0.0105
10/13	88	4.9038	0.0577	84	4.2524	0.0343	100	4.4503	0.0353	0.0080
11/9	84	4.8012	-0.0449	80	4.2524	0.0343	83	4.4575	0.0425	0.0096
11/10	80	4.9424	0.0963	73	4.2612	0.0431	81	4.4539	0.0389	0.0088
12/13	49	5.0519	0.2058	51	4.2851	0.0670	55	4.5094	0.0944	0.0214
12/14	52	5.0359	0.1898	52	4.2851	0.0670	52	4.5094	0.0944	0.0214
12/15	46	5.0600	0.2139	46	4.2851	0.0670	45	4.5094	0.0944	0.0214
2/2	36	5.0580	0.2119	36	4.2851	0.0670	30	4.5094	0.0944	0.0214
3/3	42	5.0399	0.1938	42	4.2701	0.0520	42	4.4981	0.0831	0.0188
3/22	50	4.9884	0.1423	50	4.2379	0.0198	97	4.5132	0.0982	0.0222
3/23	60	5.0001	0.1530	60	4.2322	0.0146	68	4.5019	0.0869	0.0197
6/6	76	5.0559	0.2098	92	4.2042	-0.0139	105	4.4831	0.0681	0.0154
6/7	79	5.0259	0.1798	79	4.1960	-0.0221	81	4.4831	0.0681	0.0154
6/22	87	5.0004	0.1543	104	4.2881	0.0700				
6/23	88	5.0160	0.1699	94	4.2761	0.0580				
6/27	94	5.0100	0.1639	113						
7/6	98	5.0279	0.1818	109	4.2612	0.0431				
7/12	100	5.0966	0.2505	116	5.3510	0.1329				
7/20	98	4.7977	-0.0484	99	4.1665	-0.0516				
7/26	98									

1977

1978

HORIZONTAL SPACINGS, MOVEMENTS, & STRAINS
 INTERSTATE HIGHWAY 1-30 BENTON, ARKANSAS
 THREE LAYERED SYSTEM 12'-2" FROM EDGE OF PAVEMENT

DATE	TOP OF CONCRETE			TOP OF OPEN GRADE			TOP OF BINDER					
	temp	spacing	movement	strain	temp	spacing	movement	strain	temp	spacing	movement	strain
10/4	96	5.4367			101	5.4285			98	4.0225		
10/5	92	5.5773	+0.1406	+0.0259	85	5.5499	+0.1214	+0.0224	82	4.0572	+0.0347	+0.0086
10/6	93	5.5773	0.1406	0.0259	86	5.5499	0.1214	0.0224	83	4.0572	0.0347	0.0086
10/13	88	5.5174	0.0807	0.0148	84	5.4945	0.0660	0.0122	100	4.0455	0.0230	0.0057
11/9	84	5.5321	0.0954	0.0175	80				83	4.0432	0.0207	0.0051
11/10	80	5.6474	0.2107	0.0388	73	5.5929	0.1644	0.0303	81	4.0660	0.0435	0.0108
12/13	49	5.6247	0.1880	0.0346	51	5.6247	0.1962	0.0361	55	4.0785	0.0560	0.0139
2/14	52	5.6772	0.2405	0.0442	52	5.6772	0.2487	0.0458	52	4.0763	0.0538	0.0134
12/15	46	5.6151	0.1784	0.0328	46	5.6151	0.1866	0.0344	45	4.0785	0.0560	0.0139
2/2	36	5.6606	0.2239	0.0412	36	5.6023	0.1738	0.0320	30	4.0714	0.0489	0.0122
3/3	42	5.6119	0.1752	0.0322	42	5.5590	0.1305	0.0240	42	4.0666	0.0441	0.0110
3/22	50	5.6247	0.1880	0.0346	50	5.5681	0.1396	0.0257	97	4.0690	0.0465	0.0116
3/23	60	5.6183	0.1816	0.0334	60	5.5620	0.1335	0.0246	68	4.0666	0.0441	0.0110
6/6	76	5.7283	0.2916	0.0536	92	5.6840	0.2555	0.0471	105	4.0930	0.0705	0.0175
6/7	79	5.7214	0.2847	0.0524	79	5.6873	0.2588	0.0477	81	4.0906	0.0681	0.0169
6/22	87	5.6772	0.2405	0.0442	104	5.6806	0.2521	0.0464	116	4.0858	0.0633	0.0157
6/23	88	5.7043	0.2676	0.0492	94	5.6706	0.2421	0.0446	100	4.0834	0.0609	0.0151
6/27	94	5.7111	0.2744	0.0505	113	5.6606	0.2321	0.0427	132	4.0834	0.0609	0.0151
7/6	98	5.6739	0.2372	0.0436	109	5.6772	0.2487	0.0458	120	4.0785	0.0560	0.0140
7/12	100	5.8583	0.4216	0.0775	116	5.8583	0.4298	0.0792	132			
7/20	98	5.6772	0.2405	0.0442	99	5.6472	0.2189	0.0403	100	4.0690	0.0465	0.0115
7/26	98	5.6941	0.2574	0.0473	99	5.6606	0.2321	0.0427	100	4.0690	0.0465	0.0115

1977

1978